Identifying Novel Apoptotic and Non-Apoptotic Substrates of Caspases

by

Luam Ellen Araya

A thesis submitted in partial fulfillment of the requirements for the degree of

Master of Science

Department of Biochemistry
University of Alberta

ABSTRACT

Caspases are a family of enzymes that regulate biological processes, such as inflammation and programmed cell death, through proteolysis. For example, in the intrinsic pathway of apoptosis, cell death signaling involves cytochrome c release from the mitochondria, which leads to the activation of caspase-9, and eventually the executioners, caspase-3 and -7. One key step in our understanding of these proteases is to identify their respective protein substrates. Whereas hundreds of substrates have been linked to caspase-3, only a small handful of substrates have been reported for caspase-9. Employing deep profiling by subtiligase N-terminomics, we present here an unbiased analysis of caspase-3 and caspase-9 substrates in native cell lysates. We identified 906 protein substrates associated with caspase-3, and 124 protein substrates for caspase-9. This is the most comprehensive list of caspase substrates reported for each of these proteases revealing a pool of new substrates that could not have been discovered using conventional interactomics approaches. Over half of the caspase-9 substrates were also cleaved by caspase-3, but often at unique sites, suggesting an evolved functional redundancy for these two proteases. Correspondingly, nearly half of the caspase-9 cleavage sites were not recognized by caspase-3. Our results suggest that in addition to its important role in activating the executioners, the role of caspase-9 is likely broader and more complex than previously appreciated, which includes proteolysis of key apoptotic substrates other than just caspase-3 and -7, and involvement in non-apoptotic pathways. Our results are well poised to aid the discovery of new biological functions for these two caspases. As well, we assessed the global proteome changes incurred in C2C12 cells following serum withdrawal-induced differentiation from myoblasts to myotubes; this differentiation process has been shown to involve the non-lethal activation of caspase-3. Our investigation indicates enrichment of key differentiation markers in harvested myotubes, and differential expression of proteins involved in rRNA processing in undifferentiated cells, and muscle contraction processes in differentiated myotubes, as expected. This experiment provides a starting block to further N-terminomics and phosphoproteomics work.

PREFACE

Portions of Chapter One were originally published as a review in the journal ACS Chemical Biology. Shu (Lucy) Luo and Luam Araya gathered research from the literature. Lucy Luo, Luam Araya and Olivier Julien wrote the manuscript.

> Luo, S.Y.*, Araya, L.E.* & Julien, O. (2019) Protease Substrate Identification Using N-terminomics. *ACS Chem Biol.* 14(11) 2361-2371

> *co-first author

The material in Chapter Three has been submitted for publication. Luam Araya performed the N-terminomics experiments and analysis. Ishankumar Soni performed immunoblot analysis. Luam Araya, Ishankumar Soni, Jeanne Hardy and Olivier Julien wrote the manuscript.

> Araya, L.E.*, Soni, I.V., Hardy, J.A. & Julien, O. (2021) Deorphanizing caspase-3 and caspase-9 substrates in and out of apoptosis with deep substrate profiling. *ACS Chem Biol.* (in press)

> *co-first author

ACKNOWLEDGMENTS

TABLE OF CONTENTS

List of Figures

Fig. 1.2, **1.6**, **1.7** and **2.2** were created using BioRender.com.

Fig. 3.17-3.22 were created in ProteomeDiscoverer 2.4 (Thermo Fisher).

List of Tables

List of Abbreviations:

Terms:

N-terminus = free-amine terminus of polypeptide chain

PILS = Proteomic identification of ligation sites

Molecules:

BSA = Bovine Serum Albumin

Casp3 = Human Caspase-3

Casp9 = Human Caspase-9

Casp14 = Human Caspase-14

DNA = deoxyribonucleic acid

GAPDH = glyceraldehyde-3-phosphate dehydrogenase

kDa = kilodalton

MBP = maltose-binding protein

TEV protease= Tobacco Etch Virus protease

Reagents:

2xYT = 2x Yeast Extract Tryptone growth media

ACN = Acetonitrile

AEBSF = 4-(2-aminoethyl)benzenesulfonyl fluoride hydrochloride

BME = 2-mercaptoethanol

C18 column = C18 reverse-phase sorbent resin tips for peptide desalting

CHAPS= 3-[(3-cholamidopropyl)dimethylammonio]-1-propanesulfonate

DCM = Dichloromethane

DEVD-fmk(OME) = DEVD-fluoromethylketone

DEVD-afc = DEVD-(7-amino-4-trifluoromethylcoumarin)

DICI = Diisopropylcarbodiimide

DMAP = 4-Dimethylaminopyridine

DMEM = Dulbecco's modified eagle's medium

DMF = Dimethylformamide

DMSO = dimethyl sulfoxide

DTT = 1,4 Dithiothreitol

EDTA = ethylenediaminetetraacetic acid

EtOH = Ethanol

FBS = Fetal bovine serum

Fmoc = fluorenylmethoxycarbonyl

GdnHCl = Guanidine hydrochloride

HEPES = 4-(2-Hydroxyethyl)-1-piperazineethanesulfonic acid

HOBt = Hydroxybenzotriazole

IAM = Iodoacetamide

IPTG = Isopropyl β-D-1-galactopyranoside

KCN = Potassium cyanide

LB = Luria Broth

NH_4HCO_3 = Ammonium bicarbonate

PBS = Phosphate-buffered saline

PMSF = phenylmethylsulfonyl fluoride

Rink Amide AM resin = 4-(2′,4′-Dimethoxyphenyl-Fmoc-aminomethyl)-phenoxyacetamido-aminomethyl resin

RPMI = Roswell Park Memorial Institute

TBST = Tris-buffered saline, 0.1% Tween-20

TCEP = Tris(2-carboxyethyl)phosphine hydrochloride

Tris = 2-Amino-2-(hydroxymethyl)-1,3-propanediol

TFA = trifluoroacetic acid

z-VAD-fmk = Z-Val-Ala-Asp-fluoromethylketone

Methods:

LC-MS/MS = liquid chromatography with tandem mass spectrometry

O.D. = Optical density at 600nm

SDS-PAGE = Sodium dodecyl sulfate polyacrylamide gel electrophoresis

SEC = size exclusion chromatograph

CHAPTER ONE

INTRODUCTION

1.1 Proteolysis

1.1.1 Proteolysis is a post-translational modification that regulates cellular functions

Nearly every cellular process is mediated by or involves proteins. Proteins are the driving forces that pass signals in the cell and effectuate the signal responses in pathways, such as nutrient transport and metabolism, cell growth and development and cell death.

Proteins are created through the translation of DNA into RNA, their subsequent splicing into mRNA, followed by their translation by ribosomes into a protein product. Many proteins are not fully functional upon translation and require further modification. These modifications are termed post-translational modifications (PTMs). A PTM is a biochemical modification on one or more amino acids[1]. These modifications can be reversible (such as phosphorylation) or irreversible (such as proteolysis). This allows for high protein diversity, even though there are only 20 primary amino acids encoded by DNA. There are over 140 different amino acids observed across mature proteins after post-translational modification is complete[2], with a few entries in the SwissProt database (5 as of 2019) containing over 90 annotated PTMs[3].

PTMs can occur at any stage of a protein's lifespan, from immediately after translation, to the protein's eventual degradation. They can have implications on many aspects of protein structure, such as protein structure and folding, protein stability, and subcellular localization. For example, one of the most common PTMs is ubiquitination. Ubiquitination is a process where ubiquitin, a 76-amino acid protein, is added onto lysine residues of a protein. This addition has important functional consequences for the protein in question, the most common consequence being degradation. After ubiquitination, most proteins will be targeted to the 26S proteasome for degradation[4].

There is an incredible variety of PTMs possible. Some PTMs are found in both prokaryotes and eukaryotes (such as phosphorylation[5], thiolation[6] and N-glycosylation[7]), however they are in larger variety in higher eukaryotes[2]. PTMs are mainly carried out by specialized enzymes, which recognize specific target sequences on proteins. Most often, these PTMs occur on side chains that can act as strong or weak nucleophiles (polar, acidic, and basic amino acids)[8].

Enzymes are protein catalysts, responsible for catalyzing nearly all the chemical reactions within cells, save for those catalyzed by ribozymes[9]. Enzymes catalyze reactions by binding substrates to an active site within the enzyme structure. This active site is a pocket or crevice with a specialized conformation that only accepts its substrate for binding[10]. Currently there are two

models for how substrates bind to enzyme active sites: the lock and key model and the induced fit model[11]. In the lock and key model, the substrate is a perfect fit for the active site, forming the enzyme-substrate complex. In the induced fit model, the substrate binds to the active site, though this initial binding does not have the perfect complementary chemistry. Instead, the substrate induces a conformational change in the enzyme to create the enzyme-substrate complex.

Enzymes can be placed into six categories, based on the chemical reactions they catalyse: oxidoreductases, transferases, hydrolases, lyases, isomerases and ligases[11]. Oxidoreductases catalyze redox reactions, where there is electron transfer from one molecule to another (e.g. Lactate dehydrogenase)[12]. Transferases catalyze reactions where a functional group is transferred from one molecule to another (e.g. Glutathione S-transferase)[13]. Hydrolases catalyze reactions where water is used to break a bond within a molecule (e.g. Trypsin)[14]. Lyases catalyze reactions where double bonds are created within a molecule, usually accomplished with the addition of a water, carbon dioxide or an ammonia molecule (e.g. Enolase)[15]. Isomerases catalyze reactions where a molecule shifts in structure to another shape, or isomer, of that same molecule (e.g. Triose phosphate isomerase)[16]. Finally, ligases catalyze reactions where a molecule becomes non-covalently bonded to another one. (e.g. DNA ligase I)[17]. Each of these enzyme classes can be further broken down into more specialized enzyme groups. Many of these groups, classes and families are enzyme groups that catalyze post-translational modifications. The subject of this thesis are proteases, a specific type of hydrolase that works to hydrolyze peptide bonds[18].

1.1.2 Proteases

Proteolysis is the reaction of hydrolysis of a peptide bond, a way in which proteins can be fragmented. This reaction in eukaryotic systems is often catalysed by proteases, accelerating the cleavage of the alpha-peptide bonds between amino acids[19]. The nomenclature often used to number the residues surrounding a cleavage site are counted starting at the point of cleavage[20]. For example, to indicate a sequence of four residues before and after a cleavage site ($\downarrow$), the sequence would be written as P4-P3-P2-P1$\downarrow$P1′-P2′-P3′-P4′. Residues P4-P1 are N-terminal to the cleavage site, while residues P1′-P4′ are C-terminal to the cleavage site. [20]. Proteases can be found in living and nonliving entities, from plants, animals, bacteria, and viruses. In humans, there are about 600 proteases encoded by the human genome[21].Proteases can be categorized into two groups: endopeptidases and exopeptidases[19]. Endopeptidases catalyze hydrolysis of internal peptide bonds, while exopeptidases catalyze hydrolysis of external peptide bonds (peptide bonds

of the N- or C-terminal residues on a protein). Other methods of classification based on catalysis mechanism have also been developed. Proteases are generally categorized into five families based on their catalytic mechanism: metallo-, cysteine, serine, threonine, and aspartyl proteases. Cysteine, serine, and threonine proteases hydrolyze peptide bonds by nucleophilic attack via the catalytic residues for which they are named, while metallo- and aspartyl proteases typically activate a water molecule to carry out the nucleophilic attack[22]. (**Fig. 1.1**). To a lesser extent, there is also evidence of glutamic proteases[23] which also activate a water molecule in their catalytic mechanism, though they have not yet been found in mammals.

Some proteases are promiscuous, recognizing a single amino acid in any peptide chain, and thus causing proteolysis in a wide range of protein substrates. For example, trypsin is a commonly used enzyme for protein digestion, cleaving peptide bonds on the C-terminus of any lysine or arginine in a peptide sequence. In contrast, many proteases are highly specific to longer, more distinct amino acid motifs, reflecting their regulated function in complex physiological processes. A well-known protease in this category is the tobacco etch virus (TEV) protease, which has a more stringent substrate consensus sequence ENLYFQ↓(G/S), where the proteolysis occurs after glutamine[24]. As the TEV protease is natively required for the cleavage of the TEV viral precursor polyprotein into functional viral protein units, its higher specificity can be explained by the biological importance of retaining its proper function for viral production and infectivity. Thus, the characterization of protease cleavage specificity[25–27] and identification of protease substrates is a fundamental step in the quest to understand the vital roles of proteases in various organisms. One of the most important roles that proteases carry in the cell is in programmed cell death, involving many proteases such as cathepsins[28], granzyme B[29] and caspases[30].

1.2 Cell death in response to intracellular and extracellular signals

In the average adult, 50 – 70 billion cells die every day[31]. When cells are stressed, mutate, or simply overextend their lifespan, they must find a way to cease function and die, without negatively impacting their environment or other surrounding cells, allowing new cells to take their place. As a result, these mechanisms must function under tight supervision and regulation. There are several pathways through which a cell can achieve this goal, which fall under the umbrella term of regulated cell death[32].

There are many forms of regulated cell death, most recently proposed as a family of 12 forms which oscillate between apoptotic and necrotic (or autophagic) cell morphologies during their initiation and execution[32]. These forms are distinguished by the intra- or extracellular factors which

drive their initiation, as well as the downstream signalling and resulting morphologies of death. Proposed by the Nomenclature Committee on Cell Death in 2018, this definition of regulated cell death (RCD) specifies that RCD can occur in one of two scenarios. One scenario is RCD occurring independent of exogenous signals, thereby serving as a mechanism for cell turnover (often referred to as programmed cell death (PCD)). The other scenario is that RCD can stem from external stimuli or stressors that are too strong for the cell adaptor response to cope with. Two of these forms of RCD are intrinsic and extrinsic apoptosis.

1.3 Apoptosis is a regulated cell death pathway

With the term first coined in 1972[33], apoptosis is a ubiquitous pathway for highly regulated cell death, that occurs in response to pro-death signals[34]. Morphologically, it is characterized by cytoplasmic shrinkage, membrane blebbing and fragmentation into apoptotic bodies. To elaborate, the degradation of cellular structures occurs, such as DNA fragmentation[35] and cytoskeletal protein degradation[36]. Following this, apoptotic bodies form and are phagocytosed by neighbouring cells, such as macrophages[37]. This all takes place rather quickly, on the order of minutes[38]. Apoptosis must be highly regulated to ensure that the death program is held in check until needed. Both too much and too little cell death will lead to pathology, as dysregulation of apoptosis is related to disease states, such as cancers. There are two classic mechanisms for apoptosis, the extrinsic and the intrinsic pathways, named for the signals responsible for initiating the process[39]. Outside of these two processes, the serine protease granzyme B, is also capable of mediating apoptosis through a separate cell death pathway used by cytotoxic lymphocytes to clear cells infected by viruses or other pathogens[40,41].

1.3.1 Intrinsic pathway for apoptosis

Conversely, in the intrinsic pathway for apoptosis, it is intracellular components responsible for triggering cell death. There are a variety of intrinsic stresses, such as DNA damage, survival factor deprivation, and hypoxia[42]. These stresses are recognized by cellular stress sensors, such as p53[43]. p53 is a transcriptional activator of apoptotic proteins, so is typically maintained at low level in non-stressed cells. During intrinsic apoptosis, it is phosphorylated by DNA checkpoint proteins (such as Chk2), which stabilize p53 and prevent Mouse Double Minute-2 Homolog (MDM2)-mediated p53 ubiquitination. This will prevent its degradation. MDM2 will also bind p53, preventing its nuclear export, allowing it to function as a transcriptional activator. Some proteins transcriptionally activated by p53 are the pro-apoptotic members of the Bcl2 protein family, Bcl2-Associated X-protein (BAX), Noxa, p53-upregulated modulator of apoptosis (PUMA) and BH3

Interacting Death Domain (BID)[38]. In addition to this, p53 also transcriptionally represses anti-apoptotic proteins such as the anti-apoptotic Bcl2 family members and inhibitors of apoptotic proteins (IAPs). Importantly, p53 transcriptionally activates genes that lead to an increase in reactive oxygen species (ROS), which along with the proteins above lead to mitochondrial damage and mitochondrial membrane permeabilization. This causes the release of proteins from the damaged mitochondria, such as the Second Mitochondria-derived Activator of Caspases (SMAC)/Diablo and cytochrome c because of increased mitochondrial permeability. SMAC works to inhibit IAPs, which typically bind and inhibit caspase-3[39]. Cytochrome c joins Apoptotic protease activating factor 1 (Apaf-1) upon release from the mitochondria to assemble the apoptosome, a multiprotein complex which recruits and activates the initiator pro-caspase-9. Activated caspase-9 can then activate the executioner caspase-3, which can further execute apoptosis by cleaving protein targets, leading to downstream cell death (**Fig. 1.2**).

In addition, while the pathway described above is the most common mechanism of intrinsic apoptosis, there are redundancies to maintain apoptosis in the cell. As such, typically, caspase knockout is insufficient to prevent activation of intrinsic apoptosis *in vivo*. Intrinsic apoptosis can also be triggered in a caspase-independent manner, where during MOMP, apoptosis-inducing factor (AIF) and endonuclease G (ENDOG) are relocated to the nucleus and carry out their own mass degradation events[32]. As well, the serine protease HTAR2, while being a caspase activator, is also able to generate pro-apoptotic cleavages itself, independent of caspases[44,45].

1.3.2 Extrinsic pathway for apoptosis

In the extrinsic pathway for apoptosis, extracellular components are responsible for triggering the pathway, as per the name. This can be accomplished with extracellular receptors or can be a response to cytotoxic stress outside of the cell. In the receptor-based response, a death ligand will bind to a death receptor on the surface of the cell, such as the Fas receptor or Tumor Necrosis Factor Receptor-1 (TNFR-1). In the case of the Fas receptor, the receptor will oligomerize upon binding of the Fas ligand, recruiting the Fas-Associated via Death Domain (FADD) protein to the intracellular death domain located on the Fas receptor. FADD will recruit and bind the initiator pro-caspase-8 at both of their respective Death Effector Domains (DEDs), leading to the assembly of the death-induced signaling complex (DISC)[39]. As a result of DISC formation, caspase-8 oligomerizes and activates through self-cleavage. The active caspase-8 then activates the executioner caspases-3 and -7 and downstream cell death as a result. Caspase-8 can activate the executioner caspases through two pathways. The first pathway is by cleaving Bcl2-interacting protein (BID), which leads to cytochrome c release, creating a similar downstream response to

that of the intrinsic pathway. The second way caspase-8 can activate the executioner caspases is by directly cleaving and activating caspase-3 (**Fig. 1.2**)

1.4 Dysregulation of apoptosis can lead to disease states

The dysregulation of apoptosis is well-known to be a hallmark of various disease states. For example, in all cancers, the mechanisms of cell death are limited or non-functional, typically due to a mutation, allowing cells to proliferate uncontrollably, leading to the growth and eventual metastasis of tumors in mammalian systems. Dysregulation in the opposite sense, with too much apoptosis, can also be observed in diseases. Excessive apoptosis of neurons is characteristic of neurodegenerative diseases such as Alzheimer's, Parkinson's, and Huntington's diseases[46,47].

The dysregulation of apoptosis in cancers is an extremely complex and multifaceted topic, often unique to individual cancer types, and sometimes even unique to an individual cancer patient[48]. Often, this is mediated through mutation which leads to transcriptional repression of pro-apoptotic factors, or transcriptional activation of anti-apoptotic factors, like the B-Cell Lymphoma (BCL-2) family of proteins[49]. This has consequences which lead to the dysfunction of the apoptotic cascade.

Better knowledge about how the apoptotic cascade functions, especially in terms of its activation and downstream effects, are critical to understand how these disease states manifest. The work can be a foundation to rational drug design, leading to potential therapies for those who suffer from these diseases. This thesis focuses on caspases, a family of proteases intimately involved in the initiation and execution of cell death in various forms (see **1.3** for apoptosis)

1.5. Caspases: mediators of cell death and more

In the apoptotic pathways described above, caspases play a critical role. "Caspase" is the name given to a family of cysteine aspartyl proteases, some of which were initially discovered and named interleukin converting enzymes. Their study began in 1993, with the discovery that the cell death protein-3 (ced-3) gene in *C. elegans* encodes a homolog of the independently identified human interleukin-1 converting enzyme (ICE – now caspase-1), named for its cleavage of interferon-1 beta[50]. The gene for the protein was most abundant in embryogenesis, where most programmed cell death occurs. Mutation studies determined that ced-3 was a cysteine protease required for programmed cell death. From this point, the field expanded, with some newly discovered proteins being labeled ICE enzyme while some were being labeled cell death proteins, as well as many of these proteins being discovered in other organisms before finding their human

analogues (of which there sometimes was none). This created much confusion. By 1996, 10 of the 12 human caspases had been discovered. Researchers in the field wrote a letter suggesting a change the naming of this family of proteases, to move away from prior naming systems based on homology to either ICE or CED3 and create a new family name[51]. The term "caspases" was suggested, because of their nature as <u>c</u>ysteine <u>asp</u>artic acid prote<u>ases</u>.

1.5.1 Caspase families

Most human caspases fit into three categories based on their phylogenetic relationships (which are correlated to their cell functions)[52]. These categories are the initiator, executioner and inflammatory caspases. The initiator caspases are caspase-2, -8 and -9. They are mainly responsible for cleaving the pro-domains of the executioner caspases in response to cell death signals, initiating cell death. The executioner caspases are caspase-3, -6 and -7. They work to execute cell death by cleaving pro-apoptotic targets in the cell. The inflammatory caspases are caspase-1, -4 and -5. Three human caspases remain, caspase-10, -12 and -14, of which less is known. Caspases-10 and -12 are less active caspases. Caspase-10 is highly homologous to caspase-8 (46%)[53] and is part of the initiator caspases. Caspase-12 is implicated in ER-stress-mediated apoptosis[54] and is also sometimes referred to as an inflammatory caspase. Caspase-14 is unique in that it does not seem to exhibit any cell death-related function. It is selectively expressed and activated in epidermis and hair follicles and is required for keratinocyte differentiation (**Fig. 1.4**).

The numbering of the 12 human caspases does not follow as a straightforward 1-12 sequence because of two prior identified caspases which were thought to originate from humans but were later found not to be present in humans. Caspase-11 is a murine caspase, analogous to human caspase-4, involved in pro-caspase-1 activation in macrophages[55]. Caspase-13 is a bovine caspase, which also appears to be an ortholog to human caspase-4[56].

1.5.2 Canonical roles of the caspases

To elaborate more on the cellular roles of the caspases, the inflammatory caspases-1, -4 and -5 play roles in inflammatory cell death. Caspase-1 is responsible for initiating pyroptosis, a form of programmed cell death, within the inflammasome[57]. Its recruitment to the inflammasome allows for autocatalysis[58]. Active caspase-1 will then cleave the proinflammatory cytokines pro-Interleukin-1β (pro-IL-1β) and pro-IL-11, as well as the pro-pyroptotic factor gasdermin D[59]. This leads to pore formation on the cell membrane and emptying of cytoplasmic contents.

Caspases-4 and -5 function similarly to caspase-1 as they also lead to pyroptosis, though they achieve pyroptosis in a caspase-1-independent pathway, which requires activation of the non-canonical inflammasome[58]. This is activated by cytosolic lipopolysaccharide (LPS) from gram-negative bacteria, which are recognized by caspases-4 and -5. Active caspases-4 and -5 also cleave gasdermin D, leading to pore formation. The N-terminal fragment of gasdermin D can then also activate the inflammasome, leading to caspase-1 dependent cleavage of pro-IL-β and pro-IL-11.

Caspase-12 is involved in initiating ER-stress-mediated apoptosis, also known as the unfolded protein response (UPR)[60]. This stress response can occur in either a transcription factor-dependent pathway, or a caspase-dependent pathway mediated by caspase-12. In the caspase-dependent pathway, caspase-12 migrates from the ER to the cytosol after the UPR leads to its activation. Active caspase-12 then activates caspase-9, leading to downstream caspase-3 activation and apoptosis. It is not entirely known what element of the UPR activates caspase-12, however calpains have emerged as a potential activator[61].

The initiator caspases-2, -8, -9, and -10 mainly play roles in activating the executioner caspases during various forms of cell death. Caspase-9 works to cleave caspases-3 and -7 during the intrinsic apoptotic pathway (see **1.3.1** for more detail). Caspases-8 and -10 either cleave caspases-3 and -7 directly during the extrinsic apoptotic pathway, or accomplish the same goal indirectly by cleaving BID, triggering downstream mitochondrial membrane permeabilization and caspase-9 activation (see **1.3.2** for more detail, more on caspase-9 in **2.3**). Caspase-2 is difficult to place in an apoptotic pathway, and as a result is often referred to as the "orphan caspase"[62]. Caspase-2 is implicated in p53-mediated cell death. It is activated through recruitment by RAIDD, an adaptor protein like FADD, to the PIDDosome, a complex containing the protein PIDD[63]. This recruitment alone is not sufficient to induce apoptosis, and the apoptotic pathway is unclear past this point. Caspase-2 can cleave Bid, and can directly induce cytochrome c release[64], so caspase-2 could be initiating the intrinsic apoptotic pathway, though it is currently not known. Interestingly, its substrate specificity resembles the executioner caspase-3 and -7[65].

The executioner caspases -3, -6, and -7 are the most active caspases, which have been well-studied to be responsible for a host of proteolytic cleavage events. Once activated, they work to achieve mass proteolysis in the cell, leading to the destruction of cellular structures and ultimately apoptosis of the cell (see **1.3**), However, it's been reported that activation of caspase-6 alone does not lead to apoptosis, unlike caspase-3 and -7 activation[66].

As stated earlier, Caspase-14 does not exhibit a cell death role. It is instead selectively expressed and activated in the epidermis and hair follicles and is required for keratinocyte differentiation. Currently there is only one known substrate of caspase-14, profilaggrin. Caspase-14 cleavage of profilaggrin creates filaggrin units, which accumulate in the epidermis, degrading into free amino acids and contributing to the generation of natural moisturizing factors (NMFs), which maintain epidermal hydration[67]. In addition, elevated levels of caspase-14 protect skin from UVB irradiation, as knockout mice were more UV sensitive[68].

1.5.3 Caspases are active as heterodimers

Caspases are synthesized as inactive zymogens. Each caspase is a pro-enzyme and when cleaved, becomes an active enzyme as a heterodimer. The mechanism through which this occurs is slightly different for each caspase category (**Fig 1.4**).

The initiator caspases are expressed as inactive monomers activated by autocatalytic cleavage of their pro-domain upon dimerization. For caspases-8 and -10, this is a Death Effector Domain (DED), while for caspases-2 and -9 this is a CAspase Regulatory Domain (CARD). Currently, the mechanism for how initiator caspases initially dimerize are unclear, though there have been two models proposed: an Induced Proximity model, and a Proximity-Induced Dimerization model[69]. In the Induced Proximity model, initiator caspases autoprocess when they come into close contact with each other. The Proximity-Induced Dimerization model expands upon this, hypothesizing that increased local concentrations of the initiator caspases in the apoptosome (for caspase-9) or the DISC (for caspases-8 and -10) promotes their homodimerization[70]. Following dimerization and autocatalytic cleavage, the active initiator caspase can work to cleave the executioner caspases.

The executioner caspases are expressed as constitutive dimers and as stated above, are activated by the initiator caspases. The initiator caspases work to activate the executioners by cleaving them at their inter-subunit linker regions. Once activated, they can accomplish their functions in inducing mass proteolysis in the cell (see **1.3**). The executioner caspases-3 and -7 can also trans-activate in Granzyme-B-mediated apoptosis[71]. As well, due to their similar activity against synthetic peptide substrates the executioner caspases-3 and -7 are often discussed together, but there is evidence to suggest that they cleave proteins with differing levels of efficiency, with caspase-3 being the more promiscuous enzyme[72]. Executioner caspases also seem to target initiator caspases. Depletion of caspase-3 has been shown to lead to partial caspase-9 inhibition, despite caspase-3 being the target of caspase-9 activity[73]. This suggests a feedback loop where mature caspase-3 can cleave and activate pro-caspases-9 as well, further

activating other pro-caspase-3 molecules[73]. Caspase-6, while bearing close sequence homology to caspases-3 and -7, cleaves different substrates, preferring a hydrophobic amino acid at P4 similar to the initiator caspases[65].

Like the initiator caspases, the inflammatory caspases are activated by recruitment to a larger multiprotein complex. In this case, it is recruitment to the inflammasome or the non-canonical inflammasome that activates caspases-1, -4 and -5. They are activated through autocatalytic cleavage of their CARD domains, following which they can assume their active dimerized form. Like the initiator caspases, the Proximity-Induced Dimerization model is proposed to explain their ability to autocatalyze, though it is suggested that the activation and autoproteolysis are distinctly separate events[74].

1.6 Discovery of caspase substrates

The range of knowledge about the substrates that caspases can cleave is at the same time vast and still undergoing. Some caspases have hundreds of known substrates, while others have very few. Hundreds of substrates are attributed to caspase-3/-7 during apoptosis substrates[75]. In contrast, little is known about the substrates of caspase-9, other than downstream procaspases-3/7 proteolysis.

Historically, caspase substrates were determined very slowly, first with the defining of the substrate specificity of each caspase, followed by further investigation into their cellular roles. After nearly 30 years since the discovery of the first caspase, there is still much left to be discovered about the specific substrates cleaved by many caspases. Over these years, there have been many tools designed to help aid in this endeavor. Below are the tools employed to identify the substrate specificity of the human caspases, as well as the determination of protein substrate profiles.

1.6.1 Caspases function as cysteine proteases to cleave predominantly after aspartic acid

As cysteine proteases, the active site of caspases employs a catalytic dyad at minimum, comprising a histidine and a cysteine residue within the active site. Many cysteine proteases also employ a third residue to form a catalytic triad, such as caspase-8, which also uses an arginine residue. The catalytic cysteine serves as a nucleophile to attack the peptide bond of the substrate, with the help of a water molecule (**Fig. 1.3** for a mechanism).

Caspases have been known to cleave C-terminal to aspartate residues since the discovery of caspase-1/interleukin-converting enzyme (ICE)[76]. The researchers who discovered ICE

demonstrated that it cleaved C-terminal to an aspartate[27] of interleukin-1β. To note, although caspases canonically cleave C-terminal to aspartate residues[77,78] , some can also cleave C-terminal to glutamate and phosphoserine (pS) residues, but to a much lesser extent[79]. This was determined using synthetic peptides containing DEVD↓, DEVE↓, and DEVpS↓ sequences. Recombinant caspases-3 and -7 were shown to cleave C-terminal to glutamate half as efficiently as they cleaved after aspartate (with a k_{cat}/K_m=2.7 x 10^3 $M^{-1}s^{-1}$ for Glu vs 5.5 x 10^3 $M^{-1}s^{-1}$ for Asp). Caspase-3 also cleaved phosphoserine at one-third the efficiency as aspartate (k_{cat}/K_m=1.7 x 10^3 $M^{-1}s^{-1}$ for pS vs 5.5 x 10^3 $M^{-1}s^{-1}$ for Asp)[79].

1.6.2 Determination of caspase substrate specificity

Beyond P1 specificity however, each caspase has their own preferred recognition sequence, meaning that the residues surrounding the cleaved aspartic acid will affect which caspase is able to cleave a particular aspartic acid-containing sequence.

The sequence specificity of caspases has been studied using several methods. For example, a positional scanning synthetic combinatorial library[77] approach was used, though the approach did not determine prime site specificity. This study identified the optimal recognition sequences for most human caspases (**Table 1.1**). The optimal recognition sequences for caspases-10 and -14 were later determined using the same positional scanning approach[53,80] (**Table 1.1**). The optimal peptide substrate for caspase-12 is not known. Determination of prime (P1') sit specificity was later accomplished using fluorogenic tetrapeptides[78]. It is important to note that these methods determined the optimal peptide recognition sequence, and not the consensus sequences that these caspases cleave on whole proteins. There are many factors which determine whether a caspase will cleave a recognition sequence *in vivo*, such as subcellular localization, protein structure and cleavage site accessibility, and enzyme activity, making their protein recognition sequences occasionally different. The dominant protein substrate recognition sequence has been determined for every human caspase except caspase-12 (**Table 1.1**)

Fluorescent tetrapeptide peptides are still often used when working with caspases as a method for verifying activity and determining the catalytic parameters of a protein purification[65,80,81]. Coumarin-based probes are some of the most common used for analyzing caspases. A coumarin-based caspase probe is constructed by synthesizing a tetrapeptide for the optimal recognition sequence of a caspase, followed by a coumarin (often 7-amino-4-trifluoromethylcoumarin [AFC] or 7-amino-4-methylcoumarin [AMC]). When uncleaved, the peptide does not fluoresce. However, when placed in solution with its appropriate active caspase, the probe will be cleaved, releasing

the coumarin[82]. The free AFC/AMC will generate a fluorescent signal when excited by the proper wavelength (380 nm excitation and 460 nm emission for AMC, 400 nm excitation and 505 nm emission for AFC)[77,83]. The increase of this signal can be monitored over time to determine the kinetics parameters of a caspase preparation.

1.6.3 Bioinformatic prediction of caspase substrates

There have been several computational predictive tools developed over the years to help identify potential caspase substrates. There are at least 20 computational methods proposed or available for use to predict proteolytic cleavage sites[84]. Typically, these cleavage prediction software tools will incorporate a combination of protein sequence and protein structural information, providing a theoretical measure of potential cleavage sites for a protein of interest. Some examples of these sorts of databases include ProCleave (https://procleave.erc.monash.edu)[85], iProtSub, Prediction of Protease Substrates (PoPS) (http://pops.csse.monash.edu.au/)[86], PROSPER/ PROSPRous (http://prosperous.erc.monash.edu/)[87] and CaspDB[88]. Globally, the goals of these tools are to facilitate the act of choosing potential proteolytic substrates to investigate. This is advantageous because it can provide invaluable time-saving for researchers, as it automates much of the process. The applicability of these predictor tools is often limited to well- characterized proteases or limited by the goals of the database. For example, PROSPER can only predict cleavage sites for caspases or granzyme B[89].

Despite these advantages however, there is still quite a high investment of time and work that must take place to confirm the computationally suggested protease targets and verify whether they truly are substrates in both *in vitro* and *in vivo* settings.

1.7 Proteomics

The current method of choice for identifying protease substrates is mass-spectrometry-based proteomics, but there are many challenges to overcome in order to precisely identify protease cleavage sites. For example, the balance between protein expression and protein degradation leads to constant proteolysis within a cell. In addition, cellular heterogeneity between treated and untreated samples, or healthy and disease samples, makes it difficult to distinguish meaningful induced proteolytic activity from transient background events. Moreover, proteolytic fragments of interest are often low in abundance and can be targeted for subsequent degradation due to their instability[90]. Various degradomics methods were created to overcome some of these issues, with the attempts of reliably detecting and resolving proteolytic peptides from protein substrates and background peptides.

1.7.1 N-terminomics

The N-terminomics methods essentially consist of two main objectives, labeling of the proteolytic protein fragments and enrichment of the fragments from the complex mixture. The enrichment can be achieved by modifying the cleaved peptide termini with the addition of functional groups, or by taking advantage of differentially labeled isotopes. Since carboxyl groups are less reactive than primary amines, peptide C-terminal labeling methods have been difficult to develop and thus are not as established as N-terminal profiling approaches (N-terminomics). Recent advances in tandem mass spectrometry (LC-MS/MS) have greatly accelerated the progress and sensitivity of these proteomic methods.

1.7.2 *Forward* and *reverse* N-terminomics

The *forward* discovery describes a workflow for N-terminomics application in an *in vivo* biological system. For example, human cancer cells can be treated with an apoptotic inducer to trigger massive cellular proteolysis compared to untreated cells. Both samples undergo cell lysis, N-terminal labeling, enrichment, and capture, followed by enzymatic digestion and identification by LC-MS/MS. In this analysis, labeled N-termini identified in the apoptotic samples would be subtracted from the ones that are also present in the healthy cells. *Forward* degradomics discovery is fast, relatively easy to perform, and provides a clear biological picture of protease substrates cleaved in a given biological process. For example, several studies using COFRADIC, TAILS, and subtiligase have been used to study matrix metallopeptidase activity in cancer cells[91], cathepsin function of protein degradation, and proteolysis in pancreatic tumors[92], and the N-terminal proteome of human blood samples[93]. While the *forward* experiments provide clues about biological processes, they cannot identify with certainty the protease(s) responsible for these proteolytic events. (**Fig. 1.6**)

In order to associate a protease with its substrates, the *reverse* N-terminomics method can been used. In short, endogenous proteases are first quenched in a relevant proteome lysate (e.g., cell culture, tissue, blood, or others), followed by the addition selected active protease of interest. Substrates are then identified using one of the N-terminomics methods presented above. This N-terminomics discovery approach provides direct information on the specific substrates a given protease could be targeting. Importantly, it also reveals the protease primary sequence specificity (**Fig. 1.6**). However, *reverse* N-terminomics does not provide the functional or biological significance of the proteolytic events identified and can lead to the identification of substrates from organelles that would not normally colocalize with the protease in a living cell. The *reverse*

degradomics has been successfully applied to study the role of various proteases, such as ADAMTS7[94] and matrix metalloproteinases[95,96] using TAILS, granzyme tryptases[97], and several caspases using COFRADIC[98] and subtiligase N-terminomics.

1.7.3 Subtiligase-based N-terminomics

Positive selection enables the direct labeling and capture of native N-termini and neo-N-termini on protein fragments. The difficulty arises from specifically labeling the backbone α-amines while leaving the protein ε-lysine side chains unmodified. An enzymatic N-terminomics approach was developed in this regard to selectively attach a biotin probe to N-terminal fragments generated by proteolysis. Subtiligase, an engineered peptide ligase generated from a nonspecific protease called subtilisin[99], is able to efficiently catalyze ligation between N-terminal α-amines with a peptide ester (or thioester tag; **Fig 1.7**). In untreated or apoptotic Jurkat cells, proteolytic fragments generated by cellular protease activation are N-terminally ligated by subtiligase to a designed peptide ester substrate, containing a biotin molecule for immobilization on avidin and a TEV protease cleavage site for release and recovery. Therefore, after trypsin digestion, biotinylated peptides can be easily isolated and selected from internal and C-terminal tryptic fragments for the following LC-MS/MS analysis. Importantly, the recovered peptides also contain a unique non-naturally occurring amino acid (α-amino butyric acid, Abu) derivative tag upon TEV protease cleavage, such that labeled peptides can be unambiguously distinguished from background tryptic peptides.

Despite the robustness and low false discovery rate, this enzymatic subtiligase N-terminomics approach has limitations. For example, a large amount of sample is often needed for effective enrichment and detection, often requiring milligrams of starting material due to the low efficiency of the labeling reaction (although recent advances in LC-MS/MS technology have reduced this requirement). Another major drawback is that subtiligase also has an intrinsic substrate specificity for ligation. While subtiligase has broader specificity and higher catalytic efficiency than many peptide ligases, it still possesses prime-side preferences for specific residues[99]. This would limit its application in N-terminal bioconjugation, causing an under-representation of peptides. This issue was partly resolved by mutating subtiligase at different residues to alter its P1′ and P2′ specificity, allowing one to select from a cocktail of subtiligase mutants tailored to broaden subtiligase specificity[100]. Finally, since subtiligase N-terminomics takes advantage of an enzymatic reaction as opposed to a chemical reaction, it should be possible to perform labeling in live cells.

1.7.4 Subtiligase-based N-terminomics of caspases

Subtiligase-based protease substrate profiling has been also employed in *reverse* mode, to define the substrate pools of distinct caspases. The executioner caspases (−3, −6 and −7) and initiator caspases (−2, −8 and −9) have been studied mainly in the context of apoptosis, using immortalized cancer cell lines, such as K562, Jurkat, MM1S and HEK293 cells[65,101,102], while the inflammatory caspase-1, -4, and -5 were studied in THP-1 cells[103]. In particular, the discovery of Gasdermin D as a caspase-1 substrate led to the important discovery that cleavage of Gasdermin D releases its N-terminal proteolytic domain and triggers pyroptosis[59,104]. While current advances in understanding the substrate profiles of the various caspases have been significant, there are still numerous caspases for which this information is still unknown. Caspase-14, for example, is proposed to be specifically involved in human keratinocyte differentiation, a unique function among caspases[105] An *in vitro* method to activate caspase-14 as well as the substrate cleavage sequence preferences of caspase-14 have been characterized. While select substrates of caspase-14 have been identified, such as profillagrin[68], a comprehensive substrate profiling has yet to be completed and could provide further insights into its physiological role.

In addition, the *reverse* degradomics approach has also been used to determine the rate of proteolysis of hundreds of protease substrates simultaneously using quantitative LC-MS/MS[65,101]. Selected Reaction Monitoring (SRM) is a targeted MS approach which allows for label-free quantification of digested peptides. In these studies, the *reverse* experiment was performed by adding the caspase to the cell lysate, and a series of time points were taken. The appearance of the caspase-cleaved products was enriched and labeled by subtiligase, quantified over the time-course of the experiment. This allows the measurement of the rate of proteolysis for each cleavage site. While SRM was successfully used in these studies, the recent progress and development of quantitative proteomics methods should further facilitate the measurement of proteolytic events in both *forward* and *reverse* N-terminomics paradigms[106].

1.8 Emerging non-apoptotic roles of caspases

An emerging field is the study of caspases and their involvement in non-apoptotic processes. As stated earlier, caspase-14 is required for keratinocyte differentiation, however there are also new non-apoptotic roles identified for other caspases as well.

There is evidence that caspases are active in cellular remodelling, inflammation, dendrite trimming[107], and cell differentiation. An example of caspase involvement in cell differentiation is in mouse myoblasts. Caspase-3 is required for the differentiation of C2C12 mouse myoblasts into

myotubes[108], however the relevant targets and the global proteome changes as a result of its activity are currently unknown. Caspase-2 is also required for C2C12 differentiation, as its inhibition will suppress caspase-3 activation and the induction of the cyclin-dependent kinase inhibitor p21[109]. Other examples include caspase-3 and -9 activity in the differentiation of monocytes to macrophages[110], as well as caspase-3 activity mediating embryonic stem cell differentiation[111] (See **Fig. 1.5** for more roles).

1.9 Caspase-9

A caspase of interest with relatively few information on its substrate profile is caspase-9. Caspase-9 was discovered in 1996, through cDNA constructs derived from the human chronic myelogenous leukemia cell line K562[112]. Canonically, caspase-9 is known as the initiator caspase responsible for activating caspase-3 in the intrinsic apoptotic pathway. Caspase-9 is also indirectly implicated in the extrinsic apoptotic pathway, as BID cleavage can trigger caspase-9 activation as well.

Human caspase-9 consists of a pro-domain, a large subunit and a small subunit (**Fig. 1.4**). The large and small subunits are required for catalytic activity. The pro-domain contains the CARD motif. As stated earlier, the CARD in caspase-9 selectively binds to the CARD in Apaf-1 upon formation of the apoptosome[113], allowing for dimerization followed by autocatalysis to create active, mature caspase-9. However, there is experimental evidence which suggests that caspase-9 can also be active without proteolytic processing, where mutant uncleavable caspase-9 was still able to cleave downstream caspases as long as they were also in the presence of cytosolic factors[114].

Mature caspase-9 has a reported catalytic efficiency of 2.6×10^3 $M^{-1}s^{-1}$ and a K_m of 116 µM in presence of Na-citrate as an activator, and a catalytic efficiency of 3.1×10^2 $M^{-1}s^{-1}$ with a K_m of 546 µM in presence of Apaf-1 as an activator[115].

1.9.1 Caspase-9 is implicated in non-activatory roles

Interestingly, caspase-9 has been implicated in a non-apoptotic form of cell death called paraptosis[116]. Paraptosis, an Apaf-1-independent but caspase-9-dependent form of programmed cell death[117], was first termed over two decades ago. Paraptosis occurs during cell death and neurodevelopment. It was shown that human insulin-like growth factor I receptor (IGF-IR) can be used to stimulate paraptosis cell death in HEK293T and mouse embryonic fibroblasts. Paraptosis can be inhibited by phosphatidylethanolamine binding protein (PEBP-1)[118].

1.9.2 Caspase-9 is cleaving targets other than executioner caspases

There is a growing body of evidence to suggest that casaspase-9 is playing cleavage roles beyond simply activating the executioner caspase. There are currently very few known non-caspase substrates of capase-9. A brief investigation of known caspase-9 substrates follows.

The first discovered non-caspase substrate of caspase-9 was vimentin[119], a major component of intermediate filaments. It is cleaved by caspase-9 at three sites, Asp^{85}, Asp^{259} and Asp^{429}. Vimentin is cleaved during apoptosis, and it was determined that an initiator caspase was cleaving vimentin when abolishment of executioner caspase activity did not prevent vimentin cleavage The Asp^{259} cleavage site specifically was cleaved in early apoptosis, and inhibition of caspase-9 (while other initiator caspases, like caspase-8, remained active) prevented this cleavage product[120]. Vimentin is likely not uniquely cleaved by caspase-9 in apoptosis, as two of these cleavage sites, Asp^{85} and Asp^{429}, are also cleavable by caspases -3, and -6, respectively[119]. This discovery proposed an executioner role for caspase-9 in degrading the cytoskeleton. Since the discovery of vimentin as a substrate of caspase-9, there have been discoveries of other cellular caspase-9 substrates, further suggesting that caspase-9 cleaves its own substrate profile in apoptosis.

RING2 (also known as RING1B) is cleaved by both caspases-3 and -9 at Asp^{175} and Asp^{208}, respectively[121]. RING2 is an E3 ubiquitin ligase and a member of the polycomb protein complex, which has roles in transcriptional repression of developmentally-regulated genes like the Hox genes[122,123]. RING1B is also part of the complex that maintains Histone H2A ubiquitination and transcriptional repression[124]. Caspase-mediated cleavage disrupts its transcriptional repressor activity by changing its subcellular localization from exclusively in the nucleus to being more widely distributed across the cell.

Another protein that has been shown to be cleavable by caspase-9 in vitro is Histone Deacetylase 7 (HDAC7)[125]. HDAC7, as per the name, is mainly known for deacetylating histones. HDAC7 deacetylates lysine residues on the N-terminal of core histones, effectively functioning as a transcriptional repressor[126]. It is a key regulator for genes related to immune function[127,128]. The work identifying HDAC7 as a caspase-9 substrate focused on identifying HDAC7 as a caspase-8 substrate in apoptosis, but the authors also conducted experiments in buffer with purified HDAC7 to determine if other caspases were able to cleave the protein as well. Caspase-9 was shown to be able to cleave HDAC7, albeit at a lower efficiency than caspase-8 and other caspases. HDAC7 is also cleavable by all 3 executioner caspases, as well as caspase-10. Based on this study, it is likely that caspase-9 could cleave HDAC7 during apoptosis as well, though it is not certain.

Sorting Nexin 1 and 2 (SNX1 and SNX2) are both cleavable by caspase-9[129]. Through kinetic assays, it was determined that the initiator caspase-8 is more efficient than caspase-9 at cleaving SNX2, while the opposite is true for SNX1. SNX1 and 2 are involved in intracellular protein trafficking[130], endosome signalling and endocytosis as members of a 33-protein family in mammals[131]. Both SNX1 and SNX2 are cleaved in apoptosis[129].

Another caspase-9 target is Major Vault Protein (MVP)[132]. It is cleaved by caspases-1 and -9 in epithelial cells at Asp^{441} during apoptosis. MVP, as per the name, is the major component of vaults. Vaults are ribonucleoprotein particles, whose roles are not well understood. They are associated with the nuclear envelope, the cytoskeleton, and the cytoplasm, and are likely involved in regulating signalling pathways like the MAPK pathway through its binding of kinases and phosphatases[133]. Interestingly in relation to its caspase-1 cleavage, MVP is not cleaved during pyroptosis. MVP is cytoprotective, and cleavage of MVP by caspases -1 and -9 inactivate this cytoprotectivity.

Lastly, semaphorin 7A is also cleaved by caspase-9 at Asp^{231} in mouse neuronal cells and mouse olfactory bulbs[134]. Semaphorin 7A is a membrane-anchored member of the semaphoring family of axonal guidance proteins, with roles in axonal development and immune function[135]. The protein was cleaved in apoptosis, however semaphorin 7A was also shown to be more efficiently cleaved in mouse olfactory bulbs (aged 2 years), which exhibited much higher caspase-9 activity than younger olfactory bulbs (aged 2 months). The aged olfactory bubs exhibited no caspase-3 activation, indicating no downstream effects of higher caspase-3 activity. As a result, unlike the other known substrates of caspase-9, semaphorin 7A is cleaved by caspase-9 independent of apoptosis, suggesting that caspase-9 is also active during non-apoptotic processes.

As seen by the descriptions above, there is not a single reported caspase-9 substrate whose cleavage is unique to caspase-9. They are all cleaved by other caspases as well. This does not mean that their caspase-9 cleavage is less important, however. Cleavage of a substrate by multiple caspases at the same or a similar site can indicate redundancy and specify that cleavage of that site is evolutionarily conserved and important for function. Cleavage by caspase-9 at a site distinct from other caspases, even if other caspases can cleave the substrate as well, can indicate a functional role of caspase-9 cleavage that is distinct from the cleavage by other caspases.

1.10. Thesis objectives and hypotheses

As there has never been an untargeted global proteomics profiling experiment on caspase-3 in human lysate, it is worth investigating, to determine the widest net of substrates of caspase-3. In

tandem with this, it is important to investigate the activity of caspase-9 and determine its own specific substrate profile. Prior experiments centering both of these caspases have revealed limited substrates (180 for caspase-3 for apoptotic substrates only, and none for caspase-9)[101]. As well, the lack of knowledge on the substrate-specific cleavage events, as well as the broader proteome changes of caspase-3 activity in C2C12 cells leaves much to be discovered, and likely implicates proteins that are currently unknown. This leads to the objectives and hypotheses for this thesis.

My hypotheses are the following:

1. Initiator caspases play a role in cleaving their own set of protein targets in apoptosis
2. There are apoptotic substrates of caspase-3 yet to be discovered
3. Initiator and executioner caspases are cleaving protein targets not involved in apoptosis that are currently unknown
4. The proteome of C2C12 myoblasts will incur important global caspase-3 dependent proteome changes to differentiation into myotubes

To that end, we selected an initiator caspase (caspase-9) and an executioner caspase (caspase-3) to investigate, using subtiligase N-terminomics. We also chose to conduct a label-free quantification approach to assess global proteomic changes in C2C12 myoblasts upon differentiation.

Chapter one: Figures and Table
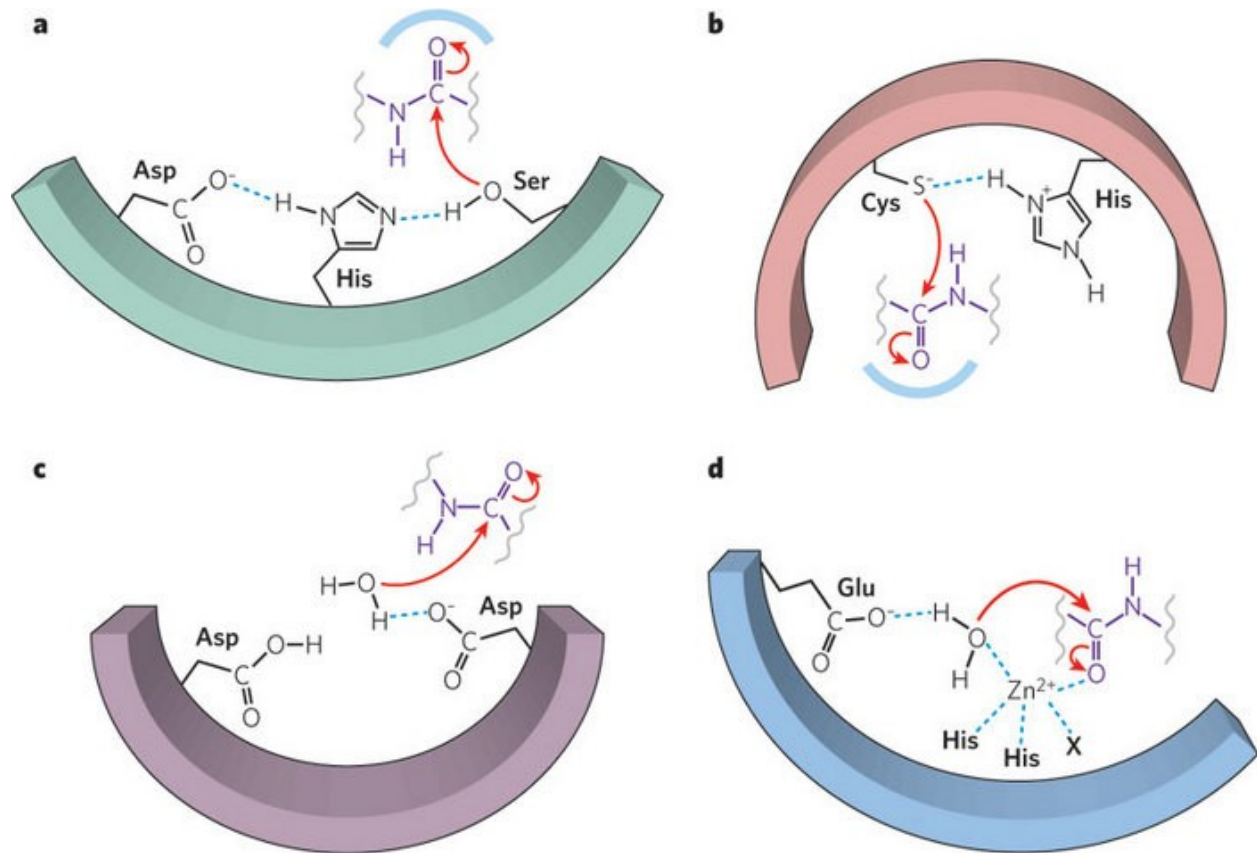
Fig. 1.1 Protease cleavage mechanisms. Proteases can be categorized into four groups according to the catalytic mechanisms they use to facilitate protein cleavage via nucleophilic attack. **A.** A serine protease, where serine serves as the nucleophile for the reaction. **B.** Cysteine proteases, where the cysteine thiol serves as the nucleophile. **C.** An aspartyl protease will activate a water molecule to serve as the nucleophile. **D.** A metalloprotease will also activate a water molecule to serve as the nucleophile. Reproduced from Erez et al. (2009) with permission[136].
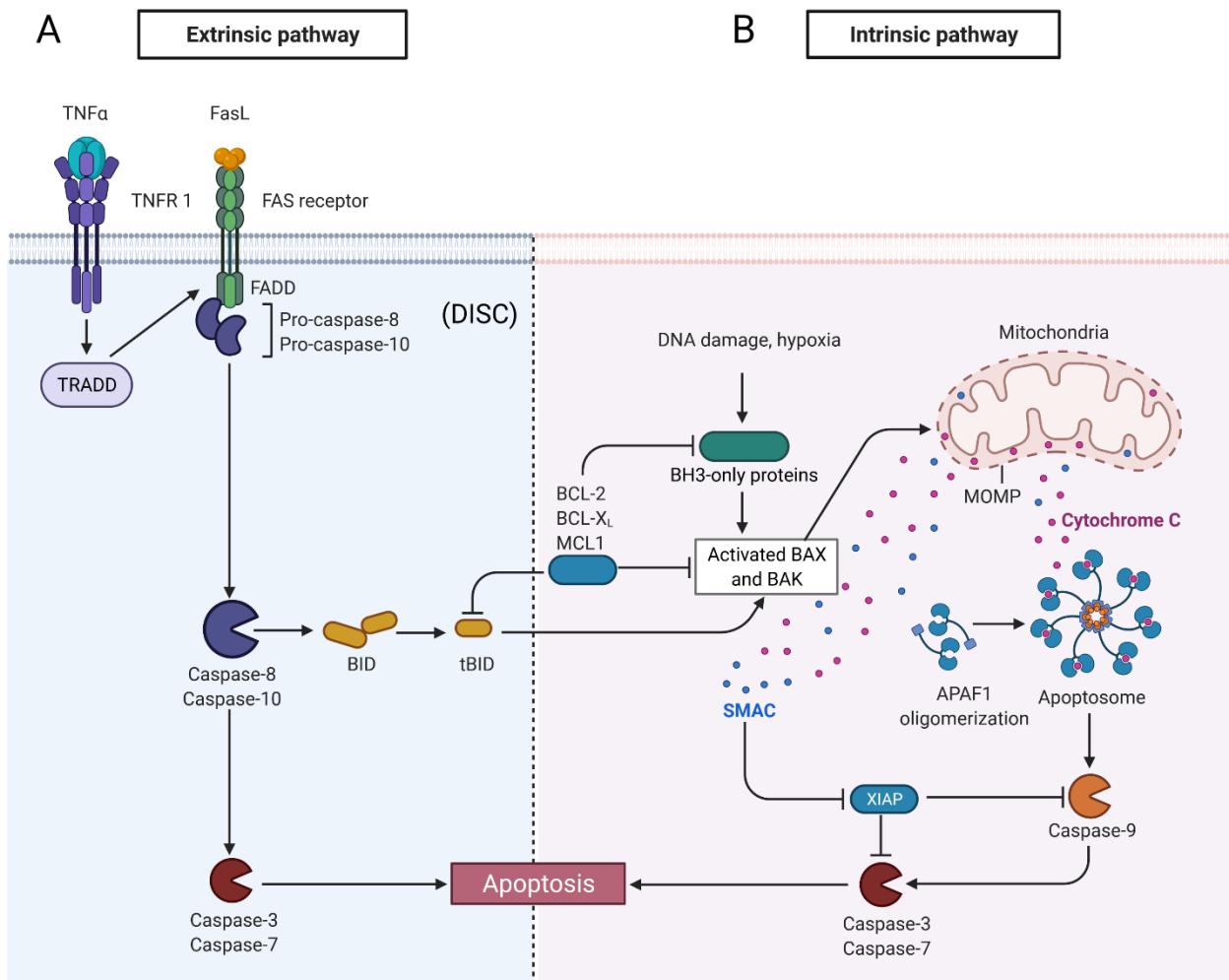
Fig. 1.2 Intrinsic and extrinsic apoptotic pathways There are many forms of programmed cell death, described above are the two pathways of apoptosis (intrinsic and extrinsic). **A.** In the intrinsic pathway, intracellular signals lead to the activation of pro-apoptotic members of the Bcl-2 family of proteins, leading to Mitochondrial Outer Membrane Permeabilization (MOMP). This leads to cytochrome C exiting the mitochondria and associating with Apoptotic Protease Activating Factor-1 (APAF1). APAF-1 will oligomerize to form the apoptosome, which will recruit pro-caspase-9 and lead to its activation. Active caspase-9 will proteolytically cleave caspases-3 and -7, allowing them to cleave various targets in the proteome and trigger apoptosis. **B.** In the extrinsic pathway, extracellular death signals will bind to death receptors such as Tumor Necrosis Factor 1 (TNF1) or the Fas receptor, leading to recruitment of Fas-Associated via Death Domain (FADD)to the death domain of the receptor, which recruits pro-caspases-8 and -10 to activate them, creating the Death Induced Signalling Complex (DISC). Active caspases-8 and -10 can either directly cleave the executioner caspases to trigger apoptosis, or they can cleave BID to lead to MOMP, and set off a similar cascade to the intrinsic apoptotic pathway.
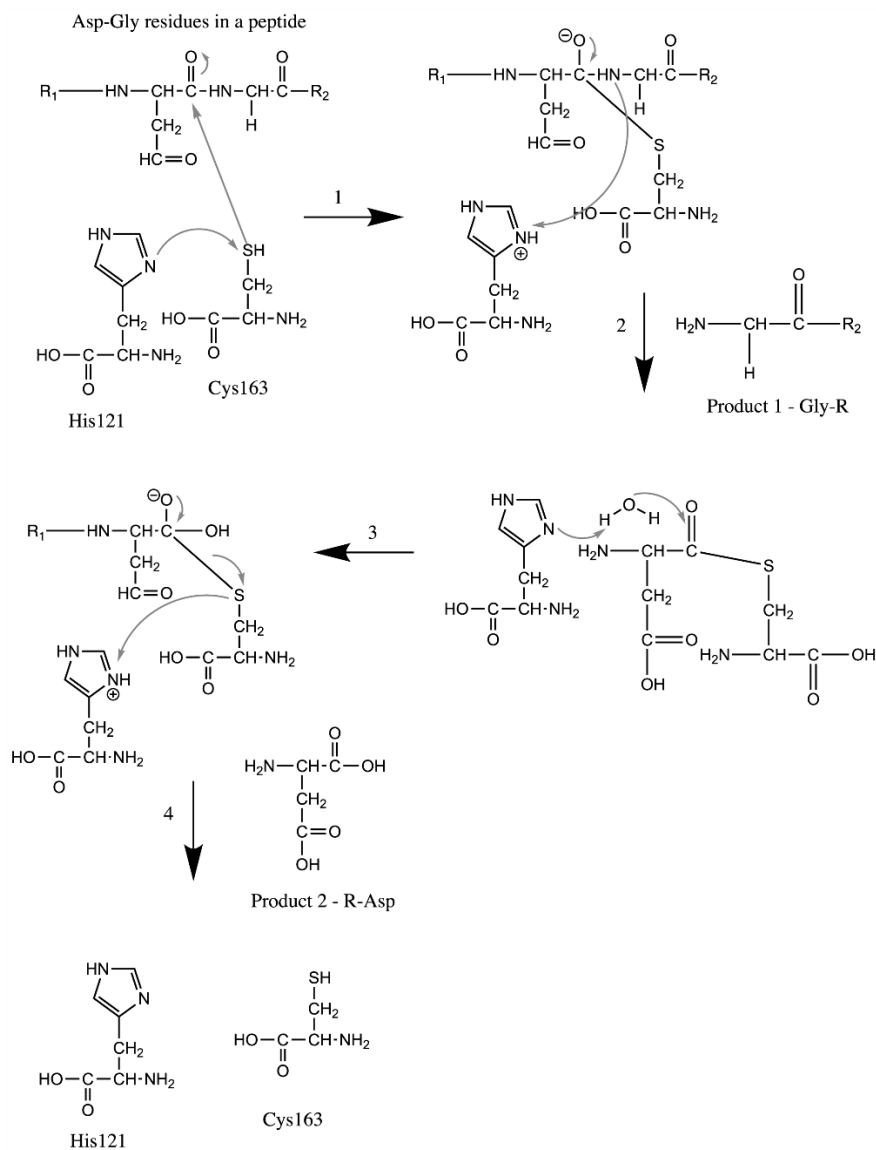
Fig. 1.3 Classic mechanism of cysteine protease cleavage. In this mechanism, the thiol from the catalytic cysteine (Cys163 in the case of caspase-3, as described in (1)) acts as a nucleophile to attack the peptide bond substrate., while the side chain of the catalytic histidine (His 121 for caspase-3) attacks the thiol. A Cys-Substrate intermediate then forms, where the substrate backbone nitrogen performs a nucleophilic attack on the newly positively charged His nitrogen. This allows the P1' residue to leave the complex, generating one cleavage products (R2), and regenerating the catalytic His. Following this, a water molecule serves as a nucleophile to the remaining portion of the Cys-Substrate intermediate (containing R1), and the catalytic his side chain attacks the water molecule. The catalytic cysteine sulfur attacks the newly positive His side chain, following which the second cleavage product (R1) is released, regenerating both catalytic residues and freeing the active site for a new substrate. Adapted from Clark, A.C. (2016)[138]

23
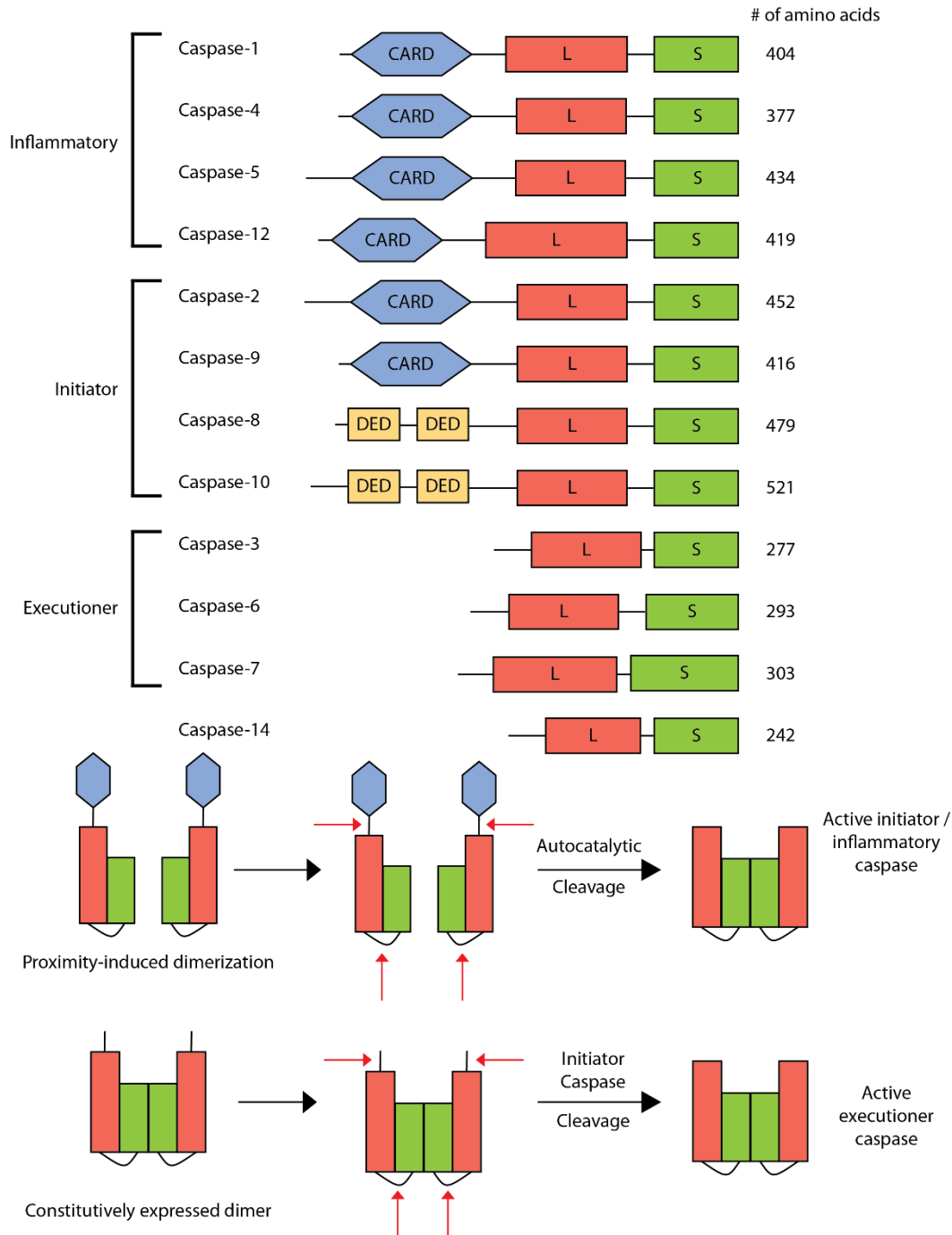
Fig. 1.4 Initiator, executioner and inflammatory caspases and their mechanisms of activation. A. Initiator and inflammatory caspases are synthesized as inactive monomers Upon dimerization of 2 monomers, they are activated through autocatalytic cleavage of their pro-domain (Death Effector Domain (DED) or Caspase Recruitment Domain (CARD)). **B.** Executioner caspases are synthesized as inactive dimers. They are activated by initiator caspase cleavage of their inter-subunit linkers. **C.** Inflammatory caspases are activated by recruitment to the inflammasome, leading to autocatalytic cleavage of their CARDs. Adapted from Shalini et al. (2015)[139]
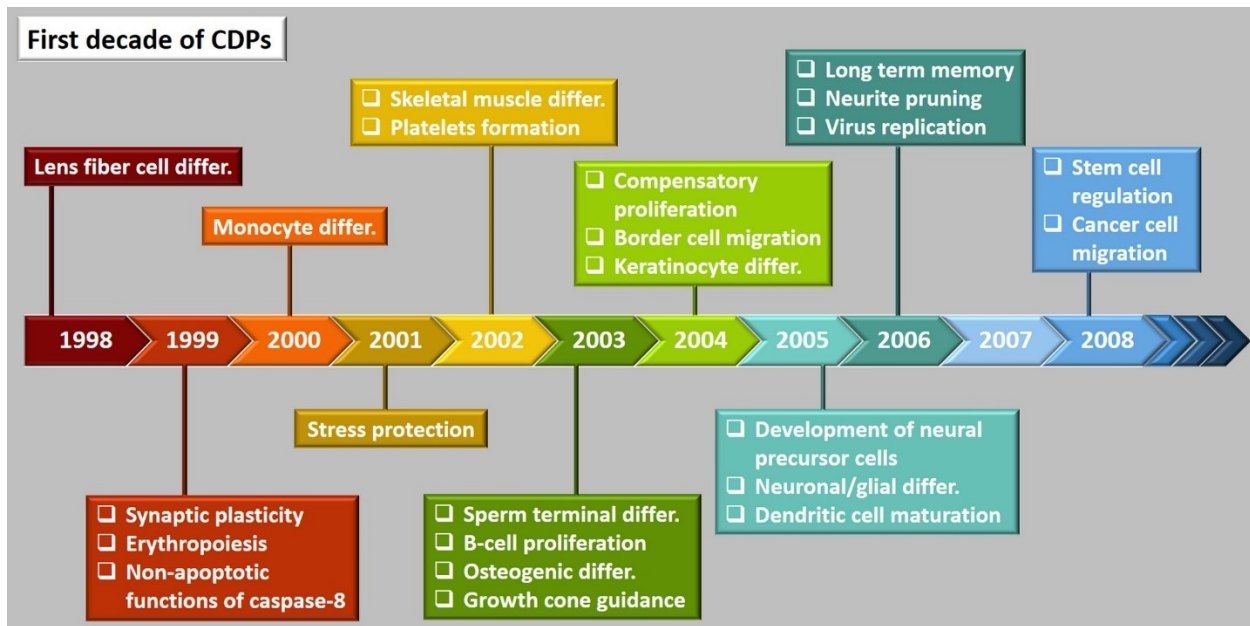
Fig. 1.5 Non-apoptotic roles of cell death proteins discovered from 1998-2008. A timeline of publications, first published in a report from a conference surrounding the topic of non-lethal roles of cell death proteins. This timeline compiles the first decade of non-apoptotic research in cell death proteins. In majority, the publications described above determined these non-apoptotic roles, mostly in mammalian cells. Starting from 1998, with the implication of caspase-3 in lens development[140,141] through to 2008, with the implication of caspases-3 and -8 in stem cell regulation[111,142,143] and caspase-3 in lung cancer cell migration[144]. In this time, there have also been non-apoptotic roles identified for cell death proteins in synaptic plasticity[145–147], erythropoiesis[148–151], non-apoptotic functions of caspase-8[152–158], monocyte differentiation[110,159,160], stress protection[161,162], skeletal muscle differentiation[108,163], platelet formation[164], sperm terminal differentiation[165–170], B-cell proliferation[171], osteogenic differentiation[172–174], growth cone guidance[175], compensatory proliferation[176–179], border cell migration[180], keratinocyte terminal differentiation[181], development of neural precursor cells[182,183], neuronal and glial differentiation[184–186], dendritic cell maturation[187], long-term memory[188], neurite pruning[189,190] and virus replication[191]. Reproduced under a Creative Commons License, created by Arama, Baena-Lopez & Fearnhead (2020)[192].
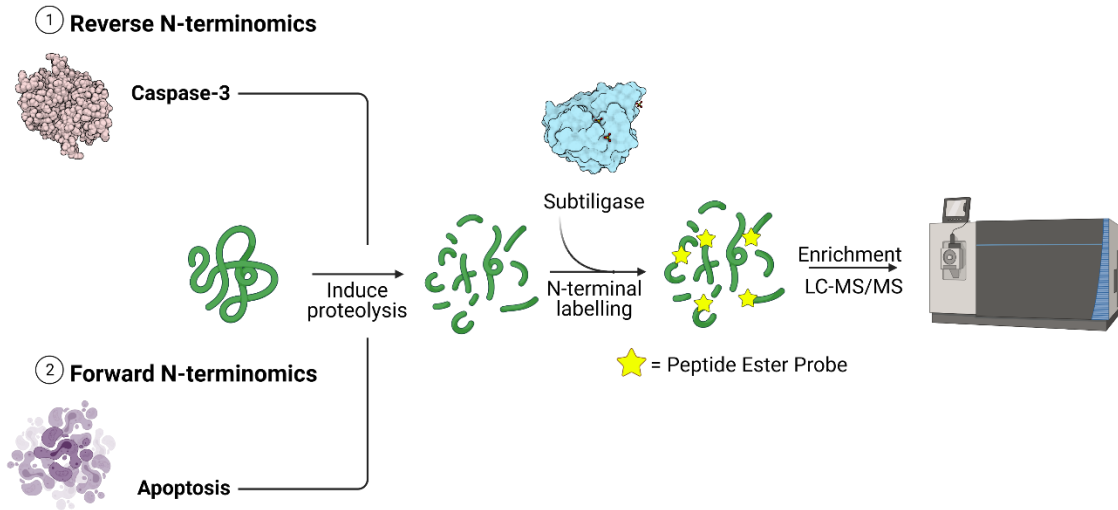
Fig. 1.6 *Forward* **and** *reverse* **N-terminomics.** The *forward* and *reverse* N-terminomics labeling experiments function similarly after the proteolytic cleavage sites are generated: Both experimental lysates are labeled at their newly generated N-termini with a peptide ester probe, mediated by subtiligase. These labeled N-termini are then enriched, trypsinized, and eluted, followed by LC-MS/MS analysis (see **Fig. 1.7** for more detail). In the *forward* experiments, the induction of a cellular process leads to endogenous protease activation, generating the observed cleavage products. The results are biologically relevant cleavages, though the identity of the protease responsible is unknown. Conversely, the *reverse* experiments the opposite is true. The cleaved products can be attributed to the added enzyme, but the biological relevance will need to be determined.
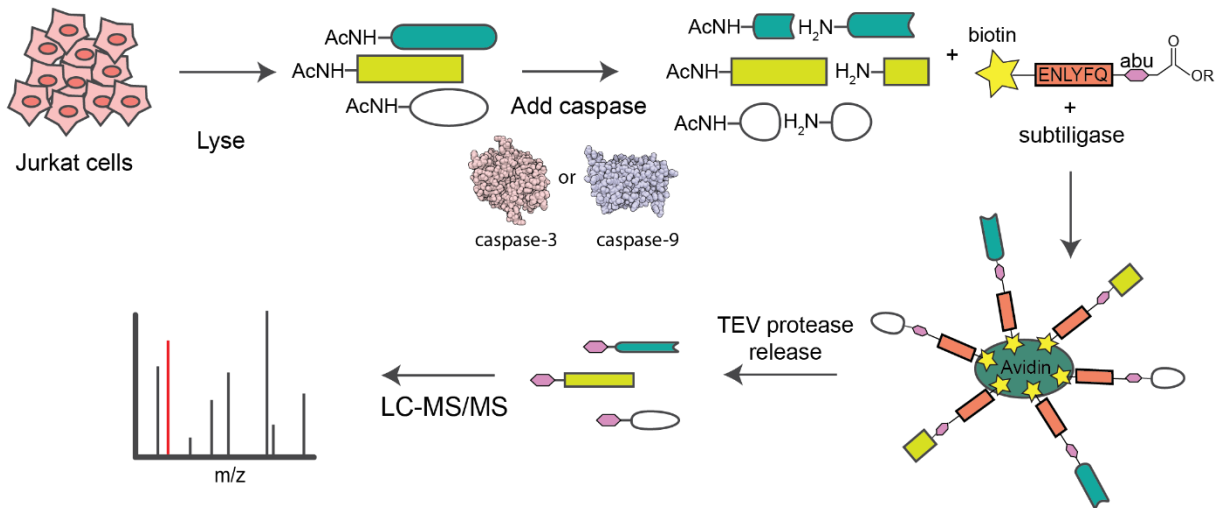
Fig. 1.7 Protease substrates identification using subtiligase N-terminomics. The method employed to identify protease substrates in this thesis is *reverse* subtiligase N-terminomics. In the *reverse* discovery, a protease of interest is added into an untreated lysate. The purified protease (in this case a caspase), is added to the lysate, which will generate caspase-specific cleavage events. The cells are then harvested and lysed, and the cleavage products are labeled with a biotin ester tag using subtiligase. The protein fragments are then enriched on neutravidin beads, digested, and released using a TEV protease site engineered in the biotin tag. This is followed by identification and quantification by tandem mass spectrometry, allowing the targets of a given protease and its sequence specificity to be defined.

Table 1.1 Optimal caspase peptide recognition sequence and protein consensus sequence for cleavage. Adapted from Table 1 of Julien, O. & Wells, J.A.[193]

Caspase	Peptide sequence	Protein sequence
-1	WEHD[77]	YVHD/FESD[103]
-2	DEHD[77]	XDEVD[65,98]
-3	DEVD[77]	DEVD[81]
-4	(W/L)EHD[77]	-
-5	(W/L)EHD[77]	-
-6	VEHD[77]	VEVD[65]
-7	DEVD[77]	DEVD[101]
-8	LETD[77]	XEXD[101]
-9	LEHD[77]	-
-10	WEHD[53]	LEHD[53]
-12	-	-
-14	WEHD[80]	HSED[67]

CHAPTER TWO
MATERIALS & METHODS

2.1 Protease DNA constructs

TEV Protease S219V (pRK793)[194,195] was a gift from David Waugh, and obtained from Addgene (plasmids 8827). The expression construct for WT caspase-3 (pET23b-Casp3-His)[196] was a gift from Guy Salvesen, and obtained from Addgene (plasmid 11821). The expression constructs for subtiligase expression (WT and M222A mutants used in *reverse* N-terminomics) were a gift from Drs Jim Wells and Amy Weeks[100]. Subtiligases were expressed and purified by Longxiang Wang, Bridgette Hartley and Shu (Lucy) Luo.

2.2 Transformations

DNA stocks ranged from 50-200 ng/µL. 2 µL of stock DNA was added to 50 µL competent BL21(DE3)pLysS and incubated for 15 minutes on ice. Then transformation was heat shocked by incubation in a 42°C water bath, followed by an incubation on ice for 2 minutes. 450 µL of LB was added to the cells, following which they were incubated at 37°C in a shaking incubator at 200 rpm for 1 hour. The cells were centrifuged at 1000 rpm for 5 minutes and most of the media removed, leaving 100 µL. Cells were resuspended in that 100 µL, which was plated in its entirety on LB agar plates with 100 µg/mL ampicillin and 12.5 µg/mL chloramphenicol. Plates were incubated overnight at 37°C and were stored at 4°C the following day.

2.3 Recombinant Caspase-3 purification and kinetics

2.3.1 Caspase expression and purification

Recombinant His-tagged caspase-3 was expressed in BL21(DE3) pLysS *E. coli*. One colony was added to 50 mL 2xYT media supplemented with ampicillin and chloramphenicol. The following morning, 25 mL of the starter culture was used to inoculate 3 L of 2xYT (Fisher Scientific) supplemented with 100 µg/mL ampicillin and 12.5 µg/mL chloramphenicol at 37°C until an O.D. of 0.6 was reached. We then induced expression for 5 h at 30°C using 0.3 mM IPTG (Fisher Scientific). Cells pellets were collected by centrifugation of the culture at 4,000 g for 20 minutes at 4°C. The supernatant was discarded and the pellet was frozen at -80°C. The following day, the pellet was thawed on ice and resuspended in 45 mL of Lysis buffer (100 mM NaCl and 100 mM Tris pH 8.0). Cells were lysed through high-pressure homogenization (Avestin Emusiflex C3), then centrifuged at 40,000 g for 45 minutes at 4°C. The clarified protein supernatant was passed through a 1-mL Ni^{2+} affinity column (Cytiva inc.), following which protein was eluted from the column using a linear gradient (Elution buffer: 500 mM NaCl, 20 mM imidazole and 100 mM Tris pH 8.0). The eluted protein purity was confirmed via SDS-PAGE. Eluted fractions were pooled

and buffer exchanged through size exclusion chromatography (HiLoad 16/600 Superdex 200 pg, Cytiva inc.), eluting in storage buffer (100 mM NaCl, 25 mM Tris pH 7.5, and 2 mM DTT). Fractions were assayed for DEVDase activity. The fractions with the highest activity were pooled and concentrated using a 10K MWCO filter spin concentrator (Cytiva inc.)

Recombinant caspase-9[114] used in *reverse* N-terminomics was expressed, purified and characterized by Ishankumar Soni. The DNA plasmid encoding caspase-9 was transformed into BL21(DE3) T7 express strain of *E. coli* (New England Biolabs), and plated on an LB-Agar dish to grow overnight at 37°C. A single colony was picked and transferred into a flask containing 50 mL LB media (Research Products International). This media was incubated at 37°C overnight to grow a seed culture. The next day, 1 mL of the seed culture was diluted one thousand times into 1 L of LB media containing 0.1 mg/mL ampicillin (Fisher BioReagents). This culture was incubated at 37°C until the desired O.D. of 1.0 was reached. IPTG (GoldBio) was added to a final concentration of 1 mM to induce expression, while also lowering the growth temperature to 25°C. Expression was performed for 4 hours. The culture was centrifuged at 5000 g for 7 minutes at 4°C, and cell pellets were collected and stored at -80°C until their use for purification. The frozen pellet was thawed and diluted in 200 mL of lysis buffer (50 mM Sodium Phosphate pH 7.0, 300 mM NaCl, 5% glycerol, and 2 mM Imidazole). Cells were lysed using a microfluidizer (Microfluidics, Inc.), and cell lysate was separated from the cell debris by centrifugation at 50,000 g for 1 hour at 4°C. Cell lysis was purified using a Hi-Trap^{TM} chelating HP column charged with Ni^{2+} (Cytiva inc.). Protein was subjected to a linear gradient (0 to 33% of elution buffer) using an elution buffer (50 mM sodium phosphate, pH = 7.0, 300 mM NaCl, 5% glycerol, and 300 mM Imidazole). Eluted protein was diluted 5 times using buffer A (20 mM Tris pH 8.5, 5% glycerol, and 2 mM DTT). Then, for further purification by anion exchange chromatography, protein was applied to Hi-Trap^{TM} Q HP column (Cytiva inc.). The column was washed and then developed with a linear gradient (0 to 30% of buffer B: 20 mM Tris pH 8.5, 1 M NaCl, 5% glycerol, and 2 mM DTT). Purity and concentration of purified caspase-9 were assessed using SDS-PAGE. The most concentrated fractions were aliquoted to store at -80°C for further usage.

2.3.2 Caspase-3 kinetic assay

Purified caspase-3 was thawed on ice and diluted in activity buffer (10 mM HEPES pH 7.4, 50 mM KCl, 1.5% sucrose, 0.1% CHAPS, 10 mM DTT) to 20 nM and 2 nM, from a 5 µM stock. Ac-DEVD-Afc probe was diluted from 5 mM stocks to 50 µM in activity buffer, followed by serial

dilution to generate several probe concentrations in a 96-well plate: These were all conducted to a final volume of 50 µL. Caspase-3 solution was added at a 1:2 dilution factor which generated final probe concentrations from 25 µM to 24 nM in stepwise serial dilutions, and final enzyme concentrations of 10 nM and 1 nM. Fluorescence assay was conducted for 1 hour to monitor DEVDase activity (Excitation: 400 nm/ Emission: 505 nm). Following this, the catalytic efficiency (k_{cat}/K_m) was determined using the assays at both enzyme concentrations, using the relative fluorescence of complete substrate cleavage.

2.4 TEV protease purification and PILS experiment

2.4.1 TEV protease purification

Recombinant His-tagged TEV Protease S219V mutant was expressed in BL2DE31pLysS. 1 colony was added to 8 mL 2xYT media supplemented with ampicillin and chloramphenicol. The following morning, 4 mL of the starter culture was used to inoculate 3 L of 2xYT (Fisher Scientific) supplemented with 100 µg/mL ampicillin and 12.5 µg/mL chloramphenicol at 37°C until an O.D. of 0.6 was reached. We then induced expression overnight at 25°C using 0.3 mM IPTG (Fisher Scientific). Cells pellets were collected by centrifugation of the culture at 4,000 g for 20 minutes at 4°C. The pellet was resuspended in 45 mL of Lysis buffer (1X PBS + 10 mM imidazole + 500 mM NaCl + 2 mM BME). Cells were lysed through high-pressure homogenization (Avestin Emusiflex C3), then centrifuged at 40,000 g for 45 minutes at 4°C. The clarified protein supernatant was passed through a 1-mL Ni^{2+} affinity column (Cytiva inc.), following which protein was collected off the column using a linear elution gradient (Elution buffer: 1X PBS, 500 mM imidazole, 100 mM NaCl, 2 mM BME, 10% glycerol). The eluted protein purity was confirmed via SDS-PAGE, then pooled. As precipitation is common with TEV protease during its purification, precipitated protein was removed by centrifugation at 4000 g for 5 minutes. The supernatant soluble protein was buffer exchanged using an Econopac DG10 column (Bio-Rad), eluting in storage buffer (25 mM Tris pH 7.5, 100 mM NaCl, 1 mM EDTA, 10% glycerol, 2 mM DTT). Following this, fractions were pooled and centrifuged at 4000 g for 5 minutes again, to remove more precipitated protein. Protein concentration was determined using a Bradford protein assay (Bio-Rad) and A280 (MW 28.6 kDa, E/1000= 31.97). Protein was supplemented with 10% glycerol, divided into aliquots and flash-frozen in liquid nitrogen, followed by storage at -80°C.

2.4.2 *E. coli* lysate streptavidin labeling test

Performed by Erik Gomez-Cardona, following protocols in Weeks & Wells[100]. The XL10 *E. coli* lysate was generated as follows: XL10 cells were plated onto LB-Agar and incubated overnight

at 37°C. The following day, 1 colony was placed into 50 mL 2xYT media and incubated overnight at 37°C while shaking at 200 rpm. The next day, cells were harvested by centrifugation at 4000 g for 15 minutes at 4°C. The cell pellet was then resuspended in 50 mL lysis buffer (10 mM pH 7.4 bicine, 1 mM PMSF and 10 mM EDTA) and incubated on ice in the dark for 15 minutes. The cells were then lysed by probe sonication at 30% amplitude in 2 second on and 2 second off intervals for a total of 1 minute. Following this, the lysate was incubated on ice in the dark for another 15 minutes. DNA was precipitated by dropwise addition of 10% (w/v) streptomycin sulfate to a final concentration of 1% (w/v), and removed by centrifugation at 10,000 g for 20 minutes at 4°C. The protein concentration was determined using a Bradford assay (Bio-Rad), and adjusted to a final concentration of 2 mg/mL. DTT was added to a final concentration of 25 mM, and the pH was adjusted to 8.5 using 1 M bicine pH 9.2. The labeling test and subsequent PILS experiment were performed on a total of 2 mg of protein.

The labeling protocol for the *reverse* N-terminomics experiment (see 2.7.4) was followed until the ACN precipitation. 50 μL pre-and post-labeling samples were collected for the labeling test blot. After the pellet was air-dried, it was resuspended in 1.5 mL TEV protease buffer (100 mM ammonium bicarbonate pH 8.0, 2 mM DTT, and 1mM EDTA). After nutation at room-temperature for 1 hour, excess non-dissolved proteins were removed by centrifugation, splitting the supernatant into 2 Eppendorf tubes after collecting a 50 μL pre-cleavage sample. In one tube, 25 μg of the newly purified TEV protease was added, and in the other 25 μg of previous TEV stock in the lab was added. Both tubes were nutated overnight at room temperature. 50 μL post-cleavage samples were collected the following day from each tube. The streptavidin blot was then completed using all the samples, using the same procedure as for *reverse* N-terminomics (see **2.7.4**) 10 μL each of the pre- and post-labeling samples, and 15 μL each of the pre- and post-cleavage samples were loaded onto the SDS-PAGE gel used for the blot.

2.4.3 Proteomic identification of ligation sites (PILS) experiment

Performed by Erik Gomez-Cardona, following the N-terminomics protocol described in **2.7.4**, without the addition of recombinant caspases.

2.5 TEVest6 peptide ester tag synthesis

Performed by Erik Gomez-Cardona. The structure of the TEVest6 probe contains a biotin tag, followed by a linker region (two Glu), the substrate recognition sequence for the TEV protease (Glu-Asn-Leu-Tyr-Phe-Gln), a mass tag (Abu), an ester group and a single Arg residue after the ester that functions as a leaving group (**Fig. 2.1**).

The tag was synthesized by solid phase synthesis, using an Fmoc-mediated chemistry. The sequence was synthesized from the C- to the N-terminus. 1 g of Rink Amide AM resin (0.89 mmol/g) was transferred to the reaction cartridge (Poly-Prep Chromatography Column, Bio-Rad) and 10 mL of DCM were added to a resin for swelling (30 minutes with constant mixing). The DCM was removed by vacuum filtration and the resin was washed three times with DMF, once with methanol, once with DCM and once with DMF (10 mL per wash).

The Fmoc-group was removed using 10 mL of 20% (vol/vol) piperidine in DMF. The resin and deprotection solution were gently agitated for 30 minutes. Afterwards, the solution was removed by vacuum filtration and the resin was washed five times with DMF (10 mL per wash). After washing, a Kaiser test (ninhydrin test) was performed to confirm the removal of the Fmoc-group. The Kaiser test reagents were prepared according to AAPPTec recommendations: For Reagent A, 16.5 mg of potassium cyanide (KCN) was dissolved in 25 mL of distilled water. A 1:50 dilution was prepared in pyridine. For Reagent B, 1 g of ninhydrin was dissolved in 20 mL of butanol. For Reagent C contains 20 g of phenol was dissolved in 10 mL of n-butanol. A few beads were transferred to a 1.5 mL Eppendorf tube three drops of each reagent were added. The mixture was heated for 5 minutes at 95°C in a heating block. The presence of a blue colour (positive test) indicates deprotection of the resin, while a yellow colour (negative test) indicates protection. For this deprotection step a positive test result was required to continue.

The loading of the first residue (Arg) was carried out for 2 hours using the Fmoc-Arg(Pbf)-OH version of that residue (4.45 mmol, 5 equivalents), HOBt (4.45 mmol, 5 equivalents) and DICI (4.45 mmol, 5 equivalents) in 8 mL of DMF. Following this Fmoc-group removal was performed for 15 minutes using 20% (vol/vol) piperidine in DMF (1.6 mL of piperidine in 6.4 mL of DMF). Five 8-mL DMF washes were then performed. The completion of the reaction was monitored with a Kaiser test (positive result needed to proceed).

The formation of an ester group in the sequences started with the addition of acetoxyacetic acid (4.45 mmol, 5 equivalents) using HOBt and DICI at the concentrations previously mentioned in 8

34

mL of DMF. This step was carried out for 2 hours. After complete addition (confirmed by a negative Kaiser test), the resin was treated with 10 mL of 2.5 M hydrazine monohydrate overnight with constant mixing. The next day at the end of the reaction, five DMF washes were performed. The ester was formed by addition of Fmoc-Abu-OH (3.56 mmol, 4 eq) to the resin using DMAP (3.56 mmol, 4 equivalents) and DICI (3.56 mmol, 4 equivalents) in 8 mL of DMF for 2 hours with constant mixing. Five DMF washes were done at the end of this step.

The following addition steps for the protected residues were done for 90 minutes with constant mixing using the Fmoc-protected version of each residue (4.45 mmol, 5 equivalents), HOBt (4.45 mmol, 5 equivalents) and DICI (4.45 mmol, 5 equivalents) in 8 mL of DMF. The completion of the reaction was monitored with a Kaiser test. If the reaction was not complete after 90 minutes, a second round of addition was performed for 30 minutes using 3 equivalents of the reagents. Before loading the next residue in the sequence, deprotection of the resin was performed as previously described.

After the final deprotection, Biotin was added to the N-termini with 9 mL of the biotin loading mixture (Biotin: 2.67 mmol, 3 equivalents dissolved in 6 mL of DMSO, and DICI/HOBt: 2.67 mmol, 3equivalents dissolved in 3 mL of DMF) for 90 minutes with constant mixing. The addition was repeated 3 times, the final product formation monitored by MALDI and a Kaiser test (negative result). Once the Kaiser test was negative and the correct mass was detected on MALDI, the resin was washed five times with 8 mL of DMF and three times with 8 mL of DCM. The resin was dried by vacuum filtration for 1 hour.

Cleavage of the final product was carried out for 2 hours with constant mixing with 10 mL of the cleavage solution (TFA/H_2O/Tripropylsilane at 95:2.5:2.5% vol/vol/vol). The solution was recovered, and the beads were washed with 5 mL of the cleavage solution. Both fractions were combined and concentrated using a Rotavap to a final volume of 5 mL. The solution was recovered and precipitated in 40 mL of cold Diethyl ether for 1 hour. The tube was spun down at 8000 g for 20 minutes. The pellet was washed twice with 40 mL of cold ether, ensuring that the pellet resuspends in solution. After the washes, the pellet was air dried and resuspended in 5-10 mL of ACN/H_2O (50/50% vol/vol) and lyophilized until fully dry. The purity of the substrate was confirmed by MALDI-TOF (Autoflex speed MALDI-TOF, Bruker). The final TEVest6 probe was dissolved in DMSO at a 50 mM stock concentration, aliquoted and stored at -80°C.

2.6 Jurkat cell culture

Jurkat cells were used for caspase-3 experiments, while Jurkat JMR (caspase-9 knockout) were used for caspase-9 experiments[197]. Jurkat and Jurkat JMR cell pellets were thawed from frozen stocks and grown in RPMI cell culture media (Gibco), supplemented with 10% fetal bovine serum (Sigma inc.), 100 µg/mL penicillin/streptomycin (Gibco) and 2 mM L-glutamine (Gibco). Cells were grown at 37°C, passing stepwise from growing in culture dishes to 4 L spinner flasks. Cells were harvested by centrifugation at 800 g for 5 minutes, washed with cold PBS and centrifuged again at 800 g for 5 minutes. Pellets were kept frozen at -80°C until required for *reverse* N-terminomics experiments.

2.7 Subtiligase-based *reverse* N-terminomics

2.7.1 Caspase-3 *reverse* N-terminomics lysate preparation.

7.5×10^8 harvested Jurkat cells were thawed on ice and resuspended in lysis buffer (5 mM EDTA, 1 mM PMSF, 4 mM IAM, 1 mM AEBSF and 0.1% Triton X-100 in 100 mM HEPES pH 7.4). Sample was incubated for 45 minutes in the dark at room temperature, then sonicated using a probe tip sonicator at 20% amplitude, 2 seconds on 5 seconds off for 5 minutes. 20 mM DTT was added to quench the IAM, to retain the activity of the caspase-3 that is added subsequently. Total protein concentration in the cell lysate was determined to be 7 mg/mL using a Bradford assay kit (Bio-Rad Laboratories). The lysate was centrifuged for 10 minutes at 4,000 g to remove cell debris. A concentrated caspase activity buffer (10x) was added to the lysate (for final concentrations of 10 mM HEPES pH 7.4, 50 mM KCl, 1.5% sucrose, 0.1% CHAPS, and 10 mM DTT). Lysates were incubated with 0.5 µM caspase-3 in the dark at room temperature for 2 hours and assayed for DEVDase activity. After 2 hours had elapsed, enzyme activity was irreversibly inhibited by treating with 100 µM z-VAD-fmk which quantitatively blocks the function of all caspases. We then proceeded with N-terminomics labeling (see below).

2.7.2 Caspase-9 *reverse* N-terminomics lysate preparation.

Performed by Ishankumar Soni (UMass Amherst). 5×10^8 Jurkat JMR cells were cultured and harvested. To lyse the cells, we directly suspended the cell pellet (without freezing) in a lysis buffer (100 mM HEPES pH 7.4, 5 mM EDTA, 1 mM PMSF, 4 mM IAM, 1 mM AEBSF, 25 µM Ac-DEVD-fmk, and 0.1% Triton X-100), and then incubated on ice in the dark for 30 minutes. Total protein concentration in the cell lysate was determined to be 10 mg/mL using a BCA assay kit

(ThermoFisher Scientific). We added 20 mM of DTT to the cell lysate to quench the IAM. The lysate was centrifuged for 10 minutes at 4,000 g to remove cell debris. A concentrated caspase-9 activity assay buffer (for final concentrations of 100 mM MES, pH = 6.5, and 10 mM DTT) was added to the lysate, following which 8 μM purified caspase-9 was added. Lysates were incubated with caspase-9 in the dark at room temperature for 4 hour and assayed for LEHDase activity. Then, the enzyme activity in treated lysates was irreversibly inhibited by treating with 100 μM z-VAD-fmk. We stored this sample at -80°C for the further usage in *reverse* N-terminomics.

2.7.3 Caspase-3 and -9 *reverse* N-terminomics.

Lysates were incubated with 1 mM TEVest6 biotin peptide ester tag[42] and subtiligase (1 μM wild-type and 1 μM M222A mutant)[100] for 2 hours. Labeling was monitored by immunoblot using a streptavidin IRDye 800CW (LI-COR inc.) (see **2.7.4**). Protein was precipitated in acetonitrile at -20°C overnight. The precipitate was recovered by centrifugation at 12,000 g, resuspended in 8 M guanidine hydrochloride and boiled with 100 mM tris(2-carboxyethyl)phosphine (TCEP) for 15 minutes. Once cooled, resuspension was treated with 4 mM IAM and incubated in the dark for 1 hour. The sample was then reduced with 20 mM DTT and precipitated in ethanol (100 proof) at -80°C overnight. The following morning, the precipitate was recovered by centrifugation and resuspended in 8 M guanidine hydrochloride, which was diluted to 4 M with water once the precipitate was dissolved. Neutravidin agarose beads were added to the resuspension and incubated overnight at room temperature on a rotator. Capture efficiency was measured by dot blot using the same streptavidin IRDye 800CW (see **2.7.5**). When a 90% capture efficiency was observed, the beads were washed with a biotin wash solution (1 mM biotin, 10 mM bicine pH 8.0), then washed with 4 M guanidine hydrochloride, then washed and resuspended in a trypsin buffer (100 mM bicine pH 8.0, 200 mM NaCl, 20 mM CaCl₂, and 1 M guanidine hydrochloride). 20 μg trypsin (Promega) was added and incubated overnight at room temperature on a rotator. The next day, the trypsin in buffer was washed from the beads using 4 M guanidine hydrochloride. The neutravidin beads were then resuspended in Tobacco Etch Virus (TEV) protease buffer (100 mM ammonium bicarbonate pH 8.0, 2 mM DTT, and 1mM EDTA). 65 μM TEV protease was added to the resuspension before they were incubated overnight at room temperature on a rotator. The next day, the supernatant was recovered and dried on a Genevac® solvent evaporator (SP Scientific). When dry, the samples were resolubilized in 5% trifluoroacetic acid (TFA) and incubated for 10 minutes at room temperature to precipitate the TEV protease. Samples were centrifuged and the supernatant was desalted using C18 desalting resin tips (PureSpeed Rainin). The eluted solution from the desalting was dried on a Genevac®.

2.7.4 *Reverse* N-terminomics labeling western blot

Western blotting was used to verify subtiligase labelling of lysates. Using a prepared 10% acrylamide SDS-PAGE gel, electrophoresis of pre- and post-subtiligase labeled lysates was performed at 180V for 40 minutes. The resulting gel was transferred onto a PVDF (Polyvinylidene fluoride) membrane (Cytiva inc.) using a Mini Trans Blot® wet transfer apparatus (Bio-Rad), transferring for 75 minutes at 35 V, using Towbin's transfer buffer (25 mM Tris base, 192 mM glycine, pH 8.3). The transferred membrane was then blocked for 45 minutes at room temperature on an orbital shaker with a 10% fish skin gelatin buffer. Following this, a fluorescent streptavidin antibody (Li-Cor Biosciences) was added at a 1:10 000 dilution in the same 10% fish skin gelatin buffer and incubated at room temperature for 1 hour at room temperature. The membrane was then washed 3 times in 1X TBST (Tris-buffered saline, 0.1% Tween-20) prior to visualizing at 2 minutes exposure each for 680 nm (for protein ladder) and 800 nm channels (Li-Cor Odyssey Fc).

2.7.5 *Reverse* N-terminomics streptavidin capture dot blot

To confirm that labeled proteins were successfully captured onto avidin beads, pre- and post-avidin capture samples from *reverse* N-terminomics were diluted 1:10 and 1:20 in water. 2 μL of each sample was dotted onto a nitrocellulose membrane and allowed to dry for 1 minute. Once dry, membrane was treated like a western blot – see **2.7.4**

2.8 *Reverse* N-terminomics immunoblotting investigation

2.8.1 Sample preparation for immunoblotting.
Performed by Ishankumar Soni (UMass Amherst). For the cleavage assays using recombinant caspase-3 and -9, the same procedure was used to prepare the samples for immunoblotting as for *reverse* N-terminomics. After the incubation with the respective caspase (or only buffer A without caspase as a control) and addition of z-VAD-fmk, we added 1xSDS blue loading dye (New England Biolabs) and denatured the samples by heating at 90°C for 10 minutes. Samples were aliquoted and stored at -80°C until the further usage.

For staurosporine (STS) induced apoptosis assays, we treated Jurkat cells (5×10^7) with either 0.5 μM of STS or DMSO (control). We incubated these cultures at 37°C for 3 hours to induce apoptosis. Then, we lysed cells following the same protocol as for N-terminomics. At last, we added 1xSDS blue loading dye (New England Biolabs) and denatured the samples by heating at 90°C for 10 minutes. These samples were also aliquoted and stored at -80°C until further usage.

2.8.2 Immunoblotting analysis

Performed by Ishankumar Soni (UMass Amherst). The samples were thawed, and the proteins separated by molecular weight using gel electrophoresis. A 12% SDS-PAGE gel was used for RECQL5, GSDMD, MFN2, PAK2, PARN, and ATXN2L and a 16% SDS-PAGE gel for NUP43, RNF126, RNF4, and RING1. The proteins were transferred from the SDS-PAGE gel to an Immobilon-P PVDF membrane (MilliporeSigma). These membranes were washed five times with TBST over a period of 30 minutes. The membranes were then blocked using OneBlock™ Western-CL Blocking Buffer (Genesee Scientific Corporation) at 4°C for 1 hour. Primary antibody solutions were prepared as follows: RECQL5 [ThermoFisher Scientific (PA5-56315); final concentration: 0.1 µg/mL], NUP43 [ThermoFisher Scientific (A303-976A); 1:5000 dilution], RNF126 [abcam (ab183102); 1:700 dilution], GSDMD [MilliporeSigma (G7422); 1:1000], MFN2 [abcam (ab205236); 1:5000 dilution], RNF4 [R&D Systems (AF7964); final concentration: 1 µg/mL], PAK2 [Cell Signaling Technology (2608); 1:5000 dilution], PARN [abcam (ab188333); 1:5000 dilution], ATXN2L [Proteintech Group, Inc. (24822-1-AP); 1:5000 dilution], and RING1 [Cell Signaling Technology (13069); 1:5000 dilution] into 10 mL of blocking buffer. After removing the blocking buffer from the membranes, they were incubated with primary antibodies solutions at 4°C overnight. The next day, the membranes were washed five times with TBST over a period of 30 minutes and subsequently incubated with secondary antibodies: RNF4, rabbit anti-goat IgG HRP antibody [R&D Systems (HAF017); 1:10,000 dilution], and for all the other antibodies, goat anti-rabbit IgG H L HRP [Genesee Scientific Corporation (20-303); 1:10,000 dilution]. The incubation for secondary antibodies was performed for 1 hour, and then the membranes were washed five times using a TBST buffer over the period of 30 minutes. At last, the signal was detected using a SuperSignal™ West Dura Extended Duration Substrate kit (ThermoFisher Scientific). The images of immunoblots were taken using ChemiDoc™ MP imaging system (Bio-Rad Laboratories) and analyzed using Image Lab software (Bio-Rad Laboratories). GAPDH protein levels were used as loading control. Each membrane was stripped by incubating with a mild stripping buffer (1.5% glycine pH 2.2, 0.1% SDS, and 1% Tween 20) for 10 minutes. The membranes were washed twice with PBS, then twice with TBST and incubated with GAPDH primary antibody [ThermoFisher Scientific (MA5-15738); 1:5000 dilution], and secondary antibody, goat anti-mouse IgG H L HRP [Genesee Scientific Corporation (20-304); 1:10,000 dilution], as described above.

2.9 C2C12 culture and differentiation

C1C12 cells[198] were thawed from liquid nitrogen and cultured in Growth medium: Dulbecco's modified eagle medium (DMEM) supplemented with 10% FBS, 1X penicillin/streptomycin and 0.2X L-glutamine. For maintenance, cells were passaged when they reached 60% confluency, determined visually using a cell imager (Life Technologies). To passage the cells, culture dishes were rinsed in PBS, then incubated for 5 minutes at 37 °C in 0.05% Trypsin-EDTA (Gibco, prepared as a 1:10 dilution from 0.5% in PBS) to detach. Once detached, tryspin was diluted in an equal volume of DMEM. Trypsinized cells were centrifuged at 500 g for 5 minutes, following which the DMEM-tryspin mix was aspirated. Cells were resuspended in fresh Growth medium and plated in a new culture dish, then incubated at 37 °C and 5% CO_2.

To differentiate C2C12 cells to myotubes, C2C12 cells were grown to confluency, following which DMEM was aspirated from culture dish, rinsed with PBS and replaced with Differentiation medium: DMEM supplemented with 2% Horse Serum, 1X penicillin/streptomycin and 0.2X L-glutamine. To monitor effects of caspase-3 inhibition on differentiation progress, z-DEVD-FMK(OME) was added at 20 µM to one dish. Media was exchanged daily into fresh Differentiation medium for 3 days. The culture dish being monitored for caspase-3 inhibition was treated to fresh 20 µM cell-permeable DEVD-FMK(OME) daily. On the fourth day, Differentiation medium was aspirated from cells and culture dish was rinsed with PBS. Following the rinse, a Versene solution (prepared in-lab: 0.5 mM EDTA in PBS) was added to cells and incubated at 37 °C for 10 minutes or until cells detached. Once detached, Versene was diluted in an equal volume of DMEM. Detached cells were centrifuged at 500 g for 5 minutes, following which the DMEM-Versene mix was aspirated. Cells were then resuspended in cold (4°C) PBS to rinse any remaining DMEM, then centrifuged at 800 g for 5 minutes. PBS was aspirated and the pellets were stored at -80°C (**Fig 2.2**).

2.10 C2C12 lysis and in-gel digest

Cell pellets were thawed on ice and resuspended in lysis buffer (8 M urea, 100 mM Tris pH 8.5, 1 mM AEBSF, 5 mM EDTA, 1 mM PMSF, 4 mM IAM, 2 % SDS). Cells were lysed by probe sonication at 40% amplitude, 2 seconds on and 2 seconds off for 2 minutes. Lysates were centrifuged at 17,500 g for 10 minutes and the supernatant was recovered in a new tube. A BCA assay (Thermo Fisher) was conducted to determine protein concentration, following which the concentrations were standardized across samples through buffer dilution. 20 ug of lysate was used for each experiment. Samples were then diluted 1:4 in 4X loading dye (250 mM Tris pH 6.8,

8% SDS, 0.2% bromophenol blue, 20% glycerol, 20% β-mercaptoethanol [BME]). Using a precast 4-20% acrylamide SDS-PAGE gel (Bio-Rad), electrophoresis of undifferentiated, differentiated and DEVD-fmk-treated lysates was performed at 180V for 40 minutes. The resulting gel was incubated in fixing solution (50% EtOH, 2% phosphoric acid) for 20 minutes, following which the gel was washed in water twice, for 20 minutes per wash. The gel was then incubated in blue-silver staining solution (10% phosphoric acid, 20% ethanol, 756 mM ammonium sulphate, 1.4 mM Coomassie Blue G-250) overnight. The following morning the gel was rinsed twice in water, for 10 minutes per wash.

For the in-gel digest, each gel lane was divided into 5 fractions. A stamp gel cutter was used to cut each lane into 1 mm x 4 mm strips, following which the gel strips were further cut into 1 mm x 1 mm cubes using a razor blade. The cut gels were placed into wells of a round-bottom 96-well plate containing 175 μL destaining solution (1:1 100 mM NH_4HCO_3: ACN). The plate was incubated at 37 °C for 10 minutes. Afterwards, the destaining solution was replaced with fresh solution, to repeat the destaining at 37 °C for 10 minutes. Typically, 4-5 destaining rounds was required to remove all traces of Coomassie dye from the gel pieces. After the final destaining solution was discarded from the plate, 175 μL of 100% ACN was added to each well and incubated at 37 °C for 10 minutes, to begin dehydrating the gel pieces. Afterwards, the ACN was removed, and the plate was incubated at 37 °C for 15 minutes to dry the wells. Once dry, 175 μL of reduction solution (prepared as 8 μL BME in 100 mM) was added to each well, followed by incubation at 37 °C for 30 minutes. Following this, excess reduction solution was removed from the wells, and 175 μL of alkylation solution was added to the wells (prepared as 10 mg/mL IAM in 100 mM NH_4HCO_3). The 96-well plate was incubated at 37 °C for 30 minutes again, following which excess alkylation solution was discarded from the wells. After alkylation, the gel pieces were washed twice with 175 μL of 100 mM NH_4HCO_3 into each well, incubating for 10 minutes at 37 °C for each wash. After washing, the gel pieces were dehydrated for a second time, repeating the ACN-drying steps from earlier. Once the gel pieces had dried and excess ACN solution had evaporated, 75 μL of digestion buffer (prepared as 20 μg lyophilized trypsin (Promega) in 3.3 mL of 50 mM NH_4HCO_3) was added to each well, to digest overnight (~1 hour after trypsin buffer addition, samples were checked to ensure that there remained excess solution after the gel pieces swelled and absorbed liquid – if there was not extra liquid, 50 μL 50 mM NH_4HCO_3 was added to the dry wells). The following day, the liquid from the round-bottom plate was transferred to an MS V-bottom plate. Following this, 75 μL extraction solution (prepared as 2% formic acid and 2% ACN in water) was added to the gel pieces and incubated for 1 hour at 37 °C, to extract shorter & hydrophilic peptides. After the incubation, the liquid was transferred to the same MS V-bottom

plate, and the gel pieces were then extracted a second time, using 75 μL of 2nd extraction solution (1:1 1st extraction solution: 100% ACN) and incubating for 1 hour at 37 °C, to extract longer & more hydrophobic peptides. After the extraction, the liquid was also transferred to the same MS V-bottom plate. The MS V-bottom plate was then dried using a Genevac® and stored at -80 °C until resolubilized for mass spectrometry. (**Fig 2.2**)

2.11 Mass spectrometry

Dried samples were resuspended in 10 μL 0.1% formic acid. Peptides were analyzed using a nanoflow-HPLC (Thermo Scientific EASY-nLC 1000 system) coupled to a Lumos (Thermo Fisher Scientific) mass spectrometer. Peptides were eluted using a 120 minute 0 – 42% linear acetonitrile gradient, followed by elution with 80% acetonitrile. Data were analyzed using ProteinProspector (v5.22.1) software against the human proteome (2017-11-01 human proteome sequence downloaded from https://www.uniprot.org). Search parameters included non-tryptic cleavage at N-termini, missed trypsin cleavages, and precursor and mass tolerance, as detailed in Supplemental File S1 for each dataset. Variable modifications such as Carbamidomethylation of Cys, oxidation of Met, deamidation of Asn and Gln and addition of aminobutyric acid (abu) were searched as well. The TEVest6 biotin ester peptide tag contains an unnatural residue, Abu that is retained on labeled peptides following TEV protease cleavage of peptides from the neutravidin beads. Search parameters included a strict false discovery rate (FDR) of 5% for proteins, 1% for peptides. The maximum number of variable modifications was set to two. Data including peak lists are available on the MS-Viewer repository with search keys mdjft1fbxv (caspase-3, replicate 1), lltypq1rr0 (caspase-3, replicate 2), 65spzmus6p (caspase-9, replicate 1) and xcn4gexgdo (caspase-9, replicate 2). Raw files can be found in the massIVE repository: MSV000087447 (caspase-3, both replicates), MSV000087448 (caspase-9, both replicates).

For the C2C12 in-solution digest, dried samples were resuspended in 20 μL 0.1% formic acid. Peptides were analyzed using the same mass spectrometer and acetonitrile gradient as above. Data were analyzed using ProteomeDiscoverer (v2.4) software (Thermo Scientific), using the SEQUEST program (Thermo Scientific) against the mouse proteome (2021-04-30 mouse proteome sequence downloaded from https://www.uniprot.org). The search parameters included only tryptic peptides, with a maximum of two missed trypsin cleavages, a precursor mass tolerance of 15 ppm and a fragment mass tolerance of 0.8 Da. Carbamidomethylation of Cys was searched as a static modification, and oxidation of Met and deamidation of Asn and Gln were once again searched as variable modifications. Other parameters included a strict false discovery

rate (FDR) of 0.01 using a decoy database, and a relaxed FDR of 0.05. A maximum number of variable modifications of 3 was set.

Volcano plots, heat maps and principal component analysis (PCA) plots were created in ProteomeDiscoverer (v2.4) (Thermo Fisher) to plot mass spectrometry results.

The volcano plots were created by comparing two experiments at a time: undifferentiated vs differentiated, DEVD-fmk-treated vs differentiated, and DEVD-fmk-treated vs undifferentiated for a total of 3 plots. A background t-test was then conducted. The protein abundance ratios were calculated directly from the grouped protein abundances. This experiment followed a non-nested design, so the median protein abundance value over 3 replicates was used as the grouped value. Following this, the abundance ratio was calculated as specified in the experiment design (in this case, differentiated/undifferentiated, DEVD-fmk/undifferentiated and DEVD-fmk/differentiated). These grouped abundances were then subjected to a background-based T-test. In this T-test, the significance of change (as demonstrated through the p-value) is related to how large the difference of a protein ratio is compared to the background. The T-test follows two assumptions. Firstly, that most proteins do not change in abundance between samples. Secondly, that the variability for proteins of similar abundance is the same. Using these two assumptions, the median change values for proteins of similar abundance was determined, allowing for the calculation of confidence intervals. These confidence intervals were then applied to proteins of interest at these similar abundances to determine statistical significance. High abundance proteins will have a "narrower" confidence interval, while low abundance proteins will have a "wider" confidence interval. Consequently, lower abundance proteins will need a larger ratio change to be considered statistically significant compared to a higher abundance protein. With increased replicates, the confidence intervals could be narrowed.

The heatmap was created by mapping the protein abundances across all replicates using a Euclidean distance function, followed by a complete linkage method. The Euclidean distance function computes the geometric distance between data points (in this case, the distance in protein abundance between replicates). Following this, the complete linkage method calculates the distance between two replicates as the greatest distance between any two objects in each replicate.

The PCA plot was created with the replicate protein abundances, with the principal components representing axes of maximal variation observed when plotting these replicate abundances.

Glu   Glu   Leu   Phe   Abu

Biotin   Glu   Asn   Tyr   Gln   Ester   Arg
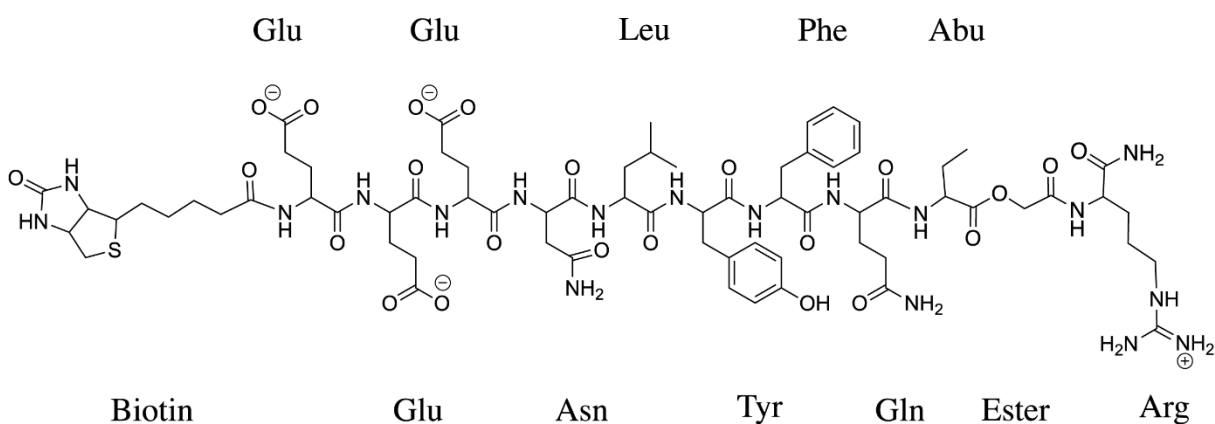
Chemical Formula: $C_{70}H_{100}N_{18}O_{23}S^{2-}$
Exact Mass: 1592.69
Molecular Weight: 1593.73

Fig. 2.1 TEVest6 peptide ester tag chemical structure. TEVest6 is a peptide ester tag containing several important features for its use in subtiligase-based N-terminomics. The ester group allows subtiligase, a peptide esterase, to label neo-N-termini with the tag. A biotin on the tag allows for the labeled peptides to be enriched using neutravidin beads. Following trypsinization on beads, the labeled peptides are cleaved from the beads using the TEV protease, taking advantage of a TEV protease cleavage site in the tag (Glu-Asn-Leu-Tyr-Phe-Gln). The eluted peptides will retain a nonstandard amino acid residue (aminobutyric acid – Abu) on their N-termini, allowing for unambiguous identification via LC-MS/MS. This tag was synthesized by Erik Gomez-Cardona.
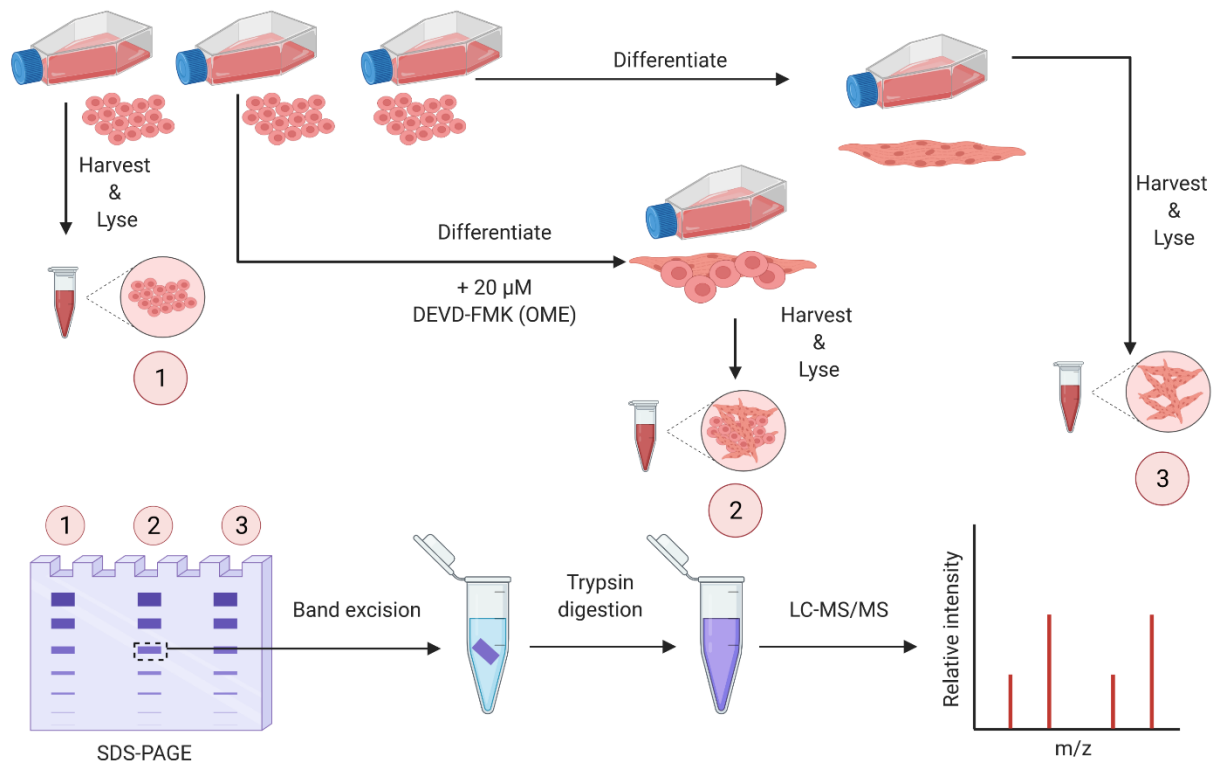
Fig. 2.2 Global proteomics workflow of C2C12 differentiation. C2C12 cells were thawed from frozen and cultured in 3 different conditions. Undifferentiated C2C12 cells were harvested, following which the unharvested C2C12 cells were made to differentiate to myotubes (through serum starvation – see Materials and Methods). The differentiation was performed under two conditions: one condition being the typical differentiation protocol, while the second condition was differentiation with the presence of 20 µM z-DEVD-fmk(OME), a cell-permeable caspase-3 inhibitor, which would work to prevent the caspase-3 dependent differentiation of C2C12. After differentiating, cells were harvested, lysed, and processed for LC-MS/MS using in-gel digestion.

CHAPTER THREE

RESULTS

3.1 TEV protease and caspase-3 purifications

3.1.1 TEV protease expression and purification

The TEV protease was expressed as a fusion construct with the Maltose Binding Protein (MBP) to aid in its solubility, and a 6xHis tag to allow for purification using a Ni^{2+} affinity column[194]. A TEV protease cleavage site is inserted in the construct between the two proteins so that when purified, the TEV protease can cleave the MBP and the two can be separated. After transforming the construct into BL21(DE3)pLysS *E. coli*, the protease was expressed in 1.5 L of Lennox LB overnight at 25°C, before harvesting the cells to lyse and purify (see **2.4.1**).

The 6xHis tag purification of the TEV protease was carried over a small elution volume (5 mL), which led to the retention of MBP in the final TEV aliquots (**Fig. 3.1**). Elution fractions A4 and A5 were pooled and subsequently buffer-exchanged into the final storage buffer. The concentration of the TEV protease was approximated by A_{280nm} using its extinction coefficient (E = 31970 $M^{-1}cm^{-1}$)[195] and molecular weight (28.6 kDa), to 6.7 mg/mL. However due to the MBP retention, a secondary indirect concentration measurement was used to correct the measurement. A Coomassie gel was used to conduct band intensity comparisons to previous TEV protease stocks in the laboratory (**Fig. 3.2**). This yielded a corrected measurement of 4.24 mg/mL for the final TEV protease yield.

3.1.2 TEV protease cleavage assay and PILS experiment

This protease preparation was then used in an N-terminomics labeling and cleavage PILS experiment to confirm its activity for intended subtiligase-based N-terminomics uses. The purified TEV protease was incorporated into a modified PILS experiment, a subtiligase-based N-terminomics experiment on a standard *E. coli* lysate (section **2.4.3**) (performed by Erik Gomez-Cardona). As part of the monitoring of subtiligase labeling of neo N-termini in the lysate, an immunoblot using a fluorescent streptavidin was performed (**Fig. 3.3**). Subsequent TEV protease cleavage of the peptide label was also monitored using this blot. The immunoblot visually demonstrated that the purified TEV protease could cleave TEVest6, as the signal intensity was markedly decreased after both 4 h and 24 h incubation with the protease.

The large band that appeared in every immunoblot lane was likely the subtiligase enzyme itself being labeled, as it corresponds to the expected molecular weight of subtiligase with the addition of TEVest6 (~1.5 kDa) (**Fig. 3.3**). As well, the immunoblot signal does not disappear entirely after a 24-hour incubation with the TEV protease. In typical subtiligase N-terminomics experiments, we

monitored TEV cleavage after a streptavidin bead-capture step, which enriched for labeled proteins. We monitored through a dot blotting approach and sought a near-disappearance of signal (of at least 90%); however, during this cleavage test we did not perform any enrichment, and rather added TEV protease directly into the labeled lysate mixture. Consequently, this meant that subtiligase was still present in the mixture and was capable of re-labeling free N-termini as well. Because we still observed a decrease in signal, we concluded the purified TEV was catalytically active.

The subsequent completion of the PILS experiment demonstrated that this TEV purification is cleaving at a similar efficiency compared to stocks in the lab (**Table 3.1**), as it resulted in the recovery of 695 labeled peptides compared to 700 labeled peptides using previously prepared TEV protease.

3.1.3 Caspase-3 expression and purification

Unlike the TEV protease, caspase-3 is not expressed as a fusion construct to another protein, it is simply expressed with a 6xHis tag to allow for purification on Ni^{2+} affinity columns[196]. Caspase-3 is constitutively expressed as a dimer. To become active, endogenous caspase-3 is cleaved between its small and large subunits (**Fig. 1.4**). This caspase-3 construct is active upon expression. After transforming the caspase-3 plasmid into BL21(DE3)pLysS *E. coli*, the protease was expressed in 1.5 L of Lennox LB for 5 h at 30°C, before harvesting the cells for lysis and purification (see **2.3.1**).

The 6xHis tag purification of caspase-3 was carried over 10 mL, which allowed for the separation of recombinant caspase-3 from most of the nonspecific protein which also bound to the Ni^{2+} column (**Fig. 3.4**). Elution fractions A7 and A8 were pooled and subsequently buffer-exchanged into the final storage buffer. The concentration of enzyme was approximated by A_{280nm} using its extinction coefficient (from Expasy ProtParam = 26400 $M^{-1}cm^{-1}$ assuming all Cys form cystines, 25900 $M^{-1}cm^{-1}$ assuming all Cys reduced) and molecular weight (28.5 kDa), to 0.65 mg/mL (20.5 µM), noting the presence of other contaminating protein bands (**Fig. 3.4**). This protease preparation was then used in an activity assay to determine its catalytic properties prior to use.

3.1.4 Caspase-3 is catalytically active

Ac-DEVD-Afc fluorescence assays were used to determine the catalytic parameters (k_{cat}/K_m) of caspase-3 stocks in the laboratory, prior to use in *reverse* N-terminomics (**2.3.2**). Fluorescence

assays were performed in parallel to previous caspase-3 stocks in the lab, diluting from 5 μM stocks to working concentrations of 1 nM and 10 nM. The catalytic efficiency for the previous stock was calculated to be 1.06 x 10^6 $M^{-1}s^{-1}$ with a K_m of 26.2 μM calculated at 1 nM and 5.76 x 10^5 $M^{-1}s^{-1}$ with a K_m of 53.7 μM calculated at 10 nM (**Fig. 3.5**). For the new purification, the efficiency was determined as 5.24 x 10^6 $M^{-1}s^{-1}$ with a K_m of 3 μM for 1 nM and 6.28 x 10^5 $M^{-1}s^{-1}$ with a K_m of 22.6 μM for 10 nM. These k_{cat}/K_m values are all within an order of magnitude of one another and comparable to a previously reported caspase-3 catalytic efficiency (k_{cat}/K_m) of 7.6 x 10^5 $M^{-1}s^{-1}$, with a K_m of 12 μM[81]. Following this, we proceeded with *reverse* N-terminomics.

3.2 Caspase-3 and -9 *reverse* N-terminomics reveals new substrates

We report 906 and 124 protein substrates targeted by caspase-3 and caspase-9, respectively. These substrates were observed by using a subtiligase-based *reverse* N-terminomics enrichment method (**Fig 1.7**). For the analyses of caspase-3 and -9 substrates to play the intended role in providing insights into their respective functions, it is critical that we assess the proteolysis of these caspases in a native environment (substrates folded and interactions maintained), while inhibiting activation of endogenous proteases[65,102].

Using *reverse* N-terminomics, the activities of caspase-3 and -9 were assessed and optimized in Jurkat lysates (**Fig. 3.6** and **3.7**). The general schematic diagram of *reverse* N-terminomics is shown (**Fig. 1.7**). During cell lysis, background proteolysis was minimized by the addition of protease inhibitors (EDTA, IAM, PMSF, AEBSF) (see **2.7.3**) which inhibits metallo- and serine proteases, attenuating the activity of endogenous cysteine proteases, such as caspases and cathepsins. Dithiothreitol was subsequently supplemented to react with excess iodoacetamide, prior to adding purified caspase. In addition, extra precautions were taken for the initiator caspase-9 assay. Jurkat JMR, a caspase-9 deficient cell line[197], was used to ensure the measurement of exogenously added caspase-9-cleaved substrates only. To ensure that the executioners caspase-3/-7 were fully inhibited and not contributing to the observed cleavage[73], Ac-DEVD-fmk was added to the lysate (**Fig. 3.7**). After monitoring caspase activity, z-VAD-fmk was added to the lysates to quench the caspases before proceeding with labeling. Subtiligase and biotin ester peptide tag were then added to label the newly generated N-termini of the cleaved products[100]. Biotinylated protein fragments were then captured on neutravidin beads, trypsinized, and released by TEV cleavage. The N-terminomics labeling and capturing efficiency were measured (**Fig. 3.8**). The eluted peptides were then identified using tandem mass spectrometry (LC-MS/MS) (**Fig. 1.7**). Importantly, the peptides that have been labeled with the biotin ester peptide tag and released by

TEV retain a nonstandard amino acid, aminobutyric acid (Abu), that allows for unambiguous identification of proteolytic products and precise location of the cleavage sites.

3.2.1 Caspase-3 and -9 cleave new and expected apoptotic substrates, enabling deorphanization

Prior subtiligase N-terminomics analysis for caspase-3 observed 180 substrates linked to apoptosis, whereas no substrates were found for caspase-9[101].This is possibly due to the low intrinsic activity of caspase-9 and the lower sensitivity of the mass spectrometers used in prior N-terminomics assessments. Thus, all caspase-9 substrates known have been reported via individual biological investigations.

In our N-terminomics analyses across two biological replicates, we found 1126 cleavage sites featuring an aspartate at P1 position (P1 = D) in 906 proteins for caspase-3 (1.2 cleavage sites per protein), and 137 cleavage sites in 124 proteins (1.1 cleavage sites per protein) for caspase-9 (**Fig. 3.9A**). The caspase-3 *reverse* N-terminomics experiments exhibited a P1 = D cleavage in 46% of its labeled N-termini (1126 out of 2437), while the caspase-9 experiment exhibited 32% (137 out of 428) (**Fig. 3.9A**). This is significantly higher than found in non-treated cell lysate, where we typically observe 6.5% of N-termini featuring a P1 = D[75], confirming strong caspase substrate proteolysis induced by the addition of exogenous caspase.

We then aligned each P1 = D peptide from the caspase-3 and caspase-9 datasets to determine the specificity of each protease in human cell lysates, where we anticipate that potential substrates are intact and properly folded (**Fig. 3.9B**)[199]. The caspase-3 cleavage sites revealed a clear DEVD↓(G/S/A) cleavage motif for amino acids P4-P1↓(P1')[20], (**Fig. 3.9B**) as expected[200]. The full list of cleavage sites recognized shows considerably greater breadth of recognized sequences than may be reflected in the sequence logo, suggesting that context of the cleavage site, in addition to the sequence, is critical to substrate recognition (**Appendix A**). The caspase-9 cleavage sites on the other hand revealed a LESD↓(G/S) cleavage motif for P4-P1↓(P1') (**Fig. 3.9B**), similar to its reported cleavage specificity for P4-P1↓ as LEHD[77]. More importantly, there is no evidence of a DEVD cleavage site motif (**Appendix A**), indicating any DEVDase activity has been fully blocked by the Ac-DEVD-fmk inhibitor (**Fig. 3.7**). Thus, these results (**Fig. 3.9B**) strongly suggest that we succeeded in inducing selective caspase proteolysis in each of our caspase-3 and caspase-9 experiments, with no or limited contamination from other activated caspases.

To determine which substrates have already been previously observed in apoptosis, we compared our results with the DegraBase, a repository containing >6000 unique N-termini (>1700 caspase cleavage sites) identified in subtiligase-based N-terminomics of cells undergoing apoptosis (**Appendix A**)[75]. Derived from previous studies, the DegraBase includes the list of proteolytic substrates from many different inducers of apoptosis, including etoposide, staurosporine, TRAIL, bortezomib and doxorubicin. This important resource does not, however, identify which protease is responsible for each cleavage event. By cross-referencing our substrates with the DegraBase, we found that many of the caspase-3 and -9 substrates identified are cleaved during apoptosis (**Appendix A**). We can now deorphanize these proteolytic events, linking them to their respective caspases. We found that 577 cleavage sites from caspase-3 (51% of observed cleavages) and 52 cleavage sites from caspase-9 (38% of observed cleavages) had not been previously identified in the DegraBase. We also looked for new substrates that were not previously reported in the DegraBase. We found 257 new caspase-3 and 20 new caspase-9 substrates (**Appendix A**). This suggests that these new substrates of caspase-3 and -9 may be present at low abundance or play roles in pathways other than apoptosis.

Comparing the results obtained in these experiments, 43% of the cleavage sites (and 40% of the substrates) observed in the caspase-9 *reverse* N-terminomics experiment were not observed in the caspase-3 experiment (**Fig. 3.9C**). This suggests that many of the substrates and the cleavage sites observed in the caspase-9 *reverse* experiments are unique to caspase-9, especially considering that caspase-3 is much more active (k_{cat}/K_m = 7.6x10^5 M^{-1}s^{-1})[81] than caspase-9 (k_{cat}/K_m = 3.3x10^3 M^{-1}s^{-1})[201]. Furthermore, we observed none of these caspase-9 cleavages in either of the two replicate experiments of caspase-3 N-terminomics. These results are further evidenced by our subsequent characterization (see below).

The distribution of subcellular localization of caspase-3 and -9 substrates is similar, with the majority of substrates being localized to either the cytoplasm or the nucleus (**Fig. 3.13A**). Our N-terminomics method is less suited to detect secreted and membrane proteins, which likely contributes to their lower appearance in our datasets. Within the caspase-3 dataset, 49% of the substrate proteins have been reported to be present in the cytoplasm, 48% in the nucleus, 6% in the mitochondria, 7% in the endoplasmic reticulum, 7% in the cell membrane, 4% in other organelles and 2% were reported to be secreted. A number of substrate proteins have been reported in more than one subcellular location. Within the caspase-9 dataset, 47% of substrate proteins were found in the cytoplasm, 55% in the nucleus, 1% in the mitochondria, 6% in the

endoplasmic reticulum, 7% in the cell membrane, 4% in other organelles and 2% were found to be secreted. Compared to the proteome, there is a higher proportion of proteins localized in the nucleus or cytoplasm (50% in caspase datasets and 25% in proteome), with lower representation of other subcellular locations (1-10% in datasets and 5-15% in proteome).

We also carried out a Reactome[202] pathway analysis to identify cellular pathways enriched in our datasets. Across both datasets, pathways with the p-values (caspase-3, caspase-9) below 5.0×10^{-2} were related to mRNA splicing (4.21×10^{-7} [38 substrates], 5.25×10^{-6} [11 substrates]), RNA metabolism (1.38×10^{-7} [95 substrates], 2.30×10^{-5} [11 substrates]) and SUMOylation of proteins (4.04×10^{-5} [32 substrates], 1.25×10^{-2} [6 substrates]), including the expected enrichment of proteins associated with apoptosis (**Fig. 3.13B** and **3.13C**). We observed more enrichment for Notch-HLH transcription (5.42×10^{-4} [9 substrates]) and HIV infection pathways (1.26×10^{-3} [35 substrates]) in the caspase-3 but not in the caspase-9 dataset. For caspase-9, we saw enrichment for mitotic prometaphase (1.85×10^{-3} [8 substrates]), Rho GTPase signaling (3.13×10^{-3} [12 substrates]) and membrane trafficking (3.60×10^{-3} [15 substrates]). Broadly, we observed enrichment of pathways often found in prior caspase N-terminomics analyses[65,203].

We also extracted the location of the caspase cleavage sites from the secondary structure of each substrate, if available (**Fig. 3.14**). As expected, the majority of the caspase cleavage sites occur in loop or disordered regions (58% for caspase-3 and 65% for caspase-9), but proteolysis also is observed in regions of α-helices (31% for caspase-3 and 23% for caspase-9) and β-sheets (11% for caspase-3 and 12% for caspase-9) suggesting that local unfolding may also be involved in substrate recognition. We further compared our results to previously published machine learning algorithms used to predict caspase cleavage sites in the human proteome based on protein surface accessibility and secondary structure[204]. Overall, almost all observed cleavage sites reported here scored above the average aspartate site found in the proteome (**Fig. 3.15**), supporting the predictions.

From the N-terminomics results, we individually examined each substrate, and selected ten targets to further investigate the cleavage sites we observed (**Table 3.3**). The intention in selecting these ten targets was to pick a mixture of cleavage sites within and outside the DegraBase. Some of these cleavage sites were observed only in the caspase-3 experiments, some only in the caspase-9 experiments, and some in both experiments. The aim of these studies is to further understand the unique and overlapping roles of these caspases. We also sought to probe in detail

substrates featuring multiple caspase cleavage sites. Moreover, for diversification, we selected substrates that belong to different functional protein families: a DNA helicase, three E3 ubiquitin ligases, a nucleoporin, a pore-forming membrane protein, a GTPase, a kinase, a ribonuclease, and a protein involved in RNA processing. It is important to mention that we reported here all of our validation attempts and did not withhold any data.

3.2.2 Caspase-9 cleaves distinct substrates from caspase-3.

As mentioned above, of the 124 caspase-9 substrates observed, 50 of them (43%) were not observed in the caspase-3 experiment (**Fig. 3.9C**), although these experiments were run using the same protocol. For further investigation into novel roles of caspase-9, we selected three caspase-9 substrates that are not cleaved by caspase-3: ATP-dependent DNA helicase Q5 (RECQL5), nucleoporin 43 (NUP43), and E3 ubiquitin-protein ligase - Ring Finger Protein 126 (RNF126).

RECQL5 is a DNA helicase involved in chromosomal and genome stability, DNA replication and double strand break repair[205–207]. The full-length RECQL5 can be divided into two parts: the N-terminal region (primarily responsible for helicase activity) composed of a helicase domain, a zinc-binding domain, and a wedge domain, and the C-terminal region (mainly involved in DNA repair during transcription) containing an internal Pol II–interacting (IRI) domain and a Set2-Rpb1–interacting (SRI) domain (**Fig. 3.10A**)[208]. As was observed in our N-terminomics experiments, RECQL5 was robustly cleaved in Jurkat cell lysates treated with caspase-9, but not caspase-3 (**Fig. 3.10B**). Importantly, RECQL5 was also cleaved in Jurkat cells treated with the general kinase inhibitor and apoptosis inducer, staurosporine (STS), which led to expected phenotypic changes associated with apoptosis (**Fig. 3.10C**). From our N-terminomics data, caspase-9 cleaves RECQL5 at D809 removing the SRI domain (**Table 3.3** and **Fig. 3.10A**). To maintain genome stability, the SRI domain of RECQL5 directly interacts with multiple binding partners, such as RNA polymerase I[209], RNA polymerase II[206,210], and proliferating cell nuclear antigen[211]. Thus, caspase-9 cleavage would prevent these interactions. From our N-terminomics data, both RECQL5 and DNA topoisomerase II alpha, which is likewise involved in DNA decatenation and cell cycle progression[212], were observed to be cleaved by caspase-9 but not caspase-3 (**Appendix A**). Given the fact that the cell cycle, DNA replication and DNA repair should be halted in the initial stage of apoptosis, our results suggest that caspase-9 also cleaves critical early apoptotic substrates. These data strongly suggested that caspase-9 can act as an executioner,

and its role is not limited to only serve as an initiator of apoptosis through cleavage of caspase-3 and -7.

RNF126 is an E3 ubiquitin ligase known to target the p21 tumor suppressor, and as such is considered a potentially useful cancer biomarker or therapeutic target[213,214]. RNF126 possesses two domains, an N-terminal zinc finger domain[215] and a C-terminal RING (Really Interesting New Gene) domain (**Fig. 3.10D**)[214]. RNF126 was readily identified in the caspase-9 N-terminomics analysis; however, it was not found as a caspase-3 substrate in our analysis nor in the DegraBase (**Table 3.3**). Consistent with the N-terminomics findings, RNF126 was cleaved by caspase-9, but not by caspase-3 (**Fig. 3.10E**). In addition, when apoptosis was induced by STS, no RNF126 cleavage was observed (**Fig. 3.10F**). Thus, RNF126 could be a new non-apoptotic substrate of caspase-9. One of the known functions of RNF126 is that its RING domain directly interacts and ubiquitinates AICDA (activation-induced cytidine deaminase), an enzyme that deaminates deoxycytidines in single-stranded DNA[216]. The exact outcome of this ubiquitination (whether AICDA is degraded or not) remains to be determined *in vivo*. AIDCA is predominantly expressed in germinal centers, and as an immune response, it produces and distributes high affinity antibodies against foreign antigens[217]. Because caspase-9 cleaves RNF126 in the RING domain at D253 (**Table 3.3** and **Fig. 3.10D**), this cleavage is likely to disrupt the ability of RNF126 to ubiquitinate AICDA.

While a number of nucleoporins have previously been reported as caspase substrates[218,219], NUP43, a component of the nucleoporin complex (NPC), was also identified as a new substrate of caspase-9 that had not been observed in previous studies. Cleavage of nucleoporins is critical as it allows entry of caspases lacking a nuclear localization signal into the nucleus[220]. NUP43 is composed of seven WD40 repeat domains, WD1 to WD7 (**Fig. 3.10G**)[221]. Although caspase-9 was robustly able to cleave NUP43 in Jurkat cell lysates, no cleavage by caspase-3 was observed (**Fig. 3.10H**). These findings are consistent with our N-terminomics analyses (**Table 3.3**). In contrast, when apoptosis was induced by STS, no NUP43 cleavage was observed (**Fig. 3.10I**) suggesting that NUP43 is not an apoptotic substrate cleaved in STS-treated cells. Induction of apoptosis by etoposide has been previously shown to result in cleavage of other nucleoporins including NUP93 and NUP96, but also did not result in cleavage of NUP43[222]. This provides increased evidence that NUP43 could be a substrate of caspase-9 under non-apoptotic conditions. The caspase-9 cleavage of NUP43 occurs in the WD1 domain at D58 (**Table 3.3** and **Fig. 3.10G**). In the NPC, NUP43 has been shown to interact with other nucleoporins, NUP85 and

Seh1[221,223]. Therefore, it remains to be discovered how the overall structure and function of NPC are changed upon caspase-9 cleavage of NUP43.

3.2.3 The majority of caspase-3 substrates are not recognized by caspase-9.

Of the 906 substrate proteins cleaved by caspase-3 in our analysis, 832 of the proteins were not cleaved by caspase-9. We selected four unique caspase-3 substrates for further analysis: gasdermin D (GSDMD), mitofusin 2 (MFN2), E3 ubiquitin-protein ligase - RING finger protein 4 (RNF4), and serine/threonine protein kinase PAK 2 (PAK2). All of these substrates were also cleaved at the expected sites when apoptosis was initiated by STS in Jurkat cells (**Fig. 3.11**), strongly suggesting that these proteins are *bona fide* apoptotic caspase-3 substrates.

GSDMD, a pore-forming membrane protein, controls membrane permeabilization during pyroptosis[224]. GSDMD is composed of two domains, GSDMD-N (N-terminal pore-forming domain) and GSDMD-C (C-terminal auto-inhibitory domain) (**Fig. 3.11A**). The full-length GSDMD remains inactive by an autoinhibitory mechanism due to the presence of GSDMD-C[225–227]. To induce pyroptosis, GSDMD is recognized by the inflammatory caspases (caspase-1, -4, -5 and -11) which cleave a linker between GSDMD-N and GSDMD-C at D275[59]. This cleavage facilitates GSDMD-N domains to oligomerize and form pores in the cell membrane[226,227]. In contrast, prior work has shown that GSDMD is readily cleaved by caspase-3 in GSDMD-N at D87[228] instead of D275[229]. Cleavage of GSDMD-N at D87 by caspase-3/-7 is critical for faithful execution of apoptosis, as it is sufficient to prevent pyroptosis[229]. Our N-terminomics datasets showed that GSDMD can be cleaved by caspase-3 at both D87 and D275, consistent with both sites reported in the DegraBase (**Table 3.3**). Mirroring the N-terminomics results, we also observed cleavage of GSDMD in Jurkat lysates incubated with caspase-3 but not caspase-9 (**Fig. 3.11B**). However, the presence of a cleavage product at 43 kDa suggest that D87 is the main caspase-3 cleavage site. As expected, GSDMD was also proteolyzed in a similar manner during STS-induced apoptosis (**Fig. 3.11C**).

MFN2 is present in the outer mitochondrial membrane and is essential for fusion of mitochondria[230]. MFN2 has also been implicated in the regulation of mitochondrial metabolism[231], apoptosis[232], shape of other organelles (e.g. endoplasmic reticulum)[233], and cell cycle progression[234]. MFN2 possesses a GTPase domain, a first coiled-coil heptad-repeat region domain, a proline-rich domain, transmembrane domains, and a second coiled-coil heptad-repeat region domain (**Fig. 3.11D**)[235]. MFN2 is cleaved by caspase-3, but not caspase-9 (**Table 3.3** and

Fig. 3.11E). Cleavage of MFN2 in Jurkat cells after induction of apoptosis (**Fig. 3.11F**) further suggests that MFN2 is a bonafide apoptotic substrate solely of caspase-3, although this cleavage has not been previously reported in earlier studies (**Table 3.3**). Caspase-3 cleaves MFN2 at D499 (**Table 3.3** and **Fig. 3.11D**). This cleavage severs the GTPase domain from the second coiled-coil heptad-repeat region domain, important components of MFN2 required to initiate and induce the fusion of mitochondria[236–238]. Thus, caspase-3 cleavage of MFN2 can prevent mitochondrial fusion. Another role of MFN2 is that it interacts with BAX (Bcl-2-associated X protein) under non-apoptotic conditions, preventing apoptosis[239]. Furthermore, reduction of MFN2 levels has been shown to render cells more sensitive to mitochondrial Ca^{2+}-dependent cell death[240]. Thus, we anticipate that caspase-3-mediated cleavage of MFN2 likewise increases the release of cytochrome c, evoking apoptosis.

RNF4 is an E3 ubiquitin ligase that recognizes SUMO-modified proteins and degrades them via ubiquitination[241]. RNF4 accumulates at the foci of DNA double strand break repair, so its deficiency leads to increased DNA damage[242]. RNF4 can be divided into two parts: the N-terminal region possessing four tandem SUMO-interacting motifs (SIMs) and the C-terminal RING domain (**Fig. 3.11G**)[243–245]. We identified RNF4 as a substrate of caspase-3, but not of caspase-9 (**Table 3.3** and **Fig. 3.11H**). Moreover, RNF4 was found to be cleaved during STS-induced apoptosis in Jurkat cells (**Fig. 3.11I**). RNF4 was cleaved by caspase-3 at D89 and D137 (**Table 3.3** and **Fig. 3.11G**) causing the removal of the N-terminal region that recognizes SUMO-modified proteins. The majority of SUMO-modified proteins regulated by RNF4 are involved in nucleic acid metabolism with a particular emphasis on SUMOylation, transcription, DNA repair, and chromosome segregation[241]. Since these types of cellular procedures must be halted during apoptosis, it is understandable that RNF4 emerged as an apoptotic substrate of caspase-3.

PAK2 is known to play a role in regulating apoptosis through reciprocal interactions with caspase-7[246]. PAK2 is composed of two domains, an auto-inhibitory domain and a kinase domain (**Fig. 3.11J**)[246,247]. PAK2 was identified as a substrate of caspase-3, but not of caspase-9 (**Table 3.3** and **Fig. 3.11K**). Moreover, it was proteolyzed after STS-induced apoptosis in Jurkat cells (**Fig. 3.11L**). In its full-length form, PAK2 stimulates cell survival by the phosphorylation and inactivation of caspase-7[246,248]. PAK2 is also a known substrate of caspase-3 and -7[246,249]. Cleavage of PAK2 by caspase-3 or -7 at D212 removes the autoinhibitory domain[247]. As a result, the kinase domain translocates from the cytoplasm to the nucleus, and phosphorylates a new set of substrates contributing to apoptosis[250]. Intriguingly, in the caspase-3 N-terminomics analysis, we did not

observe cleavage at D212, but rather observed two cleavages at D89 and D148 (**Table 3.3** and **Fig. 3.11J**). These results appear to be in line with our observation of PAK2 cleavage *in vitro* which demonstrates that PAK2 is such an excellent substrate of caspase-3 that it completely disappears on the immunoblot after incubation with caspase-3 (**Fig. 3.11K**) as well as during STS-induced apoptosis (**Fig. 3.11L**).

3.2.4 Caspase-3 and -9 share some common substrates.

Of the 906 caspase-3 substrate proteins and 124 caspase-9 substrate proteins, 74 were cleaved by both caspases. These 74 represent 57% of all caspase-9 substrate proteins identified, suggesting that there is significant redundancy between caspase-9 and -3 substrates. We selected three common substrates of caspase-3 and -9, poly (A)-specific ribonuclease (PARN), ataxin-2-like protein (ATXN2L), and E3 ubiquitin-protein ligase RING1, for further investigation.

PARN is a deadenylating nuclease that regulates mRNA turnover and non-coding RNA maturation[251,252]. PARN possesses three well-structured RNA binding domains (catalytic nuclease domain, an R3H domain, and an RRM domain)[253] and an intrinsically disordered C-terminal domain (CTD) (**Fig. 3.12A**)[254,255]. From our N-terminomics analyses, PARN was observed to be a substrate of both caspase-3 and -9, in which both caspases cleaved PARN in the CTD at the same site, D595 (**Table 3.3** and **Fig. 3.12A**). These results mirror our immunoblotting analysis (**Fig. 3.12B**). The CTD interacts with the other regions of PARN and enhances the overall thermal stability of this protein[255]. Moreover, the CTD of PARN contains a nucleolar localization signal (residues: 598-624), and interacts with the nuclear non-coding RNAs in response to DNA damage[254]. Thus, PARN cleavage by caspase-3 and -9 at D595 can not only prevent PARN access to the nucleolus but also destabilize the protein. Cleavage in the CTD appears to be crucial, as both caspase-3 and -9 execute this apoptotic role (**Fig. 3.12B**), and it is cleaved during STS-induced apoptosis (**Fig. 3.12C**). Deficiency in PARN leads to shortening of telomeres[256]. Thus, PARN inactivation would likewise be associated with the DNA fragmentation that is observed during apoptosis.

ATXN2L, a component of stress granules, plays a role in RNA processing, and possesses three domains: LSm domain, LSmAD domain, and PAM2 domain (**Fig. 3.12D**)[257]. ATXN2L is cleaved by both caspase-3 and -9, which recognize different cleavage sites: D181 and D584 for caspase-3 and D246 for caspase-9 (**Table 3.3** and **Fig. 3.12D**). These outcomes from N-terminomics analyses mirrored our immunoblotting results (**Fig. 3.12E**). Moreover, ATXN2L was readily

proteolyzed during STS-induced apoptosis demonstrating that it is an apoptotic substrate (**Fig. 3.12F**). ATXN2L appears to play a similar role to its paralog, Ataxin-2, as it interacts with Ataxin-2 itself and with Ataxin-2 interacting proteins, an RNA helicase, DDX6 (perhaps through the LSm and LSmAD domains) and Poly(A)-binding protein, PABP (perhaps through the PAM2 domain)[257]. Caspase-9 cleavage at D246 removes the LSm domain of ATXN2L (**Table 3.3** and **Fig. 3.12D**) which may prevent ATXN2L interactions with DDX6. Since caspase-3 cuts ATXN2L at two distinct sites, D181 and D584 (**Table 3.3** and **Fig. 3.12D**), these cleavages may disrupt the ability of ATXN2L to interact with DDX6 as well as PABP. Since RNA helicases (e.g. DDX6) are involved in the production of virtually all RNA types, targeting ATXN2L provides a means to block RNA production and function globally in roles including translation. These analyses underscore the observation that redundancy for key apoptotic substrates (such as global regulators of RNA metabolism) may be built into multiple caspases.

RING1 (also known as RING1A) is an E3 ubiquitin ligase that we observed to be a substrate of both caspase-3 and -9, which cleave RING1 at independent sites (**Table 3.3**). RING1 is cleaved by caspase-3 at D189 and by caspase-9 at D193 (**Table 3.3** and **Fig. 3.12G**) which are both between the RING domain[258] and a ubiquitin-like domain[259]. We observed RING1 cleavage in our *in vitro* cleavage assay for both caspase-3 and -9, correlating with our N-terminomics data (**Fig. 3.12H**). RING1 is known to degrade p53 protein causing proliferation of cancerous cells[260]. For this reason, RING1 is perhaps an unsurprising apoptotic substrate (**Fig. 3.12I**). Caspase cleavage of RING1 should protect p53 from degradation resulting in the needed ability to induce apoptosis. RING2 (also known as RING1B), which is highly homologous to RING1, was reported as a direct substrate of caspase-3 (cleaves at D175) and caspase-9 (cleaves at D208)[121]. Interestingly, these cleavages are also occurring between the RING domain and the ubiquitin-like domain of RING2. These cleavages by caspase-3 and -9 lead to the redistribution of RING2 from nuclear localization to even distribution throughout the entire cell[121]. The N-terminomics identification of RING1 as a substrate of caspase-3 and -9 (cleaving at different sites), may suggest that RING1 cleavage may lead to similar impacts on cellular localization. As was the case for ATXN2L it is tempting to speculate that a key role for RING1 in apoptosis led to evolution of cleavage sites for redundant cleavage by both caspase-3 and -9. In addition, the observation that these two caspases cleave at different sites within the same local region (D189/193) further underscores the importance of this cleavage event, perhaps even under different mechanisms of cell death that engage caspases uniquely.

3.3 C2C12 label-free quantification preliminary experiment

This experiment sought to serve as a preliminary exploration into the global proteome changes in differentiation from myoblasts to myotubes, using the C2C12 immortalized mouse myoblast cell line[198]. These cells differentiate to myotubes upon serum withdrawal (performed by switching from a 10% FBS growth media to a 2% horse serum media), and caspase-3 is required for their differentiation[108]. We sought to evaluate the proteome changes upon inhibiting caspase-3 during the serum-withdrawal period as well.

In this preliminary analysis, three samples were prepared (in biological triplicates): undifferentiated C2C12 cells, C2C12 cells which have undergone serum-withdrawal to differentiate to myotubes, and C2C12 cells which have undergone serum-withdrawal while simultaneously being treated with DEVD-fmk(OME), a cell-permeable irreversible caspase-3 inhibitor. Morphologically, the DEVD-fmk-treated cells exhibited elongation similar to that observed in the differentiated cells (**Fig. 3.16**).

In total, over 4000 (4323) proteins are observed when combining all samples. The vast majority (4145) are observed in all experiment conditions. The undifferentiated sample exhibited 25 unique proteins, the differentiated sample 3 proteins, and the differentiated sample treated with DEVD-fmk exhibited 4 unique proteins (**Fig. 3.17**).

In general, proteins classically related to myogenic differentiation were not observed in the mass spectrometry data. Common markers of myogenic differentiation myogenin, myoD, Myf-5, MRF4[261] and myosin heavy chain II are not observed. Desmin, another often-used marker of differentiation[262], is observed in both pre-differentiation and differentiated samples.

Heatmaps, volcano plots and PCA plots were created using ProteomeDiscoverer (2.4) (Thermo Fisher) software. Plotting the results on a heatmap and on a PCA plot demonstrates that the differentiated and the DEVD-fmk-treated cells exhibit high similarity, indicating that DEVD-fmk was likely unable to prevent differentiation. In the heat map, sample clustering through Euclidean distance calculations placed differentiated samples and DEVD-fmk-treated samples interchangeably, denoting similarity. This is more clearly visualized in the PCA plot, where the principal component analysis places undifferentiated cells in a PC1 range of 50-60, while differentiated and DEVD-fmk-treated cells are in a PC1 range of (**Fig. 3.21** and **3.22**).

The protein abundances were also compared in a head-to-head manner using volcano plots. Differentiated cells were compared to undifferentiated cells in one plot, and in a separate plot they were compared to DEVD-fmk-treated cells. Undifferentiated C2C12 cells were also compared to

DEVD-fmk-treated cells, for a total of 3 volcano plots (**Fig. 3.18-3.20**). To be considered a significant enrichment, proteins had to exhibit a minimum 2-fold difference in abundance between experiments. Proteins also had to exhibit a p-value below 0.05 when subjected to a t-test based on the background population of proteins.

When comparing protein abundances between undifferentiated and differentiated C2C12 experiments, we observed 421 proteins enriched in differentiated cells (**Fig. 3.18**). Desmin, the only differentiation marker observed in the dataset, was not significantly enriched in differentiated samples. In undifferentiated cells we observed 368 enriched proteins. Interestingly, nucleoporin Nup43, a protein investigated in the *reverse* N-terminomics as a substrate of caspase-9 is enriched in undifferentiated cells.

Following this, protein abundances were compared between differentiated C2C12 cells and DEVD-fmk-treated cells. We observed 255 proteins enriched in the DEVD-fmk-treated cells and in the differentiated cells we observed 154 enriched proteins, about half the number of enriched proteins observed in the previous comparison (**Fig. 3.19**).

Lastly, protein abundances between undifferentiated C2C12 cells and DEVD-fmk-treated cells were also compared. Here we observed 430 proteins enriched in DEVD-fmk-treated cells and 347 proteins enriched in undifferentiated cells. Many of the observed enriched proteins in the DEVD-fmk-treated cells are similar to those in the differentiated cells, such as Armadillo repeat-containing protein 1 (ARMC1), Myosin light chain 6B (MYL6B), MYL4 and Pregnancy Zone Protein (PZP) (**Fig. 3.20**). Many enriched proteins in undifferentiated cells are also similar to what was observed in the comparison with differentiated cells, though the levels of enrichment varied. For example, fast-type myosin-binding protein 3 (MYPC2) was one of the most enriched proteins in the undifferentiated-differentiated comparison. While it remains significantly enriched in the undifferentiated-DEVD-fmk treatment comparison, the enrichment is not as high. Interestingly, Nucleoporin NUP43, a protein chosen for investigation in our *reverse* N-terminomics experiment, is enriched in undifferentiated cells compared to differentiated cells, however it is not observed in DEVD-fmk-treated cells.

3.4.1 Reactome pathway analysis

Reactome pathway analysis was performed on the enriched proteins between sample sets. When comparing undifferentiated and differentiated C2C12 cells, the top 4 pathways for the proteins enriched in the differentiated samples were all related to muscle contraction. In undifferentiated cells, the top 3 enriched pathways related to rRNA processing, followed by the cell cycle and DNA

strand elongation. Between undifferentiated C2C12 cells and DEVD-fmk-treated cells, the DEVD-fmk-treated cells held very similar enriched pathways, with the same top 4 pathways as the differentiated cells. In this comparison, the undifferentiated cells mainly exhibited enrichment in pathways related to the cell cycle and DNA replication, though enrichment of rRNA processing was also observed.

Finally, pathway analysis between differentiated C2C12 cells and DEVD-fmk-treated cells demonstrated enrichment for pathways related to trafficking and recycling for the differentiated cells, such as PIP synthesis at the Golgi membrane. For the DEVD-fmk-treated cells, pathways such as E3 ubiquitin ligase activity and snRNP assembly were enriched.
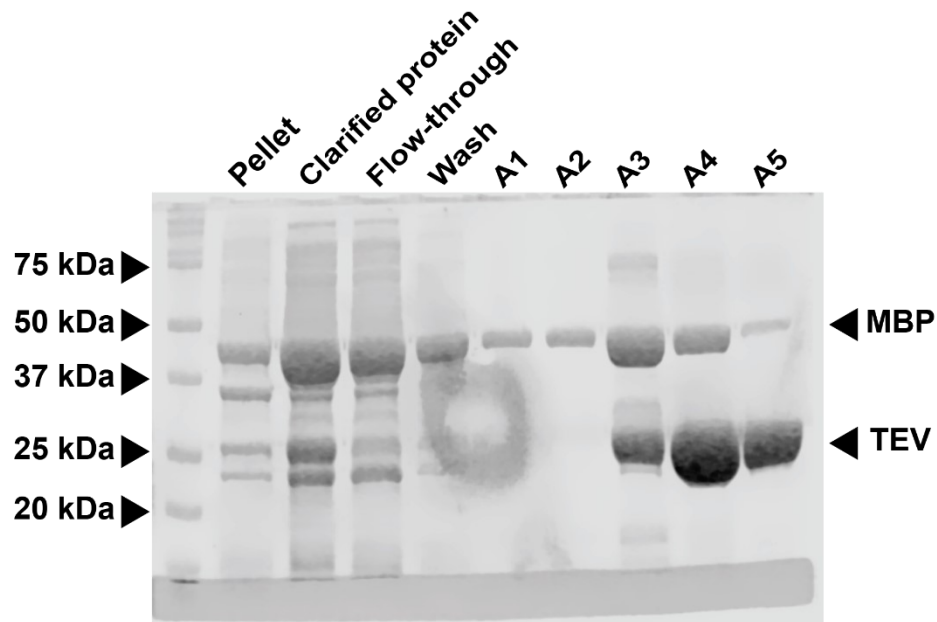
Fig. 3.1 SDS-PAGE of His-tag purification of TEV protease. Recombinant MBP-TEV protease was purified through Ni^{2+} affinity chromatography using a HisTrap column (Cytiva inc.). A 10% polyacrylamide SDS-PAGE gel was run at 180 V for 35 minutes, followed by staining with Coomassie blue dye for protein visualization. The protein construct contains MBP to improve solubility, which is auto-cleaved from the protease at a linker containing the TEV recognition sequence (ENLYFQ↓[G/S]). As seen above, the final TEV protease aliquots still contain the MBP, though because the protein is only used for N-terminomics experiments the remaining MBP does not pose a problem (see **Fig. 3.3** for a cleavage test)
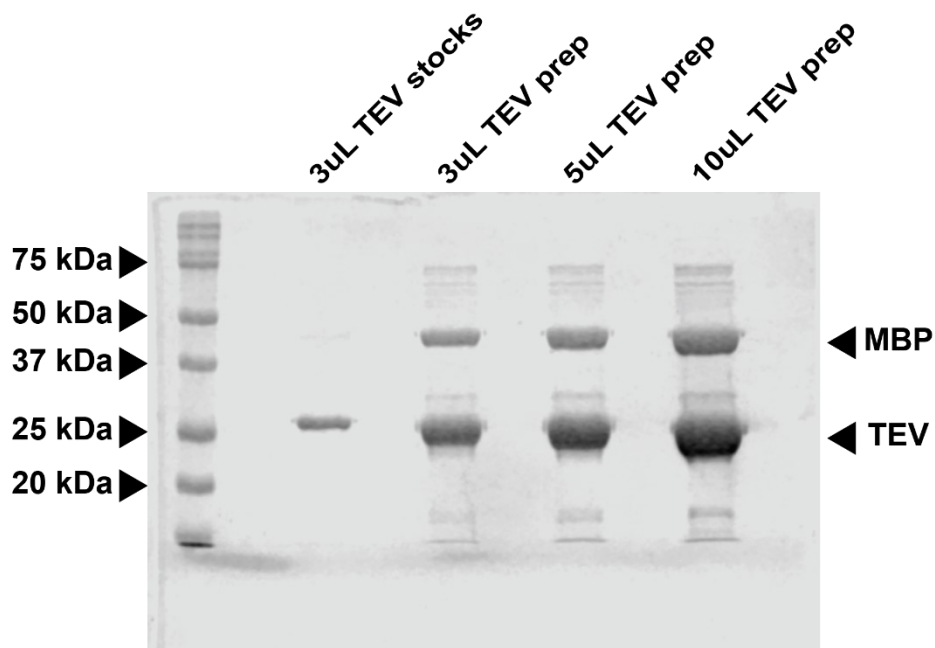
Fig. 3.2 TEV protease purification Coomassie gel concentration comparison to stocks. We compared our TEV purification aliquots with stocks in the lab because we suspected that the presence of MBP in our preparation could have influenced our readout. Using ImageJ software and the concentration of TEV stocks (1.3 mg/mL) we determined an adjusted concentration for our TEV purification of 4.24 mg/mL.
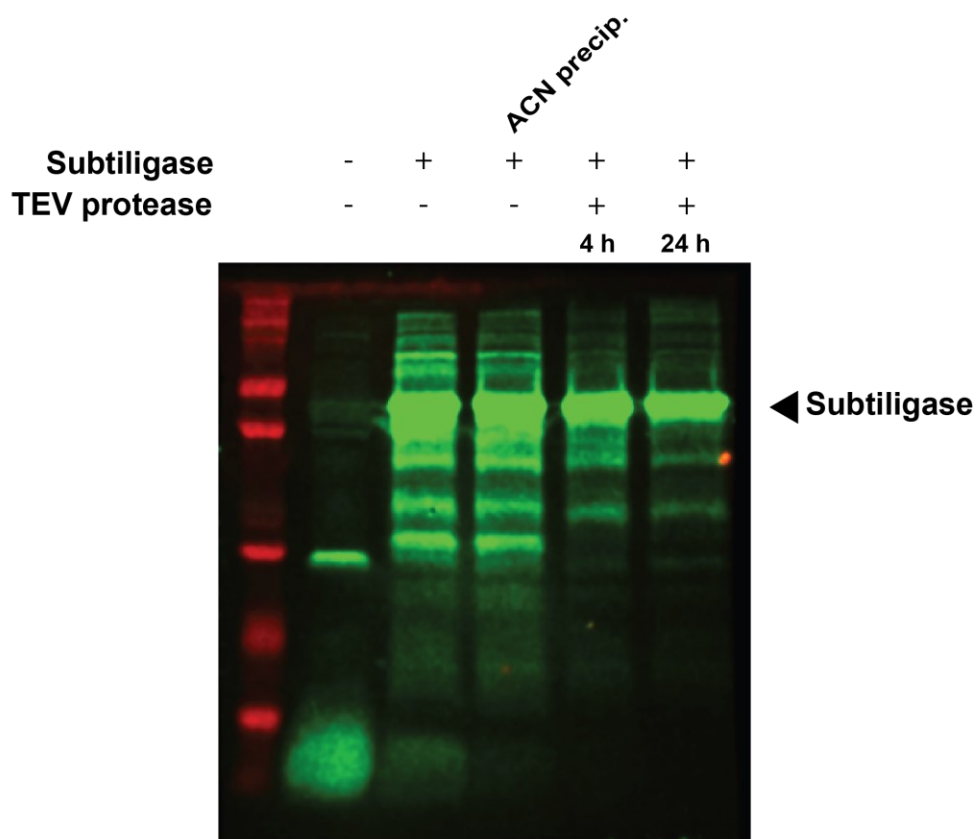
Fig. 3.3 N-terminomics-like cleavage assay of purified TEV protease. Western blot of pre (-) and post (+) labeling of *E. coli* lysate. An *E. coli* lysate was labeled with the TEVest6 biotin peptide ester tag using subtiligase as per the typical subtiligase N-terminomics protocol (-), following which the lysate was precipitated in acetonitrile (ACN) to remove excess tag in solution. Next, TEV protease is incubated for 24 h to induce cleavage of the tag from peptides, with an additional sample taken 4 h after TEV protease addition. The decrease in intensity of the signal from pre-digestion (-) to post-digestion (+) indicates that the biotin-containing TEVest6 was successfully cleaved from the labeled proteins. As subtiligase remains active in the mixture, some of the cleaved tag will be re-labeled onto the free N-termini, leading to some signal retention. The large band present in each lane is the subtiligase enzyme. This assay was performed by Erik Gomez-Cardona
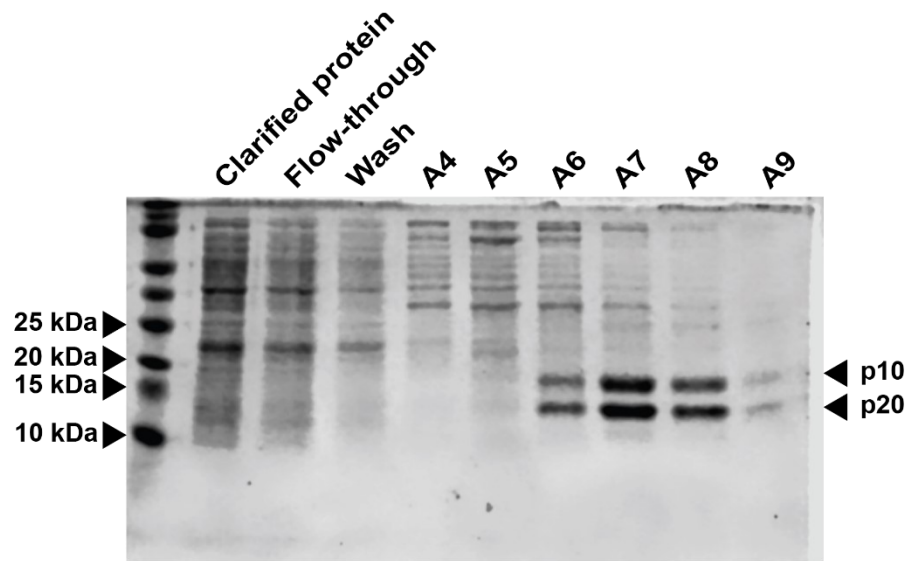
Fig. 3.4 SDS-PAGE of His-tag purification of caspase-3. Caspase-3 was purified through Ni^{2+} affinity chromatography using a HisTrap column (Cytiva inc.). A 10% polyacrylamide SDS-PAGE gel was run at 180 V for 35 minutes, followed by staining with Coomassie blue dye for protein visualization. Protein fractions eluted from the affinity column are numbered A4-A9. In fractions A6-A9, the characteristic banding patterns of the p20 and p10 subunits of caspase-3 (at 20 kDa and 10 kDa, respectively). Fractions A7 and A8 were pooled.

Caspase-3 Stocks

A

1 nM

k_{cat} = 27.90 s-1
K_m = 2.62 x 10^{-5} M
k_{cat} / K_M = 1.06 x 10^6 M^{-1} s^{-1}

B

10 nM

k_{cat} = 30.94 s-1
K_m = 5.37 x 10^{-5} M
k_{cat} / K_m = 5.76 x 10^5 M^{-1} s^{-1}

Purified Caspase-3

C

1 nM

k_{cat} = 15.73 s-1
K_m = 3.00 x 10^{-6} M
k_{cat} / K_m = 5.24 x 10^6 M^{-1} s^{-1}

D

10 nM

k_{cat} = 16.45 s-1
K_m = 22.6 x 10^{-5} M
k_{cat} / K_m = 6.28 x 10^5 M^{-1} s^{-1}
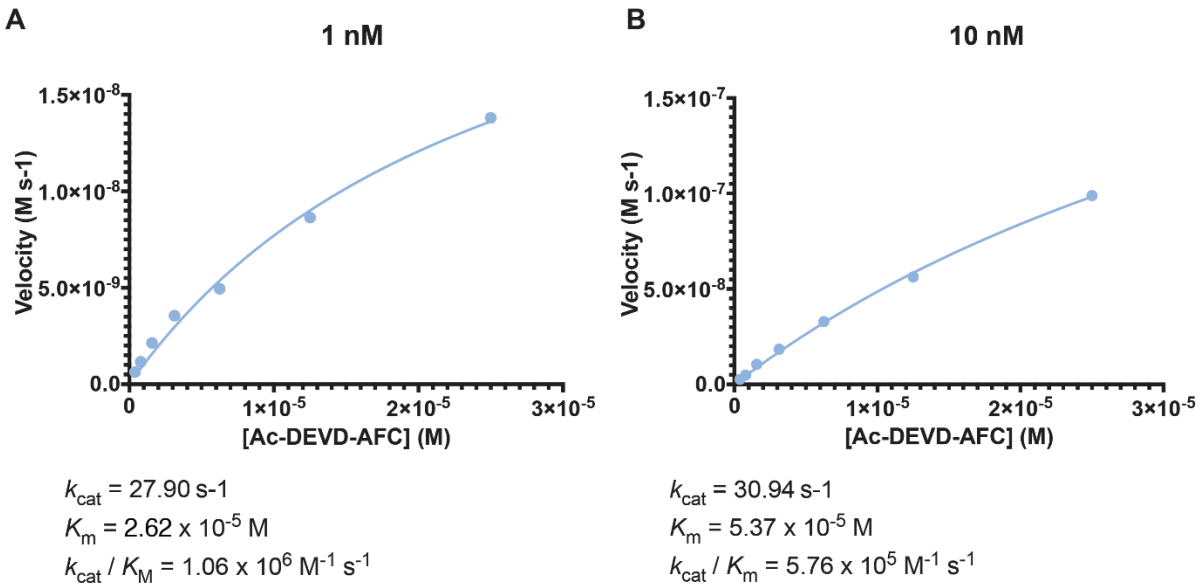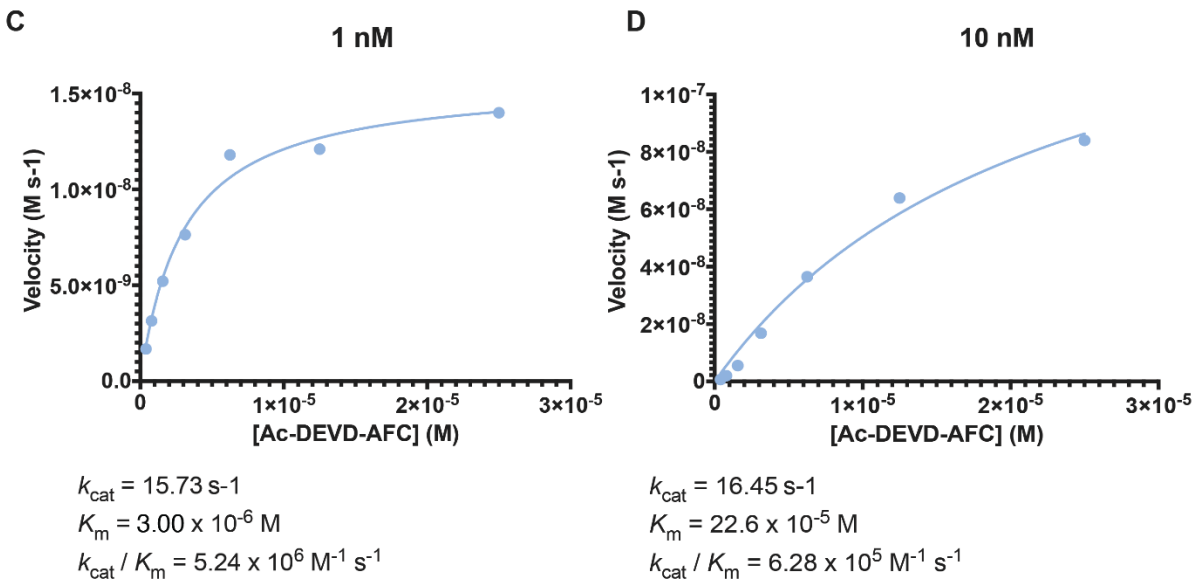
Fig. 3.5 Determining the catalytic efficiency of purified recombinant caspase-3. Purified enzyme was diluted from 5 µM stock to 100 nM and 1 nM in activity buffer (see **2.3.2**). Fluorescence assays were performed with a coumarin-based probe in serial dilution from 25 µM to 390 nM and assayed until the probe was depleted. Following this, Michaelis-Menten kinetic calculations were performed, yielding a catalytic efficiency (k_{cat}/K_m) of 1.06 x 10^6 $M^{-1}s^{-1}$ for the 1 nM experiment (**A**) and 5.76 x 10^5 $M^{-1}s^{-1}$ for the 10 nM experiment (**B**), within an order of magnitude to the kinetic parameters of a previous purification in the lab (k_{cat}/K_m = 1.06 x 10^6 $M^{-1}s^{-1}$ for 1 nM stocks (**C**), 5.76 x 10^5 $M^{-1}s^{-1}$ for 10 nM stocks (**D**)). Both values were similar to published catalytic efficiency[81].
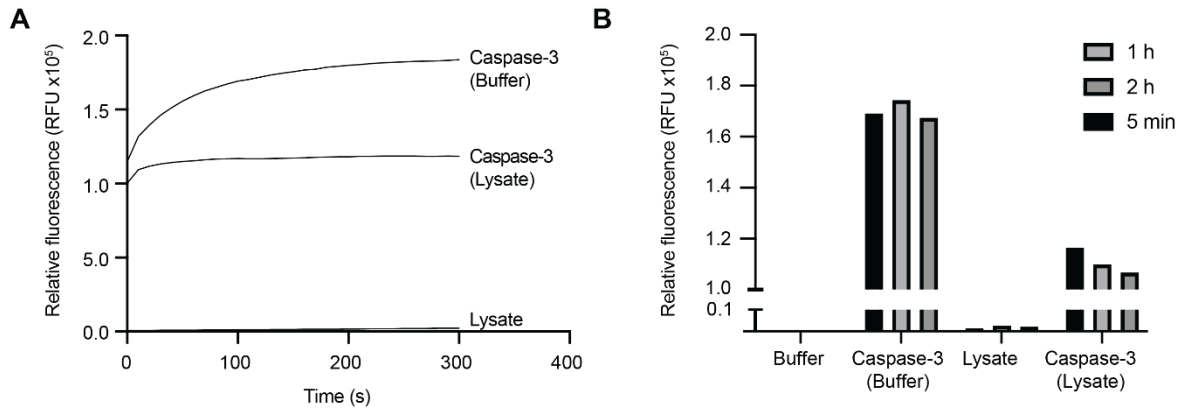
Fig. 3.6 Recombinant caspase-3 activity assay in lysate. DEVDase activity was monitored in the caspase-3 *reverse* N-terminomics experiment by sampling 5 minutes, 1 hour, and 2 hours after the addition of caspase-3 WT to Jurkat WT lysate. Caspase-3 WT induced Jurkat WT lysate was compared to uninduced lysate, caspase-3 WT in activity buffer and activity buffer alone. Assays were conducted as endpoint assays, monitoring for maximum probe cleavage. (**A**) Relative fluorescence output of assay conducted 5 minutes after inducing lysate with caspase-3. (**B**) Endpoint assay fluorescence outputs for all monitored timepoints. We observed that DEVDase probe cleavage was significantly higher in caspase-3 induced lysate than lysate alone ($3x10^3$ RFU for lysate alone vs $1x10^5$ RFU for induced lysate).
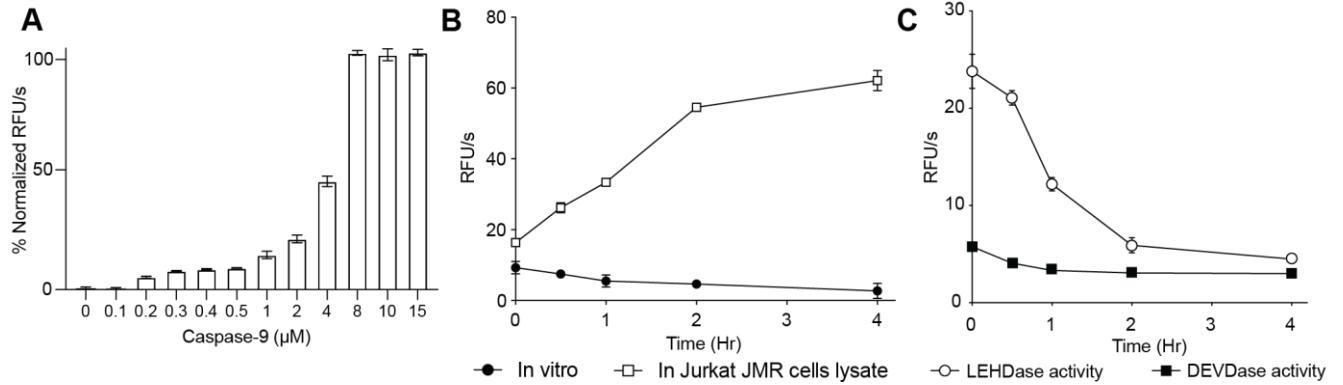
Fig. 3.7 Recombinant caspase-9 is active in cell lysates. A. Optimization of caspase-9 concentration for N-terminomics was performed using a LEHDase activity assays *in vitro* in caspase-9 activity assay buffer. Caspase-9 concentration from 0 to 15 µM was assayed to determine that the optimal LEHDase activity (in RFU/s) for 3 mM of the fluorogenic peptide substrate (Ac-LEHD-afc) is 8 µM of caspase-9. **B**. LEHDase activity of caspase-9 is higher in Jurkat JMR cells lysate than in the standard caspase-9 activity assay buffer. The increase of LEHDase activity in Jurkat JMR cells lysate over time is likely due to the activation of endogenous caspases in the lysate including caspase-3/-7/-8. **C**. To quench the background caspase activity seen in **B**, 25 µM of Ac-DEVD-fmk was added in Jurkat JMR cells lysate. This is sufficient to inhibit caspase-3/-7.
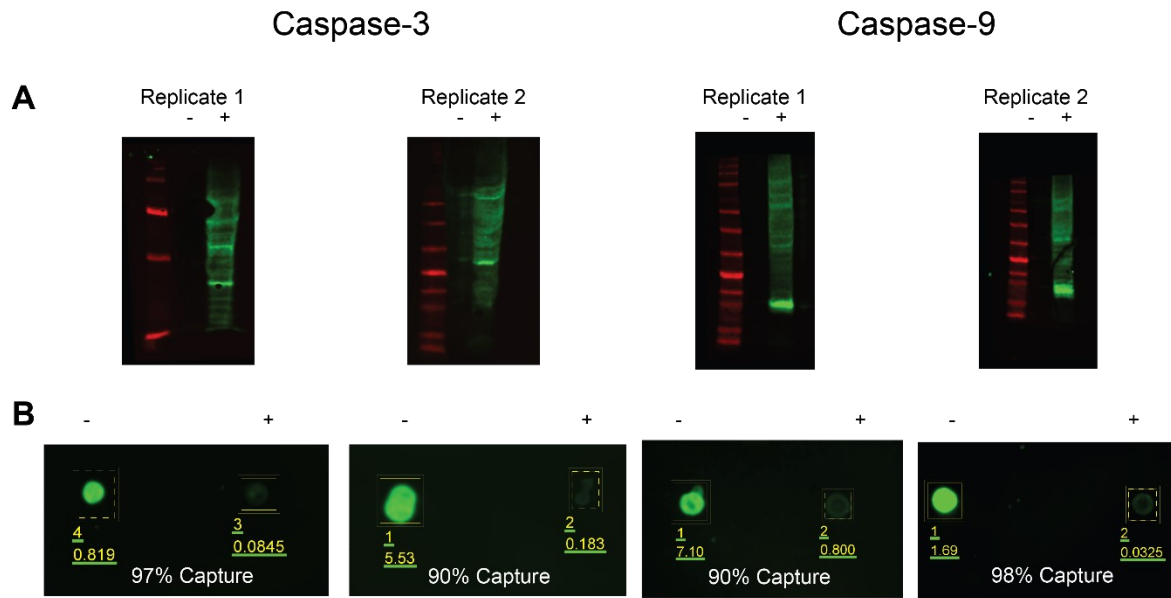
Fig. 3.8 N-terminomics labeling and capture efficiency. **A**. Western blots of pre (-) and post (+) labeling with subtiligase using TEVest6. The green signal corresponds to biotinylated proteins. **B**. Biotinylated proteins were captured on neutravidin beads. The dot blots show the pre (-) and post (+) capture. The disappearance of the signal indicates that biotinylated proteins were captured on beads, and ready to proceed for on-beads trypsin digestion and TEV release.
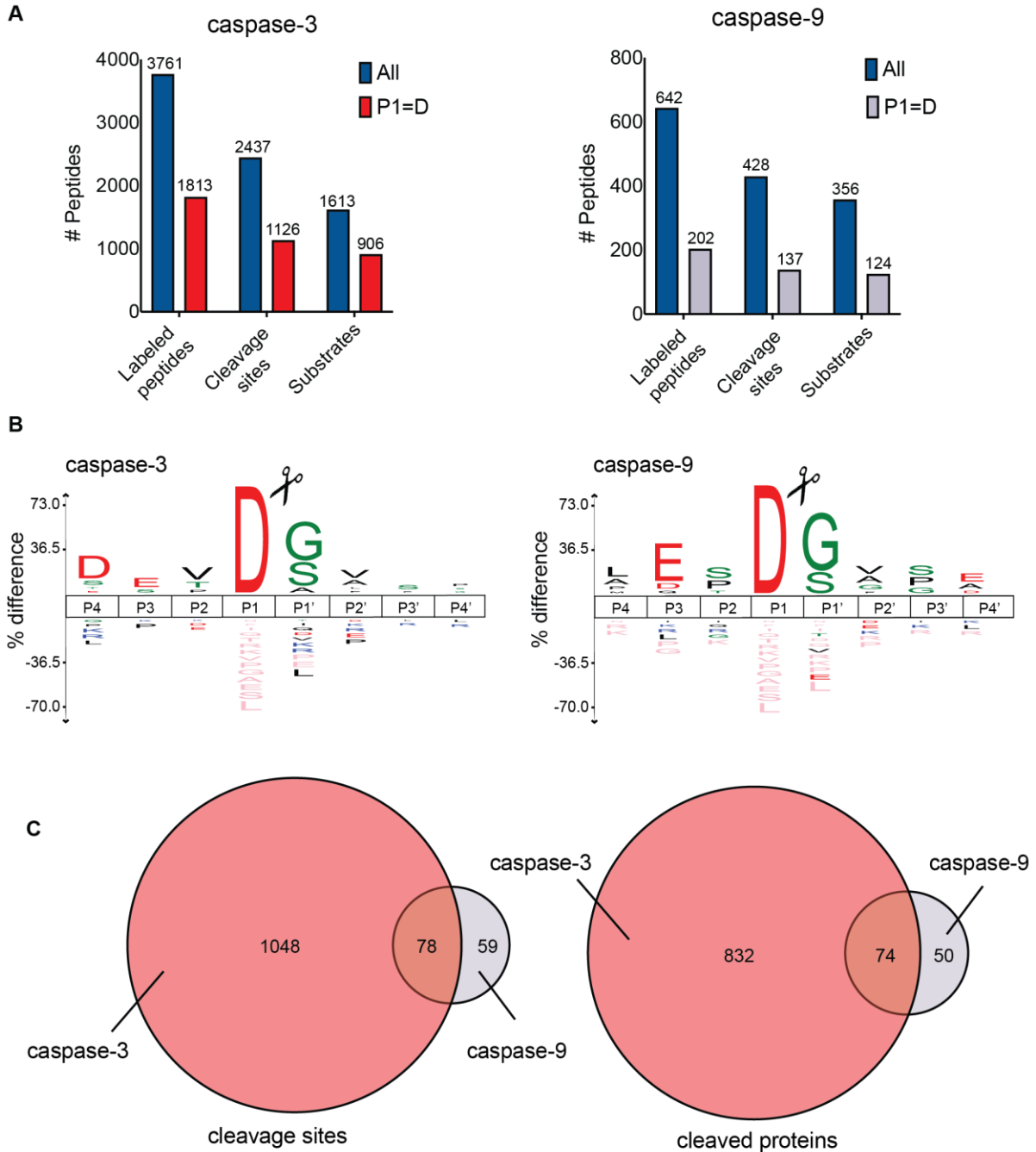
Fig. 3.9 Caspase-3 and -9 substrate discovery. **A**. We identified 906 caspase-3 putative protein substrates (1126 peptides featuring an aspartate at P1 position) and 124 caspase-9 protein substrates (137 peptides). Some of these substrate proteins are cleaved at multiple sites. **B**. The icelogo revealed a clear DEVD motif for caspase-3 and a LESD motif for caspase-9. **C**. Venn diagram showing the overlap between the peptide cleavage sites found in caspase-3 (red) and caspase-9 (orange), showing a set of cleavage sites unique to caspase-9.
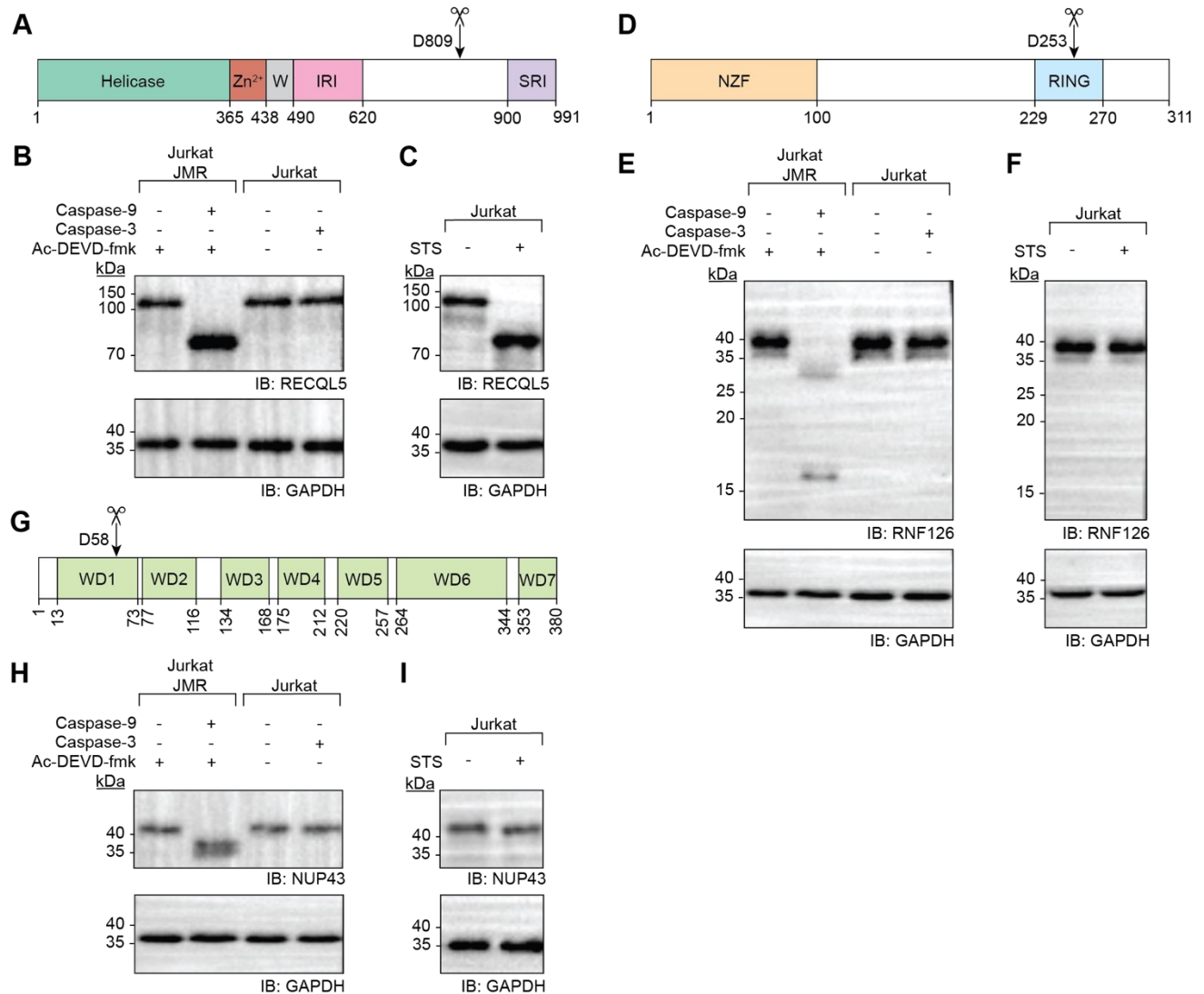
Fig. 3.10 Casapase-9-only substrate analysis via western blotting. RECQL5, RNF126, and NUP43 are the substrates of caspase-9 but not caspase-3. Staurosporine (STS) induced apoptosis results in the proteolysis of RECQL5 but not RNF126 and NUP43. **A.** Domain organization of RECQL5 comprises a helicase domain, zinc-binding domain, wedge domain, IRI domain, internal RNAPII-interacting domain, and SRI domain, Set2-Rpb1-interacting domain. Caspase-9 cleaves at D809 (N-terminomics). **B.** RECQL5 is cleaved by recombinant caspase-9 but not caspase-3. **C.** Treating Jurkat cells with 0.5 µM of STS for 3 hours revealed that RECQL5 is proteolyzed during apoptosis. **D.** RNF126 comprises a NZF domain, N-terminal zinc finger domain and RING (Really Interesting New Gene) domain. Caspase-9 cleaves at D253 (N-terminomics). **E.** RNF126 is cleaved by recombinant caspase-9 but not caspase-3. **F.** RNF126 is not cleaved during STS induced apoptosis suggesting caspase-9 has a putative non-apoptotic role. **G.** NUP43 has seven WD40 repeat (also known as Trp-Asp 40 repeat) domains. Caspase-9 cleaves at D58 (N-terminomics). **H.** NUP43 is cleaved by recombinant caspase-9 but not caspase-3. **I.** NUP43 is not cleaved during STS-induced apoptosis suggesting caspase-9 has a putative non-apoptotic role. As a loading control, each immunoblot was stripped using a stripping buffer, and then immunoblotted using an anti-GAPDH antibody. Each experiment was performed twice using two different samples on two different days.
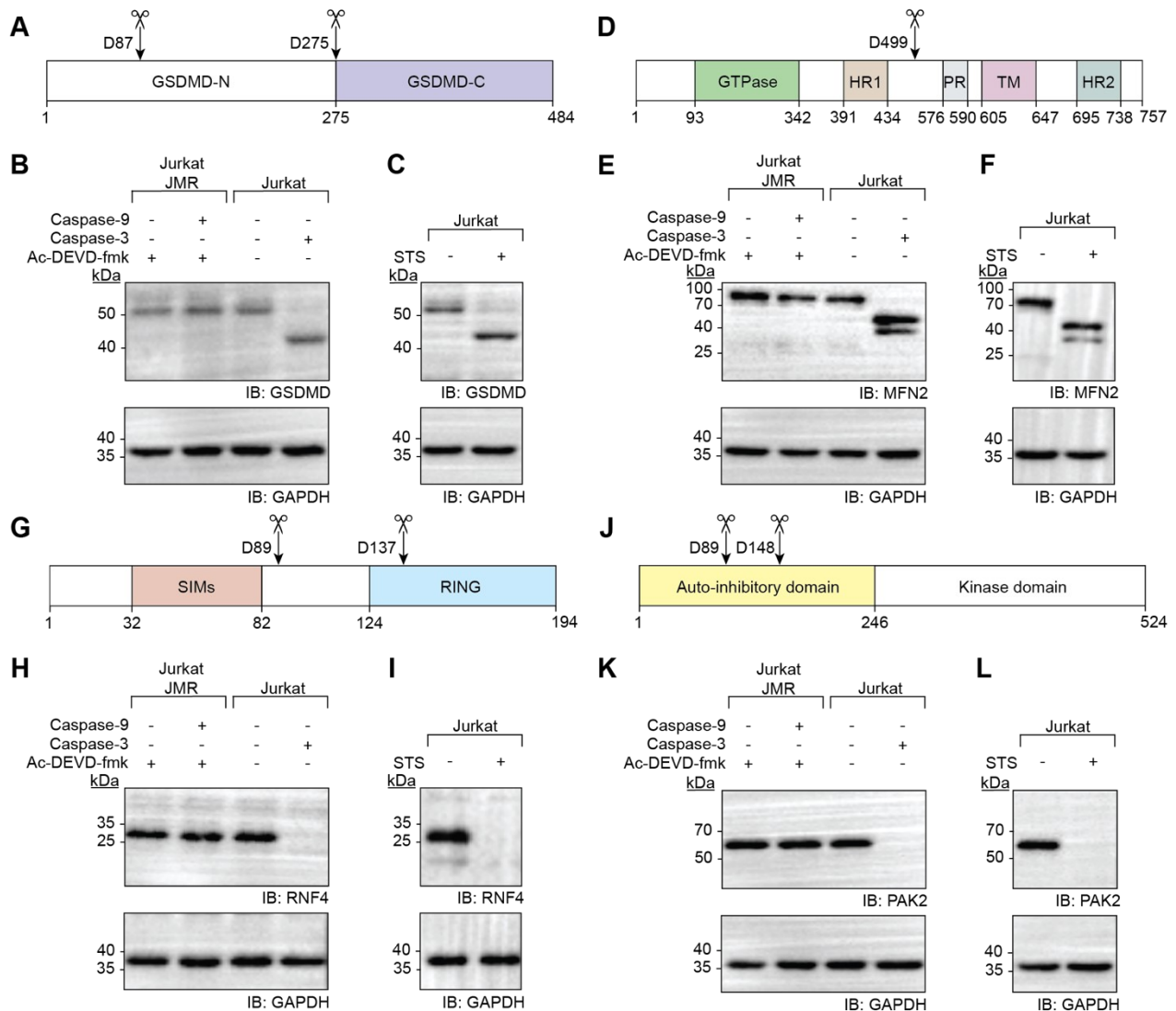
Fig. 3.11 Casapase-3-only substrate analysis via western blotting. GSDMD, MFN2, RNF4, and PAK2 are the substrates of caspase-3 but not caspase-9, and are proteolyzed during STS induced apoptosis. **A.** GSDMD is composed of two domains: GSDMD-N (N-terminal domain also known as pore forming domain) and GSDMD-C (C-terminal domain also known as auto-inhibitory domain). N-terminomics reveals caspase-3 cleavage at D87 and D275. **B.** GSDMD is cleaved by recombinant caspase-3 but not caspase-9. **C.** Jurkat cells treated with 0.5 µM of STS for 3 hours revealed that GSDMD is proteolyzed during apoptosis. **D.** MFN2 has a GTPase domain, HR1 (first coiled-coil heptad-repeat region), PR (proline-rich) domain, TM (transmembrane) domain, and HR2 (second coiled-coil heptad-repeat region) domain. N-terminomics revealed caspase-3 cleavage at D499. **E.** MFN2 is cleaved by recombinant caspase-3 but not caspase-9. **F.** MFN2 is cleaved during STS-induced apoptosis. **G.** RNF4 has four tandem SIMs [SUMO (small ubiquitin-like modifier)-interaction motifs] in the N-terminal domain between residues 32-82, and a RING domain at the C-terminal. N-terminomics revealed caspase-3 cleavage at D89 and D137. **H.** RNF4 is cleaved by recombinant caspase-3 but not caspase-9. **I.** RNF4 is cleaved during STS-induced apoptosis. **J.** PAK2 is composed of two domains: Auto-inhibitory (regulatory) and kinase domains. N-terminomics revealed caspase-3 cleavage at D89 and D148. **K.** Immunoblot analysis resembled N-terminomics data that PAK2 is cleaved by recombinant caspase-9 but not caspase-3. **L.** PAK2 is proteolyzed during STS-induced apoptosis. As a loading control, each immunoblot was stripped using a stripping buffer, and then immunoblotted using an anti-GAPDH antibody. Each experiment was performed twice using two different samples on two different days.

72
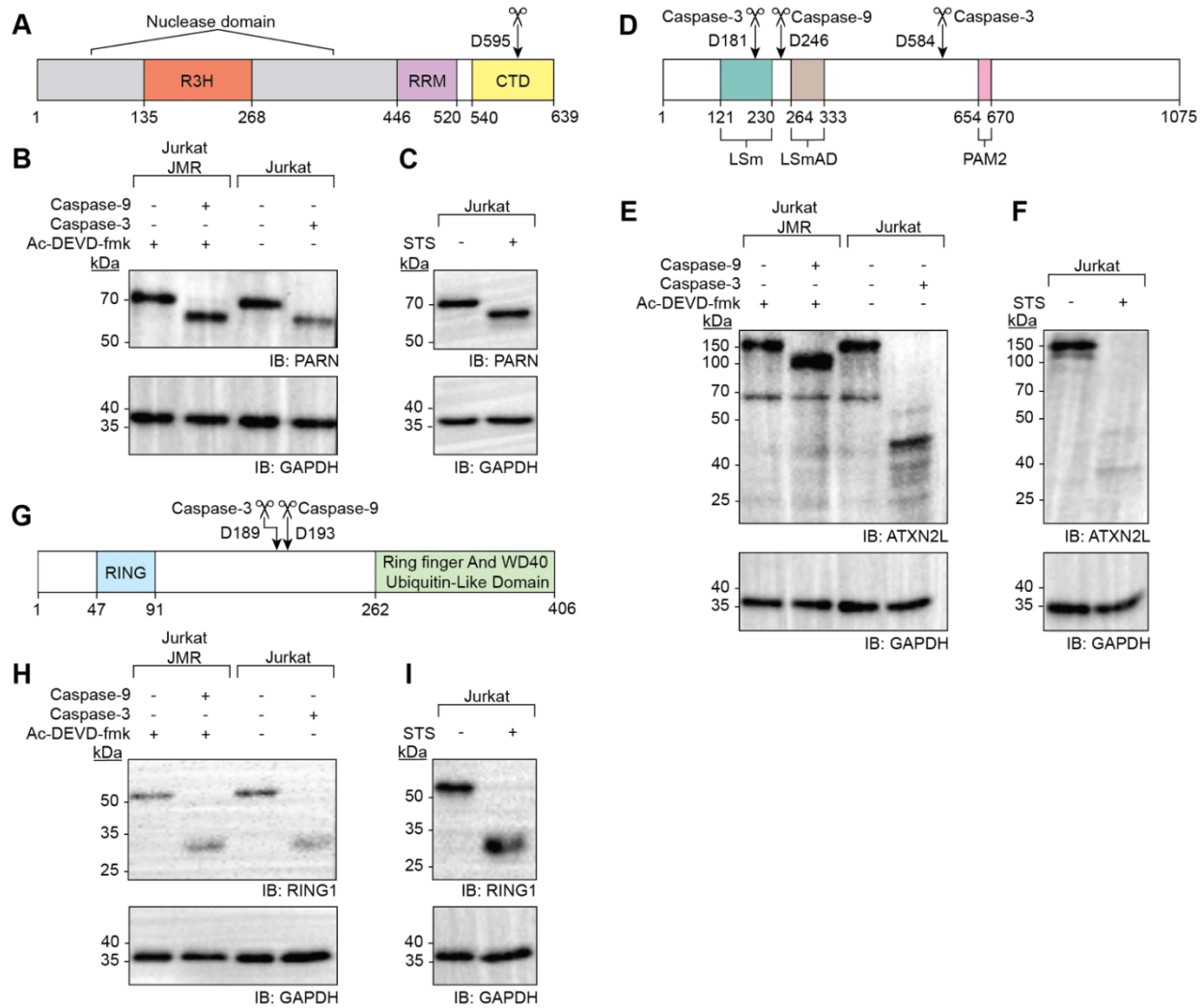
Fig. 3.12 Western blotting analysis of substrates of both caspases-3 and -9. PARN, ATXN2L, RING1 are the substrates of both caspase-9 and -3, and they are proteolyzed during STS induced apoptosis. **A.** PARN is composed of a catalytic nuclease domain (gray regions), R3H domain, RRM (RNA recognition motif) domain, and CTD, C-terminal domain. Caspase-9 cleaves at D595 (N-terminomics). **B.** PARN is cleaved by recombinant caspase-9 and -3. **C.** Treating Jurkat cells with 0.5 µM of STS for 3 hours revealed that PARN is proteolyzed during apoptosis. **D.** ATXN2L comprises a LSm (like-Sm protein) domain, LSmAD (LSm associated domain) and PAM2 (PABP-interacting motif 2) domain. N-terminomics revealed that caspase-9 cleavage occurs at D246, and caspase-3 cleavage occurs at D181 and D584. **E.** ATXN2L is cleaved by recombinant caspase-9 and -3. **F.** ATXN2L is cleaved during STS induced apoptosis. **G.** RING1 comprises a RING domain, and a Ring finger and WD40 Ubiquitin-Like Domain. N-terminomics revealed that caspase-9 cleavage occurs at D193, and caspase-3 cleavage occurs at D189. **H.** RING1 is cleaved by recombinant caspase-9 and -3. **I.** RING1 is cleaved during STS-induced apoptosis. As a loading control, each immunoblot was stripped using a stripping buffer, and then immunoblotted using an anti-GAPDH antibody. Each experiment was performed twice using two different samples on two different days.

73
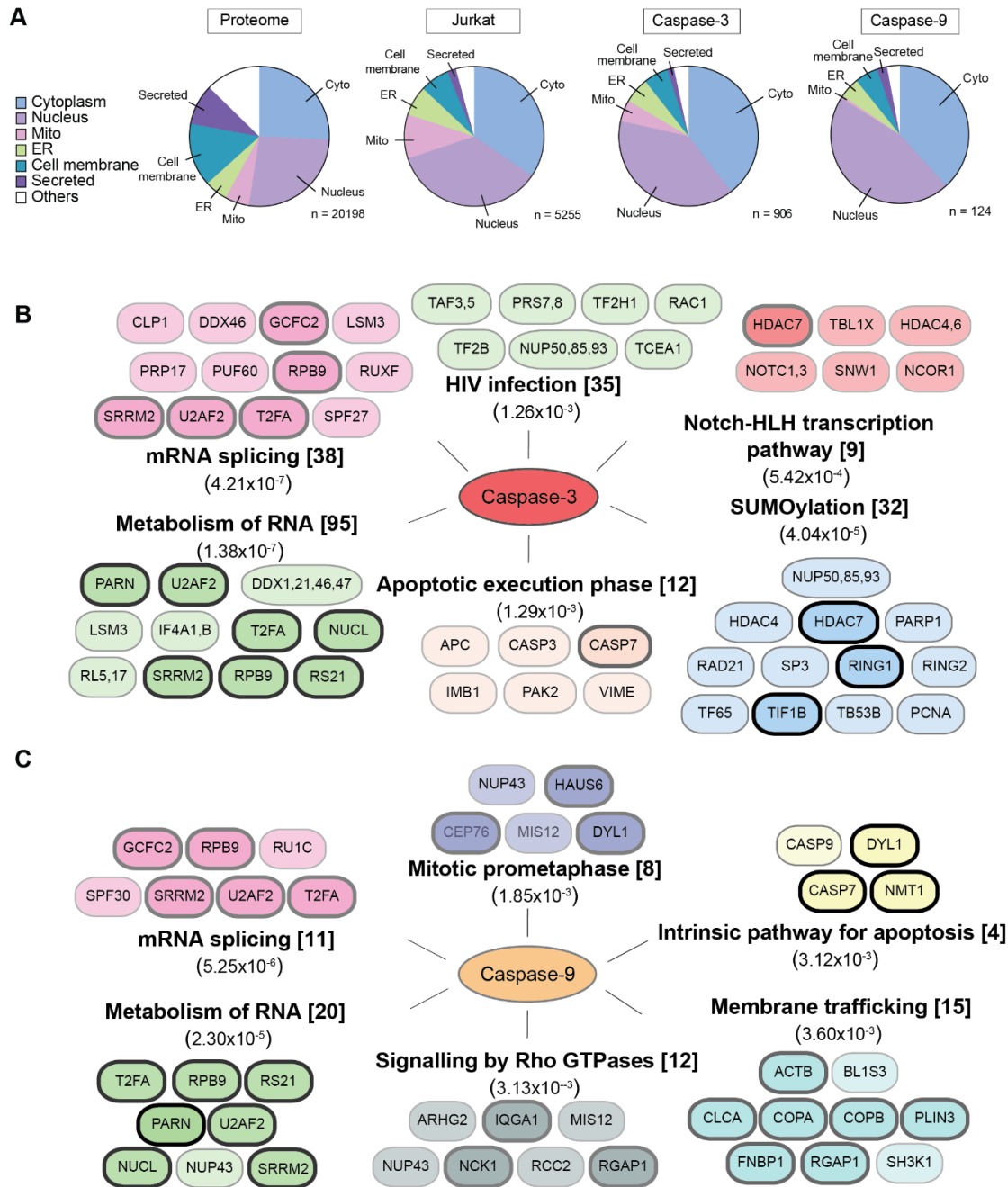
Fig. 3.13 Substrate subcellular localization and pathway enrichment in caspase-3 and caspase-9 *reverse* experiments. A. Subcellular localization of caspase-3 and caspase-9 substrates compared with those of the proteome, as well as a non-enriched Jurkat lysate proteomics experiment. **B-C.** Reactome (https://reactome.org) analysis of cellular pathways enriched in either caspase-3 or caspase-9 experiments, with their p-values in parentheses. Bolded parentheses indicate the number of proteins from the pathway recovered in the *reverse* N-terminomics datasets. Selected examples of pathway members are shown. Bolded outlined proteins indicate substrates found in both caspase-3 and caspase-9 *reverse* N-terminomics datasets.
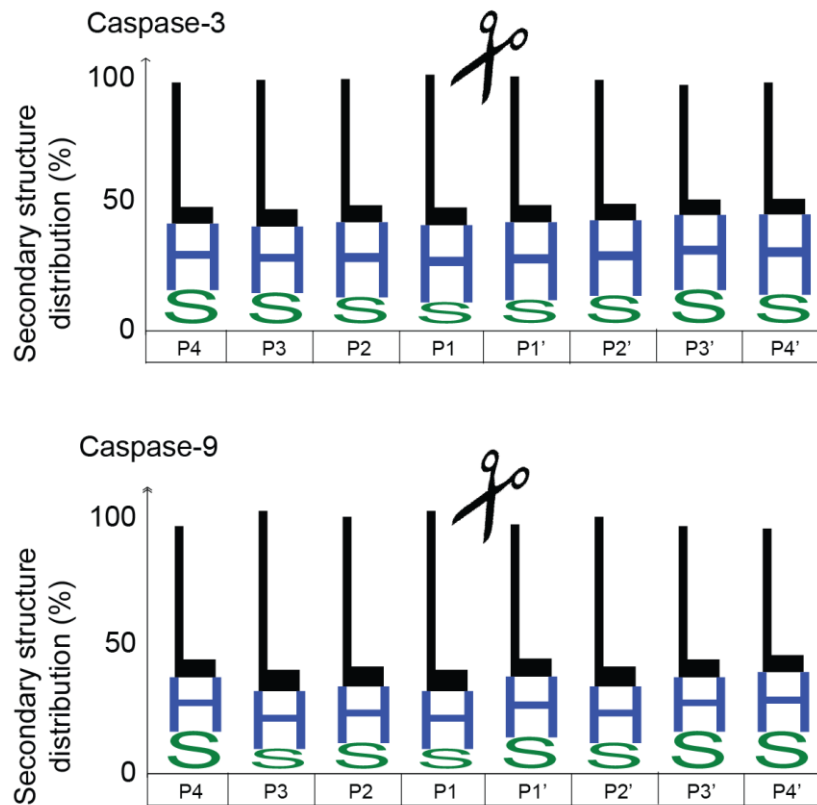
Fig. 3.14 Caspase-3 and caspase-9 cleave in secondary structures. The secondary structure distribution of the caspase cleavage sites identified in our discovery experiment of the residues from P4 to P4' are located in (caspase-3/caspase-9): 58/65% loop (L), 31/23% in alpha-helices (H), and 11/12% in beta-sheets (S). The structural data was extracted from known structures, 373 for caspase-3 and 40 for caspase-9. The secondary structure information was obtained from Barkan et al. (2010), where all possible caspase cleavage sites in the human proteome were reported.
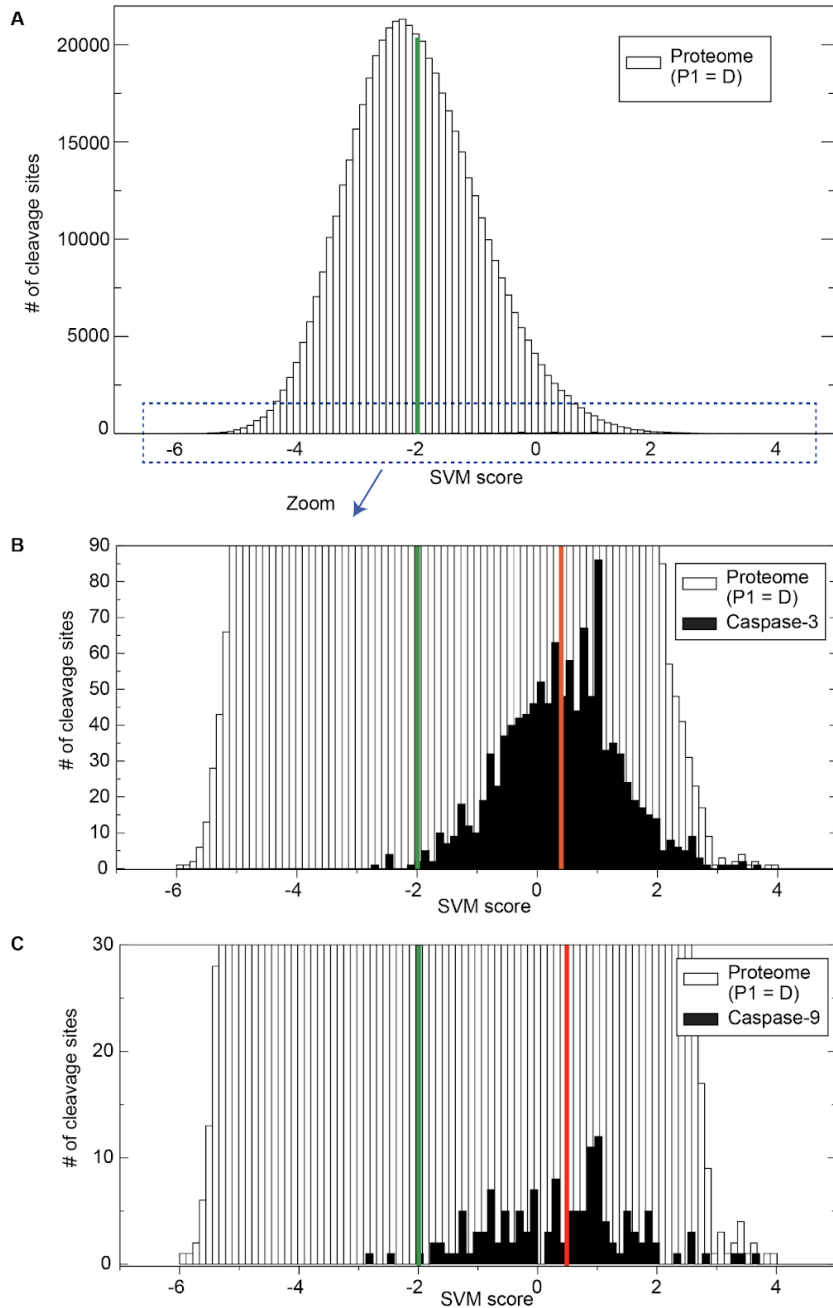
Fig. 3.15 Observed caspase-3 and caspase-9 cleavage sites correlate well with predictions.
A. Prediction of caspase cleavage sites for every tetrapeptide in the human proteome with an aspartate at P1 position (Support Vector Machine score, Barkan et al., 2010). The SVM average is 1.99 and shown in green. **B-C.** Comparison between the 1126 and 137 unique N-termini cleavage sites for caspase-3 and caspase-9 observed in our study with SVM average of 0.43 and 0.40, respectively.

C1C12 - undifferentiated
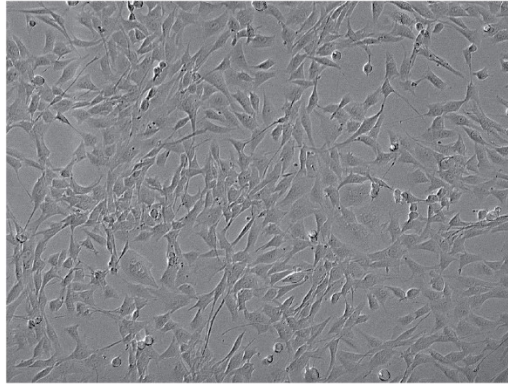
Typical differentiation   20 µM z-DEVD-fmk differentiation

Day 1
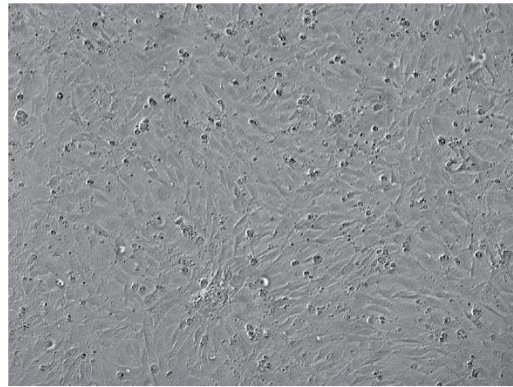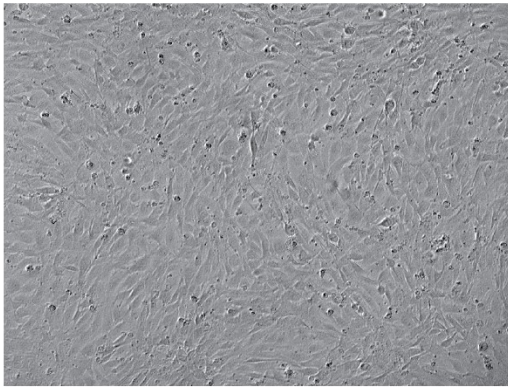
Day 4
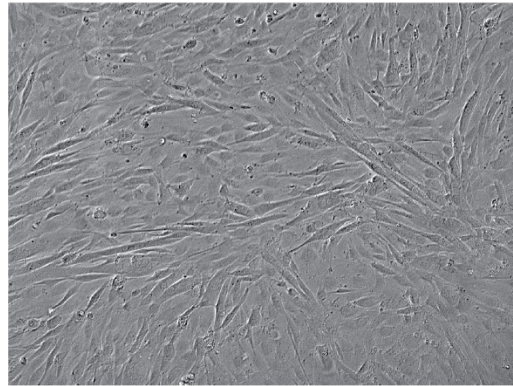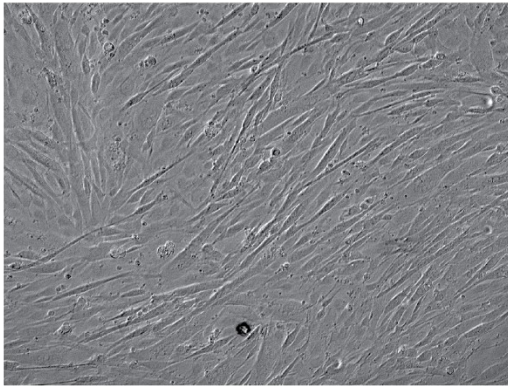
Fig. 3.16 Images of cell morphology of C2C12 cultured myoblasts upon typical and caspase-3-inhibited differentiation. Differentiating cells were imaged every day immediately following their daily media exchange. On Day 4, differentiated cells were harvested. Morphologically, the dishes do not appear to be significantly different, however the culture dish incubated with DEVD-fmk exhibited contained significantly more dead cells in media than the non-inhibited culture dish.
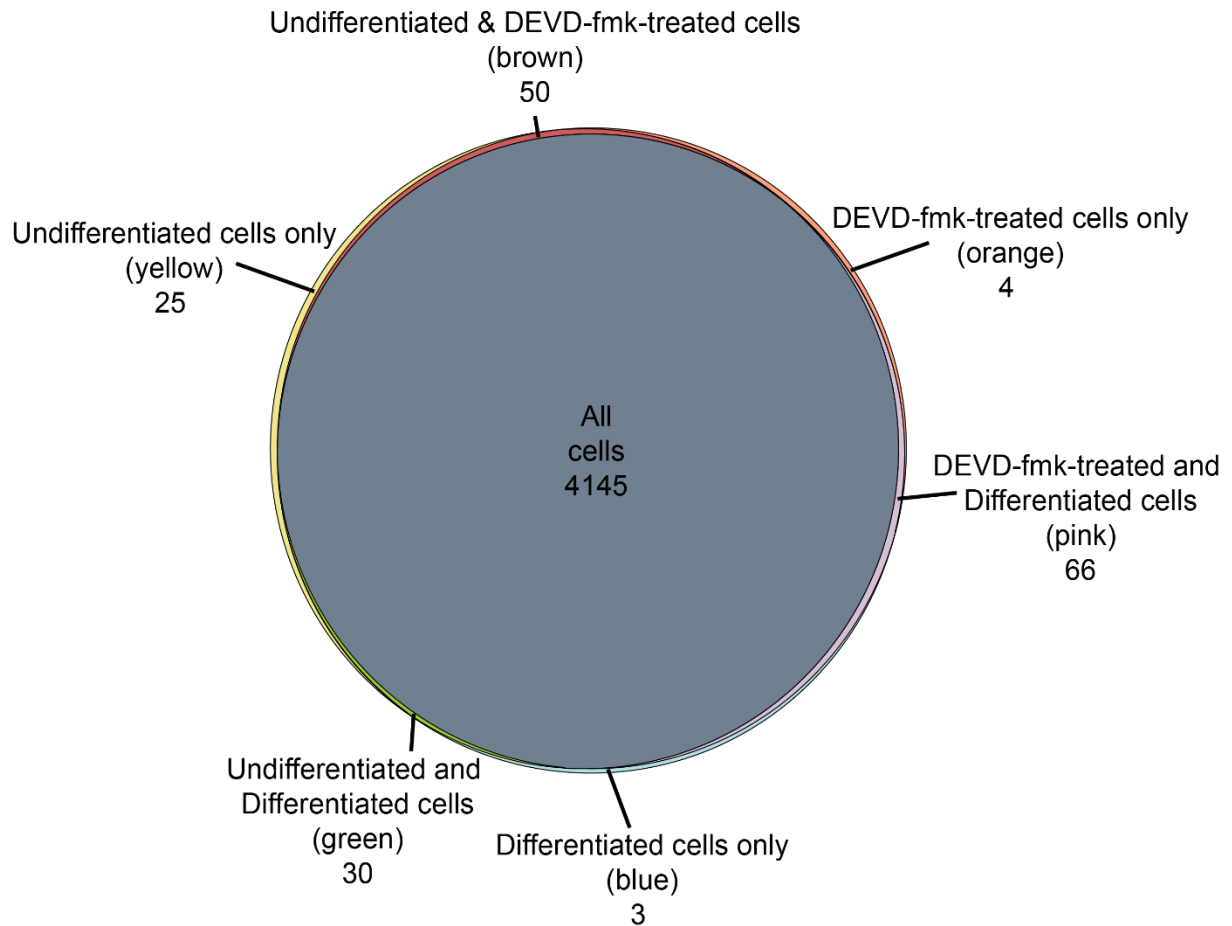
Fig. 3.17 Venn diagram showing overlaps between the proteins found in C2C12 global proteomics experiment. Diagram shows unique proteins (Undifferentiated cells in yellow, differentiated cells in blue and DEVD-fmk-treated cells in orange), protein overlaps between two conditions (Undifferentiated and differentiated in green, Undifferetiated and DEVD-fmk-treated in brown, and DEVD-fmk-treated in orange), and proteins found in all conditions (grey). The vast majority of proteins are found in all conditions.
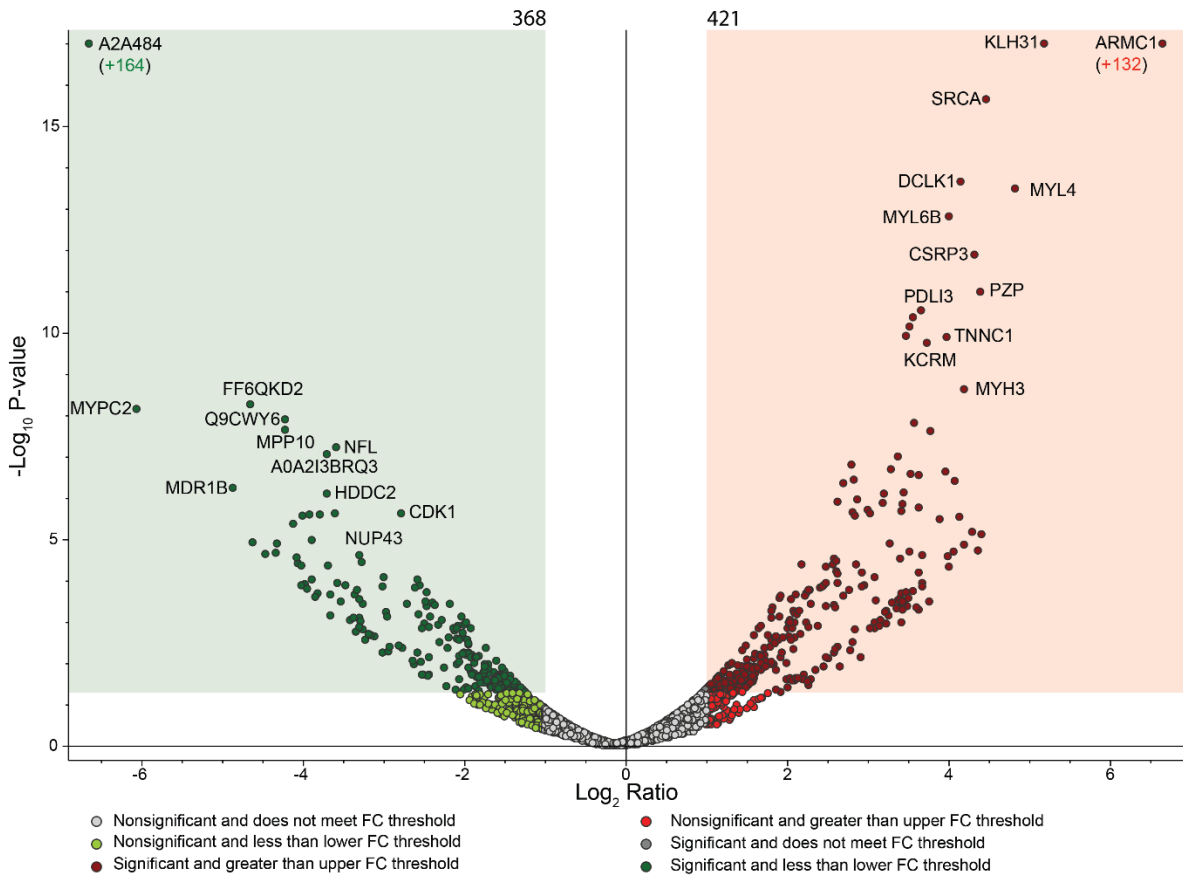
Fig. 3.18 Volcano plot of global proteome changes upon differentiation of C2C12 cells from myoblasts to myotubes. The -$\log_{10}$(p-value) is plotted against the $\log_2$(abundance ratio). The abundance ratio denotes the fold change between the sample sets, while the p-value denotes the statistical significance of this change compared to background. All colored datapoints exhibit at least a two-fold enrichment. The highlighted regions indicates either a two-fold enrichment in the differentiated samples (red) or in the undifferentiated samples (green) based on the abundance ratio, as well as a p-value below 0.05. Uniprot IDs are labeled for the most differentially expressed proteins. There were 368 enriched proteins in undifferentiated cells (green), while there were 421 enriched proteins in differentiated cells (red). Within these enriched proteins, there were 164 unique to undifferentiated cells (green text), and 132 unique to differentiated cells (red text).
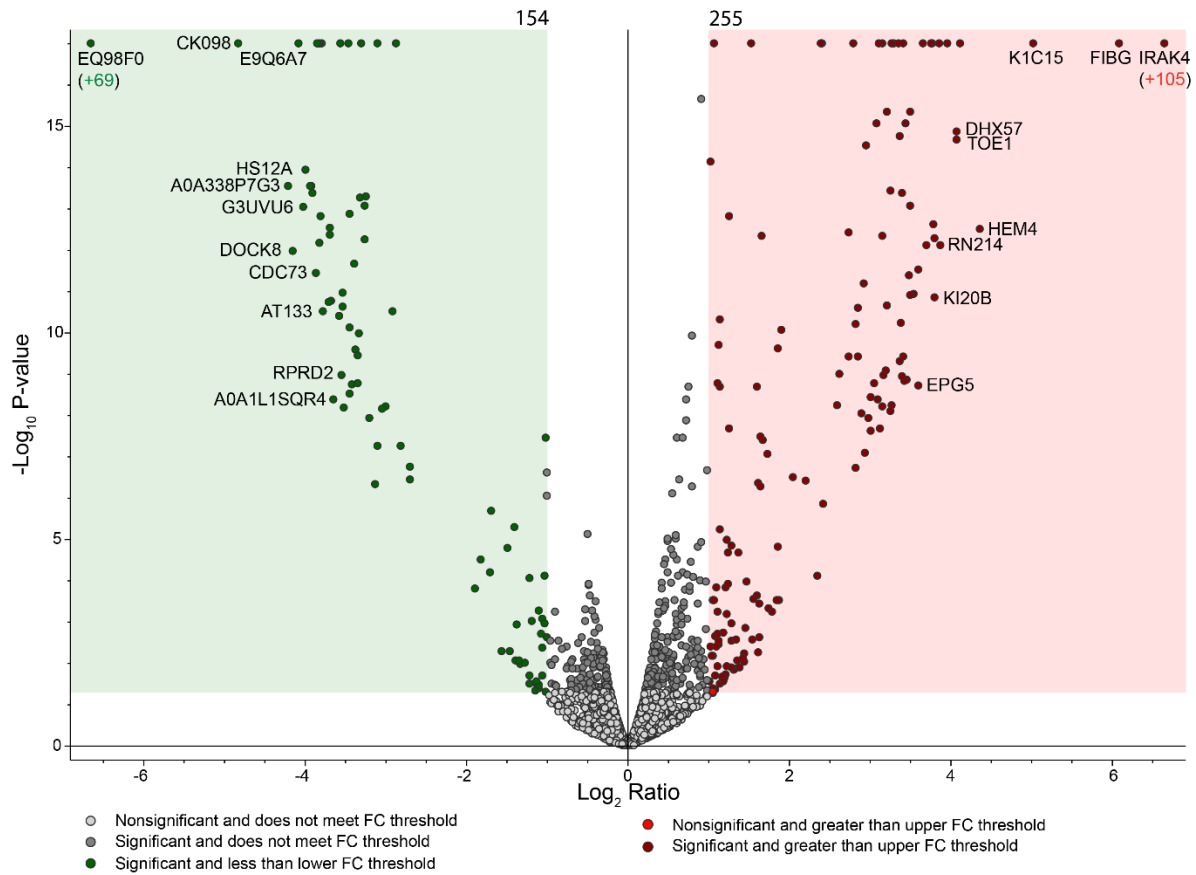
Fig. 3.19 Volcano plot of global proteome changes between serum-withdrawal of C2C12 cells with and without DEVD-fmk treatment. As in **Fig. 3.18**, the $\log_{10}$(p-value) is plotted against the $\log_2$(abundance ratio). All colored data points exhibit at least a two-fold enrichment. The highlighted regions indicates both a two-fold enrichment in the DEVD-fmk-treated cells (red) or in the differentiated cells (green) based on the abundance ratio, as well as a p-value below 0.05. There were 255 enriched proteins in the DEVD-fmk-treated cells (red), and 154 in the differentiated cells (green).
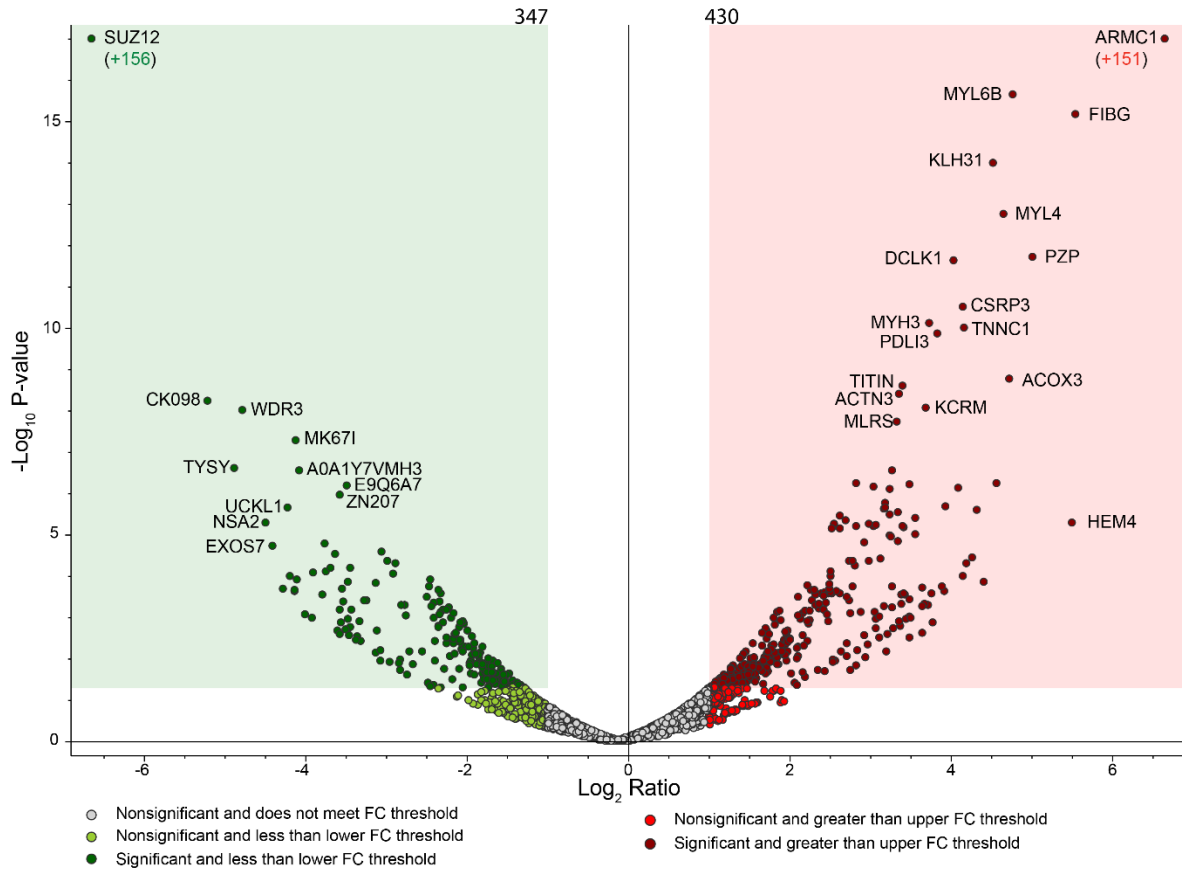
Fig. 3.20 Volcano plot of global proteome changes between serum-withdrawal of C2C12 cells with DEVD-fmk treatment and undifferentiated C2C12 cells. As in **Fig. 3.18**, the $\log_{10}$(p-value) is plotted against the $\log_2$(abundance ratio). All colored data points exhibit at least a two-fold enrichment. The highlighted regions indicates both a two-fold enrichment in the DEVD-fmk-treated cells (red) or in the undifferentiated cells (green) based on the abundance ratio, as well as a p-value below 0.05. There were 430 enriched proteins in the DEVD-fmk-treated cells (red), and 347 in the undifferentiated cells (green).
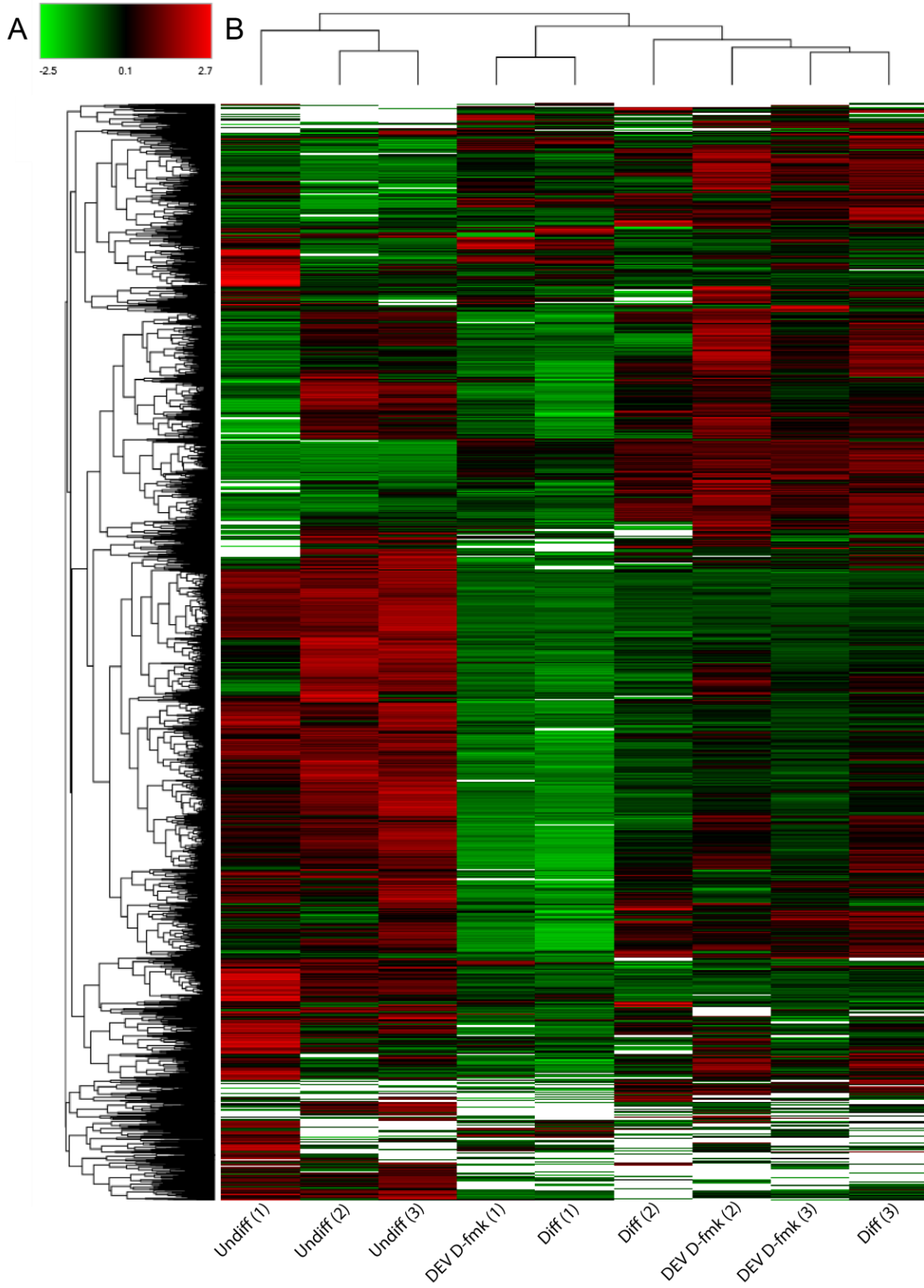
Fig. 3.21 C2C12 preliminary experiment label-free quantitation heat map. A. Each band on the heat map corresponds to a protein. In the green-red scale, enriched proteins are in red, while de-enriched proteins are green. Proteins with no enrichment or de-enrichment are in black, while proteins absent from a sample are in white. Samples with statistical similarity are clustered together on the heatmap, determining the sample order in the heatmap readout. This is also demonstrated with the dendrogam linkages in **B**. The three undifferentiated C2C12 replicates are listed first. The differentiated replicates and DEVD-fmk-treated replicates appear in a mixed order.
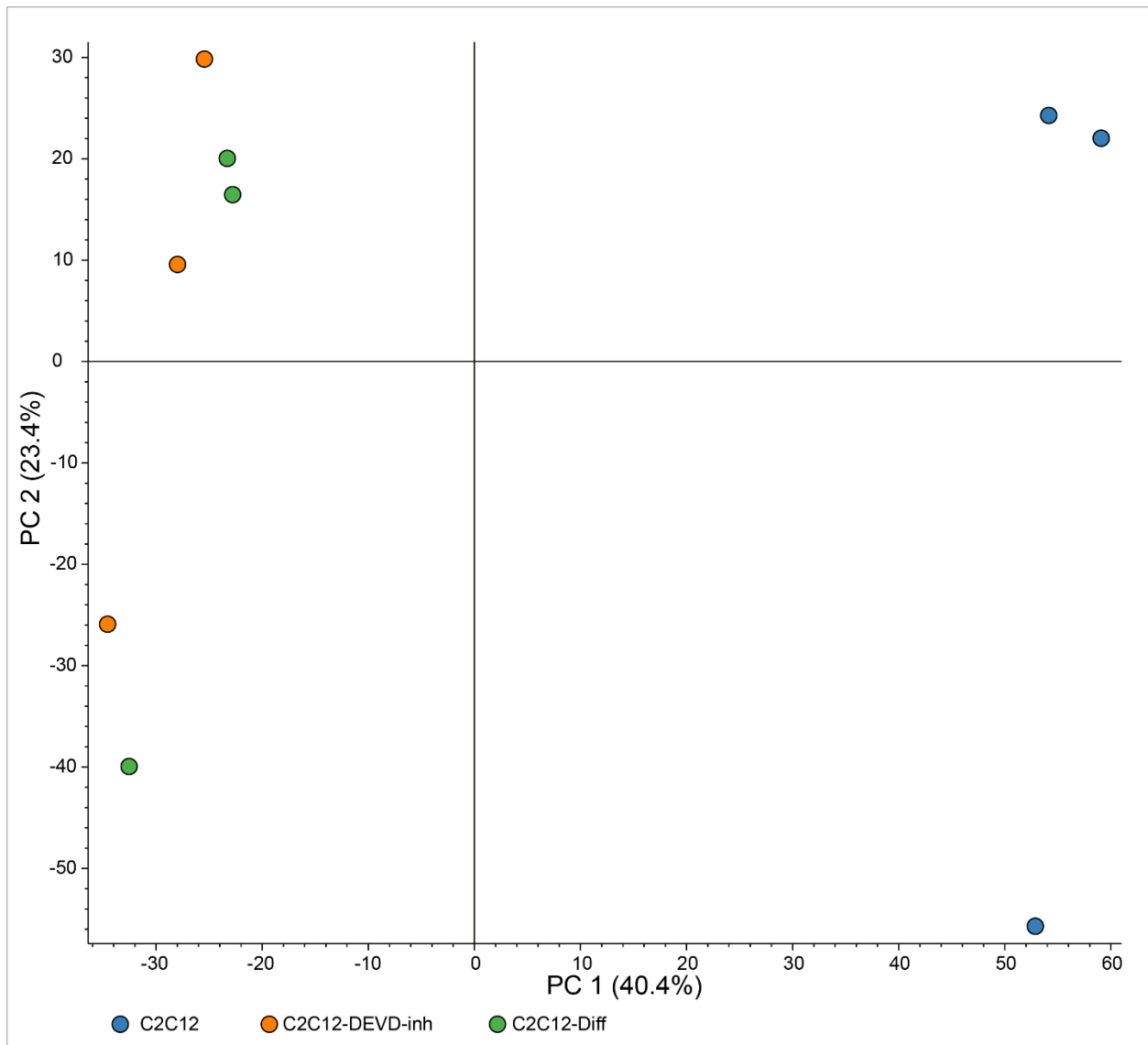
Fig. 3.22 PCA plot of C2C12 label-free quantitation replicates. Plotting the principal component 1 (PC1 - X-axis) and principal component 2 (PC2 - Y-axis) of all experimental replicates in C2C12 label-free proteomics experiment. The principal components are based on protein abundance ratios, with the percentage values corresponding to the proportion of sample variance being explained by this principal component. Undifferentiated replicates are in blue, differentiated replicates are in orange and DEVD-fmk-treated replicates are in green. Differentiated replicates and DEVD-fmk-treated replicates cluster relatively close together around PC1 scores of -35 to -20, while undifferentiated replicates cluster around PC1 scores of 50 to 60.

Table 3.1 PILS experiment peptide recovery comparisons between old TEV protease stock and purified stock

Experiment	Protein recovery	Peptide recovery	Abu-labeled peptide recovery
PILS - Old TEV stocks	488	2995	700
PILS - Newly purified TEV stocks	491	2979	695

Table 3.2 The role of caspase-9 substrates in regulating apoptosis

	Protein name	Anti-apoptotic	Evidence for implication in apoptosis/non-apoptosis, OR prior caspase cleavage	References & N-terminomics cleavage sites
1	7SK snRNA methylphosphate capping enzyme	✓	GB-caspase-3 activity increased in cells with 7SK snRNA; cell death assay revealed higher apoptosis index when 7SK snRNA was over-expressed	Ref.[4] SDCD^{178}↓S
2	ATP-dependent DNA helicase Q5	✓	RECQL-5 deficient cells resulted in replication dependent apoptosis	Ref.[5] GEED^{809}↓G
3	Calumenin	✓	Overexpression of calumenin reduced ER stress and apoptosis in tunicamycin treated cardiomyocytes	Ref.[6] YSHD^{221}↓G
4	Cell cycle control protein 50A		Cdc50A forms a complex with ATP11C to function as a flippase. Caspase cleavage (specific caspase unknown) of ATP11C results in reduction of the flippase. This results in the exposure of PdtSer as a signal of "eat me" in apoptosis	Ref.[7] DEVD^{12}↓G
5	Chromosome transmission fidelity protein 18 homolog	✓	Chtf18−/− lead to an increase in apoptotic cells	Ref.[8] PQVD^{869}↓G
6	Coatomer subunit beta'	✓	Regulates cell cycle, cell proliferation and apoptosis in PC-3 cells	Ref.[9] QELD^{854}↓G
7	Cytoplasmic protein NCK1	✓	NCK plays an antiapoptotic role following UV treatment (when depleted, apoptosis occurred faster)	Ref.[10] SVPD^{88}↓S
8	Eukaryotic translation initiation factor 4 gamma 1		Cleaved by caspase-3 during inhibition of translation in apoptotic cells. Also cleaved in apoptotic cells and degraded in human lymphoma	Ref.[11–13] LVDD^{1049}↓G

			cells in apoptosis	
9	Glycylpeptide N-tetradecanoyltransferase 1		Caspase-3 cleavage at D72. Cleavage in apoptosis leads to cytosolic relocalization – it is 64% membrane-bound prior to cleavage	Ref.[14] SETD^{72}↓S
10	Heterogeneous nuclear ribonucleoprotein K		Cleavage in apoptosis found in the nucleus and cytosol in both nonapoptotic and apoptotic cells, with an additional cleavage site in the mitochondria found in fas-induced apoptosis cells	Ref.[15] LESD^{128}↓A
11	Histone deacetylase 7		Cleaved by caspase-8 to abolish transcription repressor function (in vitro, HDAC7 was cleavable by caspase-9.	Ref.[16] LETD^{412}↓G
12	NEDD4-binding protein 1		Cleaved by caspase-8 and allows inflammatory cytokines to be produced. Reference is for mouse N4BP1 where caspase-8 cleaves at LETD^{488}/G	Ref.[17] PETD^{490}↓G
13	Nucleobindin-2		Caspase cleavage sites between 235-255 for caspase-3,-6,-7,-8,-9,and weakly -10	Ref.[18] EETD^{237}↓G VNSD^{258}↓G
14	Nucleolin	✓	Suppresses apoptosis by inhibiting Fas ligand binding; knockdown of nucleolin enhances caspase-3 activity	Ref.[19,20] EEDD^{40}↓S
15	Nucleoporin Nup43		Specifically not cleaved in apoptosis, unlike many other nucleoporin proteins	Ref.[21] LDSD^{58}↓G
16	Poly(A)-specific ribonuclease PARN	✓	PARN knockout in cells induces apoptosis in p53-dependent manner. When PARN is knocked out in p53 null cells, no apoptosis occurs. This shows PARN interacts	Ref.[22] EQTD^{595}↓S

			with p53	
17	Probable 28S rRNA (cytosine(4447)-C(5))-methyltransferase	✓	NOP2 deficient embryos induces apoptosis	Ref.[23] EEAD[207]↓G
18	Prothymosin alpha		Cleaved by caspase-3 at DDVD[99], AAVD[6], and NGRD[31]	Ref.[24] -MSD[3]↓A
19	Rac GTPase-activating protein 1	✓	Overexpression of Racgap1 decreases apoptosis; silencing racgap1 increases activity of caspase-7 and -9	[24,25] TETD[273]↓S
20	Ras GTPase-activating-like protein IQGAP1	✓	IQGAP1 silencing induces apoptosis, IQGAP1 helps in activation of caspase-1	Ref.[26,27] DEVD[8]↓G
21	Splicing factor U2AF 65 kDa subunit		A caspase cleaved U2AF in early apoptosis at MTPD[128]↓G, but it was not possible to know which caspase is cleaving U2AF	Ref.[28] MTPD[128]↓G
22	Structural maintenance of chromosomes protein 4		Many members of a complex are cleaved by the same caspase	Ref.[29] PSPD[24]↓G
23	Synapse-associated protein 1		"amino acids surrounding the putative caspase-1 cleavage site (D278) showed an additional nearby caspase-3/-7 site (DXXD) (FVSD[278]↓AFD[281]↓AC)". We saw cleavage at the same place FVSD[278]↓A. Caspase-1 and -9 are both cleaving the same site. SYAP1 proteolysis is not observed in apoptosis.	Ref.[30] FVSD[278]↓A
24	TBC1 domain family member 4 (aka AS160)		Cleaved in apoptosis. Involved in trafficking; it is a Rab GTPase-activating protein	Ref.[31] EEAD[272]↓G
25	Tubulin alpha-1B chain		Caspase-mediated cleavage of actin and tubulin is a common feature and sensitive	Ref.[32] IQPD[33]↓G

			marker of axonal degeneration in neural development and injury	
26	Tyrosine-protein kinase ZAP-70	✓	ZAP70 is required for Fas ligand-mediated PLC-γ1 activation and calcium release in Jurkat cells	Ref.[33] LNSD^{290}↓G
27	U2 snRNP-associated SURP motif-containing protein		Component of the spliceosome. Cleaved by many caspases, and other spliceosomal components are targets of caspase-3 as well	Ref.[34] DDLD^{737}↓G EELD^{704}↓G DDLD^{695}↓G EDVD^{712}↓G
28	Ubiquitin carboxyl-terminal hydrolase 5		Cleaved in apoptosis. It is also suggested that USP5 inhibition may be effective in inducing apoptotic thresholds to enhance responsiveness to TRAIL	Ref.[35] SAAD^{782}↓S

Table 3.3 Caspase-3 and caspase-9 N-terminomics substrates selected for deep interrogation.

Uniprot ID	Protein Name	Cleavage site (P1=D)	Casp3	Casp9	DegraBase	Localization
RECQ5	ATP-dependent DNA helicase Q5	GEED^{809}↓GAGG		+		C
NUP43	Nucleoporin Nup43	LDSD^{58}↓GGFE		+		N
RN126	E3 ubiquitin-protein ligase RNF126	LFHD^{253}↓GCIV		+		C
GSDMD	Gasdermin-D	DAMD^{87}↓GQIQ	+		+	C
		FLTD^{275}↓GVPA	+		+	
MFN2	Mitofusin-2	DMID^{499}↓GLKP	+			M
RNF4	E3 ubiquitin-protein ligase RNF4	DHAD^{89}↓SCVV	+			N, C
		ICMD^{137}↓GYSE	+			
PAK2	Serine/threonine-protein kinase PAK 2	VGFD^{89}↓AVTG	+		+	C
		PEKD^{148}↓GFPS	+		+	
PARN	Poly(A)-specific ribonuclease PARN	EQTD^{595}↓SCAE	+	+		N, C
ATX2L	Ataxin-2-like protein	DIVD^{181}↓TMVF	+			C, CM
		LESD^{246}↓MSNG		+		
		KEVD^{584}↓GLLT	+		+	
RING1	E3 ubiquitin-protein ligase RING1	VSSD^{189}↓SAPD		+	+	N
		SAPD^{193}↓SAPG	+			N

* complete datasets available online in Supplementary File S1.
** N= nucleus, C= cytoplasm, CM= cell membrane, M= mitochondrion

CHAPTER FOUR

DISCUSSION

4.1 TEV protease and caspase-3 purification

The preliminary protease purifications proved successful, allowing us to continue with the main study. However, both the TEV protease (**Fig. 3.1**) and the caspase-3 purification (**Fig. 3.4**) resulted in slightly impure purification products. The TEV protease aliquots retained their MBP carrier, and the caspase-3 purification retained a significant amount of nonspecific binding. For the purposes of *reverse* N-terminomics, neither of these outcomes pose a significant problem. They do not interfere with the experiment and mass spectrometry analysis we complete at the end of the experiment will only report peptides that match the human proteome. In the future, more chromatography steps should be taken to further purify these proteases for broader use. For the TEV protease, a longer elution gradient is likely sufficient to separate MBP from the protease. For caspase-3, anion exchange chromatography or size exclusion chromatography could prove helpful. The purified TEV protease was still able to cleave TEVest6 on labeled lysates. leading to very similar signal disappearance on streptavidin blots (**Fig. 3.3**) and peptide recovery on LC-MS/MS (**Table 3.1**). The impurity of the caspase-3 purification did not affect its activity, as determined by the Ac-DEVD-AFC assays (**Fig. 3.5**). The k_{cat}/K_m was similar to prior caspase-3 stocks in the lab (10 nM of prior stocks had a k_{cat}/K_m of 5.76 x 10^5 M^{-1}s^{-1}, our purification had a k_{cat}/K_m of 6.28 x 10^5 M^{-1}s^{-1}) (**Fig. 3.5**). Based on these results, we proceeded with *reverse* N-terminomics.

4.2 Caspase-3 and caspase-9 *reverse* N-terminomics

In the *reverse* N-terminomic study, we sought to discover and compare all possible caspase substrates cleaved by the executioner caspase-3 and the initiator caspase-9. We report 906 and 124 protein substrates targeted by caspase-3 and caspase-9, respectively. Of the 124 caspase-9 substrates, 50 of them were not observed in the caspase-3 experiment. Our results clearly show that caspase-3 and caspase-9 possess both common and distinct pools of protein substrates. We found that some of these substrates are cleaved during apoptosis, while others are not, suggesting new non-apoptotic roles in the biology of these two caspases.

A strength of the *reverse* N-terminomics approach is that it allows identification of new substrates that could not be identified by other means. GSDMD, MFN2, RNF4, and PAK2 are all substrates of caspase-3, but not caspase-9 (**Table 3.3** and **Fig. 3.11**). Neither RNF4 nor MFN2 had been observed as apoptotic substrates previously. GSDMD was cleaved by caspase-3 (**Table 3.3** and **Fig. 3.11**) and showed detectable cleavage product in apoptotic cells (**Fig. 3.11**), consistent with the DegraBase. In our immunoblot analyses, full length PAK2 and RNF4 were fully degraded

when incubated with caspase-3 and during STS-induced apoptosis. No cleavage products were observed (**Fig. 3.11**), suggesting that caspase-3 likely disrupts the antibody epitope for detection. We likewise interrogated three unique caspase-9 substrates, RECQL5, NUP43, and RNF126. We observed RECQL5 proteolysis during STS-induced apoptosis, but no cleavage of NUP43 and RNF126 (**Fig. 3.10**), indicating that caspase-9 plays putative non-apoptotic roles involving these substrates. Detection of PARN, ATXN2L and RING1 as the common substrates of caspase-3 and -9, again illustrates advantages of employing *reverse* N-terminomics. Both ATXN2L and RING1 were reported as apoptotic substrates in the DegraBase; nonetheless, it is our *reverse* N-terminomics analyses which revealed they are proteolyzed by caspase-3 and -9, at distinct cleavage sites. Our analyses also discovered new caspase cleavage sites for these three substrates, PARN (D595 by caspase-3 and -9), two additional cleavage sites of ATXN2L (D181 by caspase-3 and D246 by caspase-9) and one additional cleavage site of RING1 (D189 by caspase-9) (**Table 3.3**). Together these observations underscore the complementarity of both *forward* and *reverse* N-terminomics experiments to capture the nuanced suite of substrates of these proteases.

The comprehensive list of caspase-3 and caspase-9 substrates we provide here allowed us to finally deorphanize more than a thousand caspase substrates (**Appendix A**). Not surprisingly, hundreds of them have been identified before as apoptotic substrates (649 out of 906 for caspase-3 and 103 out of 124 for caspase-9). However, until now, it was unknown which caspase was most responsible for these proteolytic events. Not surprisingly, the executioner caspase-3 cleaves hundreds of apoptotic substrates. The fact that prior studies did not identify any caspase-9 substrates[101], and our literature search only found seven non-caspase substrates[119,121,125,129,132,134], our work in deorphanizing more than hundred caspase-9 substrates represents a significant milestone in the field of caspase-9 biology. Our findings clearly demonstrate that the role of caspase-9 is not only to activate caspase-3 and -7, but also to target its own set of protein substrates.

We curated the caspase-9 substrate list, searching the literature for any references to caspase or apoptosis. Of the 124 substrate proteins (137 cleavage sites) from N-terminomics, we found literature references for only 28 proteins which are reported as caspase substrates and/or are involved in apoptosis (**Table 3.2**). In contrast, of those 124 caspase-9 substrates, only 20 were not in the DegraBase[75] (**Appendix A**), which catalogues apoptotic substrates derived from 33 different experiments ranging over 7 different apoptosis inducers in 5 independent cell lines,

reporting a total of 1706 cleavage sites in 1268 proteins. Thus, most of the caspase-9 substrates identified in this study (84%) are, in fact, apoptotic substrates that were orphaned prior to this work. It is possible or even likely that proteolysis of the 20 proteins that were not found in the DegraBase (**Appendix A**) is mediated by caspase-9 in a non-apoptotic context. Of those 20 proteins that were not found in the DegraBase (**Appendix A**), references in the literature were present for only 3 substrates (ATP-dependent DNA helicase Q5, chromosome transmission fidelity protein 18 homolog, and poly(A)-specific ribonuclease PARN) as a caspase substrate and/or involved in apoptosis (**Table 3.2**), underscoring the fact this analysis had contributed to identify 17 entirely new caspase substrates which are proteolyzed by caspase-9 (**Appendix A**).

The discovery and deorphanization of more than a hundred new caspase-9 substrates provides a critical repository of information of other functions that caspase-9 activation plays, in addition to its role as a canonical apoptotic initiator. Interestingly, caspase-9 has been implicated in a non-apoptotic form of cell death, called paraptosis[116]. Paraptosis, an Apaf-1-independent but caspase-9-dependent form of programmed cell death, was first termed over two decades ago, which can occur during development and neurodegeneration[116]. It was shown that human insulin-like growth factor I receptor (IGFIR) stimulates paraptosis in HEK293T cells as well as in mouse embryonic fibroblasts[116]. Caspase-9, but not caspase-3/-7, was also shown to play a non-apoptotic role in primitive erythropoiesis[263]. Thus, it is possible that some of the caspase-9 substrates we identified play crucial roles in non-apoptotic pathways such as paraptosis and/or primitive erythropoiesis.

We also investigated 74 substrates that were cleaved by both caspase-3 and caspase-9. These proteins were cleaved at the same site by both caspases in 45% of the cases, whereas 55% were cleaved at different sites. Amongst those 74 substrates, 35 were cleaved at just one site by caspase-3 whereas 29 were cleaved at two sites and 10 were cleaved at three or more sites (such as enhancer of mRNA-decapping protein 4, which is cleaved at six sites). In contrast, 64 of the overlapping 74 substrates were cleaved at just one site by caspase-9, whereas 9 were cleaved at two sites and only 1 substrate (U2 snRNP-associated SURP motif-containing protein) was cleaved at four sites. The canonical view is that caspase cleavage at a single site leads to changes in function or localization that contribute to apoptosis. The observation of large numbers of cleavage sites in a single substrate begs the question of whether caspases play degradative roles for some key substrates.

We also observed that multiple members of the same functional complex are often targeted by caspases. For example, it's been shown that the proteasome, the condensin I complex and the spliceosome are heavily targeted by caspases during apoptosis[203,264]. Consistently, we found an enrichment for RNA splicing in both sets of caspase-3 and caspase-9 substrates. We also found that caspase-3 and caspase-9 can cleave the same substrate in the same region, but at different aspartate residues (e.g. RING1 is cleaved at D189 by caspase-9 and at D193 by caspase-3). Similarly, synapse associated protein 1 (SYAP1) was shown to be cleaved by caspase-1 at D278 and caspase-3 and -7 at D281, with a cleavage site motif, FVSD[278]↓AFD[281]↓A[265]. Interestingly, in this study, we found that SYAP1 is also cleaved by caspase-9 at the same site at caspase-1 (D278). We hypothesize that this redundancy, cleavage by different caspases that function in different biological pathways at adjacent and therefore likely functionally similar sites, may provide a means of identifying proteolytic events that are critical in multiple contexts.

4.3 C2C12 preliminary proteomics experiment

In the label-free proteomics analysis of C2C12 cells, we sought to determine the differences in protein expression during differentiation from myoblasts to myotubes. Since differentiation to myotubes is a caspase-3-dependent process[108], we also sought to determine the effects of inhibiting caspase-3 activation would have on protein levels by DEVD-fmk(OME) treatment.

The addition of DEVD-fmk(OME) was not sufficient to abolish differentiation from myoblasts to myotubes (**Fig 3.16**), as elongation and cellular fusion was still visible in microscopy images. There could be many reasons for why this was the case, such as incomplete penetration of the DEVD-fmk(OME) into the cells leaving some caspase-3 active. We chose to use DEVD-fmk(OME) to inhibit caspase-3 activity in the cell cultures rather than a pan-caspase inhibitor to reduce off-target effects in the cells not due to caspase-3 activity, but perhaps as a result we were not treating the cells as strongly as needed.

Previous publications have observed the global proteomic changes upon C2C12 differentiation[266–268]. These publications systematically evaluated several timepoints over the course of C2C12 differentiation, which we should do as well, but they did not assess proteome changes when inhibiting caspase-3/7. As these publications are over 10 years old, the mass spectrometry technology available limited their coverage. In our experiment, we were able to identify over 4000 proteins in each experimental condition, whereas prior publications typically identified ~2000 proteins. Although it is difficult to know if the lower abundance proteins will have a significant impact on the cell differentiation process. An individual protein of interest, Nucleoporin NUP43,

was enriched in undifferentiated cells. In *reverse* N-terminomics, we observed NUP43 as a site of capase-9, which did not cleave upon staurosporine-induced apoptosis. Its enrichment in undifferentiated C2C12 cells further suggests its involvement in non-apoptotic activity, with a possibility of this activity being caspase-dependent.

Heatmap and PCA plotting of the mass spectrometry results demonstrated a statistical similarity between conventionally differentiated C2C12 cells and those treated with DEVD-fmk as well (**Fig. 3.21** and **3.22**).

The Reactome analyses of head-to-head comparisons of the three conditions exhibited some notable differences. Between undifferentiated and differentiated C2C12 cells, success of differentiation was clear by the upregulation of muscle contractile proteins in the differentiated samples. Undifferentiated cells exhibited enrichment in pathways related to rRNA processing and the cell cycle. These pathway enrichments are to be expected, as myotubes should express muscle contractile proteins, and ribosomal translational control is important in stem cell homeostasis and stem cell fate[269]. Between undifferentiated C2C12 cells and DEVD-fmk-treated cells, similar pathway enrichments emerge, further cementing that DEVD-fmk treatment did not prevent myotube formation, as observed in the cell images (**Fig. 3.16**)

Overall, the label-free quantitation method is able to recover thousands of proteins. The vast majority of proteins are present in all samples, in varying amounts across the samples. Between undifferentiated C2C12 cells and serum-withdrawn cells, global differences characteristic for a change in cell fate are observed. However, treatment with DEVD-fmk is insufficient to abolish differentiation, and thus the caspase-3 dependent changes between treated and untreated serum-withdrawn samples might not hold biological relevance. It will be interesting to compare these datasets to future N-terminomics results during C2C12 differentiation.

CHAPTER FIVE

CONCLUSIONS & FUTURE DIRECTIONS

5.1 Conclusions

While there remains significant work to fully elucidate the roles and activity of caspases-3 and -9 (especially in non-apoptotic processes), this thesis' hypotheses were explored and addressed. The hypotheses (from **1.10**) are reproduced below:

1. Initiator caspases play a role in cleaving their own protein targets in apoptosis
2. There are apoptotic substrates of Caspase-3 yet to be discovered
3. Initiator and executioner caspases are cleaving protein targets uninvolved in apoptosis that are currently unknown
4. The proteome of C2C12 myoblasts will incur important global caspase-3 dependent proteome changes to differentiation into myotubes

To start, the discovery of 124 substrates in the caspase-9 *reverse* N-terminomics experiment addresses the first hypothesis, that initiator caspases are cleaving their own protein targets. From this dataset, 6 substrates of interest were selected for further western blotting analysis (**Table 3.3**). The results demonstrated that 4 caspase-9 substrates were cleaved in staurosporine-induced apoptosis (RECQL5, PARN, ATXN2L, RING1), and 2 were not (RNF126, NUP43).

Next, we identified 906 substrates in the caspase-3 *reverse* experiment. Of these substrates, we selected 7 substrates of interest (PARN, ATXN2L, RING1, GSDMD, MFN2, RNF4, PAK2) (**Table 3.3**) and performed further western blotting analysis. We linked all 7 substrate cleavages to caspase-3 activity and determined their cleavage in staurosporine-induced apoptosis as well, addressing the second hypothesis.

By comparing our *reverse* N-terminomics results with the DegraBase, we were able to identify 257 substrates previously unseen in apoptotic lysates in the caspase-3 experiment, and 20 in the caspase-9 experiment (**Appendix A**). Of the substrates we selected for further investigation, only substrates of caspase-9 were demonstrated to be uncleaved in apoptosis, partially addressing the third hypothesis. Our non-DegraBase caspase-3 subset is quite large however, so there are many more potential non-apoptotic cleavages to investigate. To conclude this project, our *reverse* N-terminomics study has deorphanized hundreds of caspase-3 and -9 protein substrates, generating the most comprehensive substrate datasets for both caspases. Most of these proteolytic events obviously play key roles in apoptosis, induced by caspase-3 and/or caspase-9 proteolysis. However, we anticipate that these datasets will provide a powerful resource for the future investigation of the roles of these caspases in apoptotic as well as non-apoptotic pathways. Lastly, through a global proteomics experiment we were able to observe 789 proteins differentially expressed between undifferentiated C2C12 cells (386 enriched) and C2C12 cells (421 enriched)

which were subjected to a 4-day differentiation through serum withdrawal. However, experiments to determine the effect of caspase-3 on these proteomes proved dubious. 409 Proteins were differentially expressed between serum-withdrawn C2C12 cells with and without DEVD-fmk(OME), but the morphology of the cells during the 4-day serum withdrawal indicate that differentiation still occurred (**Fig. 3.16**), casting doubt on those results. In addition to this, heat map and PCA plotting of the data demonstrated that the differentiated and C2C12-treated cells were statistically similar (**Fig. 3.21** and **3.22**)

5.2 Future directions

The overarching goal of this series of projects is to determine the substrate profiles of the human caspases. Moving forward, the caspase-3 and -9 *reverse* N-terminomics experiments provide a solid foundation for the exploration of other understudied caspases. There is a dearth of knowledge in the profiling of several human caspases, such as caspases-10 and -12. Of particular interest is caspase-14, where work is underway in our laboratory to prepare such an experiment (**Appendix C**). Further *reverse* N-terminomics investigation of previously studied caspases is also worth exploring. Many studies were conducted almost a decade ago, when mass spectrometers were less powerful, as evidenced by our ability to identify 124 caspase-9 substrates while previous experiments identified none[101]. Other future experiments which could help expand our knowledge of caspase cleavage could be uncovered by performing *reverse* N-terminomics using different tissues, as most studies were conducted using immortalized cell lines such as Jurkat or THP-1[65,101–103]. Along the same lines, performing N-terminomics using trypsin as the sole enzyme to generate peptides limits our potential peptide coverage. Any proteins with many Lys and/or Arg residues close together will be less likely to appear in our mass spectrometry data, because the peptides will be too short. To improve this coverage, probes and cleavage enzymes other than the TEVest6/TEV protease pair are being explored (**Appendix D**).

The data presented in the global proteomics experiment of C2C12 differentiation serves as a preliminary investigation for a larger project. To further investigate the proteomic and caspase-dependent changes upon C2C12 differentiation, the global proteomics experiment should be conducted again with another cell-permeable caspase-3 inhibitor. In the experiment presented in this thesis, DEVD-fmk(OME) was used rather than a pan-caspase inhibitor to reduce the effects of off-target caspase inhibition in the cells. Given these results, however, pan-caspase inhibitors are worth considering, such as z-VAD-fmk(OME) or QVD-OPH, which could also

mitigate potential fmk toxicity[270]. Another option is a caspase-2 siRNA, as caspase-2 is also required for C2C12 differentiation and its inhibition prevents caspase-3 activation[109]. To investigate the continued differentiation of DEVD-fmk-treated cells, a titration assay could be conducted, as well as a caspase-Glo assay (Promega) to test for endogenous caspase-3/7 activity.

This project is intended to be expanded to a forward N-terminomics analysis and global proteomic analyses of post-translational modifications as well. This is intended to gain wide knowledge on the cellular events occurring during differentiation, ultimately generate a map of caspase-regulated proteins.

BIBLIOGRAPHY

1. Carter M, Shieh J. *Biochemical Assays and Intracellular Signaling*.; 2015. doi:10.1016/b978-0-12-800511-8.00015-0

2. Uversky VN. *Posttranslational Modification*. Vol 5. Elsevier Inc.; 2013. doi:10.1016/B978-0-12-374984-0.01203-1

3. Aebersold R, Agar JN, Amster IJ, et al. How many human proteoforms are there? *Nat Chem Biol*. 2018;14(3):206-214. doi:10.1038/nchembio.2576

4. Lecker SH, Goldberg AL, Mitch WE. Protein degradation by the ubiquitin-proteasome pathway in normal and disease states. *J Am Soc Nephrol*. 2006;17(7):1807-1819. doi:10.1681/ASN.2006010083

5. Michard C, Doublet P. Post-translational modifications are key players of the Legionella pneumophila infection strategy. *Front Microbiol*. 2015;6(FEB):1-12. doi:10.3389/fmicb.2015.00087

6. Van Loi V, Rossius M, Antelmann H. Redox regulation by reversible protein S-thiolation in bacteria. *Front Microbiol*. 2015;6(MAR):1-22. doi:10.3389/fmicb.2015.00187

7. Nothaft H, Szymanski CM. New discoveries in bacterial N-glycosylation to expand the synthetic biology toolbox. *Curr Opin Chem Biol*. 2019;53:16-24. doi:10.1016/j.cbpa.2019.05.032

8. Beck-Sickinger AG, Mörl K. Posttranslational Modification of Proteins. Expanding Nature's Inventory. By Christopher T. Walsh. *Angew Chemie Int Ed*. 2006;45(7):1020-1020. doi:10.1002/anie.200585363

9. Cooper GM. The Central Role of Enzymes as Biological Catalysts. In: *The Cell: A Molecular Approach. 2nd Edition.* Sunderland (MA): Sinauer Associates; 2000. https://www.ncbi.nlm.nih.gov/books/NBK9921/.

10. Lewis T, Stone WL. *Biochemistry, Proteins Enzymes*. Treasure Island (FL): StatPearls; 2021. https://www.ncbi.nlm.nih.gov/books/NBK554481/.

11. Voet D, Voet JGV, Pratt CW. *Fundamentals of Biochemistry*. 4th ed. Hoboken (NJ): Wiley; 2013. https://search.ebscohost.com/login.aspx?direct=true&db=cat03710a&AN=alb.6771787&site=eds-live&scope=site.

12. Markert CL. Lactate dehydrogenase. Biochemistry and function of lactate dehydrogenase. *Cell Biochem Funct*. 1984;2(3):131-134. doi:10.1002/cbf.290020302

13. Townsend DM, Tew KD. The role of glutathione-S-transferase in anti-cancer drug resistance. *Oncogene*. 2003;22(47):7369-7375. doi:10.1038/sj.onc.1206940

14. Schilling O, Biniossek ML, Mayer B, et al. Specificity profiling of human trypsin-isoenzymes. *Biol Chem*. 2018;399(9):997-1007. doi:10.1515/hsz-2018-0107

15. Sun C, Xu B, Liu X, Zhang Z, Su Z. Crystal structure of enolase from Drosophila melanogaster. *Acta Crystallogr Sect Struct Biol Commun*. 2017;73(4):228-234. doi:10.1107/S2053230X17004022

16. Alber T, Banner DW, Bloomer AC, et al. On the three-dimensional structure and catalytic mechanism of triose phosphate isomerase. 1981;171:159-171.

17. Howes TRL, Tomkinson AE. DNA Ligase I, the Replicative DNA Ligase. In: MacNeill S,

ed. *The Eukaryotic Replisome: A Guide to Protein Structure and Function*. Dordrecht: Springer Netherlands; 2012:327-341. doi:10.1007/978-94-007-4572-8_17

18.   Zhu D, Wu Q, Hua L. Industrial enzymes. *Compr Biotechnol*. 2019;3(October 2018):1-13. doi:10.1016/B978-0-444-64046-8.00148-8

19.   López-Otín C, Bond JS. Proteases: Multifunctional enzymes in life and disease. *J Biol Chem*. 2008;283(45):30433-30437. doi:10.1074/jbc.R800035200

20.   Schechter I, Berger A. On the size of the active site in proteases. I. Papain. *Biochem Biophys Res Commun*. 1967;27(2):157-162. doi:https://doi.org/10.1016/S0006-291X(67)80055-X

21.   Rawlings ND, Barrett AJ, Thomas PD, Huang X, Bateman A, Finn RD. The MEROPS database of proteolytic enzymes, their substrates and inhibitors in 2017 and a comparison with peptidases in the PANTHER database. *Nucleic Acids Res*. 2018;46(D1):D624-D632. doi:10.1093/nar/gkx1134

22.   Puente XS, Sánchez LM, Overall CM, López-Otín C. Human and mouse proteases: A comparative genomic approach. *Nat Rev Genet*. 2003;4(7):544-558. doi:10.1038/nrg1111

23.   Drapeau GR. [21] Cleavage at glutamic acid with staphylococcal protease. In: *Enzyme Structure Part E*. Vol 47. Methods in Enzymology. Academic Press; 1977:189-191. doi:https://doi.org/10.1016/0076-6879(77)47023-X

24.   Tözsér J, Tropea JE, Cherry S, et al. Comparison of the substrate specificity of two potyvirus proteases. *FEBS J*. 2005;272(2):514-523. doi:10.1111/j.1742-4658.2004.04493.x

25.   Harris JL, Backes BJ, Leonetti F, Mahrus S, Ellman JA, Craik CS. Rapid and general profiling of protease specificity by using combinatorial fluorogenic substrate libraries. *Proc Natl Acad Sci U S A*. 2000;97(14):7754-7759. doi:10.1073/pnas.140132697

26.   O'Donoghue AJ, Eroy-Reveles AA, Knudsen GM, et al. Global identification of peptidase specificity by multiplex substrate profiling. *Nat Methods*. 2012;9(11):1095-1100. doi:10.1038/nmeth.2182

27.   Schilling O, Overall CM. Proteome-derived, database-searchable peptide libraries for identifying protease cleavage sites. *Nat Biotechnol*. 2008;26(6):685-694. doi:10.1038/nbt1408

28.   Cirman T, Orešić K, Mazovec GD, et al. Selective Disruption of Lysosomes in HeLa Cells Triggers Apoptosis Mediated by Cleavage of Bid by Multiple Papain-like Lysosomal Cathepsins. *J Biol Chem*. 2004;279(5):3578-3587. doi:10.1074/jbc.M308347200

29.   Thomas DA, Scorrano L, Putcha G V, Korsmeyer SJ, Ley TJ. Granzyme B can cause mitochondrial depolarization and cell death in the absence of BID, BAX, and BAK. *Proc Natl Acad Sci*. 2001;98(26):14985-14990. doi:10.1073/pnas.261581498

30.   Kumar S. Caspase function in programmed cell death. *Cell Death Differ*. 2007;14(1):32-43. doi:10.1038/sj.cdd.4402060

31.   Reed JC. Dysregulation of apoptosis in cancer. *J Clin Oncol*. 1999;17(9):2941-2953. doi:10.1200/jco.1999.17.9.2941

32. Galluzzi L, Vitale I, Aaronson SA, et al. Molecular mechanisms of cell death: Recommendations of the Nomenclature Committee on Cell Death 2018. *Cell Death Differ*. 2018;25(3):486-541. doi:10.1038/s41418-017-0012-4

33. Kerr JFR, Wyllie AH, Currie AR. Apoptosis: A basic biological phenomenon with wide-ranging implications in tissue kinetics. *Br J Cancer*. 1972;26(4):239-257. doi:10.1038/bjc.1972.33

34. Degterev A, Boyce M, Yuan J. A decade of caspases. *Oncogene*. 2003;22(53 REV. ISS. 7):8543-8567. doi:10.1038/sj.onc.1207107

35. Wyllie AH. Glucocorticoid-induced thymocyte apoptosis is associated with endogenous endonuclease activation. *Nature*. 1980;284(5756):555-556. doi:10.1038/284555a0

36. He B, Lu N, Zhou Z. Cellular and nuclear degradation during apoptosis. *Curr Opin Cell Biol*. 2009;21(6):900-912. doi:10.1016/j.ceb.2009.08.008

37. Saraste A, Pulkki K. Morphologic and biochemical hallmarks of apoptosis. *Cardiovasc Res*. 2000;45(3):528-537. doi:10.1016/S0008-6363(99)00384-3

38. Green DR. Apoptotic pathways: Ten minutes to dead. *Cell*. 2005;121(5):671-674. doi:10.1016/j.cell.2005.05.019

39. Elmore S. Apoptosis: a review of programmed cell death. *Toxicol Pathol*. 2007;35(4):495-516. doi:10.1080/01926230701320337

40. Froelich CJ, Metkar SS, Raja SM. Granzyme B-mediated apoptosis - The elephant and the blind men? *Cell Death Differ*. 2004;11(4):369-371. doi:10.1038/sj.cdd.4401381

41. Trapani JA, Smyth MJ. Functional significance of the perforin/granzyme cell death pathway. *Nat Rev Immunol*. 2002;2(10):735-747. doi:10.1038/nri911

42. Johnstone RW, Ruefli AA, Lowe SW. Apoptosis: A link between cancer genetics and chemotherapy. *Cell*. 2002;108(2):153-164. doi:10.1016/S0092-8674(02)00625-6

43. Aubrey BJ, Kelly GL, Janic A, Herold MJ, Strasser A. How does p53 induce apoptosis and how does this relate to p53-mediated tumour suppression? *Cell Death Differ*. 2018;25(1):104-113. doi:10.1038/cdd.2017.169

44. Walle L Vande, Damme P Van, Lamkanfi M, et al. Proteome-wide Identification of HtrA2 / Omi Substrates research articles. *J Proteome Res*. 2007;6:1006-1015.

45. Hegde R, Srinivasula SM, Zhang Z, et al. Identification of Omi/HtrA2 as a mitochondrial apoptotic serine protease that disrupts inhibitor of apoptosis protein-caspase interaction. *J Biol Chem*. 2002;277(1):432-438. doi:10.1074/jbc.M109721200

46. Xu X, Lai Y, Hua ZC. Apoptosis and apoptotic body: Disease message and therapeutic target potentials. *Biosci Rep*. 2019;39(1):1-17. doi:10.1042/BSR20180992

47. Ghavami S, Shojaei S, Yeganeh B, et al. Autophagy and apoptosis dysfunction in neurodegenerative disorders. *Prog Neurobiol*. 2014;112:24-49. doi:10.1016/j.pneurobio.2013.10.004

48. Wheler J, Lee JJ, Kurzrock R. Unique molecular landscapes in cancer: implications for individualized, curated drug combinations. *Cancer Res*. 2014;74(24):7181-7184. doi:10.1158/0008-5472.CAN-14-2329

49.   Singh R, Letai A, Sarosiek K. Regulation of apoptosis in health and disease: the balancing act of BCL-2 family proteins. *Nat Rev Mol Cell Biol*. 2019;20(3):175-193. doi:10.1038/s41580-018-0089-8

50.   Yuan J, Shaham S, Ledoux S, Ellis HM, Horvitz HR. The C. elegans cell death gene ced-3 encodes a protein similar to mammalian interleukin-1β-converting enzyme. *Cell*. 1993;75(4):641-652. doi:10.1016/0092-8674(93)90485-9

51.   Alnemri ES, Livingston DJ, Nicholson DW, et al. Human ICE/CED-3 Protease Nomenclature. *Cell*. 1996;87(2):171. doi:https://doi.org/10.1016/S0092-8674(00)81334-3

52.   Lamkanfi M, Declercq W, Kalai M, Saelens X, Vandenabeele P. Alice in caspase land. A phylogenetic analysis of caspases from worm to man. *Cell Death Differ*. 2002;9(4):358-361. doi:10.1038/sj.cdd.4400989

53.   Wachmann K, Pop C, van Raam BJ, et al. Activation and specificity of human caspase-10. *Biochemistry*. 2010;49(38):8307-8315. doi:10.1021/bi100968m

54.   Szegezdi E, Fitzgerald U, Samali A. Caspase-12 and ER-Stress-Mediated Apoptosis. *Ann N Y Acad Sci*. 2003;1010(1):186-194. doi:https://doi.org/10.1196/annals.1299.032

55.   Viganò E, Mortellaro A. Caspase-11: The driving factor for noncanonical inflammasomes. *Eur J Immunol*. 2013;43(9):2240-2245. doi:10.1002/eji.201343800

56.   Koenig U, Eckhart L, Tschachler E. Evidence that caspase-13 is not a human but a bovine gene. *Biochem Biophys Res Commun*. 2001;285(5):1150-1154. doi:10.1006/bbrc.2001.5315

57.   Franchi L, Eigenbrod T, Muñoz-Planillo R, Nuñez G. The inflammasome: a caspase-1-activation platform that regulates immune responses and disease pathogenesis. *Nat Immunol*. 2009;10(3):241-247. doi:10.1038/ni.1703

58.   Man SM, Karki R, Kanneganti T-D. Molecular mechanisms and functions of pyroptosis, inflammatory caspases and inflammasomes in infectious diseases. *Immunol Rev*. 2017;277(1):61-75. doi:10.1111/imr.12534

59.   Shi J, Zhao Y, Wang K, et al. Cleavage of GSDMD by inflammatory caspases determines pyroptotic cell death. *Nature*. 2015;526(7575):660-665. doi:10.1038/nature15514

60.   Morishima N, Nakanishi K, Takenouchi H, Shibata T, Yasuhiko Y. An endoplasmic reticulum stress-specific caspase cascade in apoptosis. Cytochrome c-independent activation of caspase-9 by caspase-12. *J Biol Chem*. 2002;277(37):34287-34294. doi:10.1074/jbc.M204973200

61.   Nakagawa T, Yuan J. Cross-talk between two cysteine protease families: Activation of caspase-12 by calpain in apoptosis. *J Cell Biol*. 2000;150(4):887-894. doi:10.1083/jcb.150.4.887

62.   Bouchier-Hayes L, Green DR. Caspase-2: The orphan caspase. *Cell Death Differ*. 2012;19(1):51-57. doi:10.1038/cdd.2011.157

63.   Tinel A, Tschopp J. The PIDDosome, a Protein Complex Implicated in Activation of Caspase-2 in Response to Genotoxic Stress. *Science (80-)*. 2004;304(5672):843-846. doi:10.1126/science.1095432

64.   Guo Y, Srinivasula SM, Druilhe A, Fernandes-Alnemri T, Alnemri ES. Caspase-2 induces

apoptosis by releasing proapoptotic proteins from mitochondria. *J Biol Chem*. 2002;277(16):13430-13437. doi:10.1074/jbc.M108029200

65. Julien O, Zhuang M, Wiita AP, et al. Quantitative MS-based enzymology of caspases reveals distinct protein substrate specificities, hierarchies, and cellular roles. *Proc Natl Acad Sci*. 2016;113(14):E2001 LP-E2010. http://www.pnas.org/content/113/14/E2001.abstract.

66. Gray DC, Mahrus S, Wells JA. Activation of specific apoptotic caspases with an engineered small-molecule-activated protease. *Cell*. 2010;142(4):637-646. doi:10.1016/j.cell.2010.07.014

67. Hoste E, Kemperman P, Devos M, et al. Caspase-14 is required for filaggrin degradation to natural moisturizing factors in the skin. *J Invest Dermatol*. 2011;131(11):2233-2241. doi:10.1038/jid.2011.153

68. Denecker G, Hoste E, Gilbert B, et al. Caspase-14 protects against epidermal UVB photodamage and water loss. *Nat Cell Biol*. 2007;9(6):666-674. doi:10.1038/ncb1597

69. Shi Y. Caspase activation, inhibition, and reactivation: A mechanistic view. *Protein Sci*. 2004;13(8):1979-1987. doi:10.1110/ps.04789804

70. Boatright KM, Salvesen GS. Mechanisms of caspase activation. *Curr Opin Cell Biol*. 2003;15(6):725-731. doi:10.1016/j.ceb.2003.10.009

71. Yang X, Stennicke HR, Wang B, et al. Granzyme B Mimics Apical Caspases: Description of a Unified Pathway for Trans-Activation of Executioner Caspase-3 and -7. *J Biol Chem*. 1998;273(51):34278-34283. doi:10.1074/jbc.273.51.34278

72. Walsh JG, Cullen SP, Sheridan C, Lüthi AU, Gerner C, Martin SJ. Executioner caspase-3 and caspase-7 are functionally distinct proteases. *Proc Natl Acad Sci U S A*. 2008;105(35):12815-12819. doi:10.1073/pnas.0707715105

73. Slee EA, Harte MT, Kluck RM, et al. Ordering the cytochrome c-initiated caspase cascade: hierarchical activation of caspases-2, -3, -6, -7, -8, and -10 in a caspase-9-dependent manner. *J Cell Biol*. 1999;144(2):281-292. doi:10.1083/jcb.144.2.281

74. Broz P, von Moltke J, Jones JW, Vance RE, Monack DM. Differential requirement for Caspase-1 autoproteolysis in pathogen-induced cell death and cytokine processing. *Cell Host Microbe*. 2010;8(6):471-483. doi:10.1016/j.chom.2010.11.007

75. Crawford ED, Seaman JE, Agard N, et al. The DegraBase: A Database of Proteolysis in Healthy and Apoptotic Human Cells. *Mol Cell Proteomics*. 2013;12(3):813-824. doi:10.1074/mcp.O112.024372

76. Black RA, Kronheim SR, Sleath PR. Activation of interleukin- 1β by a co-induced protease. *FEBS Lett*. 1989;247(2):386-390. doi:https://doi.org/10.1016/0014-5793(89)81376-6

77. Thornberry NA, Rano TA, Peterson EP, et al. A Combinatorial Approach Defines Specificities of Members of the Caspase Family and Granzyme B: Functional Relationships Established For Key Mediators Of Apoptosis. *J Biol Chem*. 1997;272(29):17907-17911. doi:https://doi.org/10.1074/jbc.272.29.17907

78. Stennicke HR, Renatus M, Meldal M, Salvesen GS. Internally quenched fluorescent peptide substrates disclose the subsite preferences of human caspases 1, 3, 6, 7 and 8.

Biochem J. 2000;350 Pt 2(Pt 2):563-568. https://pubmed.ncbi.nlm.nih.gov/10947972.

79.   Seaman JE, Julien O, Lee PS, Rettenmaier TJ, Thomsen ND, Wells JA. Cacidases: caspases can cleave after aspartate, glutamate and phosphoserine residues. *Cell Death Differ*. 2016;23(10):1717-1726. doi:10.1038/cdd.2016.62

80.   Mikolajczyk J, Scott FL, Krajewski S, Sutherlin DP, Salvesen GS. Activation and substrate specificity of caspase-14. *Biochemistry*. 2004;43(32):10560-10569. doi:10.1021/bi0498048

81.   Zorn JA, Wolan DW, Agard NJ, Wells JA. Fibrils colocalize caspase-3 with procaspase-3 to foster maturation. *J Biol Chem*. 2012;287(40):33781-33795. doi:10.1074/jbc.M112.386128

82.   Poręba M, Strózyk A, Salvesen GS, Drąg M. Caspase substrates and inhibitors. *Cold Spring Harb Perspect Biol*. 2013;5(8):1-20. doi:10.1101/cshperspect.a008680

83.   Rajković J, Poreba M, Caglič D, et al. Biochemical Characterization and Substrate Specificity of Autophagin-2 from the Parasite Trypanosoma cruzi. *J Biol Chem*. 2015;290(47):28231-28244. doi:10.1074/jbc.M115.687764

84.   Li F, Wang Y, Li C, et al. Twenty years of bioinformatics research for protease-specific substrate and cleavage site prediction: A comprehensive revisit and benchmarking of existing methods. *Brief Bioinform*. 2019;20(6):2150-2166. doi:10.1093/bib/bby077

85.   Li F, Leier A, Liu Q, et al. Procleave: Predicting Protease-specific Substrate Cleavage Sites by Combining Sequence and Structural Information. *Genomics Proteomics Bioinformatics*. 2020;18(1):52-64. doi:https://doi.org/10.1016/j.gpb.2019.08.002

86.   Boyd SE, Pike RN, Rudy GB, Whisstock JC, De La Banda MG. Pops: A computational tool for modeling and predicting protease specificity. *J Bioinform Comput Biol*. 2005;3(3):551-585. doi:10.1142/S021972000500117X

87.   Song J, Li F, Leier A, et al. PROSPERous: High-throughput prediction of substrate cleavage sites for 90 proteases with improved accuracy. *Bioinformatics*. 2018;34(4):684-687. doi:10.1093/bioinformatics/btx670

88.   Kumar S, van Raam BJ, Salvesen GS, Cieplak P. Caspase Cleavage Sites in the Human Proteome: CaspDB, a Database of Predicted Substrates. *PLoS One*. 2014;9(10):e110539. https://doi.org/10.1371/journal.pone.0110539.

89.   Song J, Tan H, Perry AJ, et al. PROSPER: An Integrated Feature-Based Tool for Predicting Protease Substrate Cleavage Sites. *PLoS One*. 2012;7(11). doi:10.1371/journal.pone.0050300

90.   Varshavsky A. The N-end rule pathway of protein degradation. *Genes to Cells*. 1997;2(1):13-28. doi:10.1046/j.1365-2443.1997.1020301.x

91.   Holmberg C, Ghesquière B, Impens F, et al. Mapping proteolytic processing in the secretome of gastric cancer-associated myofibroblasts reveals activation of MMP-1, MMP-2, and MMP-3. *J Proteome Res*. 2013;12(7):3413-3422. doi:10.1021/pr400270q

92.   Prudova A, Gocheva V, auf dem Keller U, et al. TAILS N-Terminomics and Proteomics Show Protein Degradation Dominates over Proteolytic Processing by Cathepsins in Pancreatic Tumors. *Cell Rep*. 2016;16(6):1762-1773. doi:10.1016/j.celrep.2016.06.086

93. Wildes D, Wells JA. Sampling the N-terminal proteome of human blood. *Proc Natl Acad Sci U S A*. 2010;107(10):4561-4566. doi:10.1073/pnas.0914495107

94. Colige A, Monseur C, Crawley JTB, Santamaria S, De Groot R. Proteomic discovery of substrates of the cardiovascular protease ADAMTS7. *J Biol Chem*. 2019;294(20):8037-8045. doi:10.1074/jbc.RA119.007492

95. King SL, Goth CK, Eckhard U, et al. TAILS N-terminomics and proteomics reveal complex regulation of proteolytic cleavage by O-glycosylation. *J Biol Chem*. 2018;293(20):7629-7644. doi:10.1074/jbc.RA118.001978

96. Prudova A, Auf Dem Keller U, Butler GS, Overall CM. Multiplex N-terminome analysis of MMP-2 and MMP-9 substrate degradomes by iTRAQ-TAILS quantitative proteomics. *Mol Cell Proteomics*. 2010;9(5):894-911. doi:10.1074/mcp.M000050-MCP201

97. Plasman K, Demol H, Bird PI, Gevaert K, Van Damme P. Substrate specificities of the granzyme tryptases A and K. *J Proteome Res*. 2014;13(12):6067-6077. doi:10.1021/pr500968d

98. Wejda M, Impens F, Takahashi N, Van Damme P, Gevaert K, Vandenabeele P. Degradomics reveals that cleavage specificity profiles of caspase-2 and effector caspases are alike. *J Biol Chem*. 2012;287(41):33983-33995. doi:10.1074/jbc.M112.384552

99. Abrahms L, Tom J, Burnier J, Butcher KA, Kossiakoff A, Wells JA. Engineering Subtilisin and Its Substrates for Efficient Ligation of Peptide Bonds in Aqueous Solution. *Biochemistry*. 1991;30(17):4151-4159. doi:10.1021/bi00231a007

100. Weeks AM, Wells JA. Engineering peptide ligase specificity by proteomic identification of ligation sites. *Nat Chem Biol*. 2018;14(1):50-57. doi:10.1038/nchembio.2521

101. Agard NJ, Mahrus S, Trinidad JC, Lynn A, Burlingame AL, Wells JA. Global kinetic analysis of proteolysis via quantitative targeted proteomics. *Proc Natl Acad Sci U S A*. 2012;109(6):1913-1918. doi:10.1073/pnas.1117158109

102. Hill ME, Macpherson DJ, Wu P, Julien O, Wells JA, Hardy JA. Reprogramming Caspase-7 Specificity by Regio-Specific Mutations and Selection Provides Alternate Solutions for Substrate Recognition. *ACS Chem Biol*. 2016;11(6):1603-1612. doi:10.1021/acschembio.5b00971

103. Agard NJ, Maltby D, Wells JA. Inflammatory Stimuli Regulate Caspase Substrate Profiles * □. *Mol Cell Proteomics*. 2010;9(5):880-893. doi:10.1074/mcp.M900528-MCP200

104. Kayagaki N, Stowe IB, Lee BL, et al. Caspase-11 cleaves gasdermin D for non-canonical inflammasome signalling. *Nature*. 2015;526(7575):666-671. doi:10.1038/nature15541

105. Lippens S, Kockx M, Knaapen M, et al. Epidermal differentiation does not involve the pro-apoptotic executioner caspases, but is associated with caspase-14 induction and processing. *Cell Death Differ*. 2000;7(12):1218-1224. doi:10.1038/sj.cdd.4400785

106. Wichmann C, Meier F, Winter SV, Brunner AD, Cox J, Mann M. MaxQuant.live enables global targeting of more than 25,000 peptides. *Mol Cell Proteomics*. 2019;18(5):982-994. doi:10.1074/mcp.TIR118.001131

107. Ertürk A, Wang Y, Sheng M. Local pruning of dendrites and spines by caspase-3-dependent and proteasome-limited mechanisms. *J Neurosci*. 2014;34(5):1672-1688.

doi:10.1523/JNEUROSCI.3121-13.2014

108. Fernando P, Kelly JF, Balazsi K, Slack RS, Megeney LA. Caspase 3 activity is required for skeletal muscle differentiation. *Proc Natl Acad Sci U S A*. 2002;99(17):11025-11030. doi:10.1073/pnas.162172899

109. Boonstra K, Bloemberg D, Quadrilatero J. Caspase-2 is required for skeletal muscle differentiation and myogenesis. *Biochim Biophys Acta - Mol Cell Res*. 2018;1865(1):95-104. doi:10.1016/j.bbamcr.2017.07.016

110. Sordet O, Rébé C, Plenchette S, et al. Specific involvement of caspases in the differentiation of monocytes into macrophages. *Blood*. 2002;100(13):4446-4453. doi:10.1182/blood-2002-06-1778

111. Fujita J, Crane AM, Souza MK, et al. Caspase Activity Mediates the Differentiation of Embryonic Stem Cells. *Cell Stem Cell*. 2008;2(6):595-601. doi:10.1016/j.stem.2008.04.001

112. Duan H, Orth K, Chinnaiyan AM, et al. ICE-LAP6, a novel member of the ICE/Ced-3 gene family, is activated by the cytotoxic T cell protease granzyme B. *J Biol Chem*. 1996;271(28):16720-16724. doi:10.1074/jbc.271.28.16720

113. Li P, Zhou L, Zhao T, et al. Caspase-9: Structure, mechanisms and clinical application. *Oncotarget*. 2017;8(14):23996-24008. doi:10.18632/oncotarget.15098

114. Stennicke HR, Deveraux QL, Humke EW, Reed JC, Dixit VM, Salvesen GS. Caspase-9 can be activated without proteolytic processing. *J Biol Chem*. 1999;274(13):8359-8362. doi:10.1074/jbc.274.13.8359

115. Pop C, Timmer J, Sperandio S, Salvesen GS. The Apoptosome Activates Caspase-9 by Dimerization. *Mol Cell*. 2006;22(2):269-275. doi:10.1016/j.molcel.2006.03.009

116. Sperandio S, De Belle I, Bredesen DE. An alternative, nonapoptotic form of programmed cell death. *Proc Natl Acad Sci U S A*. 2000;97(26):14376-14381. doi:10.1073/pnas.97.26.14376

117. Rao R V., Castro-Obregon S, Frankowski H, et al. Coupling endoplasmic reticulum stress to the cell death program. An Apaf-1-independent intrinsic pathway. *J Biol Chem*. 2002;277(24):21836-21842. doi:10.1074/jbc.M202726200

118. Sperandio S, Poksay KS, Schilling B, Crippen D, Gibson BW, Bredesen DE. Identification of new modulators and protein alterations in non-apoptotic programmed cell death. *J Cell Biochem*. 2010;111(6):1401-1412. doi:10.1002/jcb.22870

119. Nakanishi K, Maruyama M, Shibata T, Morishima N. Identification of a Caspase-9 Substrate and Detection of Its Cleavage in Programmed Cell Death during Mouse Development. *J Biol Chem*. 2001;276(44):41237-41244. doi:10.1074/jbc.M105648200

120. Morishima N. Changes in nuclear morphology during apoptosis correlate with vimentin cleavage by different caspases located either upstream or downstream of Bcl-2 action. *Genes to Cells*. 1999;4(7):401-414. doi:10.1046/j.1365-2443.1999.00270.x

121. Wong CK, Chen Z, So KL, Li D, Li P. Polycomb group protein RING1B is a direct substrate of Caspases-3 and -9. *Biochim Biophys Acta - Mol Cell Res*. 2007;1773(6):844-852. doi:https://doi.org/10.1016/j.bbamcr.2007.02.005

122. Lund AH, van Lohuizen M. Polycomb complexes and silencing mechanisms. *Curr Opin Cell Biol*. 2004;16(3):239-246. doi:https://doi.org/10.1016/j.ceb.2004.03.010

123. Cernilogar FM, Orlando V. Epigenome programming by Polycomb and Trithorax proteins. *Biochem Cell Biol*. 2005;83(3):322-331. doi:10.1139/o05-040

124. de Napoles M, Mermoud JE, Wakao R, et al. Polycomb group proteins ring1A/B link ubiquitylation of histone H2A to heritable gene silencing and X inactivation. *Dev Cell*. 2004;7(5):663-676. doi:10.1016/j.devcel.2004.10.005

125. Scott FL, Fuchs GJ, Boyd SE, et al. Caspase-8 cleaves histone deacetylase 7 and abolishes its transcription repressor function. *J Biol Chem*. 2008;283(28):19499-19510. doi:10.1074/jbc.M800331200

126. Seto E, Yoshida M. Erasers of histone acetylation: The histone deacetylase enzymes. *Cold Spring Harb Perspect Biol*. 2014;6(4):1-26. doi:10.1101/cshperspect.a018713

127. Kasler HG, Lee IS, Lim HW, Verdin E. Histone Deacetylase 7 mediates tissue-specific autoimmunity via control of innate effector function in invariant Natural Killer T cells. *Elife*. 2018;7:1-29. doi:10.7554/eLife.32109

128. Kasler HG, Verdin E. Histone Deacetylase 7 Functions as a Key Regulator of Genes Involved in both Positive and Negative Selection of Thymocytes. *Mol Cell Biol*. 2007;27(14):5184-5200. doi:10.1128/mcb.02091-06

129. Duclos CM, Champagne A, Carrier JC, Saucier C, Lavoie CL, Denault JB. Caspase-mediated proteolysis of the sorting nexin 2 disrupts retromer assembly and potentiates Met/hepatocyte growth factor receptor signaling. *Cell Death Discov*. 2017;3(November 2016). doi:10.1038/cddiscovery.2016.100

130. Teasdale RD, Collins BM. Insights into the PX (phox-homology) domain and SNX (sorting nexin) protein families: Structures, functions and roles in disease. *Biochem J*. 2012;441(1):39-59. doi:10.1042/BJ20111226

131. Cullen PJ. Endosomal sorting and signalling: an emerging role for sorting nexins. *Nat Rev Mol Cell Biol*. 2008;9(7):574-582.

132. Grossi S, Fenini G, Kockmann T, Hennig P, Di Filippo M, Beer HD. Inactivation of the Cytoprotective Major Vault Protein by Caspase-1 and -9 in Epithelial Cells during Apoptosis. *J Invest Dermatol*. 2020;140(7):1335-1345.e10. doi:10.1016/j.jid.2019.11.015

133. Steiner E, Holzmann K, Elbling L, Micksche M, Berger W. Cellular Functions of Vaults and their Involvement in Multidrug Resistance. *Curr Drug Targets*. 2006;7(8):923-934. doi:10.2174/138945006778019345

134. Ohsawa S, Hamada S, Asou H, et al. Caspase-9 activation revealed by semaphorin 7A cleavage is independent of apoptosis in the aged olfactory bulb. *J Neurosci*. 2009;29(36):11385-11392. doi:10.1523/JNEUROSCI.4780-08.2009

135. Xie J, Wang H. Semaphorin 7A as a potential immune regulator and promising therapeutic target in rheumatoid arthritis. *Arthritis Res Ther*. 2017;19(1):1-12. doi:10.1186/s13075-016-1217-5

136. Erez E, Fass D, Bibi E. How intramembrane proteases bury hydrolytic reactions in the membrane. *Nature*. 2009;459(7245):371-378. doi:10.1038/nature08146

137. Tu H, Costa M. XIAP's Profile in Human Cancer. *Biomol* . 2020;10(11). doi:10.3390/biom10111493

138. Clark AC. Caspase Allostery and Conformational Selection. *Chem Rev*. 2016;116(11):6666-6706. doi:10.1021/acs.chemrev.5b00540

139. Shalini S, Dorstyn L, Dawar S, Kumar S. Old, new and emerging functions of caspases. *Cell Death Differ*. 2015;22(4):526-539. doi:10.1038/cdd.2014.216

140. Ishizaki Y, Jacobson MD, Raff MC. A role for caspases in lens fiber differentiation. *J Cell Biol*. 1998;140(1):153-158. doi:10.1083/jcb.140.1.153

141. Zandy AJ, Lakhani S, Zheng T, Flavell RA, Bassnett S. Role of the executioner caspases during lens development. *J Biol Chem*. 2005;280(34):30263-30272. doi:10.1074/jbc.M504007200

142. Janzen V, Fleming HE, Riedt T, et al. Hematopoietic stem cell responsiveness to exogenous signals is limited by caspase-3. *Cell Stem Cell*. 2008;2(6):584-594. doi:10.1016/j.stem.2008.03.012

143. Li F, He Z, Shen J, et al. Apoptotic caspases regulate induction of iPSCs from human fibroblasts. *Cell Stem Cell*. 2010;7(4):508-520. doi:10.1016/j.stem.2010.09.003

144. Cheng YJ, Lee CH, Lin YP, et al. Caspase-3 enhances lung metastasis and cell migration in a protease-independent mechanism through the ERK pathway. *Int J Cancer*. 2008;123(6):1278-1285. doi:10.1002/ijc.23592

145. Mattson MP, Duan W. "Apoptotic" biochemical cascades in synaptic compartments: Roles in adaptive plasticity and neurodegenerative disorders. *J Neurosci Res*. 1999;58(1):152-166. doi:https://doi.org/10.1002/(SICI)1097-4547(19991001)58:1<152::AID-JNR15>3.0.CO;2-V

146. Chan SL, Griffin WST, Mattson MP. Evidence for caspase-mediated cleavage of AMPA receptor subunits in neuronal apoptosis and Alzheimer's disease. *J Neurosci Res*. 1999;57(3):315-323. doi:https://doi.org/10.1002/(SICI)1097-4547(19990801)57:3<315::AID-JNR3>3.0.CO;2-#

147. Lu C, Fu W, Salvesen GS, Mattson MP. Direct cleavage of AMPA receptor subunit GluR1 and suppression of AMPA currents by caspase-3. *NeuroMolecular Med*. 2002;1(1):69-79. doi:10.1385/NMM:1:1:69

148. De Maria R, Zeuner A, Eramo A, et al. Negative regulation of erythropoiesis by caspase-mediated cleavage of GATA-1. *Nature*. 1999;401(6752):489-493. doi:10.1038/46809

149. Zermati Y, Garrido C, Amsellem S, et al. Caspase activation is required for terminal erythroid differentiation. *J Exp Med*. 2001;193(2):247-254. doi:10.1084/jem.193.2.247

150. Carlile GW, Smith DH, Wiedmann M. Caspase-3 has a nonapoptotic function in erythroid maturation. *Blood*. 2004;103(11):4310-4316. doi:https://doi.org/10.1182/blood-2003-09-3362

151. Ribeil J-A, Zermati Y, Vandekerckhove J, et al. Hsp70 regulates erythropoiesis by preventing caspase-3-mediated cleavage of GATA-1. *Nature*. 2007;445(7123):102-105. doi:10.1038/nature05378

152. Kennedy NJ, Kataoka T, Tschopp J, Budd RC. Caspase activation is required for T cell

proliferation. *J Exp Med*. 1999;190(12):1891-1896. doi:10.1084/jem.190.12.1891

153. Sakamaki K, Inoue T, Asano M, et al. Ex vivo whole-embryo culture of caspase-8-deficient embryos normalize their aberrant phenotypes in the developing neural tube and heart. *Cell Death Differ*. 2002;9(11):1196-1206. doi:10.1038/sj.cdd.4401090

154. Salmena L, Lemmers B, Hakem A, et al. Essential role for caspase 8 in T-cell homeostasis and T-cell-mediated immunity. *Genes Dev*. 2003;17(7):883-895. doi:10.1101/gad.1063703

155. Kang T-B, Ben-Moshe T, Varfolomeev EE, et al. Caspase-8 Serves Both Apoptotic and Nonapoptotic Roles. *J Immunol*. 2004;173(5):2976 LP - 2984. doi:10.4049/jimmunol.173.5.2976

156. Black S, Kadyrov M, Kaufmann P, Ugele B, Emans N, Huppertz B. Syncytial fusion of human trophoblast depends on caspase 8. *Cell Death Differ*. 2004;11(1):90-98. doi:10.1038/sj.cdd.4401307

157. Pellegrini M, Bath S, Marsden VS, et al. FADD and caspase-8 are required for cytokine-induced proliferation of hemopoietic progenitor cells. *Blood*. 2005;106(5):1581-1589. doi:10.1182/blood-2005-01-0284

158. Barbero S, Barilà D, Mielgo A, Stagni V, Clair K, Stupack D. Identification of a critical tyrosine residue in caspase 8 that promotes cell migration. *J Biol Chem*. 2008;283(19):13031-13034. doi:10.1074/jbc.M800549200

159. Pandey P, Nakazawa A, Ito Y, Datta R, Kharbanda S, Kufe D. Requirement for caspase activation in monocytic differentiation of myeloid leukemia cells. *Oncogene*. 2000;19(34):3941-3947. doi:10.1038/sj.onc.1203751

160. Cathelin S, Rébé C, Haddaoui L, et al. Identification of Proteins Cleaved Downstream of Caspase Activation in Monocytes Undergoing Macrophage Differentiation. *J Biol Chem*. 2006;281(26):17779-17788. doi:https://doi.org/10.1074/jbc.M600537200

161. Yang JY, Widmann C. Antiapoptotic signaling generated by caspase-induced cleavage of RasGAP. *Mol Cell Biol*. 2001;21(16):5346-5358. doi:10.1128/MCB.21.16.5346-5358.2001

162. Yang J-Y, Widmann C. The RasGAP N-terminal Fragment Generated by Caspase Cleavage Protects Cells in a Ras/PI3K/Akt-dependent Manner That Does Not Rely on NFκB Activation. *J Biol Chem*. 2002;277(17):14641-14646. doi:https://doi.org/10.1074/jbc.M111540200

163. Murray TVA, McMahon JM, Howley BA, et al. A non-apoptotic role for caspase-9 in muscle differentiation. *J Cell Sci*. 2008;121(22):3786-3793. doi:10.1242/jcs.024547

164. de Botton S, Sabri S, Daugas E, et al. Platelet formation is the consequence of caspase activation within megakaryocytes. *Blood*. 2002;100(4):1310-1317. doi:https://doi.org/10.1182/blood-2002-03-0686

165. Arama E, Agapite J, Steller H. Caspase Activity and a Specific Cytochrome C Are Required for Sperm Differentiation in Drosophila. *Dev Cell*. 2003;4(5):687-697. doi:https://doi.org/10.1016/S1534-5807(03)00120-5

166. Huh JR, Vernooy SY, Yu H, et al. Multiple apoptotic caspase cascades are required in nonapoptotic roles for Drosophila spermatid individualization. *PLoS Biol*. 2004;2(1):E15-

E15. doi:10.1371/journal.pbio.0020015

167. Arama E, Bader M, Srivastava M, Bergmann A, Steller H. The two Drosophila cytochrome C proteins can function in both respiration and caspase activation. *EMBO J*. 2006;25(1):232-243. doi:10.1038/sj.emboj.7600920

168. Muro I, Berry DL, Huh JR, et al. The Drosophila caspase Ice is important for many apoptotic cell deaths and for spermatid individualization, a nonapoptotic process. *Development*. 2006;133(17):3305-3315. doi:10.1242/dev.02495

169. Arama E, Bader M, Rieckhof GE, Steller H. A Ubiquitin Ligase Complex Regulates Caspase Activation During Sperm Differentiation in Drosophila. *PLOS Biol*. 2007;5(10):e251. https://doi.org/10.1371/journal.pbio.0050251.

170. Kaplan Y, Gibbs-Bar L, Kalifa Y, Feinstein-Rotkopf Y, Arama E. Gradients of a Ubiquitin E3 Ligase Inhibitor and a Caspase Inhibitor Determine Differentiation or Death in Spermatids. *Dev Cell*. 2010;19(1):160-173. doi:https://doi.org/10.1016/j.devcel.2010.06.009

171. Woo M, Hakem R, Furlonger C, et al. Caspase-3 regulates cell cycle in B cells: a consequence of substrate specificity. *Nat Immunol*. 2003;4(10):1016-1022. doi:10.1038/ni976

172. Mogi M, Togari A. Activation of Caspases Is Required for Osteoblastic Differentiation*. *J Biol Chem*. 2003;278(48):47477-47482. doi:https://doi.org/10.1074/jbc.M307055200

173. Miura M, Chen X-D, Allen MR, et al. A crucial role of caspase-3 in osteogenic differentiation of bone marrow stromal stem cells. *J Clin Invest*. 2004;114(12):1704-1713. doi:10.1172/JCI20427

174. Szymczyk KH, Freeman TA, Adams CS, Srinivas V, Steinbeck MJ. Active caspase-3 is required for osteoclast differentiation. *J Cell Physiol*. 2006;209(3):836-844. doi:https://doi.org/10.1002/jcp.20770

175. Campbell DS, Holt CE. Apoptotic Pathway and MAPKs Differentially Regulate Chemotropic Responses of Retinal Growth Cones. *Neuron*. 2003;37(6):939-952. doi:https://doi.org/10.1016/S0896-6273(03)00158-2

176. Ryoo HD, Gorenc T, Steller H. Apoptotic Cells Can Induce Compensatory Cell Proliferation through the JNK and the Wingless Signaling Pathways. *Dev Cell*. 2004;7(4):491-501. doi:https://doi.org/10.1016/j.devcel.2004.08.019

177. Pérez-Garijo A, Martín FA, Morata G. Caspase inhibition during apoptosis causes abnormal signalling and developmental aberrations in Drosophila. *Development*. 2004;131(22):5591-5598. doi:10.1242/dev.01432

178. Huh JR, Guo M, Hay BA. Compensatory Proliferation Induced by Cell Death in the Drosophila Wing Disc Requires Activity of the Apical Cell Death Caspase Dronc in a Nonapoptotic Role. *Curr Biol*. 2004;14(14):1262-1266. doi:https://doi.org/10.1016/j.cub.2004.06.015

179. Fan Y, Bergmann A. Distinct mechanisms of apoptosis-induced compensatory proliferation in proliferating and differentiating tissues in the Drosophila eye. *Dev Cell*. 2008;14(3):399-410. doi:10.1016/j.devcel.2008.01.003

180. Geisbrecht ER, Montell DJ. A Role for Drosophila IAP1-Mediated Caspase Inhibition in

Rac-Dependent Cell Migration. *Cell*. 2004;118(1):111-125. doi:https://doi.org/10.1016/j.cell.2004.06.020

181. Okuyama R, Nguyen B-C, Talora C, et al. High Commitment of Embryonic Keratinocytes to Terminal Differentiation through a Notch1-caspase 3 Regulatory Mechanism. *Dev Cell*. 2004;6(4):551-562. doi:https://doi.org/10.1016/S1534-5807(04)00098-X

182. Kanuka H, Kuranaga E, Takemoto K, Hiratou T, Okano H, Miura M. Drosophila caspase transduces Shaggy/GSK-3beta kinase activity in neural precursor development. *EMBO J*. 2005;24(21):3793-3806. doi:10.1038/sj.emboj.7600822

183. Kuranaga E, Kanuka H, Tonoki A, et al. Drosophila IKK-Related Kinase Regulates Nonapoptotic Function of Caspases via Degradation of IAPs. *Cell*. 2006;126(3):583-596. doi:https://doi.org/10.1016/j.cell.2006.05.048

184. Fernando P, Brunette S, Megeney LA. Neural stem cell differentiation is dependent upon endogenous caspase-3 activity. *FASEB J*. 2005;19(12):1671-1673. doi:https://doi.org/10.1096/fj.04-2981fje

185. Oomman S, Strahlendorf H, Finckbone V, Strahlendorf J. Non-lethal active caspase-3 expression in Bergmann glia of postnatal rat cerebellum. *Dev Brain Res*. 2005;160(2):130-145. doi:https://doi.org/10.1016/j.devbrainres.2005.07.010

186. Oomman S, Strahlendorf H, Dertien J, Strahlendorf J. Bergmann glia utilize active caspase-3 for differentiation. *Brain Res*. 2006;1078(1):19-34. doi:https://doi.org/10.1016/j.brainres.2006.01.041

187. Santambrogio L, Potolicchio I, Fessler SP, Wong S-H, Raposo G, Strominger JL. Involvement of caspase-cleaved and intact adaptor protein 1 complex in endosomal remodeling in maturing dendritic cells. *Nat Immunol*. 2005;6(10):1020-1028. doi:10.1038/ni1250

188. Huesmann GR, Clayton DF. Dynamic role of postsynaptic caspase-3 and BIRC4 in zebra finch song-response habituation. *Neuron*. 2006;52(6):1061-1072. doi:10.1016/j.neuron.2006.10.033

189. Williams DW, Kondo S, Krzyzanowska A, Hiromi Y, Truman JW. Local caspase activity directs engulfment of dendrites during pruning. *Nat Neurosci*. 2006;9(10):1234-1236. doi:10.1038/nn1774

190. Kuo CT, Zhu S, Younger S, Jan LY, Jan YN. Identification of E2/E3 Ubiquitinating Enzymes and Caspase Activity Regulating Drosophila Sensory Neuron Dendrite Pruning. *Neuron*. 2006;51(3):283-290. doi:https://doi.org/10.1016/j.neuron.2006.07.014

191. Liu W-H, Lin Y-L, Wang J-P, et al. Restriction of vaccinia virus replication by a ced-3 and ced-4-dependent pathway in Caenorhabditis elegans. *Proc Natl Acad Sci U S A*. 2006;103(11):4174-4179. doi:10.1073/pnas.0506442103

192. Arama E, Baena-Lopez LA, Fearnhead HO. Non-lethal message from the Holy Land: The first international conference on nonapoptotic roles of apoptotic proteins. *FEBS J*. 2021;288(7):2166-2183. doi:10.1111/febs.15547

193. Julien O, Wells JA. Caspases and their substrates. *Cell Death Differ*. 2017;24(8):1380-1389. doi:10.1038/cdd.2017.44

194. Kapust RB, Tözsér J, Fox JD, et al. Tobacco etch virus protease: mechanism of autolysis

and rational design of stable mutants with wild-type catalytic proficiency. *Protein Eng Des Sel*. 2001;14(12):993-1000. doi:10.1093/protein/14.12.993

195. van den Berg S, Löfdahl P-Å, Härd T, Berglund H. Improved solubility of TEV protease by directed evolution. *J Biotechnol*. 2006;121(3):291-298. doi:https://doi.org/10.1016/j.jbiotec.2005.08.006

196. Zhou Q, Snipas S, Orth K, Muzio M, Dixit VM, Salvesen GS. Target Protease Specificity of the Viral Serpin CrmA: Analysis of five caspases. *J Biol Chem*. 1997;272(12):7797-7800. doi:https://doi.org/10.1074/jbc.272.12.7797

197. Samraj AK, Sohn D, Schulze-Osthoff K, Schmitz I. Loss of caspase-9 reveals its essential role for caspase-2 activation and mitochondrial membrane depolarization. *Mol Biol Cell*. 2007;18(1):84-93. doi:10.1091/mbc.e06-04-0263

198. Yaffe D, Saxes O. Serial passaging and differentiation of myogenic cells isolated from dystrophic mouse muscle. *Nature*. 1977;270(5639):725-727. doi:10.1038/270725a0

199. Colaert N, Helsens K, Martens L, Vandekerckhove J, Gevaert K. Improved visualization of protein consensus sequences by iceLogo. *Nat Methods*. 2009;6(11):786-787. doi:10.1038/nmeth1109-786

200. Talanian R V, Quinlan C, Trautz S, et al. Substrate Specificities of Caspase Family Proteases. *J Biol Chem*. 1997;272(15):9677-9682. doi:10.1074/jbc.272.15.9677

201. Huber KL, Serrano BP, Hardy JA. Caspase-9 CARD : core domain interactions require a properly formed active site. *Biochem J*. 2018;475(6):1177-1196. doi:10.1042/BCJ20170913

202. Fabregat A, Sidiropoulos K, Viteri G, et al. Reactome pathway analysis: a high-performance in-memory approach. *BMC Bioinformatics*. 2017;18(1):142. doi:10.1186/s12859-017-1559-2

203. Mahrus S, Trinidad JC, Barkan DT, Sali A, Burlingame AL, Wells JA. Global sequencing of proteolytic cleavage sites in apoptosis by specific labeling of protein N termini. *Cell*. 2008;134(5):866-876. doi:10.1016/j.cell.2008.08.012

204. Barkan DT, Hostetter DR, Mahrus S, et al. Prediction of protease substrates using sequence and structure features. *Bioinformatics*. 2010;26(14):1714-1722. doi:10.1093/bioinformatics/btq267

205. Hu Y, Raynard S, Sehorn MG, et al. RECQL5/Recql5 helicase regulates homologous recombination and suppresses tumor formation via disruption of Rad51 presynaptic filaments. *Genes Dev*. 2007;21(23):3073-3084. doi:10.1101/gad.1609107

206. Islam MN, Fox 3rd D, Guo R, Enomoto T, Wang W. RecQL5 promotes genome stabilization through two parallel mechanisms--interacting with RNA polymerase II and acting as a helicase. *Mol Cell Biol*. 2010;30(10):2460-2472. doi:10.1128/MCB.01583-09

207. Hu Y, Lu X, Zhou G, Barnes EL, Luo G. Recql5 plays an important role in DNA replication and cell survival after camptothecin treatment. *Mol Biol Cell*. 2009;20(1):114-123. doi:10.1091/mbc.e08-06-0565

208. Andrs M, Hasanova Z, Oravetzova A, Dobrovolna J, Janscak P. RECQ5: A Mysterious Helicase at the Interface of DNA Replication and Transcription. *Genes (Basel)*. 2020;11(2):232. doi:10.3390/genes11020232

209. Urban V, Dobrovolna J, Hühn D, Fryzelkova J, Bartek J, Janscak P. RECQ5 helicase promotes resolution of conflicts between replication and transcription in human cells. *J Cell Biol*. 2016;214(4):401-415. doi:10.1083/jcb.201507099

210. Kassube SA, Jinek M, Fang J, Tsutakawa S, Nogales E. Structural mimicry in transcription regulation of human RNA polymerase II by the DNA helicase RECQL5. *Nat Struct Mol Biol*. 2013;20(7):892-899. doi:10.1038/nsmb.2596

211. Li M, Xu X, Chang C-W, Zheng L, Shen B, Liu Y. SUMO2 conjugation of PCNA facilitates chromatin remodeling to resolve transcription-replication conflicts. *Nat Commun*. 2018;9(1):2706. doi:10.1038/s41467-018-05236-y

212. Ramamoorthy M, Tadokoro T, Rybanska I, et al. RECQL5 cooperates with Topoisomerase II alpha in DNA decatenation and cell cycle progression. *Nucleic Acids Res*. 2012;40(4):1621-1635. doi:10.1093/nar/gkr844

213. Yang X, Pan Y, Qiu Z, et al. RNF126 as a Biomarker of a Poor Prognosis in Invasive Breast Cancer and CHEK1 Inhibitor Efficacy in Breast Cancer Cells. *Clin Cancer Res*. 2018;24(7):1629-1643. doi:10.1158/1078-0432.CCR-17-2242

214. Zhi X, Zhao D, Wang Z, et al. E3 Ubiquitin Ligase RNF126 Promotes Cancer Cell Proliferation by Targeting the Tumor Suppressor p21 for Ubiquitin-Mediated Degradation. *Cancer Res*. 2013;73(1):385 LP - 394. doi:10.1158/0008-5472.CAN-12-0562

215. Krysztofinska EM, Martínez-Lumbreras S, Thapaliya A, Evans NJ, High S, Isaacson RL. Structural and functional insights into the E3 ligase, RNF126. *Sci Rep*. 2016;6:26433. doi:10.1038/srep26433

216. Delker RK, Zhou Y, Strikoudis A, Stebbins CE, Papavasiliou FN. Solubility-based genetic screen identifies RING finger protein 126 as an E3 ligase for activation-induced cytidine deaminase. *Proc Natl Acad Sci U S A*. 2013;110(3):1029-1034. doi:10.1073/pnas.1214538110

217. Choudhary M, Tamrakar A, Singh AK, Jain M, Jaiswal A, Kodgire P. AID Biology: A pathological and clinical perspective. *Int Rev Immunol*. 2018;37(1):37-56. doi:10.1080/08830185.2017.1369980

218. Ferrando-May E, Cordes V, Biller-Ckovric I, Mirkovic J, Görlich D, Nicotera P. Caspases mediate nucleoporin cleavage, but not early redistribution of nuclear transport factors and modulation of nuclear permeability in apoptosis. *Cell Death Differ*. 2001;8(5):495-505. doi:10.1038/sj.cdd.4400837

219. Cronshaw JM, Krutchinsky AN, Zhang W, Chait BT, Matunis MJ. Proteomic analysis of the mammalian nuclear pore complex. *J Cell Biol*. 2002;158(5):915-927. doi:10.1083/jcb.200206106

220. Duclos C, Lavoie C, Denault J-B. Caspases rule the intracellular trafficking cartel. *FEBS J*. 2017;284(10):1394-1420. doi:https://doi.org/10.1111/febs.14071

221. Xu C, Li Z, He H, et al. Crystal structure of human nuclear pore complex component NUP43. *FEBS Lett*. 2015;589(21):3247-3253. doi:https://doi.org/10.1016/j.febslet.2015.09.008

222. Patre M, Tabbert A, Hermann D, et al. Caspases Target Only Two Architectural Components within the Core Structure of the Nuclear Pore Complex. *J Biol Chem*. 2006;281(2):1296-1304. doi:10.1074/jbc.M511717200

223. von Appen A, Kosinski J, Sparks L, et al. In situ structural analysis of the human nuclear pore complex. *Nature*. 2015;526(7571):140-143. doi:10.1038/nature15381

224. Rühl S, Broz P. The gasdermin-D pore: Executor of pyroptotic cell death. *Oncotarget*. 2016;7(36):57481-57482. doi:10.18632/oncotarget.11421

225. Kuang S, Zheng J, Yang H, et al. Structure insight of GSDMD reveals the basis of GSDMD autoinhibition in cell pyroptosis. *Proc Natl Acad Sci U S A*. 2017;114(40):10642-10647. doi:10.1073/pnas.1708194114

226. Liu Z, Wang C, Rathkey JK, et al. Structures of the Gasdermin D C-Terminal Domains Reveal Mechanisms of Autoinhibition. *Structure*. 2018;26(5):778-784.e3. doi:10.1016/j.str.2018.03.002

227. Liu Z, Wang C, Yang J, et al. Crystal Structures of the Full-Length Murine and Human Gasdermin D Reveal Mechanisms of Autoinhibition, Lipid Binding, and Oligomerization. *Immunity*. 2019;51(1):43-49.e4. doi:10.1016/j.immuni.2019.04.017

228. Rogers C, Fernandes-Alnemri T, Mayes L, Alnemri D, Cingolani G, Alnemri ES. Cleavage of DFNA5 by caspase-3 during apoptosis mediates progression to secondary necrotic/pyroptotic cell death. *Nat Commun*. 2017;8:14128. doi:10.1038/ncomms14128

229. Taabazuing CY, Okondo MC, Bachovchin DA. Pyroptosis and Apoptosis Pathways Engage in Bidirectional Crosstalk in Monocytes and Macrophages. *Cell Chem Biol*. 2017;24(4):507-514.e4. doi:10.1016/j.chembiol.2017.03.009

230. Li Y-J, Cao Y-L, Feng J-X, et al. Structural insights of human mitofusin-2 into mitochondrial fusion and CMT2A onset. *Nat Commun*. 2019;10(1):4914. doi:10.1038/s41467-019-12912-0

231. Bach D, Pich S, Soriano FX, et al. Mitofusin-2 Determines Mitochondrial Network Architecture and Mitochondrial Metabolism: A Novel Regulatory Mechanism Altered In Obesity. *J Biol Chem*. 2003;278(19):17190-17197. doi:10.1074/jbc.M212754200

232. Sugioka R, Shimizu S, Tsujimoto Y. Fzo1, a Protein Involved in Mitochondrial Fusion, Inhibits Apoptosis. *J Biol Chem*. 2004;279(50):52726-52734. doi:10.1074/jbc.M408910200

233. de Brito OM, Scorrano L. Mitofusin-2 regulates mitochondrial and endoplasmic reticulum morphology and tethering: The role of Ras. *Mitochondrion*. 2009;9(3):222-226. doi:https://doi.org/10.1016/j.mito.2009.02.005

234. Chen K-H, Guo X, Ma D, et al. Dysregulation of HSG triggers vascular proliferative disorders. *Nat Cell Biol*. 2004;6(9):872-883. doi:10.1038/ncb1161

235. Filadi R, Pendin D, Pizzo P. Mitofusin 2: from functions to disease. *Cell Death Dis*. 2018;9(3):330. doi:10.1038/s41419-017-0023-6

236. Koshiba T, Detmer SA, Kaiser JT, Chen H, McCaffery JM, Chan DC. Structural Basis of Mitochondrial Tethering by Mitofusin Complexes. *Science (80-)*. 2004;305(5685):858 LP - 862. doi:10.1126/science.1099793

237. Cao Y-L, Meng S, Chen Y, et al. MFN1 structures reveal nucleotide-triggered dimerization critical for mitochondrial fusion. *Nature*. 2017;542(7641):372-376. doi:10.1038/nature21077

238. Qi Y, Yan L, Yu C, et al. Structures of human mitofusin 1 provide insight into mitochondrial tethering. *J Cell Biol*. 2016;215(5):621-629. doi:10.1083/jcb.201609019

239. Karbowski M, Norris KL, Cleland MM, Jeong S-Y, Youle RJ. Role of Bax and Bak in mitochondrial morphogenesis. *Nature*. 2006;443(7112):658-662. doi:10.1038/nature05111

240. Filadi R, Greotti E, Turacchio G, Luini A, Pozzan T, Pizzo P. Mitofusin 2 ablation increases endoplasmic reticulum-mitochondria coupling. *Proc Natl Acad Sci U S A*. 2015;112(17):E2174-E2181. doi:10.1073/pnas.1504880112

241. Kumar R, González-Prieto R, Xiao Z, Verlaan-de Vries M, Vertegaal ACO. The STUbL RNF4 regulates protein group SUMOylation by targeting the SUMO conjugation machinery. *Nat Commun*. 2017;8(1):1809. doi:10.1038/s41467-017-01900-x

242. Vyas R, Kumar R, Clermont F, et al. RNF4 is required for DNA double-strand break repair in vivo. *Cell Death Differ*. 2013;20(3):490-502. doi:10.1038/cdd.2012.145

243. Keusekotten K, Bade VN, Meyer-Teschendorf K, et al. Multivalent interactions of the SUMO-interaction motifs in RING finger protein 4 determine the specificity for chains of the SUMO. *Biochem J*. 2014;457(1):207-214. doi:10.1042/BJ20130753

244. Kung CC-H, Naik MT, Wang S-H, et al. Structural analysis of poly-SUMO chain recognition by the RNF4-SIMs domain. *Biochem J*. 2014;462(1):53-65. doi:10.1042/BJ20140521

245. Liew CW, Sun H, Hunter T, Day CL. RING domain dimerization is essential for RNF4 function. *Biochem J*. 2010;431(1):23-29. doi:10.1042/BJ20100957

246. Eron SJ, Raghupathi K, Hardy JA. Dual Site Phosphorylation of Caspase-7 by PAK2 Blocks Apoptotic Activity by Two Distinct Mechanisms. *Structure*. 2017;25(1):27-39. doi:10.1016/j.str.2016.11.001

247. Walter BN, Huang Z, Jakobi R, et al. Cleavage and Activation of p21-activated Protein Kinase γ-PAK by CPP32 (Caspase 3): Effects of Autophosphorylation on Activity. *J Biol Chem*. 1998;273(44):28733-28739. doi:10.1074/jbc.273.44.28733

248. Li X, Wen W, Liu K, et al. Phosphorylation of caspase-7 by p21-activated protein kinase (PAK) 2 inhibits chemotherapeutic drug-induced apoptosis of breast cancer cell lines. *J Biol Chem*. 2011;286(25):22291-22299. doi:10.1074/jbc.M111.236596

249. Rudel T, Bokoch GM. Membrane and Morphological Changes in Apoptotic Cells Regulated by Caspase-Mediated Activation of PAK2. *Science (80-)*. 1997;276(5318):1571 LP - 1574. doi:10.1126/science.276.5318.1571

250. Jakobi R, McCarthy CC, Koeppel MA, Stringer DK. Caspase-activated PAK-2 Is Regulated by Subcellular Targeting and Proteasomal Degradation. *J Biol Chem*. 2003;278(40):38675-38685. doi:10.1074/jbc.M306494200

251. Virtanen A, Henriksson N, Nilsson P, Nissbeck M. Poly(A)-specific ribonuclease (PARN): An allosterically regulated, processive and mRNA cap-interacting deadenylase. *Crit Rev Biochem Mol Biol*. 2013;48(2):192-209. doi:10.3109/10409238.2013.771132

252. Son A, Park J-E, Kim VN. PARN and TOE1 Constitute a 3' End Maturation Module for Nuclear Non-coding RNAs. *Cell Rep*. 2018;23(3):888-898. doi:10.1016/j.celrep.2018.03.089

253. He G-J, Zhang A, Liu W-F, Yan Y-B. Distinct roles of the R3H and RRM domains in poly(A)-specific ribonuclease structural integrity and catalysis. *Biochim Biophys Acta - Proteins Proteomics*. 2013;1834(6):1089-1098. doi:https://doi.org/10.1016/j.bbapap.2013.01.038

254. Duan T-L, He G-J, Hu L-D, Yan Y-B. The Intrinsically Disordered C-Terminal Domain Triggers Nucleolar Localization and Function Switch of PARN in Response to DNA Damage. *Cells*. 2019;8(8):836. doi:10.3390/cells8080836

255. He G-J, Yan Y-B. Contributions of the C-terminal domain to poly(A)-specific ribonuclease (PARN) stability and self-association. *Biochem Biophys reports*. 2019;18:100626. doi:10.1016/j.bbrep.2019.100626

256. Tummala H, Walne A, Collopy L, et al. Poly(A)-specific ribonuclease deficiency impacts telomere biology and causes dyskeratosis congenita. *J Clin Invest*. 2015;125(5):2151-2160. doi:10.1172/JCI78963

257. Kaehler C, Isensee J, Nonhoff U, et al. Ataxin-2-like is a regulator of stress granules and processing bodies. *PLoS One*. 2012;7(11):e50134-e50134. doi:10.1371/journal.pone.0050134

258. Chen J, Xu H, Zou X, et al. Snail recruits Ring1B to mediate transcriptional repression and cell migration in pancreatic cancer cells. *Cancer Res*. 2014;74(16):4353-4363. doi:10.1158/0008-5472.CAN-14-0181

259. Sanchez-Pulido L, Devos D, Sung ZR, Calonje M. RAWUL: a new ubiquitin-like domain in PRC1 ring finger proteins that unveils putative plant and worm PRC1 orthologs. *BMC Genomics*. 2008;9:308. doi:10.1186/1471-2164-9-308

260. Shen J, Li P, Shao X, et al. The E3 Ligase RING1 Targets p53 for Degradation and Promotes Cancer Cell Proliferation and Survival. *Cancer Res*. 2018;78(2):359 LP - 371. doi:10.1158/0008-5472.CAN-17-1805

261. Sabourin LA, Rudnicki MA. The molecular regulation of myogenesis. *Clin Genet*. 2000;57(1):16-25. doi:https://doi.org/10.1034/j.1399-0004.2000.570103.x

262. Capetanaki Y, Milner DJ, Weitzer G. Desmin in Muscle Formation and Maintenance: Knockouts and Consequences. *Cell Struct Funct*. 1997;22(1):103-116. doi:10.1247/csf.22.103

263. Tran HT, Fransen M, Dimitrakopoulou D, Van Imschoot G, Willemarck N, Vleminckx K. Caspase-9 has a nonapoptotic function in Xenopus embryonic primitive blood formation. *J Cell Sci*. 2017;130(14):2371-2381. doi:10.1242/jcs.186411

264. Stoehr G, Schaab C, Graumann J, Mann M. A SILAC-based approach identifies substrates of caspase-dependent cleavage upon TRAIL-induced apoptosis. *Mol Cell Proteomics*. 2013;12(5):1436-1450. doi:10.1074/mcp.M112.024679

265. Agard NJ, Maltby D, Wells JA. Inflammatory Stimuli Regulate Caspase Substrate Profiles. *Mol Cell Proteomics*. 2010;9(5):880-893. doi:10.1074/mcp.M900528-MCP200

266. Kislinger T, Gramolini AO, Pan Y, Rahman K, MacLennan DH, Emili A. Proteome Dynamics during C2C12 Myoblast Differentiation. *Mol Cell Proteomics*. 2005;4(7):887-901. doi:https://doi.org/10.1074/mcp.M400182-MCP200

267. Casadei L, Vallorani L, Gioacchini AM, et al. Proteomics-based investigation in C2C12

myoblast differentiation. *Eur J Histochem*. 2009;53(4):e31-e31. doi:10.4081/ejh.2009.e31

268. Tannu NS, Rao VK, Chaudhary RM, et al. Comparative Proteomes of the Proliferating C2C12 Myoblasts and Fully Differentiated Myotubes Reveal the Complexity of the Skeletal Muscle Differentiation Program. *Mol Cell Proteomics*. 2004;3(11):1065-1082. doi:10.1074/mcp.M400020-MCP200

269. Gabut M, Bourdelais F, Durand S. Ribosome and Translational Control in Stem Cells. *Cells*. 2020;9(2):497. doi:10.3390/cells9020497

270. Van Noorden CJF. The history of Z-VAD-FMK, a tool for understanding the significance of caspase inhibition. *Acta Histochem*. 2001;103(3):241-251. doi:https://doi.org/10.1078/0065-1281-00601

APPENDIX

APPENDIX A

CLEAVAGE SITES OBSERVED IN CASPASE-3 AND CASPASE-9 *REVERSE* N-TERMINOMICS

C3?	C9?	Cleavage Site in Degrabase?	Protein in DegraBase?	Acc #	Uniprot	P4-P1	DB Peptide	P1'	Protein Name
Casp3		Yes	Yes	Q9C0C9	UBE2O	ETPD	GSASPVEM	438	(E3-independent) E2
Casp3		Yes	Yes	Q9Y2I7	FYV1	DVFD	GHLLGSTD	1608	1-phosphatidylinosit
Casp3	Casp9	No	Yes	P17980	PRS6A	QEED	GANIDLDS	108	26S proteasome regul
Casp3		Yes	Yes	P17980	PRS6A	AEQD	GIGEEVLK	28	26S proteasome regul
Casp3		No	Yes	P35998	PRS7	DLSD	QVAPTDIE	128	26S proteasome regul
Casp3		Yes	Yes	P62195	PRS8	DEID	SIGSSRLE	253	26S proteasome regul
Casp3		No	Yes	Q92665	RT31	AVAD	SLPFDKQT	165	28S ribosomal protei
Casp3		Yes	Yes	Q96SZ5	AEDO	SDRD	AASGPEAP	35	2-aminoethanethiol d
Casp3		No	Yes	P42765	THIM	ETVD	SVIMGNVL	53	3-ketoacyl-CoA thiol
Casp3	Casp9	No	Yes	P63220	RS21	MQND	AGEFVDLY	5	40S ribosomal protei
	Casp9	No	No	Q9BRK5	CAB45	SNHD	GIVTAEEL	296	45 kDa calcium-bindi
Casp3		Yes	Yes	P08195	4F2	TEVD	MKEVELNE	110	4F2 cell-surface ant
Casp3		No	No	P13196	HEM1	VKTD	GGDPSGLL	160	5-aminolevulinate sy
Casp3		No	No	P13196	HEM1	QSPD	GTQLPSGH	88	5-aminolevulinate sy
Casp3		No	No	O43741	AAKB2	DLED	SVKPTQQA	69	5'-AMP-activated pro
Casp3		Yes	Yes	P10809	CH60	EAGD	GTTTATVL	112	60 kDa heat shock pr
Casp3		No	Yes	P10809	CH60	TVKD	GKTLNDEL	204	60 kDa heat shock pr
Casp3		No	Yes	P10809	CH60	EDVD	GEALSTLV	280	60 kDa heat shock pr
Casp3		Yes	Yes	P10809	CH60	VGYD	AMAGDFVN	505	60 kDa heat shock pr
Casp3		No	Yes	P10809	CH60	ALLD	AAGVASLL	532	60 kDa heat shock pr
Casp3		Yes	Yes	P18621	RL17	LDVD	SLVIEHIQ	111	60S ribosomal protei
Casp3		No	Yes	P46777	RL5	ESID	GQPGAFTC	137	60S ribosomal protei
	Casp9	No	Yes	Q7L2J0	MEPCE	SDCD	SVLPSNFL	179	7SK snRNA methylphos
Casp3		No	No	Q9BWD1	THIC	PLTD	SILCDGLT	145	Acetyl-CoA acetyltra
Casp3		No	No	Q9BWD1	THIC	ILCD	GLTDAFHN	150	Acetyl-CoA acetyltra
Casp3		No	No	Q9BWD1	THIC	GLTD	AFHNCHMG	154	Acetyl-CoA acetyltra
Casp3		No	No	Q9BWD1	THIC	FLTD	GTGTVTPA	242	Acetyl-CoA acetyltra
Casp3		No	Yes	P24752	THIL	IVKD	GLTDVYNK	183	Acetyl-CoA acetyltra
Casp3		No	Yes	P24752	THIL	NEQD	AYAINSYT	213	Acetyl-CoA acetyltra
Casp3		No	No	Q13085	ACACA	SLQD	GLALHIR	70	Acetyl-CoA carboxyla
Casp3		No	Yes	P60709	ACTB	LVVD	NGSGMCKA	12	Actin, cytoplasmic 1
Casp3	Casp9	Yes	Yes	P60709	ACTB	IVMD	SGDGVTHT	155	Actin, cytoplasmic 1
Casp3		Yes	Yes	P60709	ACTB	DSGD	GVTHTVPI	158	Actin, cytoplasmic 1
Casp3		Yes	Yes	P60709	ACTB	ELPD	GQVITIGN	245	Actin, cytoplasmic 1
Casp3		Yes	Yes	P60709	ACTB	GQKD	SYVGDEAQ	52	Actin, cytoplasmic 1
Casp3		No	Yes	O14639	ABLM1	ISKD	GAPYCEKD	269	Actin-binding LIM pr
Casp3		Yes	Yes	O14639	ABLM1	IETD	HWPGPPSF	568	Actin-binding LIM pr
Casp3		No	No	O96019	ACL6A	MEID	GDKGKQGG	58	Actin-like protein 6
Casp3		No	No	O15511	ARPC5	DEED	GGDGQAGP	30	Actin-related protei
Casp3		No	No	O15511	ARPC5	DGGD	GQAGPDEG	33	Actin-related protei
Casp3		Yes	Yes	P61160	ARP2	DSGD	GVTHICPV	162	Actin-related protei

Casp3		Yes	Yes	P61158	ARP3	DDLD	FFIGDEAI	60	Actin-related protei
Casp3		Yes	Yes	Q9H981	ARP8	AQGD	GLMAGNDS	480	Actin-related protei
Casp3		No	Yes	Q8N9N2	ASCC1	DEED	FYQGSMEC	35	Activating signal co
Casp3		Yes	Yes	Q9H1I8	ASCC2	DTYD	GNQVGAND	622	Activating signal co
Casp3		Yes	Yes	Q15650	TRIP4	TEPD	TTAEVKTP	123	Activating signal co
Casp3		Yes	Yes	Q15650	TRIP4	DESD	YFASDSNQ	289	Activating signal co
Casp3		Yes	Yes	O95433	AHSA1	ERAD	ATNVNNWH	19	Activator of 90 kDa
Casp3		Yes	Yes	O95433	AHSA1	HMVD	GNVSGEFT	255	Activator of 90 kDa
Casp3		No	No	Q53H12	AGK	IEPD	TISKGDFI	339	Acylglycerol kinase,
Casp3		No	Yes	P25054	APC	STPD	GFSCSSSL	1499	Adenomatous polyposi
Casp3		No	No	P28907	CD38	DSRD	LCQDPTIK	253	ADP-ribosyl cyclase/
Casp3		No	No	Q8N6S5	AR6P6	TQGD	SWGEGEVD	36	ADP-ribosylation fac
Casp3		No	No	P43652	AFAM	SNYD	GCCEGDVV	268	Afamin
Casp3		No	Yes	Q12802	AKP13	DDMD	SIIFPKPE	1453	A-kinase anchor prot
Casp3		No	Yes	Q12802	AKP13	QSLD	GFYSHGMG	1510	A-kinase anchor prot
Casp3		No	Yes	Q12802	AKP13	EEMD	SITEVPAN	1540	A-kinase anchor prot
Casp3		Yes	Yes	Q12802	AKP13	ERVD	SLVSLSEE	1642	A-kinase anchor prot
Casp3		Yes	Yes	Q9Y2D5	AKAP2	SSRD	GEFTLTTL	166	A-kinase anchor prot
Casp3		No	Yes	Q9Y2D5	AKAP2	SAVD	GTYNGTSS	71	A-kinase anchor prot
Casp3		Yes	Yes	Q9ULX6	AKP8L	LETD	MMQGGVYG	109	A-kinase anchor prot
Casp3		Yes	Yes	Q99996	AKAP9	SLLD	GVVTMTSR	1034	A-kinase anchor prot
Casp3		Yes	Yes	Q9BTE6	AASD1	EQAD	HFTQTPLD	81	Alanyl-tRNA editing
Casp3	Casp9	No	No	Q6PD74	AAGAB	AQVD	SIVDPMLD	236	Alpha- and gamma-ada
Casp3		No	Yes	P02765	FETUA	AKCD	SSPDSAED	134	Alpha-2-HS-glycoprot
Casp3		Yes	Yes	P12814	ACTN1	DHYD	SQQTNDYM	6	Alpha-actinin-1
Casp3		No	No	Q3KRA9	ALKB6	DALD	AASSPPNA	194	Alpha-ketoglutarate-
Casp3		No	No	P54920	SNAA	QNVD	SYTESVKE	258	Alpha-soluble NSF at
Casp3		No	No	Q96Q42	ALS2	TSSD	AMSSQQNV	317	Alsin
Casp3		No	No	Q6DCA0	AMERL	QHVD	SSSGRENV	57	AMMECR1-like protein
Casp3		No	No	Q01432	AMPD3	DSKD	ALSLFTVP	37	AMP deaminase 3
Casp3		Yes	Yes	Q6FIF0	ZFAN6	SQLD	STSVDKAV	107	AN1-type zinc finger
Casp3		No	No	Q6UB99	ANR11	DDRD	SLGSSGCL	495	Ankyrin repeat domai
Casp3		No	No	Q8IZ07	AN13A	TQAD	SASHITNF	449	Ankyrin repeat domai
Casp3		Yes	Yes	O43747	AP1G1	FLLD	GLSSQPLF	690	AP-1 complex subunit
Casp3		Yes	Yes	O94973	AP2A2	VFSD	SASVVAPL	691	AP-2 complex subunit
Casp3		No	Yes	P63010	AP2B1	SQPD	MAIMAVNS	83	AP-2 complex subunit
Casp3		Yes	Yes	Q13367	AP3B2	TLTD	STLVPSLL	844	AP-3 complex subunit
Casp3		No	No	O43299	AP5Z1	TEVD	GAVATDFF	216	AP-5 complex subunit
Casp3		Yes	Yes	Q9UKV3	ACINU	VSRD	SSTSYTET	664	Apoptotic chromatin
Casp3		No	No	O14727	APAF	SVTD	SVMGPKYV	272	Apoptotic protease-a
Casp3		Yes	Yes	Q9Y2X7	GIT1	DLSD	GAVTLQEY	419	ARF GTPase-activatin
	Casp9	No	Yes	Q14161	GIT2	PDYD	SVASDEDT	394	ARF GTPase-activatin
	Casp9	Yes	Yes	Q14161	GIT2	LVPD	TAEPHVAP	626	ARF GTPase-activatin

124

Casp3		No	No	O95260	ATE1	SVVD	YFPSEDFY	14	Arginyl-tRNA--protei
Casp3		Yes	Yes	Q8N2F6	ARM10	DLTD	GSYDDVLN	87	Armadillo repeat-con
Casp3		No	No	Q9NVT9	ARMC1	NMAD	GDSFNEMN	118	Armadillo repeat-con
Casp3		Yes	Yes	Q9BVC5	ASHWN	IVFD	GSSTSTSI	106	Ashwin
Casp3		No	No	Q12797	ASPH	ENPD	SSEPVVED	238	Aspartyl/asparaginyl
Casp3		No	Yes	Q99700	ATX2	STYD	SSLSSYTV	417	Ataxin-2
Casp3		No	Yes	Q8WWM7	ATX2L	DIVD	TMVFKPSD	182	Ataxin-2-like protei
	Casp9	No	Yes	Q8WWM7	ATX2L	LESD	MSNGWDPN	247	Ataxin-2-like protei
Casp3		Yes	Yes	Q8WWM7	ATX2L	KEVD	GLLTSEPM	585	Ataxin-2-like protei
Casp3	Casp9	No	Yes	Q7Z591	AKNA	EEPD	GTLGSLEV	127	AT-hook-containing t
Casp3	Casp9	Yes	Yes	Q7Z591	AKNA	LEVD	GVAATPGK	800	AT-hook-containing t
Casp3		No	Yes	Q8NBU5	ATAD1	QETD	GFSGSDLK	293	ATPase family AAA do
	Casp9	No	No	O94762	RECQ5	GEED	GAGGHSPA	810	ATP-dependent DNA he
Casp3		Yes	Yes	Q08211	DHX9	EEVD	LNAGLHGN	168	ATP-dependent RNA he
Casp3		Yes	Yes	Q08211	DHX9	DTPD	TTANAEGD	97	ATP-dependent RNA he
Casp3		Yes	Yes	Q92499	DDX1	DEAD	GLLSQGYS	374	ATP-dependent RNA he
Casp3		Yes	Yes	Q92499	DDX1	SVPD	TVHHVVVP	440	ATP-dependent RNA he
Casp3		Yes	Yes	Q9NUU7	DD19A	MATD	SWALAVDE	5	ATP-dependent RNA he
Casp3	Casp9	Yes	Yes	Q9GZR7	DDX24	AESD	ALPDDTVI	297	ATP-dependent RNA he
Casp3		No	Yes	Q9GZR7	DDX24	MFAD	GQMDDLVC	42	ATP-dependent RNA he
Casp3		No	Yes	O00571	DDX3X	YDKD	SSGWSSSK	57	ATP-dependent RNA he
Casp3		Yes	Yes	Q14562	DHX8	AEMD	SIPMGLNK	500	ATP-dependent RNA he
Casp3		No	No	P29374	ARI4A	IEVD	SIAEESQE	1031	AT-rich interactive
Casp3		No	No	Q4LE39	ARI4B	IEVD	SVAGELQD	1073	AT-rich interactive
Casp3		Yes	Yes	O43491	E41L2	PQID	GGAGGDSG	913	Band 4.1-like protei
Casp3		No	No	Q9HCM4	E41L5	DELD	ALLASLTE	637	Band 4.1-like protei
Casp3		Yes	Yes	P51572	BAP31	AAVD	GGKLDVGN	165	B-cell receptor-asso
Casp3		Yes	Yes	Q6ZNE5	BAKOR	DLVD	SVDDAEGL	29	Beclin 1-associated
Casp3		No	No	Q14457	BECN1	EASD	GGTMENLS	106	Beclin-1
Casp3		No	Yes	O43252	PAPS1	DVND	CVQQVVEL	212	Bifunctional 3'-phos
Casp3		Yes	Yes	P07814	SYEP	DQVD	IAVQELLQ	930	Bifunctional glutama
Casp3		Yes	Yes	P13995	MTDC	DNVD	GLLVQLPL	128	Bifunctional methyle
Casp3		No	Yes	Q9Y223	GLCNE	DGPD	CSCGSHGC	579	Bifunctional UDP-N-a
	Casp9	Yes	Yes	Q6QNY0	BL1S3	AETD	SEPEPEPE	65	Biogenesis of lysoso
Casp3		No	No	Q9UL45	BL1S6	SSPD	GALTRPPY	11	Biogenesis of lysoso
Casp3		Yes	Yes	P11274	BCR	CGVD	GDYEDAEL	244	Breakpoint cluster r
Casp3		No	No	Q4AC94	C2CD3	DSAD	SFKKLPLN	2224	C2 domain-containing
Casp3		No	Yes	P27708	PYR1	GTPD	GTCYPPPP	1887	CAD protein
Casp3		Yes	Yes	P49069	CAMLG	VATD	GGERPGVP	10	Calcium signal-modul
Casp3		No	Yes	P49069	CAMLG	DKLD	SFIKPPEC	116	Calcium signal-modul
Casp3		No	No	Q13555	KCC2G	NATD	GIKGSTES	377	Calcium/calmodulin-d
	Casp9	Yes	Yes	Q9P1Z2	CACO1	EEAD	GGSDILLV	135	Calcium-binding and
Casp3		No	No	O75177	CREST	YYPD	GHGDYAYQ	275	Calcium-responsive t

125

Casp3	Casp9			ID	Gene	P4-P1	P1'-P8'	Pos	Description
Casp3		No	Yes	Q5T5Y3	CAMP1	SKPD	SFFLEPLM	589	Calmodulin-regulated
Casp3		No	No	Q08AD1	CAMP2	SYVD	GFIGTWPK	422	Calmodulin-regulated
Casp3		Yes	Yes	Q9P1Y5	CAMP3	DEGD	GSPAGAED	862	Calmodulin-regulated
Casp3		No	Yes	P27797	CALR	DQTD	MHGDSEYN	122	Calreticulin
Casp3		No	Yes	O43852	CALU	EEYD	YMKDIVVQ	187	Calumenin
	Casp9	No	Yes	O43852	CALU	YSHD	GNTDEPEW	222	Calumenin
Casp3		No	Yes	O43852	CALU	YDHD	AFLGAEEA	51	Calumenin
Casp3		No	No	P51817	PRKX	ETPD	GAPALCPS	26	cAMP-dependent prote
Casp3		No	Yes	Q9UBL0	ARP21	EYTD	STGIDLHE	144	cAMP-regulated phosp
Casp3		Yes	Yes	Q9UBL0	ARP21	VNPD	GTPAIYNP	495	cAMP-regulated phosp
Casp3		No	No	Q03060	CREM	SQHD	GSITASLT	28	cAMP-responsive elem
Casp3		Yes	Yes	Q14444	CAPR1	DQLD	AVSKYQEV	95	Caprin-1
Casp3		Yes	Yes	Q6JBY9	CPZIP	EEVD	GQHPAQEE	273	CapZ-interacting pro
	Casp9	No	No	Q8IV04	TB10C	LQDD	SSSLGSDS	19	Carabin
Casp3		No	No	O75976	CBPD	AGPD	AAGPLLPG	121	Carboxypeptidase D
Casp3		No	Yes	P42574	CASP3	IETD	SGVDDDMA	176	Caspase-3
Casp3		Yes	Yes	P42574	CASP3	ESMD	SGISLDNS	29	Caspase-3
Casp3		No	Yes	P55210	CASP7	ELDD	GIQADSGP	194	Caspase-7
Casp3	Casp9	Yes	Yes	P55210	CASP7	IQAD	SGPINDTD	199	Caspase-7
	Casp9	No	No	P55211	CASP9	PEPD	ATPFQEGL	316	Caspase-9
Casp3	Casp9	No	No	P55211	CASP9	DQLD	AISSLPTP	331	Caspase-9
Casp3		No	Yes	P11717	MPRI	DFCD	GHSPAVTI	277	Cation-independent m
Casp3		No	Yes	P11717	MPRI	EAVD	GSQTETEK	504	Cation-independent m
Casp3		No	No	O43310	CTIF	EDGD	GINLNDIE	155	CBP80/20-dependent t
Casp3		No	Yes	Q03701	CEBPZ	DDFD	FAGSFQGP	956	CCAAT/enhancer-bindi
Casp3		No	No	A5YKK6	CNOT1	SSLD	AISPVQID	705	CCR4-NOT transcripti
Casp3		No	Yes	P14209	CD99	DLAD	GVSGGEGK	98	CD99 antigen
Casp3		No	No	Q86Y37	CACL1	AAVD	GFRQPLPP	31	CDK2-associated and
Casp3		Yes	Yes	Q9BTV7	CABL2	ISLD	GRPPSLGP	59	CDK5 and ABL1 enzyme
Casp3		No	Yes	Q96SN8	CK5P2	NDTD	SLSCDSGS	1694	CDK5 regulatory subu
Casp3		Yes	Yes	Q96SN8	CK5P2	DDLD	GINPNAGL	32	CDK5 regulatory subu
Casp3		Yes	Yes	Q8N163	CCAR2	AAPD	AGAEPITA	293	Cell cycle and apopt
Casp3		No	No	Q99638	RAD9A	DDID	SYMIAMET	305	Cell cycle checkpoin
Casp3	Casp9	No	Yes	Q9NV96	CC50A	DEVD	GGPPCAPG	13	Cell cycle control p
Casp3		Yes	Yes	P30260	CDC27	SYID	SAVISPDT	237	Cell division cycle
Casp3		Yes	Yes	P30260	CDC27	ISPD	TVPLGTGT	244	Cell division cycle
Casp3		Yes	Yes	Q9BWT1	CDCA7	DSCD	SFASDNFA	40	Cell division cycle-
Casp3		No	Yes	P49454	CENPF	CVPD	SSSLSSLG	1484	Centromere protein F
Casp3		Yes	Yes	Q5SW79	CE170	GEID	SVTSSGTA	1325	Centrosomal protein
Casp3		Yes	Yes	Q5SW79	CE170	SDVD	TASTISLV	937	Centrosomal protein
Casp3		No	No	Q8TEP8	CE192	LSTD	SLIKIDHL	1810	Centrosomal protein
Casp3	Casp9	Yes	Yes	Q8TAP6	CEP76	FVTD	SVEQELPS	75	Centrosomal protein
Casp3		No	No	Q96ST8	CEP89	SHQD	GFPGSPPA	184	Centrosomal protein

	Casp9	Yes	Yes	Q8IW35	CEP97	LEDD	GVADESVK	434	Centrosomal protein
Casp3		Yes	Yes	Q8IW35	CEP97	ARVD	AALPPGEG	8	Centrosomal protein
Casp3		Yes	Yes	Q96L14	C170L	GEID	SVTSSGTA	51	Cep170-like protein
Casp3		No	No	Q9HD42	CHM1A	EQVD	SLIMQIAE	148	Charged multivesicul
Casp3		No	No	P0DP91	ERPG3	SVGD	GLSTSAVG	53	Chimeric ERCC6-PGBD3
Casp3		Yes	Yes	Q9Y232	CDYL	TAVD	GFQSESPE	211	Chromodomain Y-like
Casp3		No	Yes	Q14839	CHD4	TAVD	GYETDHQD	364	Chromodomain-helicas
Casp3		No	Yes	Q14839	CHD4	VCKD	GGELLCCD	458	Chromodomain-helicas
Casp3		No	No	Q8WVB6	CTF18	DEID	GAPVAAIN	439	Chromosome transmiss
Casp3	Casp9	No	No	Q8WVB6	CTF18	PQVD	GSPPGLEG	870	Chromosome transmiss
Casp3		Yes	Yes	Q9P2M7	CING	SSVD	SLINKFDS	174	Cingulin
Casp3		No	No	Q9ULV3	CIZ1	ITVD	AVGCFEGD	736	Cip1-interacting zin
Casp3		No	Yes	Q9UPT6	JIP3	DIID	STPELDMC	347	C-Jun-amino-terminal
Casp3		Yes	Yes	O60271	JIP4	ELED	GVVYQEEP	6	C-Jun-amino-terminal
Casp3	Casp9	Yes	Yes	P09496	CLCA	DAVD	GVMNGEYY	77	Clathrin light chain
Casp3		Yes	Yes	Q16630	CPSF6	DYMD	TLPPTVGD	55	Cleavage and polyade
Casp3		No	Yes	Q8N684	CPSF7	DLID	IYADEEFN	10	Cleavage and polyade
Casp3		Yes	Yes	Q8N684	CPSF7	DQID	LYDDVLTA	30	Cleavage and polyade
Casp3		Yes	Yes	Q7Z460	CLAP1	VSRD	GGAASPAT	1219	CLIP-associating pro
Casp3		No	Yes	O75122	CLAP2	ESVD	GNRPSSAA	17	CLIP-associating pro
Casp3		Yes	Yes	P53621	COPA	TGVD	LFGTTDAV	189	Coatomer subunit alp
Casp3	Casp9	Yes	Yes	P53621	COPA	LDED	GFVEATEG	857	Coatomer subunit alp
Casp3	Casp9	Yes	Yes	P35606	COPB2	QELD	GKPASPTP	855	Coatomer subunit bet
Casp3		No	Yes	P48444	COPD	NFVD	KLKSEGET	241	Coatomer subunit del
Casp3		No	No	Q8IWY9	CDAN1	FEVD	TVAPEHGL	777	Codanin-1
Casp3		No	Yes	P23528	COF1	AVSD	GVIKVFND	10	Cofilin-1
Casp3	Casp9	Yes	Yes	Q6P1N0	C2D1A	LSPD	GLMIPEDG	31	Coiled-coil and C2 d
Casp3		No	Yes	Q96MW1	CCD43	DEKD	DSGATTMN	150	Coiled-coil domain-c
Casp3		No	Yes	Q16204	CCDC6	SDTD	GAGGNSSS	12	Coiled-coil domain-c
Casp3		Yes	Yes	Q15003	CND2	DEPD	HTAVGDHE	381	Condensin complex su
Casp3		Yes	Yes	Q6IBW4	CNDH2	ADLD	AVPMSLSY	460	Condensin-2 complex
Casp3		No	No	Q9UP83	COG5	SVVD	GYCATLEE	282	Conserved oligomeric
Casp3		No	No	P83436	COG7	ELVD	AVYDPYKP	350	Conserved oligomeric
Casp3		Yes	Yes	Q9NZB2	F120A	NHVD	SAYFPGSS	450	Constitutive coactiv
Casp3		Yes	Yes	Q13098	CSN1	NAPD	AIPESGVE	115	COP9 signalosome com
Casp3		Yes	Yes	O75367	H2AY	ASAD	STTEGTPA	173	Core histone macro-H
Casp3		Yes	Yes	Q86X95	CIR1	VPTD	GSGPSMHP	160	Corepressor interact
Casp3		Yes	Yes	P17544	ATF7	ARTD	SVIIADQT	44	Cyclic AMP-dependent
Casp3		Yes	Yes	P16220	CREB1	QTTD	GQQILVPS	230	Cyclic AMP-responsiv
Casp3		Yes	Yes	P21127	CD11B	TEGD	YVPDSPAL	406	Cyclin-dependent kin
Casp3		No	Yes	Q00534	CDK6	MEKD	GLCRADQQ	5	Cyclin-dependent kin
Casp3		Yes	Yes	O60583	CCNT2	DVRD	HYIAAQVE	455	Cyclin-T2
Casp3		Yes	Yes	O43169	CYB5B	SGSD	GKGQEVET	11	Cytochrome b5 type B

Casp3		No	Yes	Q9Y6G9	DC1L1	DDED	GQNLWSCI	45	Cytoplasmic dynein 1
Casp3	Casp9	Yes	Yes	P16333	NCK1	SVPD	SASPADDS	89	Cytoplasmic protein
Casp3		Yes	Yes	Q2VPK5	CTU2	DAAD	SATAFGAQ	402	Cytoplasmic tRNA 2-t
Casp3		No	Yes	Q14008	CKAP5	SDLD	SNQTHSSG	1999	Cytoskeleton-associa
Casp3		No	No	P53384	NUBP1	AHID	GAVIITTP	194	Cytosolic Fe-S clust
Casp3		No	No	Q9HCK1	ZDBF2	VSAD	SVFPLQSV	542	DBF4-type zinc finge
Casp3		No	Yes	Q5BKZ1	ZN326	NSLD	SFGGRNQG	121	DBIRD complex subuni
Casp3		No	No	Q5TAQ9	DCAF8	SSTD	GRTDLANG	10	DDB1- and CUL4-assoc
Casp3		No	Yes	Q9BTC0	DIDO1	DGTD	CTSIGTIE	350	Death-inducer oblite
Casp3		No	Yes	Q9BTC0	DIDO1	AQPD	SVYCSNDC	410	Death-inducer oblite
Casp3		Yes	Yes	Q96BY6	DOC10	EETD	SSENNLHA	328	Dedicator of cytokin
Casp3		Yes	Yes	Q96N67	DOCK7	LERD	STEVEIST	419	Dedicator of cytokin
Casp3		No	No	O75398	DEAF1	VHTD	GSIVETTG	155	Deformed epidermal a
Casp3		Yes	Yes	Q9BU89	DOHH	QEVD	AIGQTLVD	9	Deoxyhypusine hydrox
Casp3		No	Yes	Q96JH7	VCIP1	ETTD	GCVADALG	1177	Deubiquitinating pro
Casp3		No	Yes	Q96JH7	VCIP1	LCVD	AAGHFPIG	965	Deubiquitinating pro
Casp3		Yes	Yes	Q86XP1	DGKH	SQTD	SVPGPAVA	699	Diacylglycerol kinas
Casp3		No	Yes	P09622	DLDH	TKAD	GGTQVIDT	169	Dihydrolipoyl dehydr
Casp3		No	No	Q9Y2H0	DLGP4	ESAD	SIEIYVPE	980	Disks large-associat
Casp3		Yes	Yes	Q2NKX8	ERC6L	DEDD	SFKDTSSI	1036	DNA excision repair
Casp3		No	Yes	Q15054	DPOD3	TYLD	GEGCIVTE	395	DNA polymerase delta
Casp3	Casp9	Yes	Yes	P23025	XPA	AAAD	GALPEAAA	6	DNA repair protein c
Casp3		No	No	Q06609	RAD51	AQVD	GAAMFAAD	275	DNA repair protein R
Casp3		Yes	Yes	P49736	MCM2	EEED	GEELIGDG	69	DNA replication lice
Casp3	Casp9	Yes	Yes	P49736	MCM2	PELD	AYEAEGLA	89	DNA replication lice
Casp3	Casp9	Yes	Yes	P33991	MCM4	LQSD	GAAAEDIV	133	DNA replication lice
Casp3		No	Yes	P33991	MCM4	LDFD	VSSPLTYG	86	DNA replication lice
Casp3	Casp9	Yes	Yes	P33992	MCM5	FYSD	SFGGDAQA	14	DNA replication lice
Casp3		No	Yes	P33992	MCM5	VLAD	GGVVCIDE	439	DNA replication lice
Casp3		No	Yes	Q14566	MCM6	DKCD	FTGTLIVV	244	DNA replication lice
Casp3		Yes	Yes	Q14566	MCM6	SGVD	GYETEGIR	275	DNA replication lice
	Casp9	No	Yes	P11388	TOP2A	PQED	GVELEGLK	1252	DNA topoisomerase 2-
Casp3		Yes	Yes	Q92547	TOPB1	DVKD	ALAALETP	842	DNA topoisomerase 2-
Casp3		No	No	P29372	3MG	SSSD	AAQAPAEQ	37	DNA-3-methyladenine
Casp3		No	No	Q2KHR2	RFX7	SNTD	GALQKPSN	480	DNA-binding protein
Casp3		No	Yes	P78527	PRKDC	DWVD	GEPTEAEK	2984	DNA-dependent protei
Casp3		Yes	Yes	P78527	PRKDC	VDQD	GDPSDRME	3212	DNA-dependent protei
Casp3		No	Yes	P78527	PRKDC	PCLD	GYLKTSAL	798	DNA-dependent protei
Casp3		No	Yes	O15446	RPA34	LEVD	MALGSPEM	201	DNA-directed RNA pol
Casp3		No	No	Q3B726	RPA43	AASD	GSLVGQAG	17	DNA-directed RNA pol
Casp3	Casp9	Yes	Yes	P36954	RPB9	MEPD	GTYEPGFV	5	DNA-directed RNA pol
Casp3		No	Yes	Q9NVU0	RPC5	AGTD	SFNGHPPQ	544	DNA-directed RNA pol
Casp3		Yes	Yes	O60216	RAD21	DDID	VAQQFSLN	129	Double-strand-break

Casp3		Yes	Yes	O60216	RAD21	DSPD	SVDPVEPM	280	Double-strand-break
Casp3		No	Yes	O60216	RAD21	TMTD	QTTLVPNE	293	Double-strand-break
Casp3		Yes	Yes	P55265	DSRAD	VRPD	GHSQGAPN	215	Double-stranded RNA-
Casp3		Yes	Yes	Q8NBA8	DTWD2	DSAD	GLWELPVE	54	DTW domain-containin
Casp3		No	No	Q6XUX3	DUSTY	MEGD	GVPWGSEP	5	Dual serine/threonin
Casp3		Yes	Yes	Q02750	MP2K1	PAPD	GSAVNGTS	17	Dual specificity mit
Casp3		No	No	Q16829	DUS7	TESD	GSPVPSSQ	234	Dual specificity pro
Casp3		No	No	Q9UJW0	DCTN4	HEVD	SHYCPSCL	48	Dynactin subunit 4
Casp3		No	Yes	O00429	DNM1L	DFAD	ACGLMNNN	504	Dynamin-1-like prote
Casp3		Yes	Yes	O00429	DNM1L	GVGD	GVQEPTTG	580	Dynamin-1-like prote
Casp3	Casp9	No	No	P63167	DYL1	MQQD	SVECATQA	21	Dynein light chain 1
Casp3		Yes	Yes	P49792	RBP2	HETD	GGSAHGDD	1158	E3 SUMO-protein liga
Casp3		Yes	Yes	P49792	RBP2	ALDD	SVSSSSVH	2237	E3 SUMO-protein liga
Casp3		Yes	Yes	P49792	RBP2	EERD	GQYFEPVV	2307	E3 SUMO-protein liga
Casp3		Yes	Yes	P49792	RBP2	DVAD	ATSEVEVS	2491	E3 SUMO-protein liga
Casp3		No	Yes	P49792	RBP2	STTD	SVYTGGTE	2777	E3 SUMO-protein liga
Casp3		No	Yes	P49792	RBP2	EEPD	SITKSISS	2798	E3 SUMO-protein liga
Casp3		No	Yes	P49792	RBP2	SFAD	LASSNSGD	2853	E3 SUMO-protein liga
Casp3	Casp9	Yes	Yes	Q7Z6Z7	HUWE1	LERD	GGSGNSTI	2360	E3 ubiquitin-protein
Casp3		Yes	Yes	Q7Z6Z7	HUWE1	STRD	SAVAISGA	2931	E3 ubiquitin-protein
Casp3	Casp9	Yes	Yes	Q7Z6Z7	HUWE1	LSPD	GLPEEQPQ	3665	E3 ubiquitin-protein
Casp3		No	Yes	O43164	PJA2	VHTD	SYDPDGKH	167	E3 ubiquitin-protein
Casp3		Yes	Yes	Q7Z6E9	RBBP6	ESLD	TAAVVQVG	1679	E3 ubiquitin-protein
Casp3		No	Yes	Q7Z6E9	RBBP6	IMTD	AVVIPCCG	269	E3 ubiquitin-protein
Casp3		No	Yes	Q7Z6E9	RBBP6	VSPD	ALIANKFL	308	E3 ubiquitin-protein
Casp3		No	Yes	Q7Z6E9	RBBP6	NKTD	SLFVLPSR	973	E3 ubiquitin-protein
	Casp9	Yes	Yes	Q06587	RING1	VSSD	SAPDSAPG	190	E3 ubiquitin-protein
Casp3		No	Yes	Q06587	RING1	SAPD	SAPGPAPK	194	E3 ubiquitin-protein
Casp3		Yes	Yes	Q99496	RING2	AITD	GLEIVVSP	35	E3 ubiquitin-protein
	Casp9	No	No	Q9BV68	RN126	LFHD	GCIVPWLE	254	E3 ubiquitin-protein
Casp3		No	Yes	Q63HN8	RN213	HMVD	GQPLAEDS	2509	E3 ubiquitin-protein
Casp3		Yes	Yes	Q63HN8	RN213	MAVD	AVAEPANA	274	E3 ubiquitin-protein
Casp3		No	No	P78317	RNF4	ICMD	GYSEIVQN	138	E3 ubiquitin-protein
Casp3		No	No	P78317	RNF4	DHAD	SCVVSSDD	90	E3 ubiquitin-protein
Casp3		Yes	Yes	Q9UPN9	TRI33	SELD	ALASLENH	830	E3 ubiquitin-protein
Casp3		No	No	Q14669	TRIPC	ENMD	GSNPALNV	1112	E3 ubiquitin-protein
Casp3		No	No	Q14669	TRIPC	TITD	SSSAASTS	196	E3 ubiquitin-protein
Casp3		No	No	Q8IWV8	UBR2	LELD	ASTSAVLD	1072	E3 ubiquitin-protein
Casp3		Yes	Yes	Q5T4S7	UBR4	SAVD	SVAGEHSV	2904	E3 ubiquitin-protein
Casp3		Yes	Yes	O95071	UBR5	TCSD	ASSIASSA	620	E3 ubiquitin-protein
Casp3	Casp9	No	Yes	Q86UK7	ZN598	EEED	GGPALQEL	557	E3 ubiquitin-protein
Casp3		Yes	Yes	Q15075	EEA1	AKPD	GLVTDSSA	128	Early endosome antig
Casp3		No	No	Q5JPI9	EFMT2	SGAD	GGGGAAVA	7	EEF1A lysine methylt

Casp3		Yes	Yes	Q8N3D4	EH1L1	DRAD	GAAPGVAS	1202	EH domain-binding pr
Casp3		No	No	Q9P2K8	E2AK4	DGLD	SVEAAAPP	695	eIF-2-alpha kinase G
Casp3		Yes	Yes	Q14657	LAGE3	GGVD	TAAAPAGG	29	EKC/KEOPS complex su
Casp3		No	Yes	P38117	ETFB	VVTD	GVKHSMNP	33	Electron transfer fl
Casp3	Casp9	Yes	Yes	P68104	EF1A1	AIVD	MVPGKPMC	404	Elongation factor 1-
Casp3		No	Yes	P13639	EF2	TLTD	SLVCKAGI	38	Elongation factor 2
Casp3		Yes	Yes	P13639	EF2	PFPD	GLAEDIDK	612	Elongation factor 2
Casp3		Yes	Yes	P49411	EFTU	DAVD	TYIPVPAR	245	Elongation factor Tu
Casp3		No	No	Q9NZ08	ERAP1	MEVD	ALNSSHPV	412	Endoplasmic reticulu
Casp3		No	No	Q9NZ08	ERAP1	DLWD	SMASICPT	481	Endoplasmic reticulu
Casp3		No	No	Q9NZ08	ERAP1	CPTD	GVKGMDGF	490	Endoplasmic reticulu
Casp3		No	No	Q96RQ1	ERGI2	ASAD	GLVYEPTV	106	Endoplasmic reticulu
Casp3		No	No	Q9Y282	ERGI3	DAMD	VAGEQQLD	91	Endoplasmic reticulu
	Casp9	Yes	Yes	P14625	ENPL	VDVD	GTVEEDLG	29	Endoplasmin
Casp3		No	No	Q9UPY3	DICER	STSD	GSPVMAVM	1254	Endoribonuclease Dic
Casp3		Yes	Yes	P42892	ECE1	DLVD	SLSEGDAY	34	Endothelin-convertin
Casp3	Casp9	Yes	Yes	Q6P2E9	EDC4	EEND	SLGADGTH	486	Enhancer of mRNA-dec
Casp3		No	Yes	Q6P2E9	EDC4	LGAD	GTHGAGAM	491	Enhancer of mRNA-dec
Casp3		Yes	Yes	Q6P2E9	EDC4	LQLD	GSLTMSSS	663	Enhancer of mRNA-dec
	Casp9	No	Yes	Q6P2E9	EDC4	LEPD	SMASAASA	768	Enhancer of mRNA-dec
Casp3		Yes	Yes	Q6P2E9	EDC4	LGLD	GGPGDGDR	797	Enhancer of mRNA-dec
Casp3		No	Yes	Q6P2E9	EDC4	STPD	SQVWPTAP	824	Enhancer of mRNA-dec
Casp3		Yes	Yes	Q6P2E9	EDC4	DSQD	ASAEQSDH	874	Enhancer of mRNA-dec
Casp3		No	No	P61916	NPC2	GSVD	GVIKEVNV	32	Epididymal secretory
Casp3		No	Yes	Q96HE7	ERO1A	EVPD	GIKSASYK	112	ERO1-like protein al
Casp3		Yes	Yes	Q3B7T1	EDRF1	DFID	SVGNDVDV	116	Erythroid differenti
Casp3		No	Yes	Q9H501	ESF1	NSTD	GEMCDKDA	231	ESF1 homolog
Casp3		Yes	Yes	P32519	ELF1	VTLD	GIPEVMET	146	ETS-related transcri
Casp3		Yes	Yes	P60842	IF4A1	EIVD	SFDDMNLS	33	Eukaryotic initiatio
Casp3		No	Yes	Q8IYD1	ERF3B	DQVD	MESPGSAP	20	Eukaryotic peptide c
Casp3		No	No	Q9NZJ5	E2AK3	DVED	GTMDGNDE	774	Eukaryotic translati
Casp3		Yes	Yes	P55884	EIF3B	-MQD	AENVAVPE	4	Eukaryotic translati
Casp3	Casp9	Yes	Yes	Q99613	EIF3C	EDED	GVSAATFL	190	Eukaryotic translati
Casp3		No	Yes	Q99613	EIF3C	DQKD	GYRKNEGY	891	Eukaryotic translati
	Casp9	No	Yes	O75822	EIF3J	GDSD	SWDADAFS	13	Eukaryotic translati
	Casp9	Yes	Yes	Q04637	IF4G1	LVDD	GGWNTVPI	1050	Eukaryotic translati
Casp3		No	Yes	P78344	IF4G2	GLAD	MFGQMPGS	374	Eukaryotic translati
	Casp9	Yes	Yes	O43432	IF4G3	VEAD	GQTEEILD	479	Eukaryotic translati
Casp3		Yes	Yes	P23588	IF4B	NKVD	GMNAPKGQ	532	Eukaryotic translati
Casp3		Yes	Yes	Q15056	IF4H	DEVD	SLKEALTY	94	Eukaryotic translati
Casp3		No	No	P55010	IF5	DMLD	GFIKKFVL	91	Eukaryotic translati
Casp3		No	Yes	P63241	IF5A1	ETGD	AGASATFP	12	Eukaryotic translati
Casp3		Yes	Yes	P63241	IF5A1	DDLD	FETGDAGA	7	Eukaryotic translati

130

Casp3		No	No	Q93063	EXT2	TAID	GLSLDQTH	662	Exostosin-2
Casp3		No	No	Q9HAV4	XPO5	IQKD	SLDQFDCK	1125	Exportin-5
Casp3		No	Yes	Q9BSJ8	ESYT1	THVD	SPLEAPAG	963	Extended synaptotagm
Casp3		No	No	Q99504	EYA3	FSTD	GFSGSGGS	389	Eyes absent homolog
Casp3		Yes	Yes	Q08945	SSRP1	TQED	GVDPVEAF	174	FACT complex subunit
Casp3		Yes	Yes	Q92945	FUBP2	SQGD	SISSQLGP	129	Far upstream element
Casp3		Yes	Yes	Q96I24	FUBP3	AKID	SIPHLNNS	35	Far upstream element
Casp3		Yes	Yes	P49327	FAS	PGLD	GAQIPRDP	1166	Fatty acid synthase
Casp3		Yes	Yes	P49327	FAS	TNTD	GFKEQGVT	255	Fatty acid synthase
Casp3		No	Yes	O14526	FCHO1	PSPD	SWVPRPGT	491	F-BAR domain only pr
Casp3		No	Yes	O60907	TBL1X	TVFD	GRPIESLS	126	F-box-like/WD repeat
Casp3		Yes	Yes	O60907	TBL1X	SLID	AVMPDVVQ	137	F-box-like/WD repeat
Casp3		No	No	Q9BZ67	FRMD8	VSSD	GGCEAALG	244	FERM domain-containi
Casp3		No	No	Q96AC1	FERM2	DAHD	GSPLSPTS	198	Fermitin family homo
Casp3		No	No	Q96AC1	FERM2	DEVD	AALSDLEI	348	Fermitin family homo
Casp3		Yes	Yes	Q86UX7	URP2	DVLD	SLTTIPEL	345	Fermitin family homo
Casp3		Yes	Yes	Q9Y613	FHOD1	DVTD	ALEQQGME	300	FH1/FH2 domain-conta
Casp3		Yes	Yes	Q9Y613	FHOD1	CSLD	GALPLGAQ	47	FH1/FH2 domain-conta
Casp3		No	No	P23142	FBLN1	SDVD	GVTCEDID	476	Fibulin-1
Casp3		No	No	P98095	FBLN2	IMAD	GVSCEDIN	714	Fibulin-2
Casp3		Yes	Yes	P21333	FLNA	VTYD	GVPVPGSP	1049	Filamin-A
Casp3		Yes	Yes	P21333	FLNA	VTYD	GSPVPSSP	1337	Filamin-A
Casp3		Yes	Yes	P21333	FLNA	DNAD	GTQTVNYV	1505	Filamin-A
Casp3		Yes	Yes	P21333	FLNA	DTRD	AEMPATEK	26	Filamin-A
Casp3		Yes	Yes	O75369	FLNB	DNGD	GTHTVTYT	1477	Filamin-B
Casp3		No	Yes	O75369	FLNB	DFLD	GVYAFEYY	509	Filamin-B
Casp3		No	Yes	Q5T1M5	FKB15	DDTD	FLSPSGGA	12	FK506-binding protei
Casp3		Yes	Yes	Q5T1M5	FKB15	SSRD	SAAPSPIP	307	FK506-binding protei
Casp3		Yes	Yes	Q9P0K8	FOXJ2	GSVD	GGAVAAGA	213	Forkhead box protein
Casp3		Yes	Yes	O43524	FOXO3	TAAD	SMIPEEED	55	Forkhead box protein
Casp3		No	No	P98177	FOXO4	ELLD	GLNLTSSH	309	Forkhead box protein
Casp3		Yes	Yes	Q8IVH2	FOXP4	SFPD	GLVHPPTS	407	Forkhead box protein
Casp3	Casp9	Yes	Yes	Q96RU3	FNBP1	ESPD	GSYTEEQS	520	Formin-binding prote
Casp3		Yes	Yes	Q8N3X1	FNBP4	AEID	AITAPQPA	154	Formin-binding prote
Casp3		Yes	Yes	Q8N3X1	FNBP4	EEGD	GSVSGSSP	426	Formin-binding prote
Casp3		Yes	Yes	Q8N3X1	FNBP4	SSVD	STISSSSS	778	Formin-binding prote
Casp3		No	Yes	P51116	FXR2	NRTD	GSISGDRQ	600	Fragile X mental ret
Casp3		Yes	Yes	Q01543	FLI1	SLFD	SAYGAAAH	21	Friend leukemia inte
Casp3		Yes	Yes	O15117	FYB1	DNQD	GVTHSDGA	441	FYN-binding protein
Casp3		Yes	Yes	O15117	FYB1	THSD	GAGNLDEE	447	FYN-binding protein
Casp3		No	No	Q9BQS8	FYCO1	TETD	SLDPNAAE	1307	FYVE and coiled-coil
Casp3		Yes	Yes	Q92917	GPKOW	DSGD	GAGPSPEE	38	G patch domain and K
Casp3	Casp9	Yes	Yes	Q92917	GPKOW	ALAD	GVVSQAVK	99	G patch domain and K

Casp3		Yes	Yes	Q9UKJ3	GPTC8	SNLD	GKKEDEDP	357	G patch domain-conta
Casp3		Yes	Yes	Q06547	GABP1	TMPD	GQQVLTVP	304	GA-binding protein s
Casp3		No	Yes	Q8TAK5	GABP2	AEVD	AVVVTEGE	413	GA-binding protein s
Casp3		No	No	Q8WW33	GTSF1	TYTD	SLDPEKLL	8	Gametocyte-specific
Casp3		Yes	Yes	P57764	GSDMD	FLTD	GVPAEGAF	276	Gasdermin-D
Casp3		Yes	Yes	P57764	GSDMD	DAMD	GQIQGSVE	88	Gasdermin-D
Casp3		No	No	Q6PJI9	WDR59	DILD	GVDEFIES	331	GATOR complex protei
Casp3	Casp9	No	No	P16383	GCFC2	SDSD	GAEESPAE	21	GC-rich sequence DNA
Casp3		Yes	Yes	P06396	GELS	DQTD	GLGLSYLS	404	Gelsolin
Casp3		Yes	Yes	Q9P107	GMIP	DLGD	GLENGLGS	473	GEM-interacting prot
Casp3		Yes	Yes	Q9P107	GMIP	DTKD	GGGEVSSQ	843	GEM-interacting prot
Casp3		No	Yes	Q8WUA4	TF3C2	EEVD	GAPRDEDF	241	General transcriptio
Casp3		No	Yes	P29083	T2EA	DERD	STNRASFK	121	General transcriptio
	Casp9	Yes	Yes	P29083	T2EA	IDMD	AFQEREEG	304	General transcriptio
	Casp9	No	Yes	P35269	T2FA	MSSD	ASDASGEE	220	General transcriptio
Casp3		Yes	Yes	P35269	T2FA	QEVD	YMSDGSSS	273	General transcriptio
Casp3		No	No	P32780	TF2H1	SNMD	GNSGDADC	337	General transcriptio
Casp3		No	No	Q13888	TF2H2	AHLD	GNTEPGLT	278	General transcriptio
Casp3		Yes	Yes	P78347	GTF2I	VVVD	GMPPGVSF	908	General transcriptio
Casp3		No	No	O60318	GANP	ESTD	SLGGLSPS	425	Germinal-center asso
Casp3		No	No	O60318	GANP	DSFD	SASEGSEG	577	Germinal-center asso
Casp3		Yes	Yes	Q3V6T2	GRDN	DSQD	SSSVGSNS	1442	Girdin
Casp3		No	Yes	Q3V6T2	GRDN	EERD	GLHFLPHA	220	Girdin
Casp3		Yes	Yes	P14314	GLU2B	DDMD	GTVSVTEL	227	Glucosidase 2 subuni
	Casp9	No	Yes	P14314	GLU2B	LDTD	GDGALSEA	244	Glucosidase 2 subuni
Casp3		No	Yes	P14314	GLU2B	TQTD	ATSFYDRV	265	Glucosidase 2 subuni
Casp3		No	Yes	O94925	GLSK	GETD	AFGNSEGK	114	Glutaminase kidney i
Casp3		No	No	Q06210	GFPT1	SRVD	STTCLFPV	261	Glutamine--fructose-
Casp3		Yes	Yes	Q2TAL8	QRIC1	LTVD	SAHLYSAT	291	Glutamine-rich prote
Casp3		Yes	Yes	O76003	GLRX3	DRLD	GAHAPELT	102	Glutaredoxin-3
Casp3		No	Yes	P04406	G3P	LWRD	GRGALQNI	199	Glyceraldehyde-3-pho
Casp3		Yes	Yes	P41250	GARS	SSMD	GAGAEEVL	57	Glycine--tRNA ligase
Casp3		No	No	P13807	GYS1	NSVD	TATSSSLS	713	Glycogen [starch] sy
Casp3	Casp9	No	Yes	P30419	NMT1	SETD	SAQDQPVK	73	Glycylpeptide N-tetr
Casp3		Yes	Yes	Q9H3P7	GCP60	VSVD	GLTLSPDP	16	Golgi resident prote
Casp3		No	Yes	Q13439	GOGA4	EEAD	SQGCVQKT	1726	Golgin subfamily A m
Casp3		No	Yes	Q14789	GOGB1	ESID	GKLPSTDQ	1246	Golgin subfamily B m
Casp3		No	Yes	Q14789	GOGB1	EEQD	SLSMSTRP	1802	Golgin subfamily B m
Casp3		No	Yes	Q14789	GOGB1	DVTD	AQIKNELL	1947	Golgin subfamily B m
Casp3		No	Yes	Q14789	GOGB1	ASPD	GSQNLVYE	3019	Golgin subfamily B m
Casp3		Yes	Yes	Q92538	GBF1	DHSD	SASVHDMD	369	Golgi-specific brefe
Casp3		Yes	Yes	Q3T8J9	GON4L	VCMD	SFQPMDDS	482	GON-4-like protein
Casp3		No	Yes	P28799	GRN	VMVD	GSWGCCPM	145	Granulins

Casp3		No	Yes	P28799	GRN	SCPD	GYTCCR	293	Granulins
Casp3		No	Yes	Q6Y7W6	GGYF2	DDRD	SLPEWCLE	284	GRB10-interacting GY
Casp3		No	Yes	Q9UQC2	GAB2	ESTD	SLRNVSSA	127	GRB2-associated-bind
Casp3		No	No	Q9UQC2	GAB2	SMSD	GVGSFLPG	429	GRB2-associated-bind
Casp3		No	Yes	O75791	GRAP2	DIND	GHCGTGLG	242	GRB2-related adapter
Casp3		Yes	Yes	Q8IWJ2	GCC2	LVQD	GVASPATP	8	GRIP and coiled-coil
Casp3		No	No	Q8WWP7	GIMA1	DTPD	IFSSQVSK	86	GTPase IMAP family m
Casp3	Casp9	Yes	Yes	Q14C86	HDHD5	DLPD	SASQAAHP	1103	GTPase-activating pr
Casp3		Yes	Yes	Q14C86	GAPD1	CSAD	SVAFPVLT	1133	GTPase-activating pr
Casp3		No	Yes	Q14C86	GAPD1	QFVD	GYKQLGFQ	85	GTPase-activating pr
Casp3		No	No	Q15382	RHEB	QFVD	SYDPTIEN	34	GTP-binding protein
Casp3		No	No	Q8TBN0	R3GEF	AEVD	CSSTNTCA	296	Guanine nucleotide e
Casp3		Yes	Yes	P36915	GNL1	QQTD	SAMEPTGP	344	Guanine nucleotide-b
Casp3	Casp9	No	Yes	Q9BXW7	HAUS6	ATHD	GAPELGAG	336	Haloacid dehalogenas
Casp3		Yes	Yes	Q92574	TSC1	TEED	GVPSTSPM	639	Hamartin
Casp3		No	No	Q7Z4H7	HAUS6	ELID	SLGSNPFL	569	HAUS augmin-like com
Casp3		Yes	Yes	O00165	HAX1	TLRD	SMLKYPDS	128	HCLS1-associated pro
Casp3		No	Yes	O00165	HAX1	NDLD	SQVSQEGL	189	HCLS1-associated pro
Casp3		No	No	Q7Z4H3	HDDC2	DFYD	STAGKFNH	170	HD domain-containing
Casp3		Yes	Yes	Q6AI08	HEAT6	AEKD	GVSSSFSS	381	HEAT repeat-containi
Casp3		No	Yes	Q00613	HSF1	SEGD	GFAEDPTI	505	Heat shock factor pr
Casp3		No	No	Q03933	HSF2	DYLD	SIDCSLED	366	Heat shock factor pr
	Casp9	Yes	Yes	Q7Z4V5	HDGR2	ADSD	GAKPEPVA	242	Hepatoma-derived gro
Casp3		No	No	Q9NQG7	HPS4	EDVD	GVCESHAA	496	Hermansky-Pudlak syn
Casp3		Yes	Yes	P51991	ROA3	SRED	SVKPGAHL	116	Heterogeneous nuclea
Casp3	Casp9	Yes	Yes	P52597	HNRPF	GLSD	GYGFTTDL	252	Heterogeneous nuclea
Casp3		Yes	Yes	P31943	HNRH1	VEMD	WVLKHTGP	95	Heterogeneous nuclea
Casp3	Casp9	Yes	Yes	P61978	HNRPK	LESD	AVECLNYQ	129	Heterogeneous nuclea
Casp3		Yes	Yes	P61978	HNRPK	SAID	TWSPSEWQ	351	Heterogeneous nuclea
	Casp9	Yes	Yes	Q8WVV9	HNRLL	FRHD	GYGSHGPL	290	Heterogeneous nuclea
Casp3		Yes	Yes	O60506	HNRPQ	DYYD	YYGYDYHN	469	Heterogeneous nuclea
Casp3		Yes	Yes	Q9BUJ2	HNRL1	SGPD	GHYAMDNI	97	Heterogeneous nuclea
	Casp9	Yes	Yes	Q1KMD3	HNRL2	AEPD	ASEKPAEA	127	Heterogeneous nuclea
Casp3		Yes	Yes	P56524	HDAC4	STVD	VATALPLQ	34	Histone deacetylase
Casp3		Yes	Yes	Q9UBN7	HDAC6	DMAD	SMLMQGSR	1089	Histone deacetylase
Casp3	Casp9	Yes	Yes	Q8WUI4	HDAC7	LETD	GGGPGQVV	413	Histone deacetylase
Casp3		No	No	P0C0S5	H2AZ	EELD	SLIKATIA	99	Histone H2A.Z
Casp3		No	No	Q9UPP1	PHF8	DEQD	SLGACFKD	840	Histone lysine demet
Casp3		No	Yes	Q03164	KMT2A	SHLD	GSSSSEMK	2282	Histone-lysine N-met
Casp3		Yes	Yes	Q9UMN6	KMT2B	EQLD	GVDDGTDS	2063	Histone-lysine N-met
Casp3		No	Yes	O14686	KMT2D	DEPD	ALYVACQG	387	Histone-lysine N-met
Casp3		No	Yes	Q9H9B1	EHMT1	LETD	GLQEVPLC	513	Histone-lysine N-met
Casp3		No	No	Q4FZB7	KMT5B	SYTD	CAPSPVGC	668	Histone-lysine N-met

Casp3	Casp9			Acc	Gene				Description
Casp3		No	Yes	O15047	SET1A	TEVD	LAVLADLA	1253	Histone-lysine N-met
Casp3		Yes	Yes	Q9BYW2	SETD2	DSHD	SIKELDSL	648	Histone-lysine N-met
Casp3		No	Yes	Q9BYW2	SETD2	SKTD	AVLMTSDD	693	Histone-lysine N-met
Casp3		Yes	Yes	O43719	HTSF1	TQTD	AGGEPDSL	34	HIV Tat-specific fac
Casp3	Casp9	Yes	Yes	O43719	HTSF1	GEPD	SLGQQPTD	40	HIV Tat-specific fac
Casp3	Casp9	Yes	Yes	O43719	HTSF1	FSND	GASSSTAN	81	HIV Tat-specific fac
Casp3		Yes	Yes	P13747	HLAE	TAVD	TAAQISEQ	159	HLA class I histocom
Casp3		Yes	Yes	Q8NCD3	HJURP	DRTD	GSVQAAAW	92	Holliday junction re
Casp3	Casp9	No	No	O95475	SIX6	AEGD	GTPEVLGV	211	Homeobox protein SIX
Casp3		Yes	Yes	Q16543	CDC37	SVWD	HIEVSDDE	9	Hsp90 co-chaperone C
Casp3		Yes	Yes	Q01581	HMCS1	DGVD	AGKYTIGL	44	Hydroxymethylglutary
Casp3		No	No	O00629	IMA3	SDID	GDYRVQNT	64	Importin subunit alp
Casp3		No	No	O00505	IMA4	SDVD	ADFKAQNV	64	Importin subunit alp
Casp3		Yes	Yes	O60684	IMA7	LLMD	SYVSSTTG	70	Importin subunit alp
Casp3		No	Yes	Q14974	IMB1	DMVD	YLNELRES	757	Importin subunit bet
Casp3		No	Yes	Q14974	IMB1	DHTD	GVVACAAG	813	Importin subunit bet
Casp3		Yes	Yes	Q07820	MCL1	TSTD	GSLPSTPP	158	Induced myeloid leuk
Casp3		Yes	Yes	Q9Y6Y0	NS1BP	NLLD	GQAEVFGS	239	Influenza virus NS1A
Casp3		Yes	Yes	Q15181	IPYR	DDPD	AANYNDIN	166	Inorganic pyrophosph
Casp3		No	No	Q9NX62	IMPA3	EHVD	AADQEVIL	138	Inositol monophospha
Casp3		No	No	Q96DU7	IP3KC	FWTD	GQTEPAAA	93	Inositol-trisphospha
Casp3		No	No	Q68E01	INT3	SCYD	NAEAAFSD	531	Integrator complex s
Casp3		No	No	Q6P9B9	INT5	ACVD	ALLDTSVQ	211	Integrator complex s
Casp3		No	No	P05107	ITB2	CECD	TINCERYN	538	Integrin beta-2
Casp3		No	Yes	Q9H0C8	ILKAP	NVRD	GRVLGVLE	281	Integrin-linked kina
Casp3		Yes	Yes	Q9H0C8	ILKAP	SSTD	SGSGGPLL	40	Integrin-linked kina
Casp3		No	Yes	Q9H0C8	ILKAP	SSGD	SGSLATSI	59	Integrin-linked kina
Casp3		No	Yes	Q7Z5L9	I2BP2	SLPD	SSLATSAP	496	Interferon regulator
Casp3		Yes	Yes	Q9H1B7	I2BPL	NHVD	GSSKPAVL	133	Interferon regulator
Casp3		No	Yes	Q12906	ILF3	VMPD	GSGIYDPC	288	Interleukin enhancer
Casp3		No	No	Q0D2I5	IFFO1	VHPD	GVGVQIDT	226	Intermediate filamen
Casp3		Yes	Yes	Q27J81	INF2	DLVD	AVTPGPQP	1052	Inverted formin-2
	Casp9	Yes	Yes	Q27J81	INF2	AEAD	STSEGLED	1147	Inverted formin-2
Casp3		Yes	Yes	Q6DN90	IQEC1	DFAD	AITELEDA	235	IQ motif and SEC7 do
Casp3		No	Yes	P50213	IDH3A	VIVD	GVVQSIKL	163	Isocitrate dehydroge
Casp3		No	Yes	P48735	IDHP	VCPD	GKTIEAEA	339	Isocitrate dehydroge
Casp3		Yes	Yes	Q96N16	JKIP1	METD	AVQMANEE	18	Janus kinase and mic
Casp3		Yes	Yes	Q8N9B5	JMY	DHCD	SLPSVLQV	723	Junction-mediating a
Casp3		No	No	Q9HDC5	JPH1	VLHD	AAAAADSP	179	Junctophilin-1
Casp3		Yes	Yes	Q9BWU0	NADAP	DSLD	AFMSEMK	538	Kanadaptin
Casp3		Yes	Yes	Q07666	KHDR1	TGPD	ATVGGPAP	76	KH domain-containing
Casp3		No	No	O75525	KHDR3	ETYD	SYGQEEWT	315	KH domain-containing
Casp3		No	No	O60333	KIF1B	IRED	GGTLGVFS	520	Kinesin-like protein

Casp3		No	Yes	O00139	KIF2A	QDVD	ATNPNYEI	190	Kinesin-like protein
Casp3		No	Yes	Q8NG31	KNL1	EVTD	SHTVFIDC	1195	Kinetochore scaffold
Casp3		Yes	Yes	Q13601	KRR1	TVPD	GWKEPAFS	39	KRR1 small subunit p
Casp3		Yes	Yes	Q9Y4X4	KLF12	LSVD	HFQTQTEP	74	Krueppel-like factor
Casp3		Yes	Yes	P42166	LAP2A	EERD	SGSFVAFQ	442	Lamina-associated po
Casp3		No	Yes	P42167	LAP2B	FRID	GPVISEST	272	Lamina-associated po
Casp3		Yes	Yes	Q6PKG0	LARP1	DFGD	AINWPTPG	173	La-related protein 1
Casp3		No	Yes	Q6PKG0	LARP1	SQTD	FSQLLNCP	496	La-related protein 1
Casp3		Yes	Yes	Q71RC2	LARP4	VQKD	GLNQTTIP	574	La-related protein 4
Casp3		No	Yes	Q71RC2	LARP4	ESTD	GMILGPED	91	La-related protein 4
Casp3		Yes	Yes	P46379	BAG6	DEQD	GASAETEP	1002	Large proline-rich p
Casp3		No	Yes	P42704	LPPRC	TYTD	YVIPCFDS	480	Leucine-rich PPR mot
Casp3		Yes	Yes	P42704	LPPRC	DRLD	SSAVLDTG	742	Leucine-rich PPR mot
Casp3		Yes	Yes	Q9Y2L9	LRCH1	DRAD	GLHSEFMN	406	Leucine-rich repeat
Casp3		Yes	Yes	Q9Y608	LRRF2	IIPD	GTPNGDVS	532	Leucine-rich repeat
Casp3	Casp9	Yes	Yes	Q8N1G4	LRC47	TEAD	AVSGQLPD	526	Leucine-rich repeat-
Casp3		No	No	Q9UIQ6	LCAP	DVVD	LAKEPCLH	30	Leucyl-cystinyl amin
Casp3		No	No	Q96PV6	LENG8	SDSD	SSYSGNEC	406	Leukocyte receptor c
Casp3		Yes	Yes	O60711	LPXN	EELD	ALLEELER	6	Leupaxin
Casp3		No	Yes	Q9UGP4	LIMD1	ECLD	GVPFTVDS	572	LIM domain-containin
Casp3		No	Yes	O43561	LAT	VLPD	STPATSTA	168	Linker for activatio
Casp3		Yes	Yes	P50851	LRBA	SSVD	SAQASDMG	1757	Lipopolysaccharide-r
Casp3		Yes	Yes	P50851	LRBA	PTVD	SVSQDPVS	1785	Lipopolysaccharide-r
Casp3		Yes	Yes	Q13136	LIPA1	TLTD	GVLDINHE	219	Liprin-alpha-1
Casp3		No	No	Q86W92	LIPB1	EEND	GNIILGAT	440	Liprin-beta-1
Casp3		Yes	Yes	Q8ND30	LIPB2	DLSD	GTCEPGLA	32	Liprin-beta-2
Casp3		No	No	Q9P260	K1468	DEAD	STIPKENS	446	LisH domain and HEAT
Casp3		No	No	O95573	ACSL3	NSLD	GLASVLYP	76	Long-chain-fatty-aci
Casp3		No	No	P01130	LDLR	LCPD	GFQLVAQR	343	Low-density lipoprot
Casp3		No	Yes	Q12912	IRAG2	SSTD	GTITSSDP	96	Lymphoid-restricted
Casp3		No	Yes	Q9Y4C1	KDM3A	DFWD	GFEDVPNR	1026	Lysine-specific deme
Casp3		No	Yes	Q9Y4C1	KDM3A	VQDD	SCVNIVAQ	535	Lysine-specific deme
Casp3		No	No	O75164	KDM4A	DYSD	STEVKFEE	459	Lysine-specific deme
Casp3		No	No	O75164	KDM4A	SSRD	SISSDSET	520	Lysine-specific deme
Casp3		No	No	O94953	KDM4B	TSRD	CVQLGPPS	971	Lysine-specific deme
Casp3		Yes	Yes	Q9H3R0	KDM4C	DEVD	GAEVPNPD	397	Lysine-specific deme
Casp3		No	No	P41229	KDM5C	DCPD	GLVCLSHI	727	Lysine-specific deme
Casp3		No	No	Q8IU60	DCP2	FETD	AVYDLPSS	368	m7GpppN-mRNA hydrola
Casp3		No	Yes	Q8IVS2	FABD	LLRD	ATGAEEEA	42	Malonyl-CoA-acyl car
Casp3		Yes	Yes	Q8WXG6	MADD	TDQD	SVIGVSPA	1178	MAP kinase-activatin
Casp3		Yes	Yes	P43243	MATR3	DETD	LANLGDVA	681	Matrin-3
Casp3		Yes	Yes	P43243	MATR3	ENAD	GQSDENKD	764	Matrin-3
Casp3		Yes	Yes	Q8IWI9	MGAP	DSKD	SVGDSLSG	572	MAX gene-associated

Casp3		Yes	Yes	O60244	MED14	DMMD	SLISQLQP	995	Mediator of RNA poly
Casp3		No	No	Q9NVC6	MED17	VGLD	GTETYLPP	26	Mediator of RNA poly
Casp3		No	No	Q9Y4F3	MARF1	QSHD	GSSTNCSP	956	Meiosis regulator an
Casp3	Casp9	Yes	Yes	Q9Y5V3	MAGD1	SEPD	GATAQTSA	223	Melanoma-associated
Casp3		Yes	Yes	Q9Y5V3	MAGD1	TSAD	GSQAQNLE	232	Melanoma-associated
Casp3		Yes	Yes	Q9UNF1	MAGD2	SEKD	SSSMMQTL	23	Melanoma-associated
Casp3		Yes	Yes	O00562	PITM1	DFID	AFASPVEA	379	Membrane-associated
Casp3		Yes	Yes	Q8N108	MIER1	PSAD	MLVHDFDD	28	Mesoderm induction e
Casp3		Yes	Yes	Q9NZL9	MAT2B	NQPD	AASQLNVD	108	Methionine adenosylt
Casp3	Casp9	No	Yes	P53582	MAP11	CETD	GCSSEAKL	13	Methionine aminopept
Casp3		No	Yes	P54105	ICLN	DYED	GMEVDTTP	217	Methylosome subunit
Casp3		No	Yes	P54105	ICLN	MEVD	TTPTVAGQ	222	Methylosome subunit
Casp3		No	Yes	Q9H7H0	MET17	CCPD	GHMQHAVL	408	Methyltransferase-li
Casp3		No	Yes	Q8WYQ5	DGCR8	NDVD	ALLEEGLC	249	Microprocessor compl
Casp3		Yes	Yes	Q8WYQ5	DGCR8	DEPD	SMGADPGP	397	Microprocessor compl
Casp3		Yes	Yes	Q9UPN3	MACF1	DTTD	GYMGVNQA	3794	Microtubule-actin cr
Casp3		Yes	Yes	Q9UPN3	MACF1	DAPD	GSDASQLL	5088	Microtubule-actin cr
	Casp9	Yes	Yes	Q9NU22	MDN1	VDTD	SHAEQGPA	5128	Midasin
Casp3		Yes	Yes	Q9GZY8	MFF	DFLD	LERPPTTP	132	Mitochondrial fissio
Casp3		No	Yes	O95202	LETM1	EGVD	SLNVKELQ	369	Mitochondrial proton
Casp3		No	Yes	O95202	LETM1	DVQD	YSEDLQEI	579	Mitochondrial proton
Casp3		No	Yes	O95202	LETM1	GQID	GLISQLEM	621	Mitochondrial proton
Casp3		No	No	O95140	MFN2	DMID	GLKPLLPV	500	Mitofusin-2
Casp3		No	No	Q13164	MK07	DGED	GSAEPPGP	13	Mitogen-activated pr
Casp3		No	No	Q9Y2U5	M3K2	SYPD	NHQEFSDY	243	Mitogen-activated pr
Casp3		No	No	Q9UI95	MD2L2	SVCD	AVLDHNPP	135	Mitotic spindle asse
Casp3		Yes	Yes	Q969V6	MRTFA	DSSD	ALSPEQPA	122	MKL/myocardin-like p
Casp3		Yes	Yes	Q9ULH7	MKL2	DSSD	ALSPDQPA	183	MKL/myocardin-like p
Casp3		No	No	Q96BX8	MOB3A	TISD	GCTEQSCP	82	MOB kinase activator
Casp3		No	No	P47974	TISD	SDRD	SYLSGSLS	458	mRNA decay activator
Casp3		Yes	Yes	Q96T58	MINT	STTD	SIQEPVVL	1575	Msx2-interacting pro
Casp3		No	Yes	P22234	PUR6	ELLD	SPGKVLLQ	27	Multifunctional prot
Casp3		No	Yes	Q8NI22	MCFD2	NIID	GVLRDDDK	123	Multiple coagulation
Casp3		Yes	Yes	Q8NI22	MCFD2	KNND	GYIDYAEF	134	Multiple coagulation
Casp3		Yes	Yes	Q96EY5	MB12A	LSLD	AASQPSKG	173	Multivesicular body
	Casp9	Yes	Yes	Q9BQG0	MBB1A	PAED	GTPAATGG	1195	Myb-binding protein
Casp3		Yes	Yes	P35579	MYH9	DTLD	STAAQQEL	1154	Myosin-9
Casp3		No	Yes	P35579	MYH9	EEVD	GKADGAEA	1949	Myosin-9
Casp3		No	No	Q13496	MTM1	TSRD	GVNRDLTE	26	Myotubularin
Casp3		Yes	Yes	Q13614	MTMR2	VSSD	SISTSADN	49	Myotubularin-related
Casp3		Yes	Yes	Q9HCE5	MET14	ESAD	SIGAVLNS	30	N6-adenosine-methylt
Casp3		No	No	Q9P032	NDUF4	VYVD	SKDPVSSL	72	NADH dehydrogenase [
Casp3		No	No	O95299	NDUAA	TTGD	GKPLATDY	101	NADH dehydrogenase [

Casp3		No	No	O95299	NDUAA	HYPD	STTGDGKP	96	NADH dehydrogenase [
Casp3		Yes	Yes	P28331	NDUS1	DVMD	AVGSNIVV	256	NADH-ubiquinone oxid
Casp3		No	Yes	P28331	NDUS1	VFVD	GQSVMVEP	38	NADH-ubiquinone oxid
Casp3		Yes	Yes	Q13765	NACA	EEQD	STQATTQQ	43	Nascent polypeptide-
Casp3		No	No	P15882	CHIN	DERD	STGQDGVS	173	N-chimaerin
Casp3		No	No	Q9HCH0	NCK5L	TTPD	STQLRPPQ	528	Nck-associated prote
Casp3	Casp9	Yes	Yes	O75113	N4BP1	PETD	GLSPSVAS	491	NEDD4-binding protei
Casp3		No	No	Q8IXH7	NELFD	DEAD	GGQQEDDS	27	Negative elongation
Casp3		No	No	Q6ZNJ1	NBEL2	PDPD	GFYHALSP	1344	Neurobeachin-like pr
Casp3		No	No	P21359	NF1	SSMD	SAAGCSGT	669	Neurofibromin
Casp3		No	Yes	P46531	NOTC1	TCVD	QVGGYSCT	1247	Neurogenic locus not
Casp3		No	Yes	P46531	NOTC1	ACVD	GVNTYNCR	275	Neurogenic locus not
Casp3		No	No	Q9UM47	NOTC3	SCQD	GVGSFSCS	867	Neurogenic locus not
Casp3		No	Yes	Q14697	GANAB	AEGD	GAQPEETP	198	Neutral alpha-glucos
Casp3		Yes	Yes	P43007	SATT	GYLD	SAQAGPAA	13	Neutral amino acid t
Casp3		No	No	Q8NDF8	PAPD5	NMLD	GYRPSMLY	352	Non-canonical poly(A
Casp3		No	Yes	Q15233	NONO	MMPD	GTLGLTPP	423	Non-POU domain-conta
Casp3		Yes	Yes	Q96MG7	NSE3	VLRD	GFAEEAPS	42	Non-structural maint
Casp3		No	No	O60443	DFNA5	DMPD	AAHGISSQ	271	Non-syndromic hearin
Casp3		No	No	O60524	NEMF	NYPD	TTIDLSHL	780	Nuclear export media
Casp3		Yes	Yes	Q00653	NFKB2	PGLD	GIIEYDDF	11	Nuclear factor NF-ka
Casp3		No	Yes	P19838	NFKB1	AHVD	STTYDGTT	714	Nuclear factor NF-ka
Casp3		Yes	Yes	O95644	NFAC1	TRPD	GAPALESP	111	Nuclear factor of ac
Casp3		Yes	Yes	Q7Z417	NUFP2	NRVD	GSKPIWKY	275	Nuclear fragile X me
Casp3		No	Yes	Q7Z417	NUFP2	AGTD	GNVYPPGG	425	Nuclear fragile X me
Casp3		Yes	Yes	Q7Z417	NUFP2	SGTD	SVLQDMSL	452	Nuclear fragile X me
Casp3		Yes	Yes	Q14980	NUMA1	TQPD	GTSVPGEP	1748	Nuclear mitotic appa
Casp3		No	Yes	Q14980	NUMA1	SSLD	SLGDVFLD	1792	Nuclear mitotic appa
Casp3		Yes	Yes	Q14980	NUMA1	EEPD	SANSSFYS	1830	Nuclear mitotic appa
Casp3		No	Yes	O75694	NU155	AAVD	GISLHLQD	854	Nuclear pore complex
Casp3		Yes	Yes	Q9UKX7	NUP50	TLVD	KVSNPKTN	127	Nuclear pore complex
Casp3		Yes	Yes	Q9BW27	NUP85	EELD	GEPTVTLI	6	Nuclear pore complex
Casp3		Yes	Yes	Q8N1F7	NUP93	DALD	FTQESEPS	158	Nuclear pore complex
Casp3		No	Yes	Q9UHQ1	NARF	LACD	SCMTAEEG	58	Nuclear prelamin A r
Casp3		No	No	Q15788	NCOA1	SDID	SLSVKPDK	59	Nuclear receptor coa
Casp3		No	No	Q15788	NCOA1	DRMD	GAVTSVTI	838	Nuclear receptor coa
Casp3		Yes	Yes	Q9HCD5	NCOA5	DSFD	GRGPPGPE	154	Nuclear receptor coa
Casp3		Yes	Yes	O75376	NCOR1	ALVD	AAASAPQM	1827	Nuclear receptor cor
Casp3		Yes	Yes	Q9Y618	NCOR2	EIID	GLSEQENL	378	Nuclear receptor cor
Casp3		Yes	Yes	P49116	NR2C2	SLAD	GIDTSGGG	334	Nuclear receptor sub
Casp3		Yes	Yes	Q86WB0	NIPA	TEPD	ASAPAEPG	450	Nuclear-interacting
Casp3	Casp9	Yes	Yes	P80303	NUCB2	EETD	GLDPNDFD	238	Nucleobindin-2
	Casp9	Yes	Yes	P80303	NUCB2	VNSD	GFLDEQEL	259	Nucleobindin-2

Casp3		Yes	Yes	P78316	NOP14	DLND	GFVLDKDD	320	Nucleolar protein 14
Casp3		Yes	Yes	Q9Y2X3	NOP58	SQMD	GLIPGVEP	125	Nucleolar protein 58
Casp3		No	Yes	Q76FK4	NOL8	SMED	GSPYVNGS	616	Nucleolar protein 8
Casp3		Yes	Yes	Q9NR30	DDX21	RLLD	SVPPTAIS	585	Nucleolar RNA helica
	Casp9	No	Yes	P19338	NUCL	EEDD	SSGEEVVI	41	Nucleolin
Casp3		No	Yes	P06748	NPM	DSMD	MDMSPLRP	7	Nucleophosmin
	Casp9	No	No	Q8NFH3	NUP43	LDSD	GGFEGDHQ	59	Nucleoporin Nup43
Casp3		Yes	Yes	P12270	TPR	HRTD	GFAEAIHS	2148	Nucleoprotein TPR
Casp3		No	No	Q6DKJ4	NXN	DMTD	SLRDYTNL	381	Nucleoredoxin
Casp3		Yes	Yes	Q99733	NP1L4	ERLD	NVPHTPSS	47	Nucleosome assembly
Casp3	Casp9	Yes	Yes	Q99733	NP1L4	SFSD	GVPSDSVE	9	Nucleosome assembly
Casp3		No	Yes	Q12830	BPTF	TVTD	SLTTTGGT	1790	Nucleosome-remodelin
Casp3		No	Yes	Q9NZT2	OGFR	DCED	GEAAGARD	28	Opioid growth factor
Casp3		Yes	Yes	Q8N6M0	OTU6B	NKID	SVAVNISN	81	OTU domain-containin
Casp3		Yes	Yes	Q8N573	OXR1	TSAD	GHIESSAL	539	Oxidation resistance
Casp3		No	No	Q9H1P3	OSBL2	EFFD	AVTGFDSD	10	Oxysterol-binding pr
Casp3		Yes	Yes	Q9H4L5	OSBL3	TITD	SSSGVFDS	171	Oxysterol-binding pr
Casp3		No	No	Q9BZF2	OSBL7	TTAD	SFSSLNPE	365	Oxysterol-binding pr
Casp3		No	Yes	Q96ST3	SIN3A	DIID	GLRKNPSI	683	Paired amphipathic h
Casp3		Yes	Yes	Q504Q3	PAN2	SEFD	SFSQVTES	467	PAN2-PAN3 deadenylat
	Casp9	No	No	Q96RG2	PASK	PAED	GGSDAGMC	558	PAS domain-containin
Casp3		Yes	Yes	P49023	PAXI	DDLD	ALLADLES	6	Paxillin
Casp3		No	No	Q5JVF3	PCID2	DSRD	GASCAELV	22	PCI domain-containin
Casp3		No	No	Q8WUA2	PPIL4	DLPD	ADIKPPEN	233	Peptidyl-prolyl cis-
Casp3		Yes	Yes	Q15154	PCM1	EDGD	GAGAGTTV	1552	Pericentriolar mater
Casp3		Yes	Yes	Q15154	PCM1	SEED	GRGEPAME	194	Pericentriolar mater
Casp3	Casp9	Yes	Yes	O60664	PLIN3	AEAD	GSTQVTVE	10	Perilipin-3
Casp3		No	Yes	O60664	PLIN3	EAVD	ATRGAVQS	153	Perilipin-3
Casp3		Yes	Yes	O60664	PLIN3	TSLD	GFDVASVQ	220	Perilipin-3
Casp3		Yes	Yes	O60664	PLIN3	STCD	MVSAAYAS	41	Perilipin-3
	Casp9	No	No	O60346	PHLP1	LEAD	AASAPTGV	383	PH domain leucine-ri
Casp3		No	Yes	Q9P1Y6	PHRF1	DEED	GASCSTFF	946	PHD and RING finger
Casp3		Yes	Yes	Q92576	PHF3	SIAD	ALSSTSNI	1158	PHD finger protein 3
Casp3		Yes	Yes	Q92576	PHF3	EEND	FFNSFTTV	1398	PHD finger protein 3
Casp3		No	Yes	Q92576	PHF3	GNID	GNVSCSEN	1627	PHD finger protein 3
Casp3		Yes	Yes	Q8IZ21	PHAR4	MVLD	SVEAGDTT	21	Phosphatase and acti
Casp3		No	No	Q8TCU6	PREX1	DQAD	SAFPLLSL	822	Phosphatidylinositol
Casp3		No	No	Q8NEB9	PK3C3	AEID	SSQIITSP	442	Phosphatidylinositol
Casp3		Yes	Yes	Q9UBF8	PI4KB	FSVD	SITSQESK	489	Phosphatidylinositol
Casp3		No	Yes	O00750	P3C2B	DGSD	GGVSSSPG	136	Phosphatidylinositol
Casp3		No	Yes	O00750	P3C2B	VDYD	GINDAITR	230	Phosphatidylinositol
Casp3	Casp9	No	No	P78356	PI42B	CEND	GVGGNLLC	311	Phosphatidylinositol
Casp3		No	Yes	Q13492	PICAL	AVDD	AIPSLNPF	432	Phosphatidylinositol

Casp3		Yes	Yes	O14523	C2C2L	IMPD	GTIVTTVT	443	Phospholipid transfe
Casp3		No	No	Q8NB49	AT11C	DAVD	GATESAEL	485	Phospholipid-transpo
Casp3		No	No	P46019	KPB2	DELD	HYINHLLQ	662	Phosphorylase b kina
Casp3		No	No	Q9H814	PHAX	ESVD	SSEESFSD	65	Phosphorylated adapt
Casp3		Yes	Yes	Q99569	PKP4	DQWD	GVGPIPGL	804	Plakophilin-4
Casp3		Yes	Yes	Q8TD55	PKHO2	DVPD	SGPPVFAP	180	Pleckstrin homology
Casp3		Yes	Yes	O43660	PLRG1	NATD	SYVHKQYP	76	Pleiotropic regulato
Casp3		No	No	O43157	PLXB1	DTLD	AYPCGSDH	374	Plexin-B1
Casp3		Yes	Yes	P09874	PARP1	DEVD	GVDEVAKK	215	Poly [ADP-ribose] po
Casp3		Yes	Yes	P09874	PARP1	VEVD	GFSELR	73	Poly [ADP-ribose] po
Casp3	Casp9	No	No	O95453	PARN	EQTD	SCAEPLSE	596	Poly(A)-specific rib
Casp3		Yes	Yes	Q86W56	PARG	DEID	VVPESPLS	257	Poly(ADP-ribose) gly
Casp3		Yes	Yes	Q15365	PCBP1	PPLD	AYSIQGQH	221	Poly(rC)-binding pro
Casp3		No	Yes	Q15365	PCBP1	ASLD	ASTQTTHE	276	Poly(rC)-binding pro
Casp3		Yes	Yes	Q15366	PCBP2	TGSD	SASFPHTT	206	Poly(rC)-binding pro
Casp3		Yes	Yes	Q9UHX1	PUF60	QGTD	SIKMENGQ	41	Poly(U)-binding-spli
Casp3		Yes	Yes	Q86U42	PABP2	DPGD	GAIEDPEL	112	Polyadenylate-bindin
Casp3		Yes	Yes	Q96GD3	SCMH1	DSMD	SASNPTNL	512	Polycomb protein SCM
Casp3		Yes	Yes	P26599	PTBP1	AAVD	AGMAMAGQ	173	Polypyrimidine tract
Casp3		No	No	Q92989	CLP1	TIPD	SCLPLGMS	337	Polyribonucleotide 5
Casp3		No	No	Q9HBE1	PATZ1	GAAD	GGPADVGG	82	POZ-, AT hook-, and
Casp3		Yes	Yes	Q9NQV6	PRD10	ESVD	GSDPLATL	116	PR domain zinc finge
Casp3		No	Yes	Q96AQ6	PBIP1	DRQD	GLREQLQA	248	Pre-B-cell leukemia
Casp3		Yes	Yes	Q7Z5W3	BN3D2	TELD	GGSVKETA	9	Pre-miRNA 5'-monopho
Casp3		Yes	Yes	Q6UN15	FIP1	VDLD	SFEDKPWR	159	Pre-mRNA 3'-end-proc
Casp3		Yes	Yes	O60508	PRP17	SNID	GFLGPWAK	191	Pre-mRNA-processing
Casp3		Yes	Yes	O60508	PRP17	DEKD	VAKPSEEE	205	Pre-mRNA-processing
Casp3		Yes	Yes	O95391	SLU7	TVVD	AVNAAPLS	8	Pre-mRNA-splicing fa
Casp3		Yes	Yes	O75934	SPF27	VVVD	ALPYFDQG	15	Pre-mRNA-splicing fa
Casp3		Yes	Yes	O95926	SYF2	VLVD	SAEEGSLA	13	Pre-mRNA-splicing fa
Casp3		No	Yes	Q8IY81	SPB1	EEKD	GISDSDSS	614	pre-rRNA processing
Casp3	Casp9	Yes	Yes	Q2NL82	TSR1	CATD	AVDDMEEG	333	Pre-rRNA-processing
Casp3		No	No	Q969E8	TSR2	AATD	GVCPQPEP	159	Pre-rRNA-processing
Casp3		Yes	Yes	Q96IZ0	PAWR	EEPD	GVPEKGKS	132	PRKC apoptosis WT1 r
Casp3	Casp9	Yes	Yes	P46087	NOP2	EEAD	GGLQINVD	208	Probable 28S rRNA (c
Casp3		No	Yes	Q9NUL7	DDX28	ASPD	AVTTITSS	349	Probable ATP-depende
Casp3		Yes	Yes	Q7L014	DDX46	EEVD	LQTALTGY	303	Probable ATP-depende
Casp3		No	Yes	Q9H0S4	DDX47	EEHD	SPTEASQP	9	Probable ATP-depende
Casp3		Yes	Yes	Q8IY37	DHX37	DLGD	GGQDGGEQ	574	Probable ATP-depende
Casp3		Yes	Yes	Q9H6S0	YTDC2	FRVD	GIPNDSSD	1084	Probable ATP-depende
Casp3		No	No	Q15751	HERC1	SYVD	GWFGGECG	3020	Probable E3 ubiquiti
Casp3		No	Yes	Q7Z333	SETX	NQCD	SVVLNGTV	1444	Probable helicase se
Casp3		Yes	Yes	P42694	HELZ	FQND	GIVQPNPS	1145	Probable helicase wi

Casp3		Yes	Yes	Q99848	EBP2	DKLD	FLEGDQKP	212	Probable rRNA-proces
Casp3		No	No	Q8WWH5	TRUB1	DTLD	STGRVTEE	164	Probable tRNA pseudo
Casp3		No	Yes	Q53EL6	PDCD4	SSRD	SGRGDSVS	71	Programmed cell deat
Casp3		No	Yes	P12004	PCNA	DNAD	TLALVFEA	98	Proliferating cell n
Casp3		Yes	Yes	P46013	KI67	DSKD	SVAQGTTN	174	Proliferation marker
Casp3		Yes	Yes	P46013	KI67	ESAD	GLQGETQL	279	Proliferation marker
Casp3		Yes	Yes	P13674	P4HA1	DEPD	AFKELGTG	440	Prolyl 4-hydroxylase
Casp3	Casp9	No	Yes	P07602	SAP	AKSD	VYCEVCEF	313	Prosaposin
Casp3		Yes	Yes	P07602	SAP	QPKD	GGFCEVCK	406	Prosaposin
Casp3		No	Yes	Q15185	TEBP	PEVD	GADDDSQD	143	Prostaglandin E synt
Casp3		Yes	Yes	P11171	41	AAVD	SADRSPRP	551	Protein 4.1
Casp3		No	No	Q9H2C2	ARV1	GNVD	GVAATPTA	18	Protein ARV1
Casp3		Yes	Yes	Q96NL8	CH037	DDLD	SLINEILE	65	Protein C8orf37
Casp3		No	No	Q9Y2B0	CNPY2	INPD	GSQSVVEV	62	Protein canopy homol
	Casp9	Yes	Yes	Q96RK0	CIC	IADD	GFGTTDID	457	Protein capicua homo
Casp3	Casp9	No	No	Q6UXH1	CREL2	EECD	SSCVGCTG	261	Protein disulfide is
Casp3		No	No	Q6UXH1	CREL2	GMVD	TAKKNFGG	48	Protein disulfide is
Casp3		No	Yes	P30101	PDIA3	AKVD	CTANTNTC	85	Protein disulfide-is
Casp3		Yes	Yes	P49257	LMAN1	VQSD	GTVPFWAH	62	Protein ERGIC-53
Casp3		Yes	Yes	Q6P1L5	F117B	DIPD	GHRAPPPL	375	Protein FAM117B
Casp3		No	No	Q9NWS6	F118A	DRVD	STTLLGNA	319	Protein FAM118A
Casp3		No	No	Q8IXS8	F126B	LSVD	SVELTPMK	419	Protein FAM126B
Casp3		Yes	Yes	Q5VWN6	F208B	VEVD	SSSASTTL	1208	Protein FAM208B
Casp3		Yes	Yes	Q8NCA5	FA98A	GWTD	GGSGGGGG	387	Protein FAM98A
Casp3		Yes	Yes	Q96ED9	HOOK2	DTPD	SLSPETYG	161	Protein Hook homolog
Casp3		No	No	Q02156	KPCE	SSPD	GQLMSPGE	384	Protein kinase C eps
Casp3		No	No	Q96GA3	LTV1	DDYD	SAGLLSDE	206	Protein LTV1 homolog
Casp3		Yes	Yes	Q86UE4	LYRIC	SRHD	GKEVDEGA	184	Protein LYRIC
Casp3		No	Yes	Q86UE4	LYRIC	VLTD	SGSLDSTI	214	Protein LYRIC
	Casp9	No	No	Q9H081	MIS12	TFFD	ELHNVGRD	161	Protein MIS12 homolo
Casp3		Yes	Yes	Q9HAS0	NJMU	DSED	GSPSGTNA	58	Protein Njmu-R1
Casp3		Yes	Yes	Q13438	OS9	EAAD	SASGAPND	342	Protein OS-9
Casp3		Yes	Yes	O14974	MYPT1	TQTD	SISRYETS	886	Protein phosphatase
Casp3		No	No	O75688	PPM1B	KCVD	GKGPTEQL	212	Protein phosphatase
Casp3		No	Yes	O15355	PPM1G	CSGD	GVGAPRLP	17	Protein phosphatase
Casp3		No	Yes	Q76I76	SSH2	DRID	FFSALEK	652	Protein phosphatase
Casp3		No	Yes	P29590	PML	ALLD	SSHSELKC	220	Protein PML
Casp3		No	Yes	Q86U86	PB1	SELD	LMPYTPPQ	1355	Protein polybromo-1
Casp3		No	No	Q5THK1	PR14L	SDRD	SVCTCVEK	1299	Protein PRR14L
Casp3		Yes	Yes	Q9Y520	PRC2C	SVTD	YTTPSSSL	2190	Protein PRRC2C
	Casp9	No	Yes	Q9P258	RCC2	GDED	GLELDGAP	56	Protein RCC2
Casp3		Yes	Yes	Q13123	RED	ERRD	GVNKDYEE	109	Protein Red
Casp3		Yes	Yes	Q13123	RED	DIGD	YVPSTTKT	325	Protein Red

Casp3		Yes	Yes	Q9H714	PACER	DTTD	SVGSASPH	111	Protein RUBCNL-like
Casp3		Yes	Yes	Q7L099	RUFY3	TEGD	GQITAILD	255	Protein RUFY3
Casp3		No	Yes	Q99590	SCAFB	PDVD	SSNICTVQ	429	Protein SCAF11
Casp3	Casp9	Yes	Yes	Q99590	SCAFB	MECD	SFCSDQNE	723	Protein SCAF11
Casp3		Yes	Yes	O75880	SCO1	DEID	SITTLPDL	189	Protein SCO1 homolog
Casp3		Yes	Yes	P55735	SEC13	NTVD	TSHEDMIH	10	Protein SEC13 homolo
Casp3		Yes	Yes	P55735	SEC13	SHED	MIHDAQMD	15	Protein SEC13 homolo
Casp3		No	Yes	Q9UPR3	SMG5	EAPD	SLNGPLGP	551	Protein SMG5
Casp3		Yes	Yes	Q8ND04	SMG8	QSTD	SLGTYPAD	705	Protein SMG8
	Casp9	Yes	Yes	P18583	SON	LESD	SFLKFDSE	154	Protein SON
Casp3		No	Yes	A3KN83	SBNO1	FDID	GGDAGLAT	28	Protein strawberry n
Casp3		Yes	Yes	Q9BVV6	TALD3	VDID	SISNSSAD	808	Protein TALPID3
Casp3		No	Yes	Q9C0D5	TANC1	VAVD	AAPPNQGG	1640	Protein TANC1
Casp3		Yes	Yes	Q9UNS1	TIM	LSMD	SVVPFDAA	580	Protein timeless hom
Casp3		Yes	Yes	O15027	SC16A	VHPD	SVSSSYSS	342	Protein transport pr
Casp3		Yes	Yes	O15027	SC16A	SHSD	SLASQQSV	838	Protein transport pr
Casp3		No	Yes	O95487	SC24B	TVAD	SLSCPVMQ	296	Protein transport pr
Casp3		Yes	Yes	Q9GZM5	YIPF3	DAAD	AAAAEEED	69	Protein YIPF3
Casp3	Casp9	Yes	Yes	P06454	PTMA	-MSD	AAVDTSSE	4	Prothymosin alpha
Casp3		No	No	Q14517	FAT1	SDSD	SIQKPSWD	4322	Protocadherin Fat 1
Casp3		No	No	P15498	VAV	DLYD	CVENEEAE	162	Proto-oncogene vav
Casp3		No	Yes	Q14671	PUM1	QWRD	SAWGTSDH	175	Pumilio homolog 1
Casp3		No	Yes	Q14671	PUM1	SRRD	SLTGSSDL	709	Pumilio homolog 1
Casp3		Yes	Yes	Q7L2E3	DHX30	DVTD	FLSMTQQD	207	Putative ATP-depende
Casp3		No	Yes	Q7L2E3	DHX30	TQQD	SHAPLRDS	215	Putative ATP-depende
Casp3		Yes	Yes	Q96T37	RBM15	DRSD	GSAPSTST	751	Putative RNA-binding
Casp3		No	Yes	Q8NDT2	RB15B	FALD	AAAAAAVG	290	Putative RNA-binding
Casp3		Yes	Yes	Q6P996	PDXD1	DNVD	AAELVETI	585	Pyridoxal-dependent
Casp3		No	No	P32322	P5CR1	DLID	AVTGLSGS	169	Pyrroline-5-carboxyl
Casp3		No	No	Q96C36	P5CR2	DLID	AVTGLSGS	169	Pyrroline-5-carboxyl
Casp3		No	Yes	P11498	PYC	NNVD	AVHPGYGF	113	Pyruvate carboxylase
Casp3		No	Yes	P11498	PYC	DVVD	VAADSMSG	796	Pyruvate carboxylase
Casp3		Yes	Yes	P11177	ODPB	TVRD	AINQGMDE	38	Pyruvate dehydrogena
Casp3		No	Yes	P14618	KPYM	AVLD	GADCIMLS	355	Pyruvate kinase PKM
Casp3		No	No	Q9Y3P9	RBGP1	VSSD	SVSTLNSE	16	Rab GTPase-activatin
Casp3		No	Yes	P26374	RAE2	TTID	GLNATKNF	356	Rab proteins geranyl
Casp3	Casp9	Yes	Yes	Q9H0H5	RGAP1	TETD	SVGTPQSN	274	Rac GTPase-activatin
Casp3		Yes	Yes	Q96D71	REPS1	TQFD	SNIAPADP	439	RalBP1-associated Ep
Casp3		Yes	Yes	Q96D71	REPS1	ADPD	TAIVHPVP	448	RalBP1-associated Ep
Casp3	Casp9	Yes	Yes	Q96D71	REPS1	TVAD	GYSSSDSF	512	RalBP1-associated Ep
Casp3		Yes	Yes	Q96D71	REPS1	SSSD	SFTSDPEQ	518	RalBP1-associated Ep
Casp3		No	No	P0DJD1	RGPD2	DVAD	AASEVEVS	1508	RANBP2-like and GRIP
Casp3		Yes	Yes	Q8TEU7	RPGF6	CSVD	SMSAALQD	1283	Rap guanine nucleoti

Casp3	Casp9	No	Yes	Q8TEU7	RPGF6	LFSD	GGLSQSQD	696	Rap guanine nucleoti
Casp3		No	No	P47736	RPGP1	QSMD	AMGLSNKK	444	Rap1 GTPase-activati
Casp3		No	No	Q6R327	RICTR	VGVD	ATTMDTDC	1245	Rapamycin-insensitiv
Casp3		Yes	Yes	Q9H2L5	RASF4	SSTD	SSGPLEEA	123	Ras association doma
Casp3		Yes	Yes	Q8WWW0	RASF5	SIYD	AIKEVNLA	264	Ras association doma
Casp3	Casp9	Yes	Yes	P46940	IQGA1	DEVD	GLGVARPH	9	Ras GTPase-activatin
Casp3		No	Yes	P63000	RAC1	VMVD	GKPVNLGL	48	Ras-related C3 botul
Casp3		No	Yes	Q92766	RREB1	ELVD	AFCAPDTV	747	Ras-responsive eleme
Casp3		No	Yes	O00559	RCAS1	LEPD	YFKDMTPT	94	Receptor-binding can
Casp3		No	Yes	P08575	PTPRC	THAD	SQTPSAGT	113	Receptor-type tyrosi
Casp3		No	No	Q8N5W9	RFLB	DSPD	SGLPPSPS	29	Refilin-B
Casp3		No	No	Q8N5W9	RFLB	LEPD	AAAATPAA	62	Refilin-B
Casp3		No	No	Q9H4X1	RGCC	DLSD	ALCEFDAV	31	Regulator of cell cy
Casp3		No	No	Q9H4X1	RGCC	CEFD	AVLADFAS	37	Regulator of cell cy
Casp3		Yes	Yes	O43665	RGS10	HDSD	GSSSSSHQ	15	Regulator of G-prote
Casp3		Yes	Yes	Q92900	RENT1	GQLD	AQVGPEGI	76	Regulator of nonsens
Casp3		Yes	Yes	Q8WUF5	IASPP	SSLD	GLGGTGKD	295	RelA-associated inhi
Casp3		Yes	Yes	P35249	RFC4	DEAD	SMTSAAQA	154	Replication factor C
Casp3		No	Yes	P27694	RFA1	QALD	GVSISDLK	424	Replication protein
Casp3		No	No	Q15293	RCN1	DRID	NDGDGFVT	93	Reticulocalbin-1
Casp3		No	Yes	Q9NQC3	RTN4	TFSD	SSPIEIID	862	Reticulon-4
Casp3		No	Yes	Q9NQC3	RTN4	NAPD	GAGSLPCT	906	Reticulon-4
Casp3		No	No	Q6NW40	RGMB	SAVD	GFDSEFCK	76	RGM domain family me
Casp3		Yes	Yes	P52566	GDIR2	DELD	SKLNYKPP	20	Rho GDP-dissociation
Casp3		No	No	Q14CB8	RHG19	ICND	SSLRGQPI	31	Rho GTPase-activatin
Casp3		Yes	Yes	P42331	RHG25	SRTD	SFSSMTSD	395	Rho GTPase-activatin
	Casp9	Yes	Yes	Q7Z6I6	RHG30	LEND	SIEAAEGE	364	Rho GTPase-activatin
Casp3	Casp9	No	Yes	Q7Z6I6	RHG30	PSPD	GCLCPCSL	908	Rho GTPase-activatin
Casp3		Yes	Yes	P98171	RHG04	DVLD	SFQTSPST	404	Rho GTPase-activatin
Casp3		No	Yes	Q92619	HMHA1	EDCD	AGCLPAEE	263	Rho GTPase-activatin
Casp3		Yes	Yes	Q92619	HMHA1	DGAD	AVFPGPSL	40	Rho GTPase-activatin
Casp3		Yes	Yes	Q92619	HMHA1	VDPD	GGAGASAF	663	Rho GTPase-activatin
Casp3		Yes	Yes	Q9NZN5	ARHGC	THSD	GAISPFTP	1465	Rho guanine nucleoti
	Casp9	Yes	Yes	Q92974	ARHG2	AEED	GGSGMALP	627	Rho guanine nucleoti
	Casp9	Yes	Yes	Q92974	ARHG2	LEPD	SGGNTSPG	691	Rho guanine nucleoti
Casp3		No	Yes	P08134	RHOC	IEVD	GKQVELAL	50	Rho-related GTP-bind
Casp3		Yes	Yes	P08134	RHOC	DSPD	SLENIPEK	91	Rho-related GTP-bind
Casp3		No	Yes	Q99575	POP1	EVMD	AGCQESAG	775	Ribonucleases P/MRP
Casp3		Yes	Yes	Q9H6W3	RIOX1	DLGD	ALPGGAAV	78	Ribosomal oxygenase
Casp3		No	Yes	Q14137	BOP1	DELD	QFLDKMDD	171	Ribosome biogenesis
Casp3		No	No	Q2QD12	RPEL1	DVMD	GHFVPNIT	41	Ribulose-phosphate 3
Casp3		No	No	Q9UFD9	RIM3A	SSPD	GLLSTHAS	276	RIMS-binding protein
Casp3		No	No	Q8N5U6	RNF10	CSSD	SALGPTST	654	RING finger protein

Casp3		Yes	Yes	Q5W0B1	OBI1	SELD	SMMSESDN	543	RING finger protein
Casp3		No	No	Q9C0B0	UNK	AAGD	SVPVSPSS	353	RING finger protein
Casp3		No	No	Q9UBF6	RBX2	DVED	GEETCALA	7	RING-box protein 2
Casp3		Yes	Yes	Q15633	TRBP2	DARD	GNEVEPDD	235	RISC-loading complex
Casp3		No	Yes	Q9Y5B0	CTDP1	GERD	GLCGLGNG	540	RNA polymerase II su
Casp3		Yes	Yes	Q9H6T3	RPAP3	SEED	GIHVDSQK	125	RNA polymerase II-as
Casp3		Yes	Yes	Q9H6T3	RPAP3	DVPD	STTAAAPE	452	RNA polymerase II-as
Casp3		Yes	Yes	P38159	RBMX	DTRD	YAPPPR	234	RNA-binding motif pr
Casp3		Yes	Yes	P38159	RBMX	SYRD	SYESYGNS	284	RNA-binding motif pr
Casp3		No	No	Q8IXT5	RB12B	SGVD	SLSNFIES	105	RNA-binding protein
Casp3		Yes	Yes	Q5T8P6	RBM26	YDTD	GYNPEAPS	432	RNA-binding protein
Casp3	Casp9	Yes	Yes	Q9P2N5	RBM27	YEPD	GYNPEAPS	488	RNA-binding protein
Casp3		Yes	Yes	Q9NW13	RBM28	DEED	GVFDDEDE	245	RNA-binding protein
Casp3		Yes	Yes	Q96EV2	RBM33	GESD	GFFHPEGQ	999	RNA-binding protein
Casp3		Yes	Yes	Q14498	RBM39	ERTD	ASSASSFL	332	RNA-binding protein
Casp3		No	No	Q96LT9	RBM40	TEVD	ASNIGFGK	357	RNA-binding protein
Casp3		Yes	Yes	Q9Y5S9	RBM8A	EDYD	SVEQDGDE	56	RNA-binding protein
Casp3		Yes	Yes	Q9Y5S9	RBM8A	DVLD	LHEAGGED	7	RNA-binding protein
Casp3		No	No	Q6ZN04	MEX3B	ASTD	SYFGGGTS	299	RNA-binding protein
	Casp9	No	No	Q6ZN04	MEX3B	PSPD	GCPELQPT	355	RNA-binding protein
Casp3		No	No	Q9NRX1	PNO1	LCGD	GLLSGKEE	67	RNA-binding protein
Casp3		No	No	Q9HBD1	RC3H2	NSLD	GYYSVACQ	741	Roquin-2
Casp3		No	Yes	Q6PCB5	RSBNL	TSSD	STSSVLGP	714	Round spermatid basi
Casp3		Yes	Yes	Q5JTH9	RRP12	LTVD	AVKLHNEL	55	RRP12-like protein
Casp3		No	No	Q9Y3B9	RRP15	NEND	GESSVGTN	82	RRP15-like protein
Casp3		Yes	Yes	O43865	SAHH2	SMPD	AMPLPGVG	6	S-adenosylhomocystei
Casp3		Yes	Yes	O43865	SAHH2	SSTD	SYSSAASY	74	S-adenosylhomocystei
Casp3		No	Yes	Q9NSI8	SAMN1	DSMD	SLYSGQSS	128	SAM domain-containin
Casp3		No	Yes	Q9NSI8	SAMN1	SNRD	SFRLDDDG	151	SAM domain-containin
	Casp9	No	Yes	Q9UHR5	S30BP	PESD	GEAGIEAV	24	SAP30-binding protei
Casp3		Yes	Yes	Q14BN4	SLMAP	DTTD	AQMDEQDL	465	Sarcolemmal membrane
Casp3		Yes	Yes	Q15424	SAFB1	DLFD	SAHPEEGD	263	Scaffold attachment
Casp3		Yes	Yes	Q15424	SAFB1	DSRD	GWGGYGSD	797	Scaffold attachment
Casp3		No	Yes	Q14151	SAFB2	DGTD	GLLDSFCD	154	Scaffold attachment
Casp3		Yes	Yes	Q14151	SAFB2	DLFD	SAHPEEGD	262	Scaffold attachment
Casp3		Yes	Yes	Q14151	SAFB2	DSRD	GWGGYGSD	821	Scaffold attachment
Casp3		No	No	Q08AF3	SLFN5	DVMD	SQEALAFL	130	Schlafen family memb
Casp3		No	Yes	Q9H4L4	SENP3	MAED	GVRGSPPV	208	Sentrin-specific pro
Casp3		No	No	Q9BQF6	SENP7	SSSD	GSLESYQN	207	Sentrin-specific pro
Casp3		No	No	Q9BQF6	SENP7	SNTD	AAKPTYTF	708	Sentrin-specific pro
Casp3		No	Yes	Q13501	SQSTM	VICD	GCNGPVVG	130	Sequestosome-1
Casp3		No	Yes	P34897	GLYM	DLPD	GGHLTHGY	169	Serine hydroxymethyl
	Casp9	No	Yes	Q9UQ35	SRRM2	FQSD	SSSYPTVD	1142	Serine/arginine repe

Casp3		Yes	Yes	Q9UQ35	SRRM2	SYVD	GSSFDPQR	148	Serine/arginine repe
Casp3		Yes	Yes	Q96IZ7	RSRC1	IESD	SFVQQTFR	239	Serine/Arginine-rela
Casp3		Yes	Yes	Q8N1F8	S11IP	DLSD	SLSSGGVV	373	Serine/threonine-pro
Casp3		Yes	Yes	Q9Y6E0	STK24	AETD	GQASGGSD	326	Serine/threonine-pro
Casp3		No	No	Q13188	STK3	DELD	SHTMVKTS	323	Serine/threonine-pro
Casp3		Yes	Yes	Q13043	STK4	TMTD	GANTMIEH	350	Serine/threonine-pro
Casp3		No	No	Q5VT25	MRCKA	RTVD	STPLSVHT	985	Serine/threonine-pro
Casp3		No	No	Q8TDX7	NEK7	CLLD	GVPVALKK	57	Serine/threonine-pro
Casp3		Yes	Yes	Q13177	PAK2	PEKD	GFPSGTPA	149	Serine/threonine-pro
Casp3		Yes	Yes	Q13177	PAK2	VGFD	AVTGEFTG	90	Serine/threonine-pro
Casp3		Yes	Yes	Q9BRS2	RIOK1	NVTD	SVINKVTE	130	Serine/threonine-pro
Casp3		Yes	Yes	Q9H4A3	WNK1	SSVD	SAHSDVAS	1070	Serine/threonine-pro
Casp3		No	No	O75460	ERN1	PQTD	GVTIGDKG	323	Serine/threonine-pro
Casp3		Yes	Yes	Q96QC0	PP1RA	GFLD	ALNSAPVP	294	Serine/threonine-pro
Casp3		Yes	Yes	Q13362	2A5G	MVVD	AANSNGPF	15	Serine/threonine-pro
Casp3		No	No	P30154	2AAB	DGDD	SLYPIAVL	21	Serine/threonine-pro
Casp3		No	No	Q5MIZ7	P4R3B	DFPD	NYEKFMET	744	Serine/threonine-pro
Casp3		Yes	Yes	Q9UPN7	PP6R1	SSVD	GQLELLAQ	297	Serine/threonine-pro
Casp3		Yes	Yes	P50454	SERPH	QTTD	GKLPEVTK	183	Serpin H1
Casp3		No	Yes	P02768	ALBU	DRAD	LAKYICEN	284	Serum albumin
Casp3		Yes	Yes	Q8NEF9	SRFB1	SEKD	SVVSLESQ	212	Serum response facto
	Casp9	No	Yes	Q96B97	SH3K1	SESD	GGDSSSTK	185	SH3 domain-containin
Casp3		No	No	Q96HL8	SH3Y1	NGPD	KIIPAHVI	34	SH3 domain-containin
Casp3		No	Yes	A0MZ66	SHOT1	TDTD	GAAETCVS	130	Shootin-1
Casp3	Casp9	Yes	Yes	A0MZ66	SHOT1	AEAD	SSSPTGIL	492	Shootin-1
Casp3		No	No	Q8NBJ9	SIDT2	GSTD	GLVDSAGT	371	SID1 transmembrane f
Casp3		No	Yes	Q9NTI5	PDS5B	EEVD	VFQGSSPV	1412	Sister chromatid coh
Casp3		No	Yes	O60232	SSA27	TCAD	CGTILLQD	56	Sjoegren syndrome/sc
Casp3		Yes	Yes	A0A096LF	SIM26	DQKD	GSASEVPS	45	Small integral membr
Casp3		No	Yes	P62306	RUXF	VSVD	GYMNMQLA	38	Small nuclear ribonu
Casp3		Yes	Yes	P62306	RUXF	EYID	GALSGHLG	53	Small nuclear ribonu
Casp3		Yes	Yes	Q5T8I9	HENMT	SVVD	GNFEEVPR	14	Small RNA 2'-O-methy
Casp3		Yes	Yes	Q8NCG7	DGLB	TELD	GGDQEVLT	549	Sn1-specific diacylg
Casp3		No	Yes	Q13573	SNW1	DFGD	GGAFPEIH	61	SNW domain-containin
Casp3		Yes	Yes	Q96AG3	S2546	DGFD	GLGYRGGA	11	Solute carrier famil
Casp3		No	Yes	Q92673	SORL	DCQD	GRDEANCP	1500	Sortilin-related rec
Casp3		Yes	Yes	Q9UMY4	SNX12	DLTD	AYGPPSNF	22	Sorting nexin-12
Casp3		Yes	Yes	Q96RF0	SNX18	PDLD	GSSSAGVG	181	Sorting nexin-18
Casp3		No	Yes	O95219	SNX4	EHTD	GQSVLTDS	95	Sorting nexin-4
Casp3		No	Yes	Q9Y5X1	SNX9	AFLD	SLSASTAQ	82	Sorting nexin-9
Casp3		No	No	Q8N0X7	SPART	FLVD	GVCTVANC	497	Spartin
Casp3		No	No	Q8N0X7	SPART	HAVD	SAVNVGVT	593	Spartin
Casp3		Yes	Yes	Q13813	SPTN1	DSLD	SVEALIKK	1479	Spectrin alpha chain

Casp3		No	No	Q9UM82	SPAT2	DDVD	LYTDSEPR	337	Spermatogenesis-asso
Casp3		Yes	Yes	Q86XZ4	SPAS2	ESVD	SLSEGLET	146	Spermatogenesis-asso
Casp3		No	No	Q9Y657	SPIN1	SRAD	AGHAGVSA	17	Spindlin-1
Casp3		Yes	Yes	Q12874	SF3A3	DDKD	GLRKEELN	66	Splicing factor 3A s
Casp3		Yes	Yes	O75533	SF3B1	VGLD	STGYYDQE	35	Splicing factor 3B s
Casp3		Yes	Yes	Q13435	SF3B2	EAMD	GSETPQLF	777	Splicing factor 3B s
Casp3		No	Yes	Q13435	SF3B2	DFSD	MVAEHAAK	863	Splicing factor 3B s
Casp3	Casp9	Yes	Yes	P26368	U2AF2	MTPD	GLAVTPTP	129	Splicing factor U2AF
Casp3	Casp9	No	Yes	Q9H7N4	SFR19	AESD	GEGALQVD	455	Splicing factor, arg
Casp3		No	Yes	Q96SB4	SRPK1	QETD	SCTPITSE	413	SRSF protein kinase
Casp3		No	No	O94864	ST65G	HSTD	SLMGSSPV	395	STAGA complex 65 sub
Casp3		No	Yes	Q7KZF4	SND1	VTVD	YIRPASPA	421	Staphylococcal nucle
Casp3		No	No	Q12770	SCAP	DQPD	LTCLIDTN	873	Sterol regulatory el
Casp3		No	Yes	O43815	STRN	ELTD	SASVLDNF	227	Striatin
Casp3		Yes	Yes	O43815	STRN	NEAD	SLTYDIAN	437	Striatin
Casp3		Yes	Yes	Q5VSL9	STRP1	DNLD	AFNERDPY	366	Striatin-interacting
	Casp9	Yes	Yes	Q9NTJ3	SMC4	PSPD	GASSDAEP	25	Structural maintenan
Casp3		No	No	Q9UBS9	SUCO	SVVD	SSSLPEVK	859	SUN domain-containin
Casp3		Yes	Yes	Q9NQ55	SSF1	AEPD	GDHNITEL	246	Suppressor of SWI4 1
	Casp9	Yes	Yes	O75940	SPF30	ASSD	SFASTQPT	63	Survival of motor ne
Casp3		No	No	Q92537	SUSD6	IMVD	GVQVALPS	169	Sushi domain-contain
Casp3		No	No	Q9P0W2	HM20B	GDCD	GFSTFDVP	179	SWI/SNF-related matr
	Casp9	No	No	Q96A49	SYAP1	FVSD	AFDACNLN	279	Synapse-associated p
Casp3		No	No	Q96A49	SYAP1	DAFD	ACNLNQED	282	Synapse-associated p
Casp3		No	No	Q96A49	SYAP1	GKID	GIIDKTII	94	Synapse-associated p
Casp3		Yes	Yes	Q99536	VAT1	TGED	ASSPPPKT	16	Synaptic vesicle mem
Casp3		No	No	O43426	SYNJ1	SSLD	GFKDSFDL	1460	Synaptojanin-1
Casp3		No	Yes	Q9UMZ2	SYNRG	DFQD	ASKSGSLD	464	Synergin gamma
Casp3		No	Yes	Q9UMZ2	SYNRG	DKYD	ALKEEASP	714	Synergin gamma
Casp3		Yes	Yes	Q86Y82	STX12	DLID	SIEANVES	218	Syntaxin-12
Casp3		Yes	Yes	O15400	STX7	DVID	SIEANVEN	205	Syntaxin-7
Casp3		Yes	Yes	Q9Y490	TLN1	QNVD	SRDPVQLN	206	Talin-1
Casp3		Yes	Yes	Q9H5J8	TAF1D	DSLD	HVTSDAVE	11	TATA box-binding pro
Casp3		Yes	Yes	P82094	TMF1	ERID	SFSVQSLD	328	TATA element modulat
Casp3		Yes	Yes	Q92804	RBP56	QQHD	SYSQNQQS	141	TATA-binding protein
Casp3		No	No	Q4KMP7	TB10B	SYLD	SVSLMSGT	272	TBC1 domain family m
Casp3		No	No	Q8TC07	TBC15	DALD	SSSILYAR	60	TBC1 domain family m
Casp3	Casp9	Yes	Yes	O60343	TBCD4	EEAD	GTDTHLGL	273	TBC1 domain family m
Casp3		Yes	Yes	O60343	TBCD4	DGTD	THLGLPAG	276	TBC1 domain family m
Casp3		No	Yes	P01733	TVBL3	KHTD	AGVIQSPR	21	T-cell receptor beta
Casp3		Yes	Yes	Q6PIZ9	TRAT1	TLVD	SFSPESQA	155	T-cell receptor-asso
Casp3		No	No	P40200	TACT	TLVD	VSALRPNT	422	T-cell surface prote
Casp3		Yes	Yes	P78371	TCPB	VRVD	STAKVAEI	260	T-complex protein 1

Casp3		No	Yes	P78371	TCPB	VTND	GATILKNI	67	T-complex protein 1
Casp3		No	Yes	P50991	TCPD	TDMD	NQIVVSDY	262	T-complex protein 1
Casp3		Yes	Yes	P48643	TCPE	VDKD	GDVTVTND	66	T-complex protein 1
Casp3		No	Yes	P48643	TCPE	VTND	GATILSMM	74	T-complex protein 1
Casp3		No	Yes	Q99832	TCPH	EGTD	SSQGIPQL	15	T-complex protein 1
Casp3		No	Yes	O15040	TCPR2	TVRD	GLEMSGCS	365	Tectonin beta-propel
Casp3	Casp9	Yes	Yes	Q6NXR4	TTI2	MELD	SALEAPSQ	5	TELO2-interacting pr
Casp3		Yes	Yes	Q9Y4R8	TELO2	EIVD	GGVPQAQL	475	Telomere length regu
Casp3		Yes	Yes	Q9BSI4	TINF2	SVTD	SVNLAEPM	208	TERF1-interacting nu
Casp3		Yes	Yes	Q5VYS8	TUT7	EHTD	SAAGDTGI	514	Terminal uridylyltra
Casp3		Yes	Yes	Q8IWB9	TEX2	VLAD	GLSVSQAP	97	Testis-expressed pro
Casp3		Yes	Yes	Q6DKK2	TAB1	QGAD	GAAAEDGA	82	Tetratricopeptide re
Casp3		No	No	Q6PID6	TTC33	DVVD	NDEGNWLH	35	Tetratricopeptide re
Casp3		No	Yes	O95801	TTC4	DVMD	SFLEKFQS	16	Tetratricopeptide re
Casp3		Yes	Yes	O95801	TTC4	LFLD	GLSTENPH	255	Tetratricopeptide re
Casp3		No	No	Q15750	TAB1	STVD	GLQVTQLN	197	TGF-beta-activated k
Casp3		No	No	P52888	THOP1	DMAD	AASPCSVV	14	Thimet oligopeptidas
Casp3		No	Yes	Q86V81	THOC4	DKMD	MSLDDIIK	7	THO complex subunit
Casp3		Yes	Yes	Q86V81	THOC4	DLFD	SGFGGGAG	94	THO complex subunit
Casp3		No	Yes	P35443	TSP4	DDND	GIPDLVPP	671	Thrombospondin-4
Casp3		Yes	Yes	P04818	TYSY	DFLD	SLGFSTR	120	Thymidylate synthase
Casp3		Yes	Yes	P63313	TYB10	DKPD	MGEIASFD	7	Thymosin beta-10
Casp3		Yes	Yes	Q9Y2W1	TR150	VRMD	SFDEDLAR	575	Thyroid hormone rece
Casp3		Yes	Yes	Q96HA7	TONSL	DDTD	GLTPQLEE	499	Tonsoku-like protein
Casp3		Yes	Yes	Q5JTV8	TOIP1	DDQD	SSHSSVTT	227	Torsin-1A-interactin
Casp3		Yes	Yes	Q5JTV8	TOIP1	MQND	SILKSELG	305	Torsin-1A-interactin
Casp3		Yes	Yes	Q12888	TP53B	DGLD	ASSPGNSF	1479	TP53-binding protein
Casp3		Yes	Yes	Q9UKE5	TNIK	ETHD	GTVAVSDI	853	TRAF2 and NCK-intera
Casp3		No	Yes	Q9UKE5	TNIK	SHAD	SFSGSISR	892	TRAF2 and NCK-intera
Casp3		No	No	Q9Y2L5	TPPC8	MTVD	GIGALPGC	854	Trafficking protein
Casp3		No	Yes	P51532	SMCA4	DYSD	SLTEKQWL	1382	Transcription activa
Casp3		Yes	Yes	P23193	TCEA1	NARD	TYVSSFPR	125	Transcription elonga
Casp3		Yes	Yes	Q99081	HTF4	DLLD	FSAMFSPP	23	Transcription factor
Casp3		Yes	Yes	Q9UGU0	TCF20	HETD	GHGLAEAT	1220	Transcription factor
Casp3		Yes	Yes	P20290	BTF3	QSVD	GKAPLATG	176	Transcription factor
Casp3		No	No	Q04206	TF65	DCRD	GFYEAELC	98	Transcription factor
Casp3		No	Yes	P08047	SP1	QTVD	GQQLQFAA	184	Transcription factor
Casp3		Yes	Yes	P08047	SP1	VQQD	GSGQIQII	200	Transcription factor
Casp3		Yes	Yes	Q02447	SP3	NSID	SAGIQLHP	531	Transcription factor
Casp3		No	No	Q02446	SP4	GELD	SSVTEVLG	749	Transcription factor
Casp3		Yes	Yes	Q00403	TF2B	TSVD	LITTGDFM	208	Transcription initia
Casp3		No	Yes	Q00403	TF2B	NHPD	AILVEDYR	21	Transcription initia
Casp3		No	Yes	Q00403	TF2B	SRLD	ALPRVTCP	9	Transcription initia

Casp3		No	No	Q5VWG9	TAF3	DSTD	LAPPSPEP	239	Transcription initia
Casp3		No	No	Q15542	TAF5	GEVD	SAGAEVTS	138	Transcription initia
Casp3		No	No	Q15542	TAF5	QQID	AMVGSLAG	354	Transcription initia
Casp3	Casp9	No	Yes	Q13263	TIF1B	SSGD	GGAAGDGT	106	Transcription interm
Casp3		No	Yes	Q13263	TIF1B	AATD	AQDANQCC	146	Transcription interm
Casp3		No	Yes	Q13263	TIF1B	DAQD	ANQCCTSC	149	Transcription interm
Casp3		No	Yes	Q13263	TIF1B	TCRD	CQLNAHKD	232	Transcription interm
Casp3		Yes	Yes	Q13263	TIF1B	LSLD	GADSTGVV	686	Transcription interm
Casp3		Yes	Yes	Q9UNY4	TTF2	DQLD	STGRPLVI	827	Transcription termin
Casp3		No	No	Q96BN2	TADA1	STPD	GAGSLPWP	79	Transcriptional adap
Casp3		Yes	Yes	P46100	ATRX	ASTD	GVDKLSGK	920	Transcriptional regu
Casp3		Yes	Yes	P49711	CTCF	NQTD	GGEVVQDV	47	Transcriptional repr
Casp3		No	Yes	Q86YP4	P66A	LNTD	GDMRVTPE	44	Transcriptional repr
Casp3		No	Yes	Q96PN7	TREF1	DTRD	GLGLPVGS	64	Transcriptional-regu
Casp3		Yes	Yes	Q96PN7	TREF1	NSID	GSNVTVTP	761	Transcriptional-regu
Casp3		Yes	Yes	Q04726	TLE3	VSAD	GQMQPVPF	456	Transducin-like enha
Casp3		No	Yes	P61586	RHOA	DSPD	SLENIPEK	91	Transforming protein
Casp3		No	No	Q9UI10	EI2BD	VQTD	AFVSNELD	451	Translation initiati
Casp3		No	No	P43307	SSRA	NDVD	MSWIPQET	253	Translocon-associate
Casp3		Yes	Yes	O94876	TMCC1	AEID	GVPTHPTA	94	Transmembrane and co
Casp3		Yes	Yes	Q9NUM4	T106B	DAYD	GVTSENMR	20	Transmembrane protei
Casp3		Yes	Yes	Q5JRA6	TGO1	DQTD	STGGPAFL	710	Transport and Golgi
Casp3		Yes	Yes	Q13428	TCOF	SGVD	SAVGTLPA	1102	Treacle protein
Casp3		Yes	Yes	Q13428	TCOF	DDPD	GKQEAKPQ	1243	Treacle protein
Casp3		Yes	Yes	P22102	PUR2	LEGD	GGPNTGGM	226	Trifunctional purine
Casp3		Yes	Yes	P22102	PUR2	SGVD	IAAGNMLV	444	Trifunctional purine
Casp3		Yes	Yes	Q96RS0	TGS1	TSHD	GHQQLSEV	344	Trimethylguanosine s
Casp3		No	Yes	Q96RS0	TGS1	DEQD	CVTQEVPD	602	Trimethylguanosine s
Casp3		Yes	Yes	Q8NDV7	TNR6A	TTVD	SISVNTSL	1543	Trinucleotide repeat
Casp3		No	No	Q9HCJ0	TNR6C	SAMD	SFPSHPQT	1237	Trinucleotide repeat
Casp3		No	Yes	Q7Z2T5	TRM1L	SALD	SAPTPASA	45	TRMT1-like protein
Casp3		Yes	Yes	P23381	SYWC	AEED	FVDPWTVQ	84	Tryptophan--tRNA lig
Casp3		No	Yes	O75157	T22D2	LLLD	GQLAAAAA	92	TSC22 domain family
Casp3	Casp9	Yes	Yes	P68363	TBA1B	IQPD	GQMPSDKT	34	Tubulin alpha-1B cha
Casp3		No	Yes	P68363	TBA1B	QFVD	WCPTGFKV	346	Tubulin alpha-1B cha
Casp3		No	Yes	P68363	TBA1B	VGVD	SVEGEGEE	439	Tubulin alpha-1B cha
Casp3		No	Yes	P07437	TBB5	ELVD	SVLDVVR	115	Tubulin beta chain
Casp3		No	Yes	P07437	TBB5	ESCD	CLQGFQLT	129	Tubulin beta chain
Casp3		No	Yes	P07437	TBB5	LQLD	RISVYYNE	46	Tubulin beta chain
Casp3		Yes	Yes	Q15814	TBCC	TKVD	AAPGIPPA	154	Tubulin-specific cha
Casp3		No	Yes	Q9BTW9	TBCD	SRLD	GNLLTQPG	172	Tubulin-specific cha
Casp3		No	No	Q9Y2W6	TDRKH	TETD	ASLSTLLT	518	Tudor and KH domain-
Casp3		No	No	Q9H7E2	TDRD3	DEED	LGNARPSA	262	Tudor domain-contain

Casp3		No	No	P25445	TNR6	DEPD	CVPCQEGK	82	Tumor necrosis facto
Casp3		No	Yes	O43399	TPD54	TQSD	LYKKTQET	125	Tumor protein D54
	Casp9	Yes	Yes	O43399	TPD54	LLSD	SMTDVPVD	21	Tumor protein D54
Casp3		Yes	Yes	Q5T0D9	TPRGL	DSVD	SAGTSPTA	10	Tumor protein p63-re
Casp3		No	Yes	Q9UIG0	BAZ1B	EVPD	GEWQCPAC	1224	Tyrosine-protein kin
Casp3	Casp9	Yes	Yes	P43403	ZAP70	LNSD	GYTPEPAR	291	Tyrosine-protein kin
Casp3		No	Yes	P54577	SYYC	TQHD	SKKAGAEV	145	Tyrosine--tRNA ligas
	Casp9	No	Yes	P09234	RU1C	FYCD	YCDTYLTH	8	U1 small nuclear rib
	Casp9	No	Yes	O15042	SR140	DDLD	GAPIEEEL	696	U2 snRNP-associated
	Casp9	Yes	Yes	O15042	SR140	EELD	GAPLEDVD	705	U2 snRNP-associated
	Casp9	Yes	Yes	O15042	SR140	EDVD	GIPIDATP	713	U2 snRNP-associated
Casp3		Yes	Yes	O15042	SR140	DDLD	GVPIKSLD	726	U2 snRNP-associated
Casp3	Casp9	Yes	Yes	O15042	SR140	DDLD	GVPLDATE	738	U2 snRNP-associated
Casp3		Yes	Yes	O43290	SNUT1	HAID	SFREGETM	265	U4/U6.U5 tri-snRNP-a
Casp3		Yes	Yes	P62310	LSM3	DDVD	QQQTTNTV	7	U6 snRNA-associated
Casp3		Yes	Yes	P83369	LSM11	TRTD	GSSVGGTF	306	U7 snRNA-associated
Casp3		Yes	Yes	Q9NPG3	UBN1	DESD	SFIDNSEA	137	Ubinuclein-1
Casp3		Yes	Yes	Q14694	UBP10	LALD	GSSNVEAE	126	Ubiquitin carboxyl-t
Casp3		Yes	Yes	Q14694	UBP10	LEND	GVSGGLGQ	139	Ubiquitin carboxyl-t
Casp3		Yes	Yes	Q14694	UBP10	NSTD	SVSDIVPD	218	Ubiquitin carboxyl-t
Casp3		No	Yes	Q70CQ2	UBP34	HTVD	SCISDMKT	3367	Ubiquitin carboxyl-t
Casp3		Yes	Yes	Q9P275	UBP36	SCGD	GVPAPQKV	96	Ubiquitin carboxyl-t
Casp3		Yes	Yes	P45974	UBP5	DDLD	AEAAMDIS	768	Ubiquitin carboxyl-t
Casp3	Casp9	Yes	Yes	P45974	UBP5	SAAD	SISESVPV	783	Ubiquitin carboxyl-t
Casp3	Casp9	Yes	Yes	Q93009	UBP7	ALSD	GHNTAEED	51	Ubiquitin carboxyl-t
Casp3	Casp9	Yes	Yes	Q14157	UBP2L	MEND	SSNLDPSQ	299	Ubiquitin-associated
Casp3		Yes	Yes	Q9NT62	ATG3	DDGD	GGWVDTYH	105	Ubiquitin-like-conju
Casp3		No	No	P68543	UBX2A	YFVD	SLFEEAQK	39	UBX domain-containin
Casp3		No	Yes	Q9NYU2	UGGG1	FNLD	GAPYGYTP	1377	UDP-glucose:glycopro
Casp3		Yes	Yes	Q3KQV9	UAP1L	CQVD	GVPQVVEY	300	UDP-N-acetylhexosami
Casp3		Yes	Yes	Q96C57	CL043	ASVD	SAVAATTP	205	Uncharacterized prot
Casp3		No	No	Q96B23	CR025	VQKD	GVADSTVI	45	Uncharacterized prot
Casp3	Casp9	Yes	Yes	Q6ZSR9	YJ005	PATD	GLSEPDVF	118	Uncharacterized prot
Casp3		Yes	Yes	Q9HCM1	K1551	SSVD	GVQTLAQT	360	Uncharacterized prot
Casp3		No	Yes	Q9HCM1	K1551	NQVD	SVLPNPVY	502	Uncharacterized prot
Casp3		Yes	Yes	Q13459	MYO9B	VCVD	SLTSDKAS	1704	Unconventional myosi
Casp3		No	No	Q6PIF6	MYO7B	EDVD	GLAEYTFP	967	Unconventional myosi
Casp3		Yes	Yes	Q49AR2	CE022	TNCD	SSSEGLEK	197	UPF0489 protein C5or
Casp3		No	No	Q7Z3J2	CP062	SVLD	GTDPLSMF	75	UPF0505 protein C16o
Casp3		No	No	A6NDU8	CE051	HEVD	TSVSGAGC	237	UPF0600 protein C5or
Casp3		No	Yes	Q15853	USF2	VGVD	GAAQRPGP	121	Upstream stimulatory
Casp3		No	No	Q9P2Y5	UVRAG	IPVD	SAVAVECD	659	UV radiation resista
Casp3		No	Yes	Q709C8	VP13C	DVHD	SKNTLTTG	1406	Vacuolar protein sor

Casp3	Casp9			UniProt	Gene	Motif	Sequence	Pos	Description
Casp3		No	Yes	Q5THJ4	VP13D	AVPD	SVALESDS	2604	Vacuolar protein sor
	Casp9	Yes	Yes	Q5THJ4	VP13D	LESD	SVGTYLPG	2611	Vacuolar protein sor
Casp3		No	No	Q8N1B4	VPS52	DEVD	VHIQANLE	59	Vacuolar protein sor
Casp3		No	No	Q8N3P4	VPS8	DTID	SHSYDTSS	97	Vacuolar protein sor
Casp3		No	Yes	P49748	ACADV	DKSD	SHPSDALT	54	Very long-chain spec
Casp3		Yes	Yes	Q9P0L0	VAPA	SKQD	GPMPKPHS	157	Vesicle-associated m
Casp3		Yes	Yes	P08670	VIME	IDVD	VSKPDLTA	260	Vimentin
Casp3		Yes	Yes	P08670	VIME	CEVD	ALKGTNES	332	Vimentin
Casp3		Yes	Yes	P08670	VIME	TNLD	SLPLVDTH	430	Vimentin
Casp3		No	Yes	P08670	VIME	ETRD	GQVINETS	452	Vimentin
Casp3		Yes	Yes	P08670	VIME	DSVD	FSLADAIN	86	Vimentin
Casp3		Yes	Yes	P08670	VIME	SLAD	AINTEFKN	91	Vimentin
Casp3		Yes	Yes	Q9UI12	VATH	GAVD	AAVPTNII	12	V-type proton ATPase
Casp3		No	No	Q5SRD0	WAC2D	DSGD	IFSTGTGS	102	WASH complex subunit
Casp3		No	No	Q5SRD0	WAC2D	DNID	IFADLTVK	236	WASH complex subunit
Casp3		No	No	Q5SRD0	WAC2D	DLFD	SGDIFSTG	99	WASH complex subunit
Casp3		Yes	Yes	Q9H6R7	WDCP	SICD	GSIALDAE	509	WD repeat and coiled
Casp3		No	No	Q8IWB7	WDFY1	LESD	SCQKCEQP	286	WD repeat and FYVE d
Casp3		No	No	Q8TBZ3	WDR20	SVMD	GAIASGVS	452	WD repeat-containing
Casp3		No	No	Q9H7D7	WDR26	NNLD	SVSLLIDH	329	WD repeat-containing
Casp3		Yes	Yes	O43379	WDR62	SACD	GLLQPPVD	1302	WD repeat-containing
Casp3		No	No	Q9NW82	WDR70	TGSD	ASGPDPQL	14	WD repeat-containing
Casp3		Yes	Yes	Q96MX6	WDR92	NAID	GIGGLGIG	119	WD repeat-containing
Casp3		No	Yes	Q92558	WASF1	DHMD	GSYSLSAL	248	Wiskott-Aldrich synd
Casp3		Yes	Yes	P13010	XRCC5	NAVD	ALIDSMSL	456	X-ray repair cross-c
Casp3		Yes	Yes	P16989	YBOX3	EMKD	GVPEGAQL	270	Y-box-binding protei
Casp3	Casp9	Yes	Yes	Q9BYJ9	YTHD1	TVVD	GQPGFHSD	165	YTH domain-containin
	Casp9	Yes	Yes	Q9Y5A9	YTHD2	AMID	GQSAFANE	167	YTH domain-containin
Casp3		Yes	Yes	Q9Y5A9	YTHD2	NGVD	GNGVGQSQ	368	YTH domain-containin
Casp3		Yes	Yes	Q7Z739	YTHD3	AITD	GQAGFGND	169	YTH domain-containin
Casp3		No	No	Q9ULJ3	ZBT21	TVGD	AATTAAAS	451	Zinc finger and BTB
Casp3		No	No	Q9ULJ3	ZBT21	DSED	SSCLPEDL	861	Zinc finger and BTB
Casp3		Yes	Yes	Q8NCN2	ZBT34	GDVD	SVTVGAEE	136	Zinc finger and BTB
Casp3		No	No	O95365	ZBT7A	PDVD	GLAASTLL	313	Zinc finger and BTB
Casp3		Yes	Yes	O75152	ZC11A	DATD	KVNKVGEI	349	Zinc finger CCCH dom
Casp3		No	Yes	O75152	ZC11A	SSSD	SSPPEVSG	737	Zinc finger CCCH dom
Casp3		No	Yes	Q6PJT7	ZC3HE	TKGD	SVEKNQGT	421	Zinc finger CCCH dom
Casp3	Casp9	No	Yes	Q8WU90	ZC3HF	EVDD	SVSVNDID	326	Zinc finger CCCH dom
Casp3		Yes	Yes	Q86VM9	ZCH18	DVRD	TVLEPYAD	362	Zinc finger CCCH dom
	Casp9	Yes	Yes	Q9UPT8	ZC3H4	LEDD	GAEETQDT	68	Zinc finger CCCH dom
	Casp9	Yes	Yes	Q9UPT8	ZC3H4	LEPD	SFSEGGPP	742	Zinc finger CCCH dom
Casp3		Yes	Yes	Q8IWR0	Z3H7A	DLLD	SAPETNET	292	Zinc finger CCCH dom
Casp3		No	No	Q9UGR2	Z3H7B	DKPD	SFMEETNS	393	Zinc finger CCCH dom

Casp3		Yes	Yes	Q7Z2W4	ZCCHV	NNAD	GVATDITS	434	Zinc finger CCCH-typ
Casp3	Casp9	Yes	Yes	Q7Z2W4	ZCCHV	LVND	SLSDVTST	492	Zinc finger CCCH-typ
Casp3		No	No	Q8N5A5	ZGPAT	VEGD	GILPPLRT	264	Zinc finger CCCH-typ
Casp3		Yes	Yes	P37275	ZEB1	SVTD	AADCEGVP	50	Zinc finger E-box-bi
Casp3		No	No	Q68DK2	ZFY26	DCKD	SLSEDLAS	527	Zinc finger FYVE dom
Casp3		Yes	Yes	Q9UHR6	ZNHI2	EELD	NAPGSDAA	145	Zinc finger HIT doma
Casp3		No	Yes	Q9UBW7	ZMYM2	NDVD	FSTSSFSR	155	Zinc finger MYM-type
Casp3		Yes	Yes	Q14202	ZMYM3	TLGD	GINSSQTK	202	Zinc finger MYM-type
Casp3		Yes	Yes	P17028	ZNF24	VEED	SILIIPTP	10	Zinc finger protein
	Casp9	No	No	O43296	ZN264	PECD	GLGTADGV	160	Zinc finger protein
Casp3		No	No	Q86YH2	Z280B	TFTD	SLHHPVST	151	Zinc finger protein
Casp3		No	No	Q53GI3	ZN394	SQRD	GLLPVKVE	35	Zinc finger protein
Casp3		No	No	Q8N8E2	ZN513	SEGD	SLGARPGL	73	Zinc finger protein
Casp3		Yes	Yes	Q969S3	ZN622	LGVD	SVDKDAMN	122	Zinc finger protein
Casp3		Yes	Yes	Q9H582	ZN644	SCVD	SFGSPLGL	616	Zinc finger protein
Casp3		Yes	Yes	O15015	ZN646	MVVD	SVLEDIVN	1006	Zinc finger protein
Casp3		No	Yes	O15015	ZN646	EALD	SAGYGHIC	953	Zinc finger protein
Casp3		No	No	Q8IZM8	ZN654	DRVD	ACSDQDNV	529	Zinc finger protein
Casp3		No	Yes	Q8N1G0	ZN687	SDPD	GGDSPLPA	1188	Zinc finger protein
	Casp9	No	No	Q5CZA5	ZN805	PKHD	GLGTADSV	160	Zinc finger protein
Casp3		No	No	Q9UKS7	IKZF2	NNMD	GPISLIRP	382	Zinc finger protein
Casp3		No	No	Q9UKS7	IKZF2	EAID	GYITCDNE	8	Zinc finger protein
Casp3		No	No	P14373	TRI27	MMLD	CGHNICCA	31	Zinc finger protein
Casp3		Yes	Yes	Q92785	REQU	ISQD	GSSLEALL	116	Zinc finger protein
Casp3		No	No	O95159	ZFPL1	EEVD	SASAAPAF	172	Zinc finger protein-
Casp3		Yes	Yes	Q15942	ZYX	LEID	SLSSLLDD	150	Zyxin

150

APPENDIX B

CAPILLARY WESTERN ANALYSIS OF SELECTED CLEAVAGE TARGETS IN CASPASE-3 AND CASPASE-9 *REVERSE* N-TERMINOMICS

Capillary Western Analysis of Selected Cleavage Targets in Caspase-3 and Capsase-9 Reverse N-terminomics

The intention with performing capillary Western blots was to observe the appearance of cleavage sites observed in our caspase-3 and caspase-9 N-terminomics experiments – an alternative to standard immunoblots. When analyzing the cleavage sites observed in our caspase-3 and -9 *reverse* N-terminomics experiments, we thought to conduct an experiment where we could generate these cleavages over time and determine the cleavage efficiency of substrates of interest. With this experiment we would gain knowledge on whether a substrate cleaved by both caspases-3 and -9 was more efficiently cleaved by one caspase. We decided to do this experiment using the Wes capillary electrophoresis system (ProteinSimple) in the lab of Dr. David Westaway.

Capillary Western Protocol:

Caspase-3 and Caspase-9-induced lysates were created using the same protocol for N-terminomics (see Thesis Chapter Two), quenching caspase activity with z-VAD-fmk at 15 minutes, 30 minutes, 1 hour and 2 hours of caspase incubation. A separate sample was also incubated for 2 hours with no caspase addition to serve as a control, in case long-term incubation at room temperature could be causing the observed cleavages. Samples were prepared following standard protocol for utilized capillary western system (Wes capillary western system, ProteinSimple). Lysates were diluted in 0.1X Sample buffer to a final concentration of 1.25 mg/mL of protein. 5x Mastermix was added to the samples, following which they were denatured for 5 minutes at 95°C, vortexed and briefly centrifuged. 4 μL of sample was loaded into each sample well of a Capillary western plate, followed by 10 μL of antibody diluent in the second row, 10 μL of primary antibody at its appropriate dilution (typically 1:50) in the third row, 10 μL of appropriate secondary antibody in the third row (arrives pre-diluted), 15 μL of an equal-part solution containing luminol-S and peroxide in the fourth row and several 500 μL wells of wash buffer at the bottom of the plate. The plate was briefly centrifuged, then assayed for 3 hours using "Compass for SW" software.

Substrates of interest (and the antibodies used):

GAPDH (control) (Cell Signalling) – recognizes carboxy terminal region

Nucleoporin Nup43 (Thermo Fisher) – recognizes amino acids 330-380

Poly(A)-specific ribonuclease PARN (Abcam) – recognizes amino acids 400-500

E3 ubiquitin-protein ligase RNF126 (Abcam) – recognizes amino acids 106-119

E3 ubiquitin-protein ligase RING1 (Cell Signalling) – recognizes region surrounding Pro316

ATP-dependent DNA helicase Q5 (RECQL5) (Thermo Fisher) – recognizes amino acids 582-681.

E3 ubiquitin-protein ligase RNF4 (RND Systems) – exact target location unknown

N-chimaerin (Thermo Fisher) – recognizes amino acids 1-200

Mitofusin-2 (AbCam) – recognizes amino acids 561-757

Ataxin-2-like protein (PTGlab) – recognizes amino acids 712-1062

Gasdermin-D (Sigma Aldrich) – recognizes amino acids 126-138

An important element to consider when deciding to use capillary Westerns is the associated cost. It can be expensive. At time of writing, a set of 8 capillary plates (which can hold 24 samples each) costs $1322CAD, and the required antibody kit costs $341CAD. This amounts to $1663CAD - $208CAD per plate – $8.67CAD per sample.

For more information on performing capillary westerns, see https://www.proteinsimple.com/, and reach out to the Westaway lab to be trained on the machine.

Results:

In general, the cleavage products observed in *reverse* N-terminomics were able to be reproduced for most cleavage sites (more details for each cleavage site below). However, for most substrates we were unable to ascertain cleavage efficiency by observing appearance of cleavage, because most cleavage sites appeared before the 15-minute timepoint. Because of this, for the last few targets we tested, we elected to run the 30 minutes, 1-hour and 2-hour timepoints only, to fit more samples into a single Wes plate. Another limitation for using the Wes capillary western system for this type of experiment is that a lot of optimization is required to determine the best concentration for each antibody. This is possible to accomplish when there is only one sample to analyze, where multiple antibody concentrations can be tested on the same sample. For our experiments with many samples however, it is impractical.

*Note: most proteins on capillary Westerns migrate at higher apparent molecular weights than their actual weights/, and higher than they would appear on a conventional western blot. As well, there can be slight variation between different sample types, where they might not migrate the same despite probing for the same protein.

Legend for all ProteinSimple outputs:

C3 = Caspase-3 *reverse* N-terminomics experiment

C9 = Caspase-9 *reverse* N-terminomics experiment

Samples – 0h, 15min, 1h, 2h, 2hneg (2-hour negative control)

GAPDH (control)

Protein MW: ~34kDa full-length.

Cleavage products expected: none

Observed: Full-length was the only expected, and it was observed
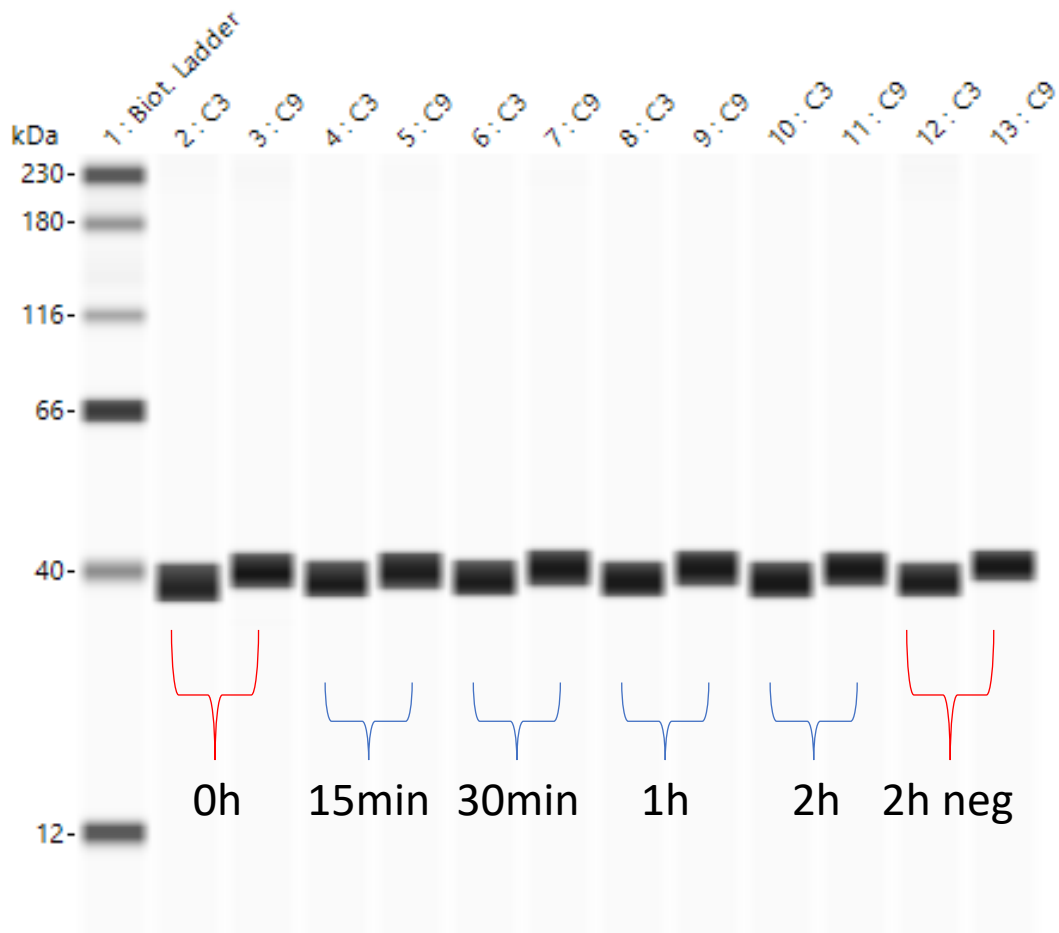
Chromatogram (All samples):
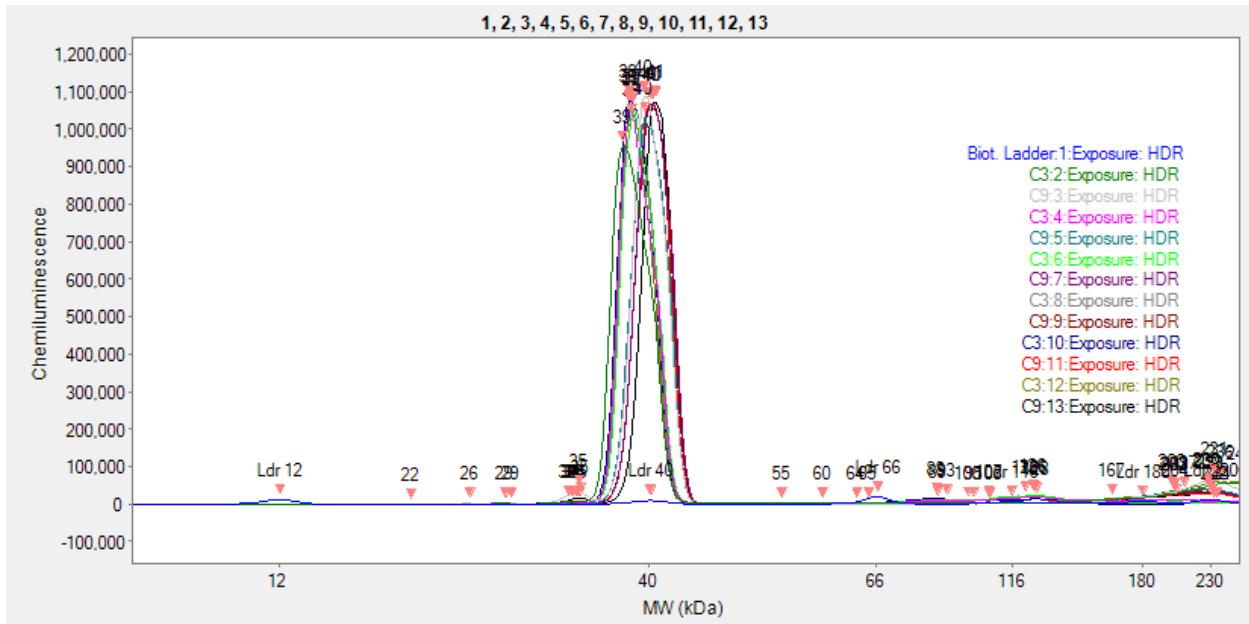
Chromatogram (0h C3 and C9 and 2h C3 and C9):
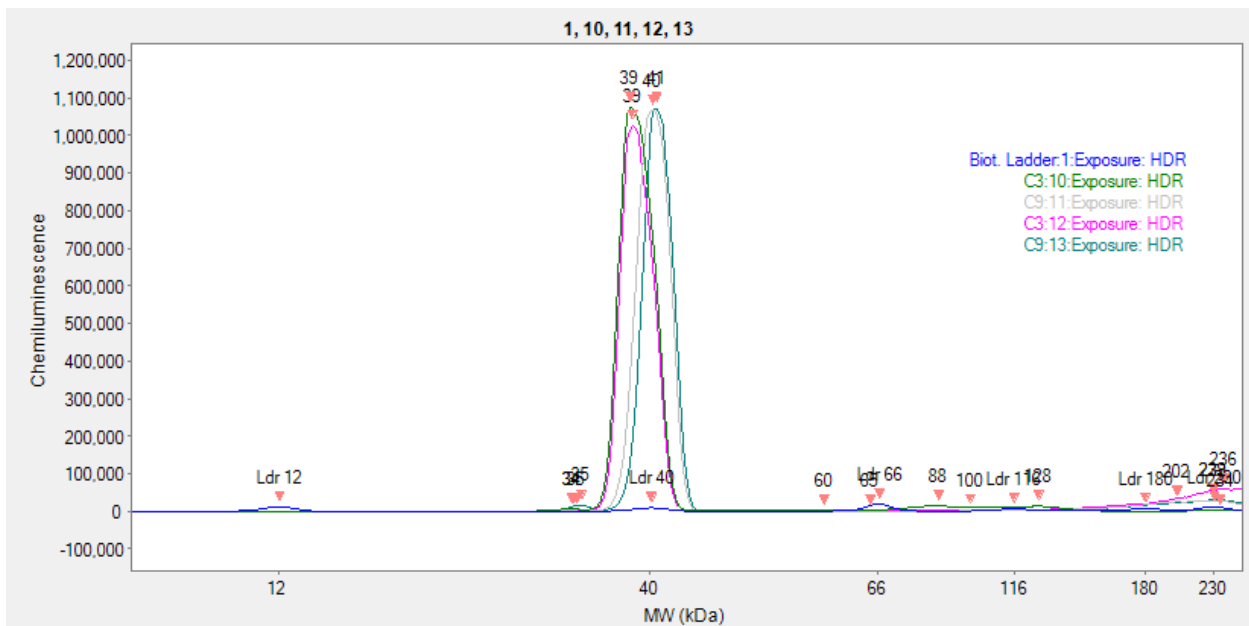
C3 0h
C3 2h
C9 0h
C9 2h

Nucleoporin Nup43 (Observed in caspase-3 datasets, not caspase-9. Not found in the DegraBase)

Protein MW: 42.1kDa

Cleavage products expected: 35.5kDa (Cleavage at LDSD(58)-GG).

Observed: no cleavage, nonspecific binding at ~100kDa which increased over time irrespective of caspase addition.
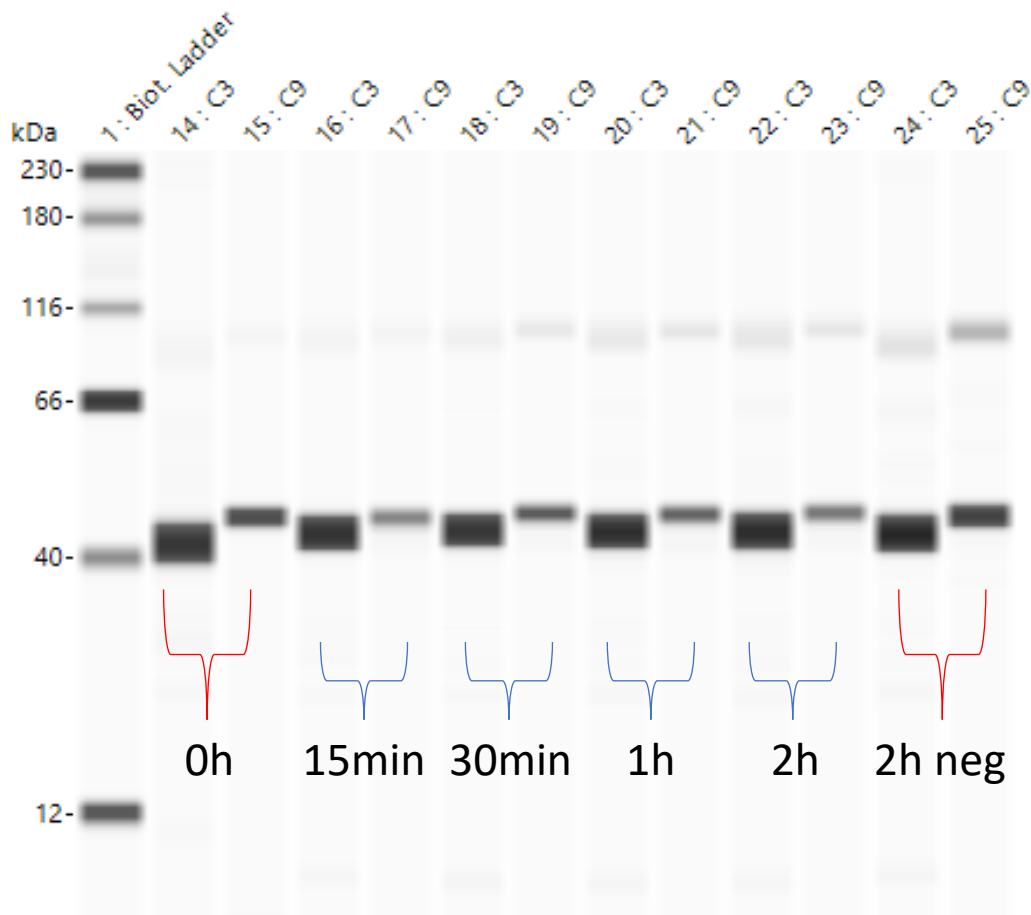
Chromatogram (all samples):
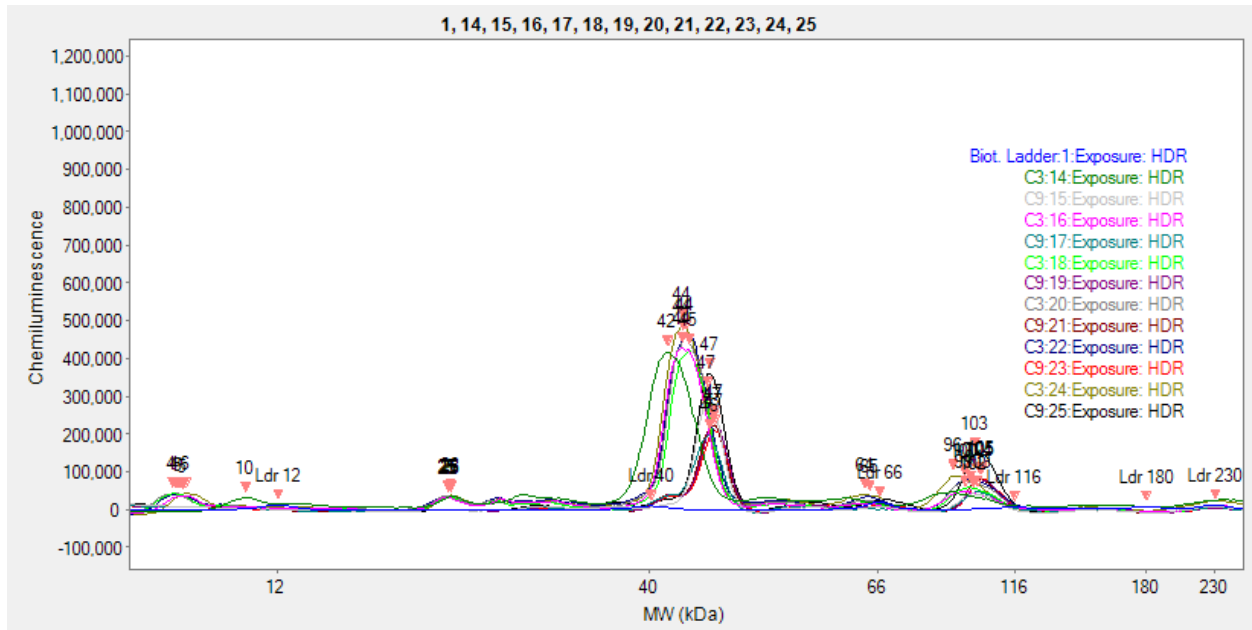
Chromatogram (0h C3 and C9 and 2h C3 and C9):
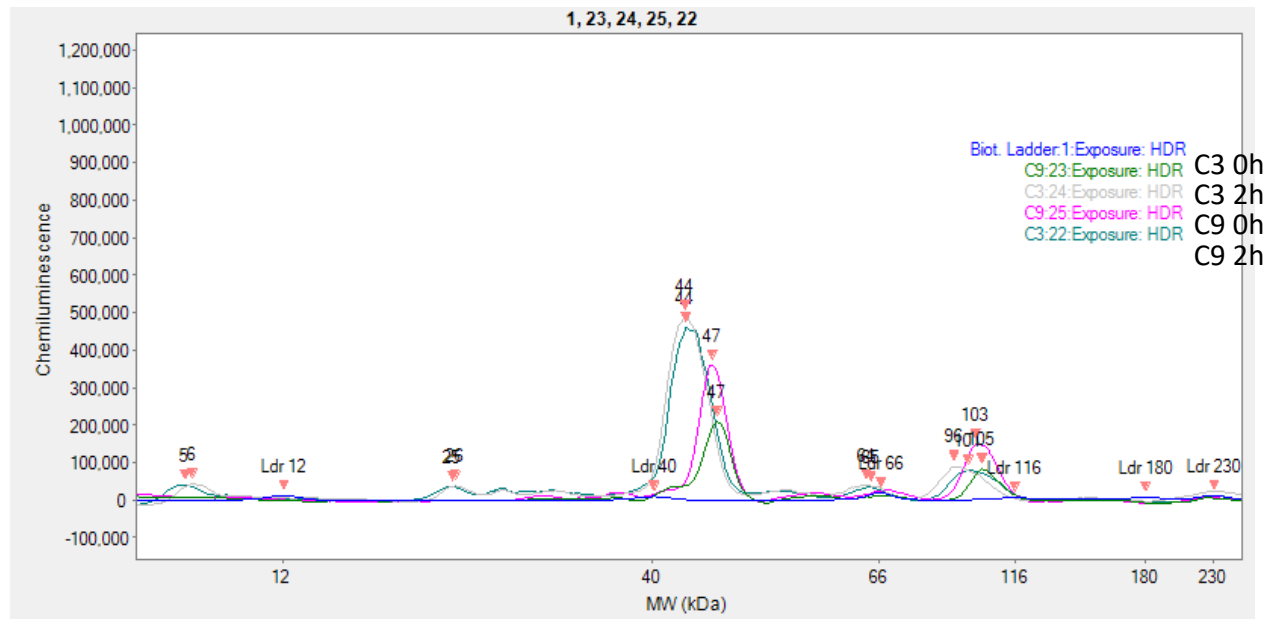
Poly(A)-specific ribonuclease PARN (Observed in caspase-3 and caspase-9 experiments. Not found in the DegraBase)

Protein MW: 73.4kDa

Cleavage products expected: 68.6kDa (cleavage at EQTD(596)-SC)

Observed: Cleavage was observed in the caspase-3 samples, the caspase-9 samples appeared to degrade rather than cleave.
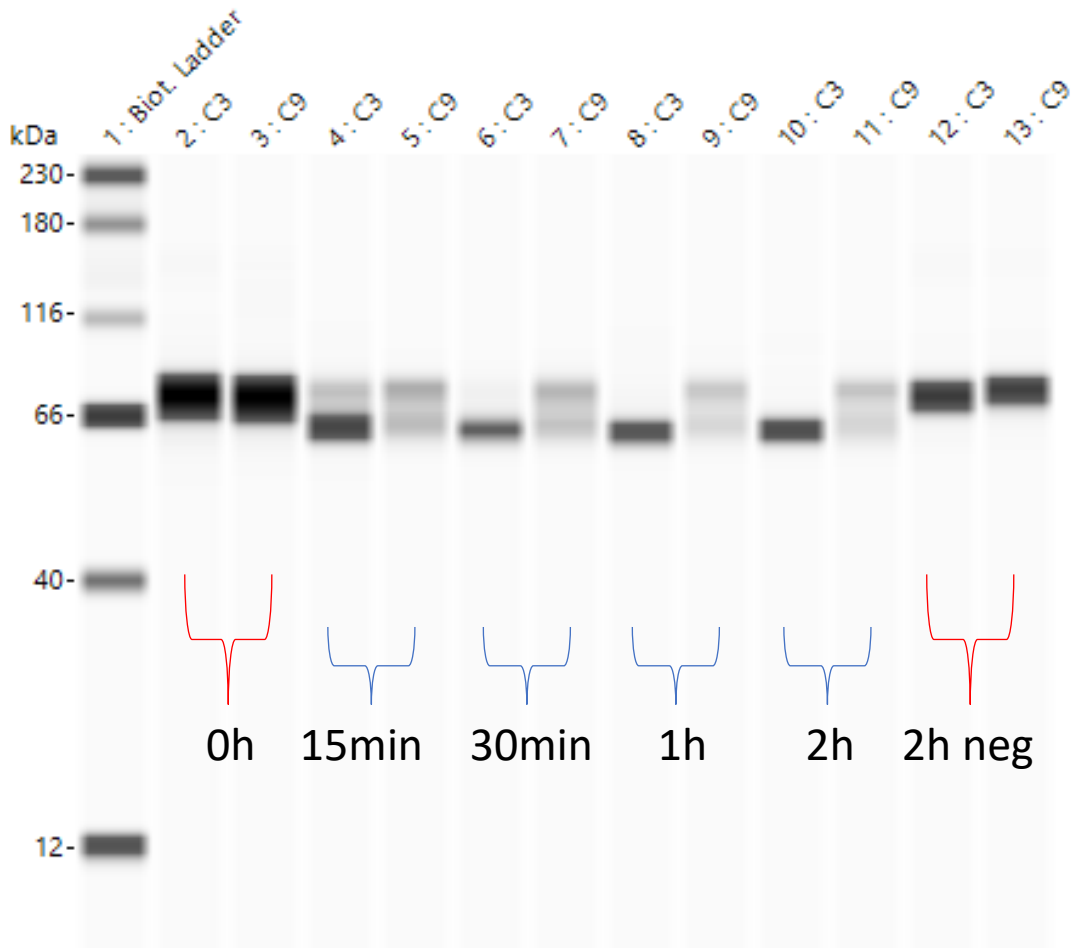
Chromatogram (all samples):
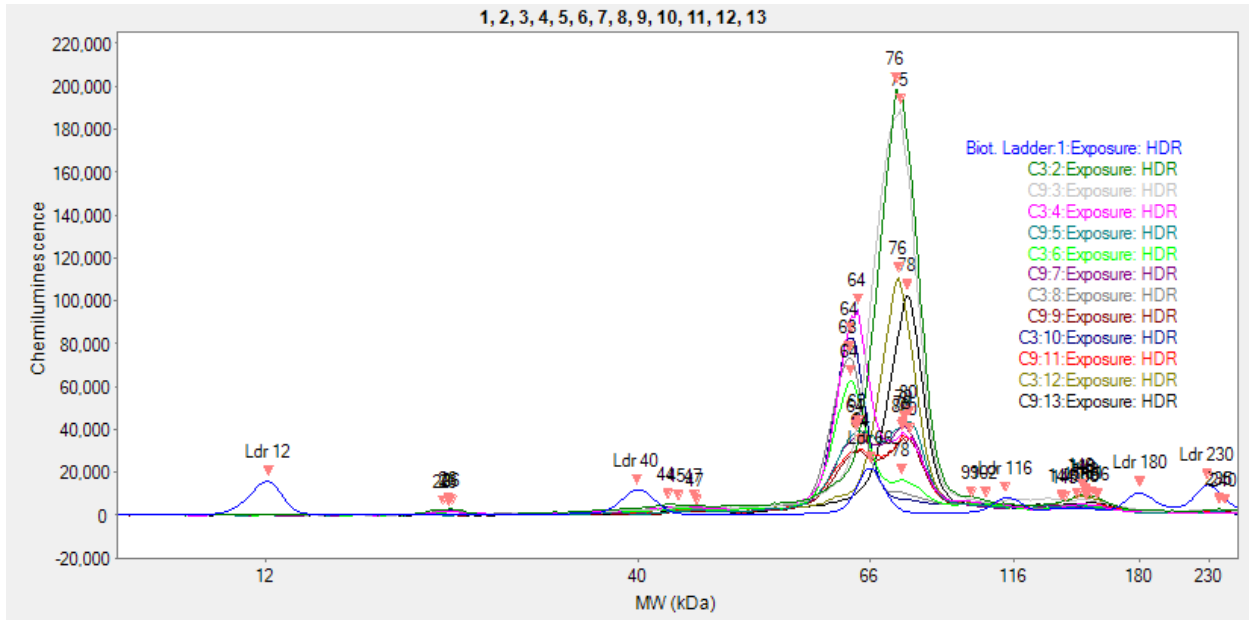
Chromatogram (0h C3 and C9 and 2h C3 and C9):
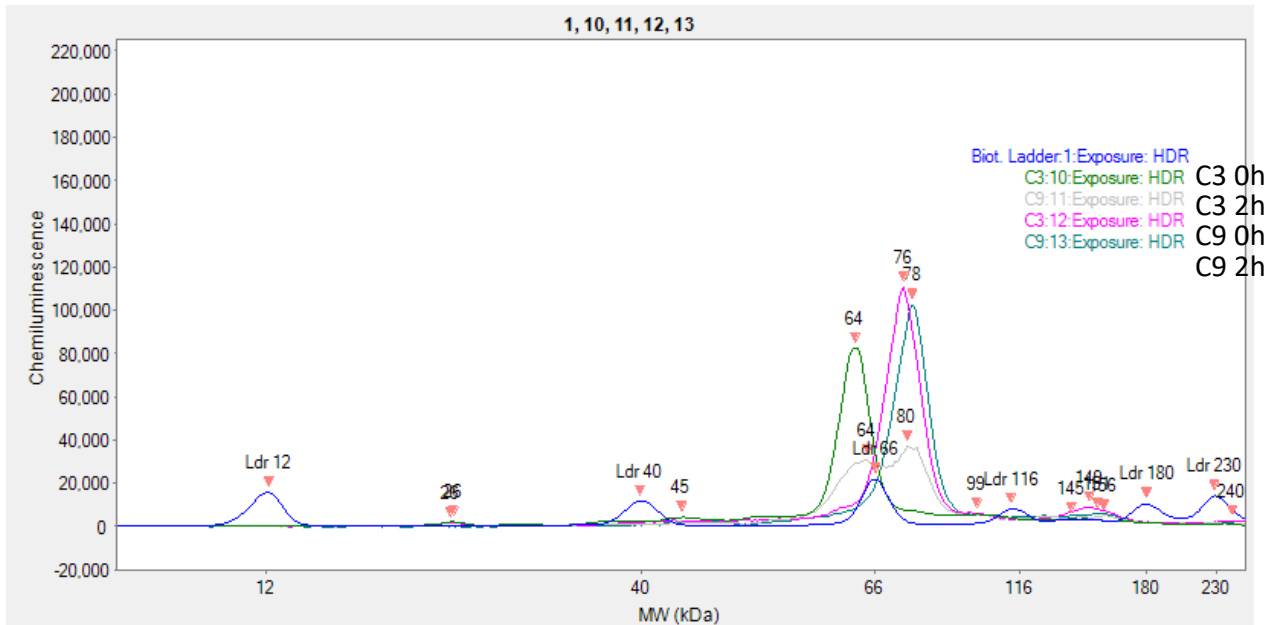
E3 ubiquitin-protein ligase RNF126 (Observed in caspase-9 experiment only. Not found in the DegraBase)

Protein MW: 34kDa

Cleavage products expected: 28 kDa (cleavage at LFHD(253)-GC)

Observed: Very low signal, appeared to cleave in the caspase-3 experiment rather than caspase-9. Would require antibody optimization to be certain.
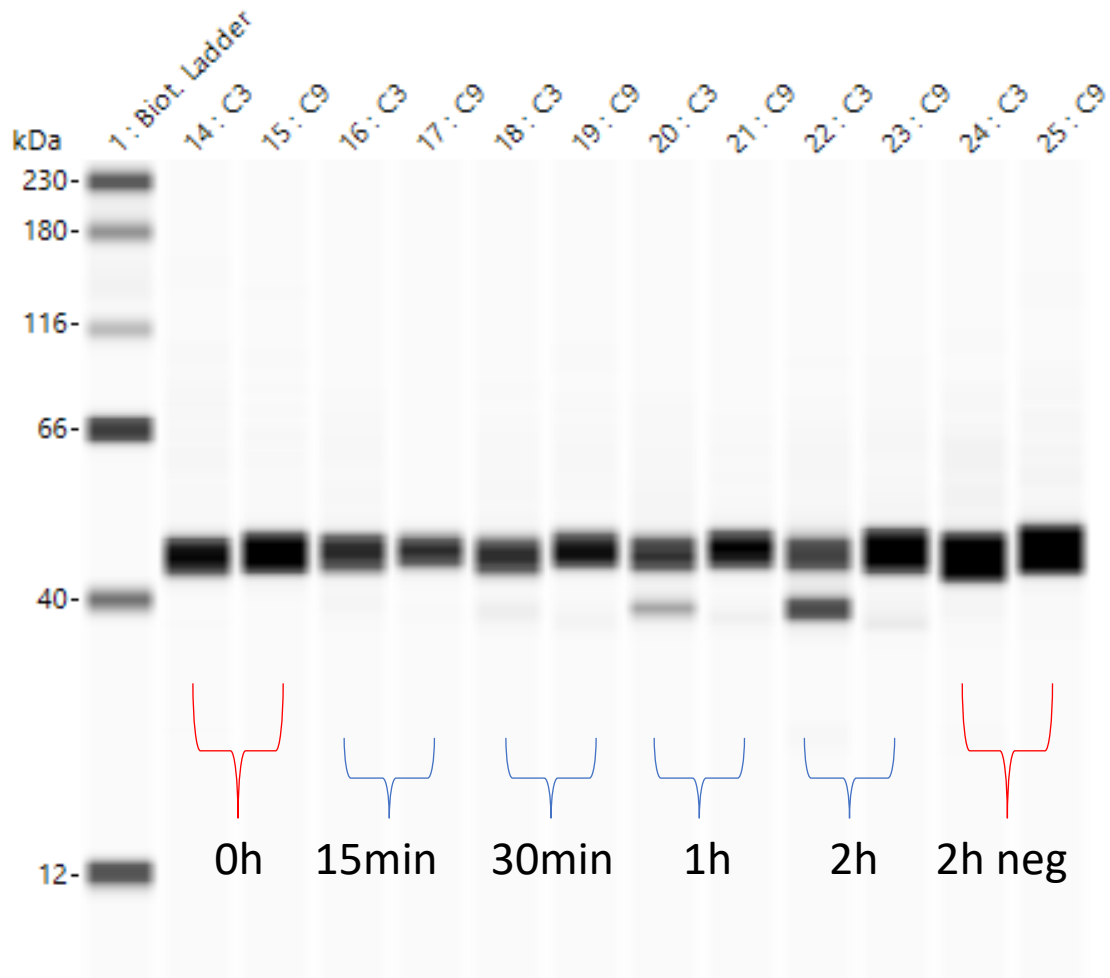
Chromatogram (all samples):
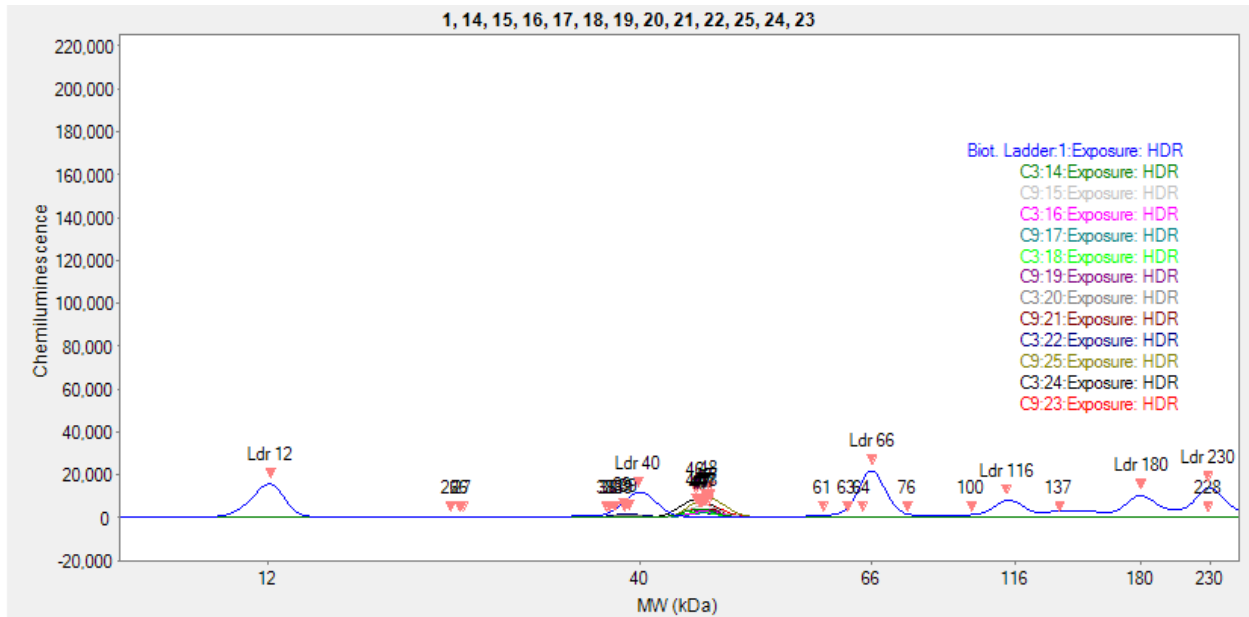
Chromatogram (0h C3 and C9 and 2h C3 and C9):
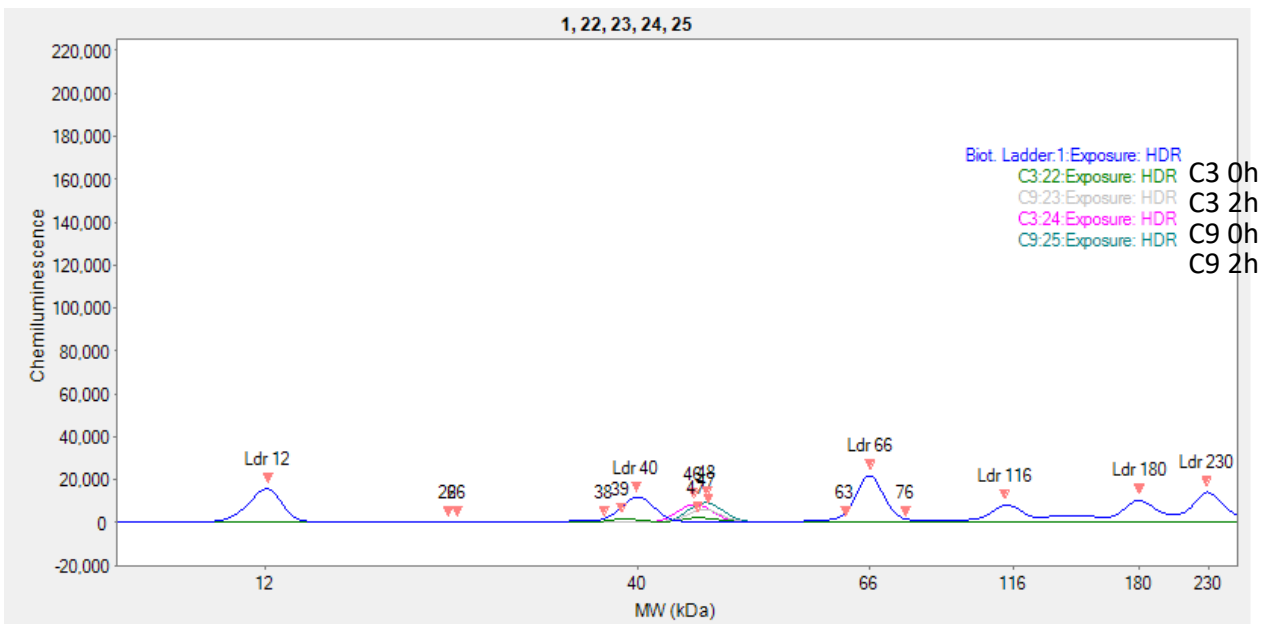
E3 ubiquitin-protein ligase RING1 (Observed in both caspase-3 and caspase-9 experiments. Found in the DegraBase)

Protein MW: 42.2kDa

Cleavage products expected: 21kDa - caspase-9 (cleavage at VSSD(189)-SA) and 21kDa - caspase-3 (cleavage at SAPD(193)-SA)

Observed: Very low signal as well, though appears to be cleaved by both enzymes (in the case of caspase-9 it is very faint)
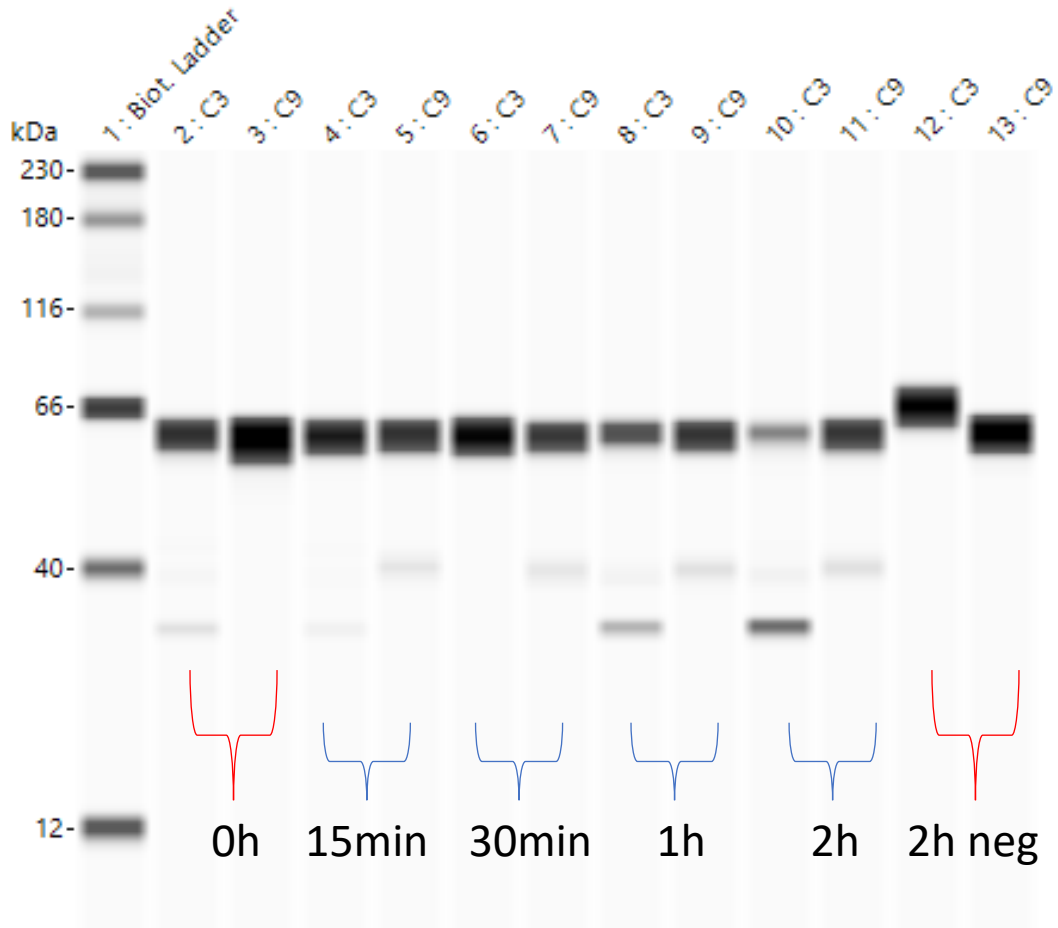
Chromatogram (all samples):
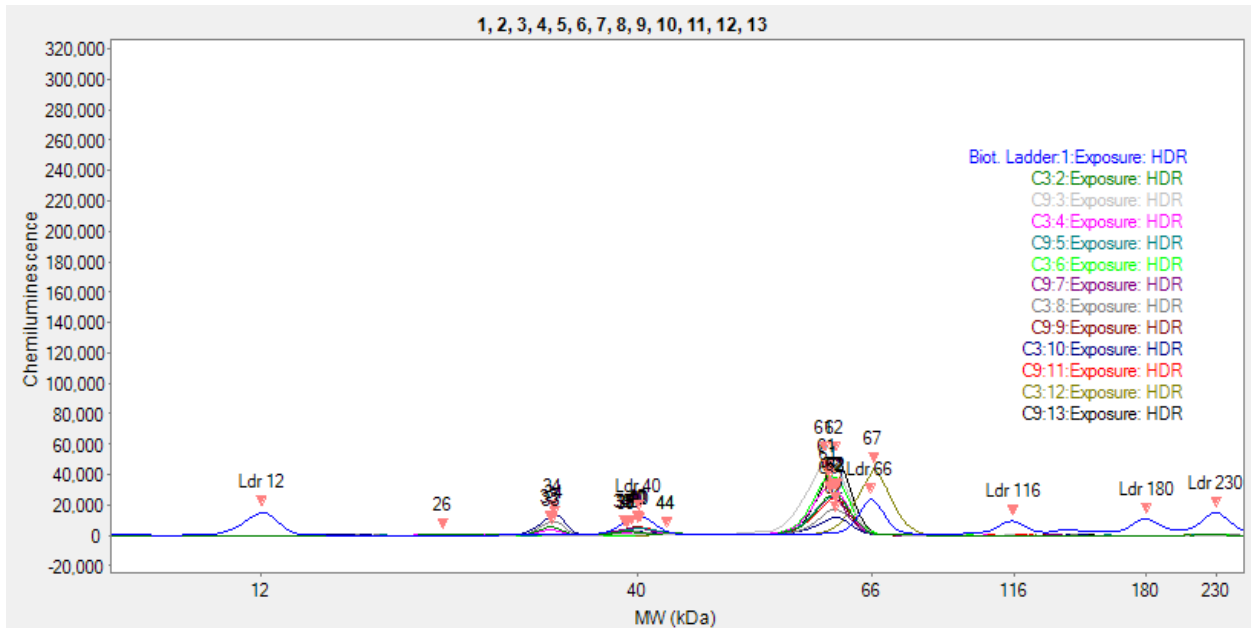
Chromatogram (0h C3 and C9 and 2h C3 and C9):
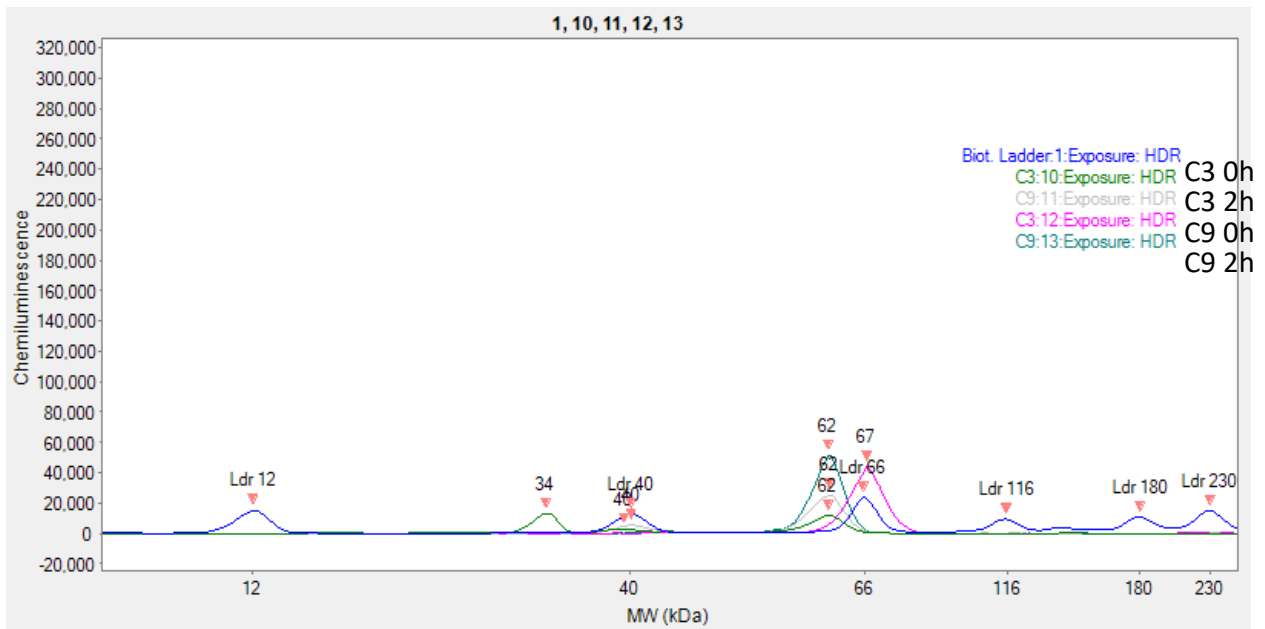
ATP-dependent DNA helicase Q5 (RECQL5) (Observed in caspase-9 experiment. Not found in the DegraBase)

Protein MW: 108kDa

Cleavage products expected: 89kDa (cleavage at GEED(809)-GA)

Observed: Evidently cleaved by caspase-9 and not caspase-3
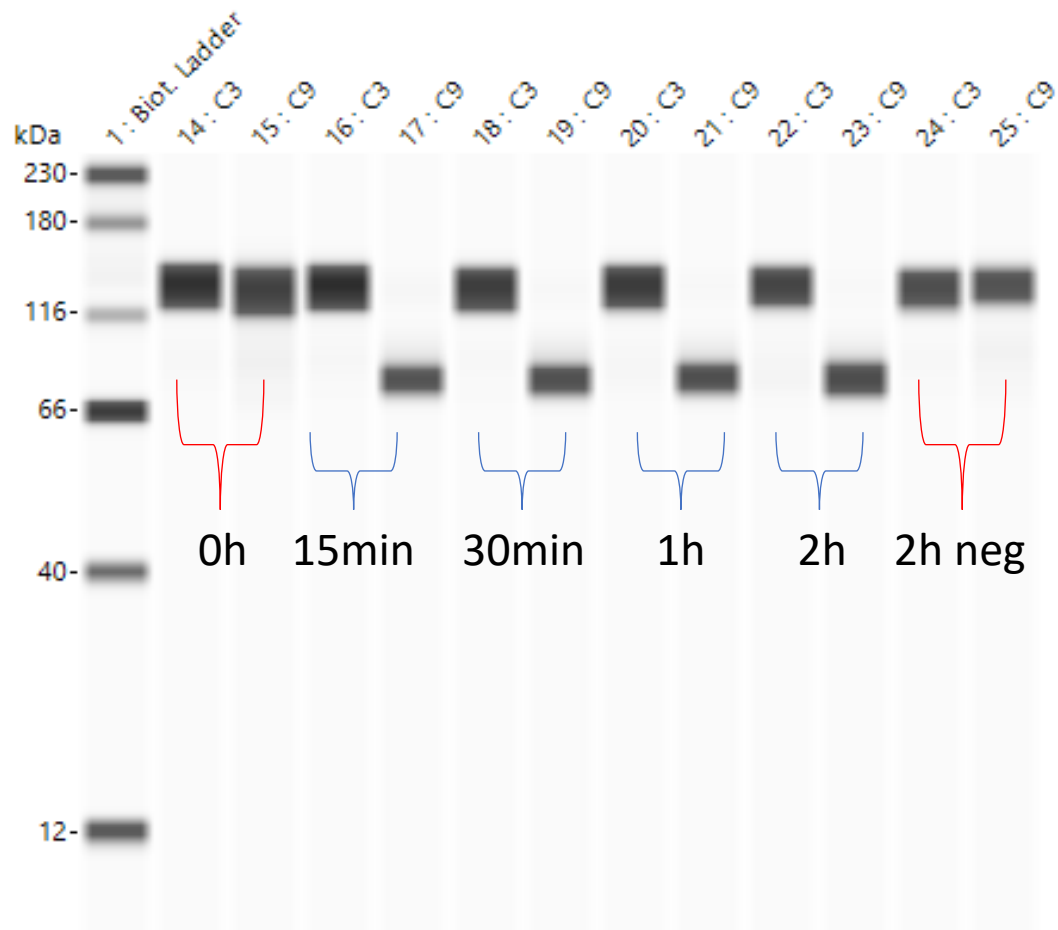
Chromatogram (all samples):
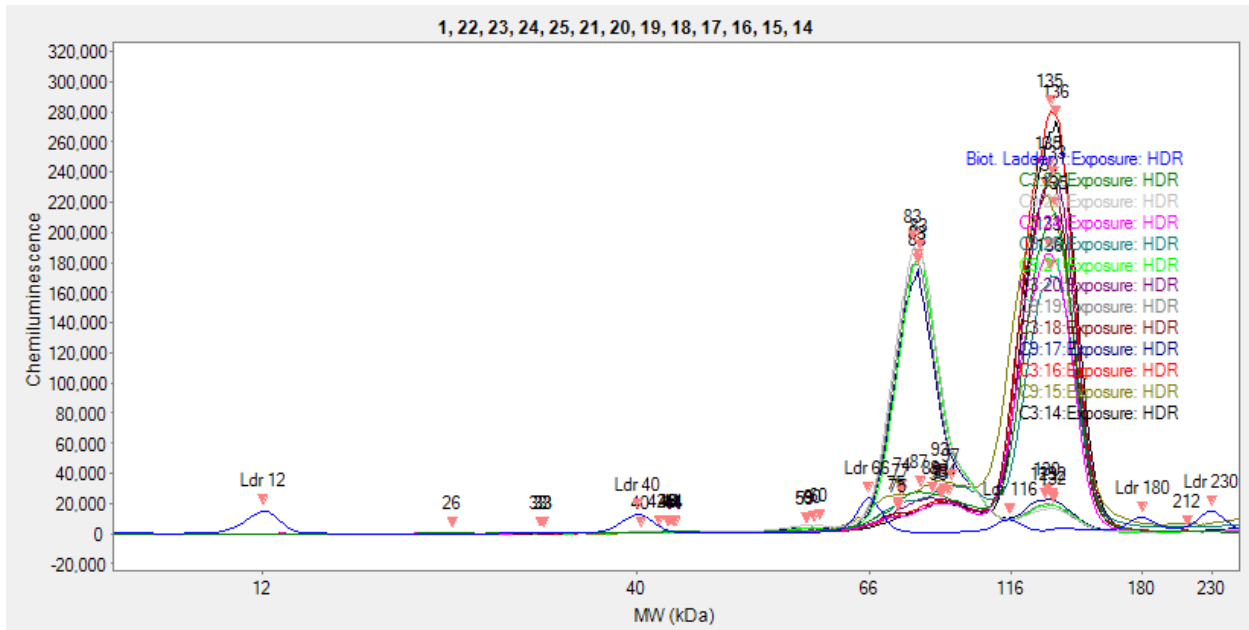
Chromatogram (0h C3 and C9 and 2h C3 and C9):
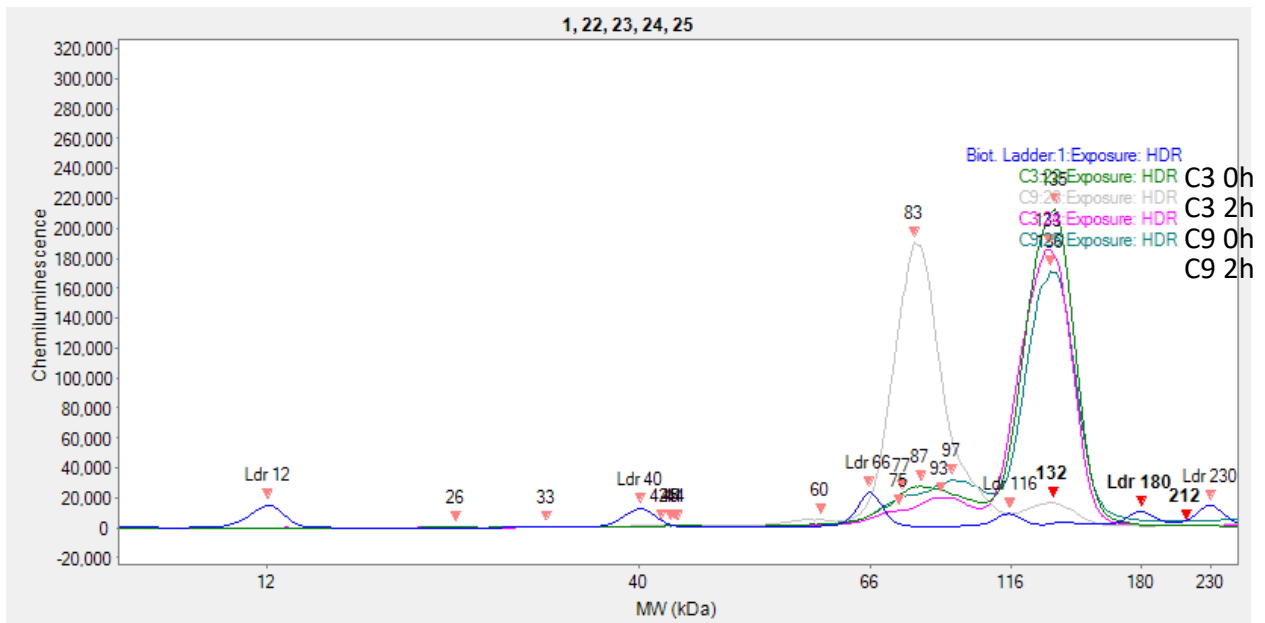
E3 ubiquitin-protein ligase RNF4 (Observed in caspase-3 experiment only. Not found in the DegraBase)

Protein MW: 21.3kDa

Cleavage products expected:

Observed: Appears degraded in both caspase-3 and caspase-9 samples, to a much more dramatic extent in the caspase-3 sample however. Though in the case of the caspase-9 dataset, the 2-hour negative control appears also degraded, so it's likely that the RNF4 degradation is not due to caspase-9's activity.
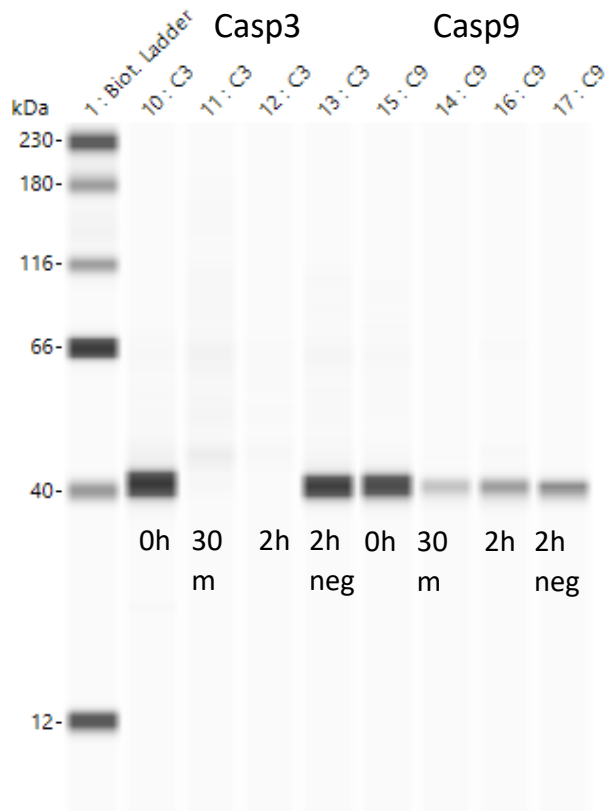
Chromatogram (all samples):
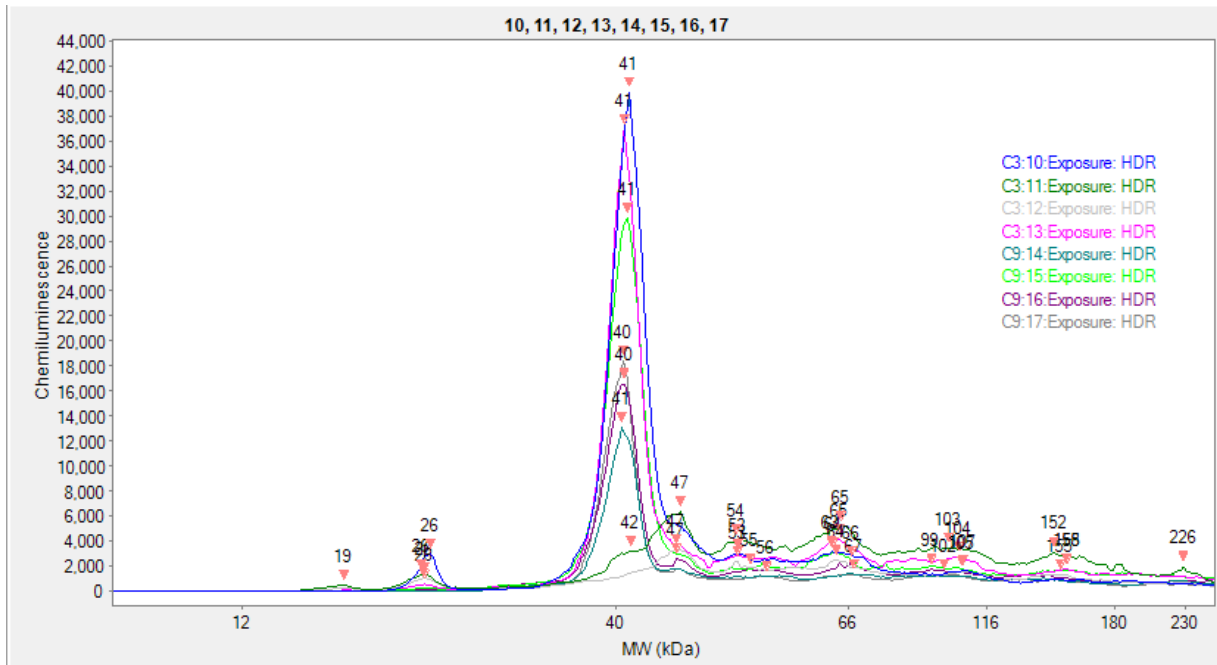
Chromatogram (0h C3 and C9 and 2h C3 and C9):
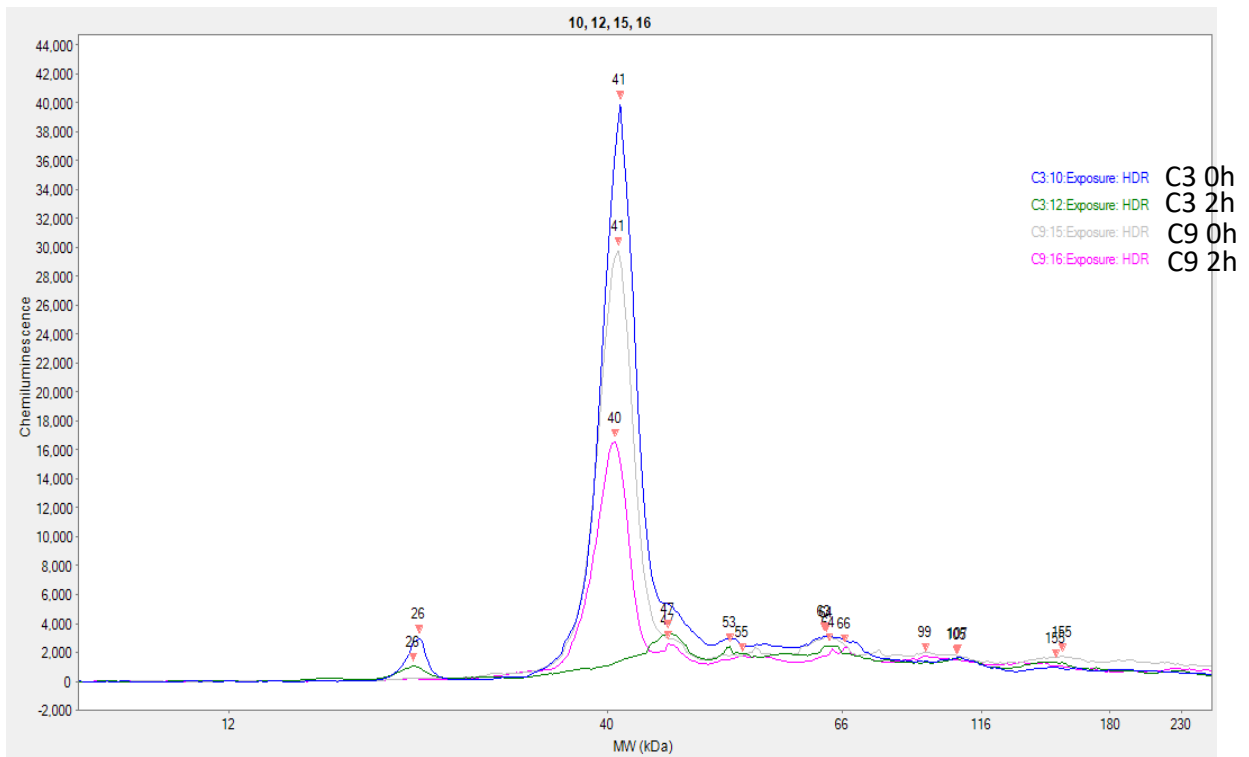
N-chimaerin (Observed in caspase-3 experiment. Not found in the DegraBase)

Protein MW: 53.2kDa

Cleavage products expected: 20.3kDa (cleavage at DERD(172)-ST)

Observed: Significant non-specific binding, many bands. In the caspase-3 samples it looks like the band at ~50kDa disappears over time. In the caspase-9 samples this does not look like the case. However in the caspae-9 samples there is also a strong band that appears 30 minutes and 2 hours after caspase-9 addition, which we believe to be nonspecific binding of the antibody to caspase-9.
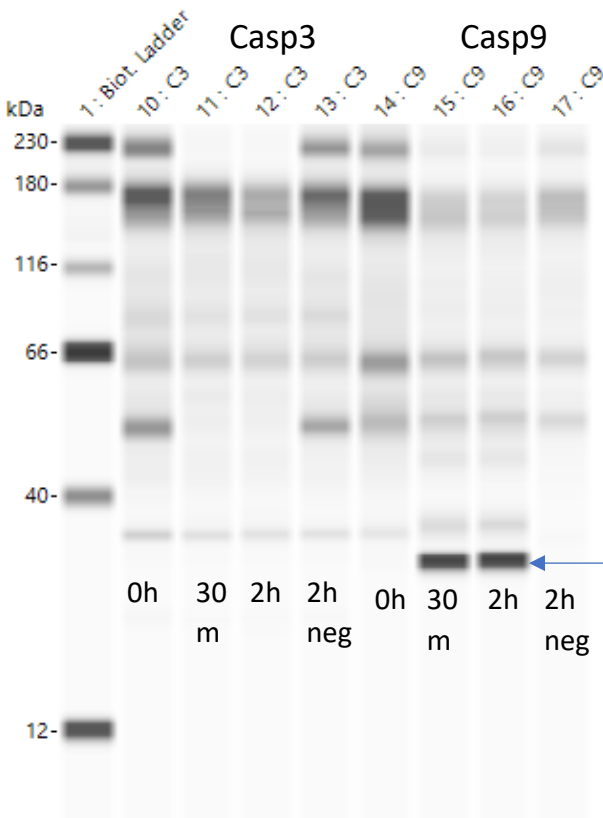
We think low band is C9 artifact – need a C9-only blot to confirm

Chromatogram (all samples):
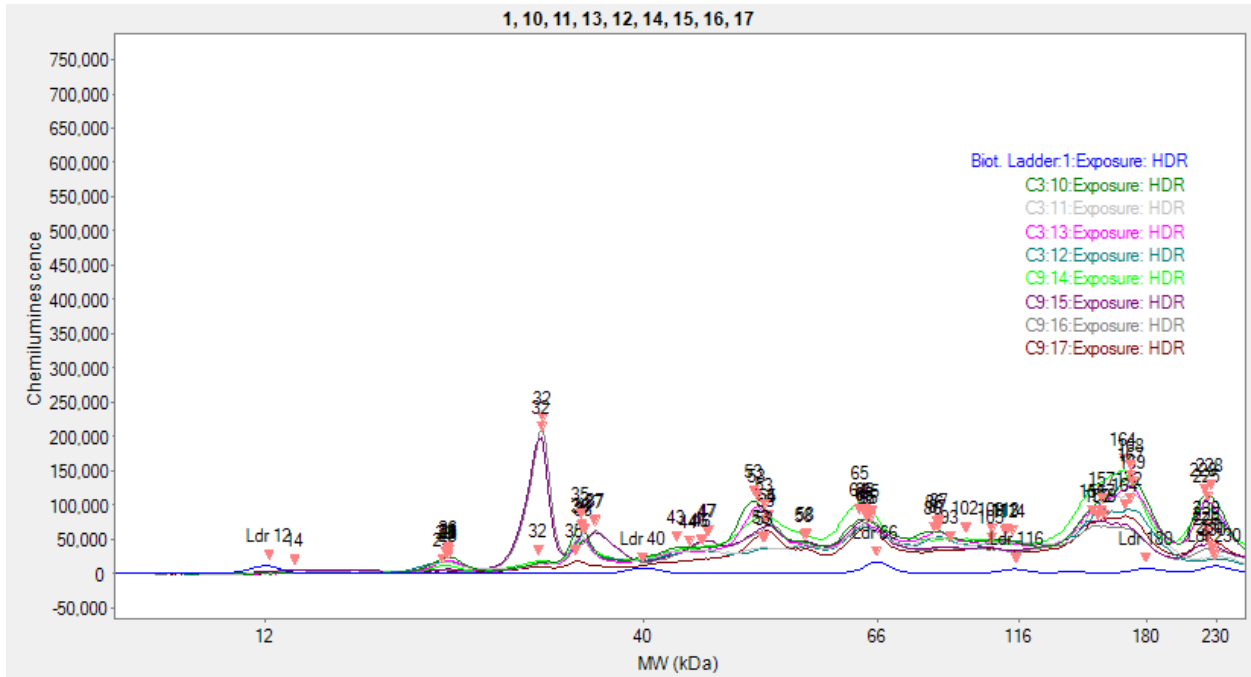
Chromatogram (0h C3 and C9 and 2h C3 and C9):
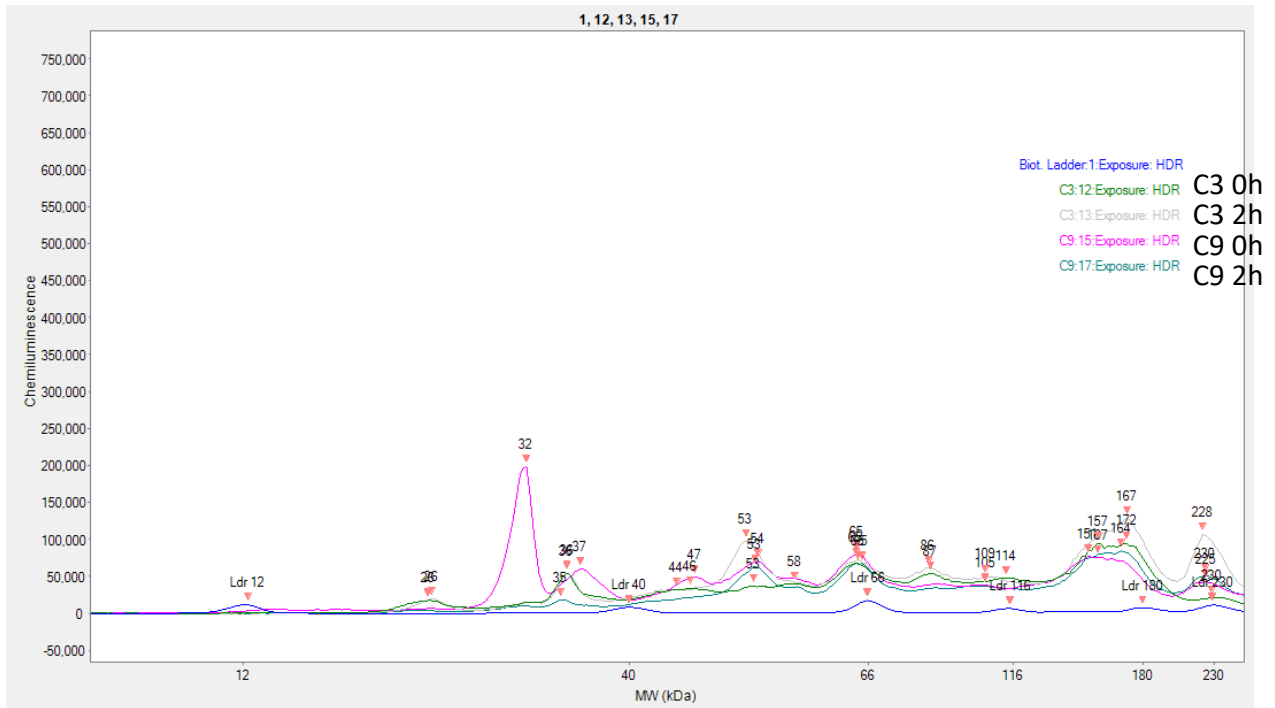
Mitofusin-2 (Observed in caspase-3 experiment only. Not found in the DegraBase)

Protein MW: 86.4kDa

Cleavage products expected: 29.2kDa (cleavage at DMID(499)-GL)

Observed: Signal was too low to draw significant conclusions. However it appears that the signal globally reduces in the caspase-3 samples much more strongly than in the case of caspase-9, suggesting cleavage. The 2-hour negative control of the caspase-3 sample appears overloaded.
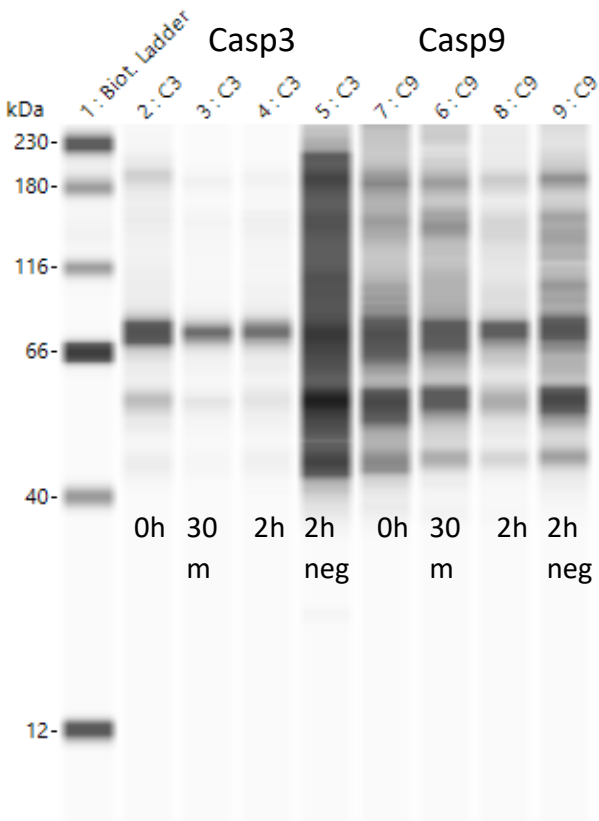
Chromatogram (all samples):
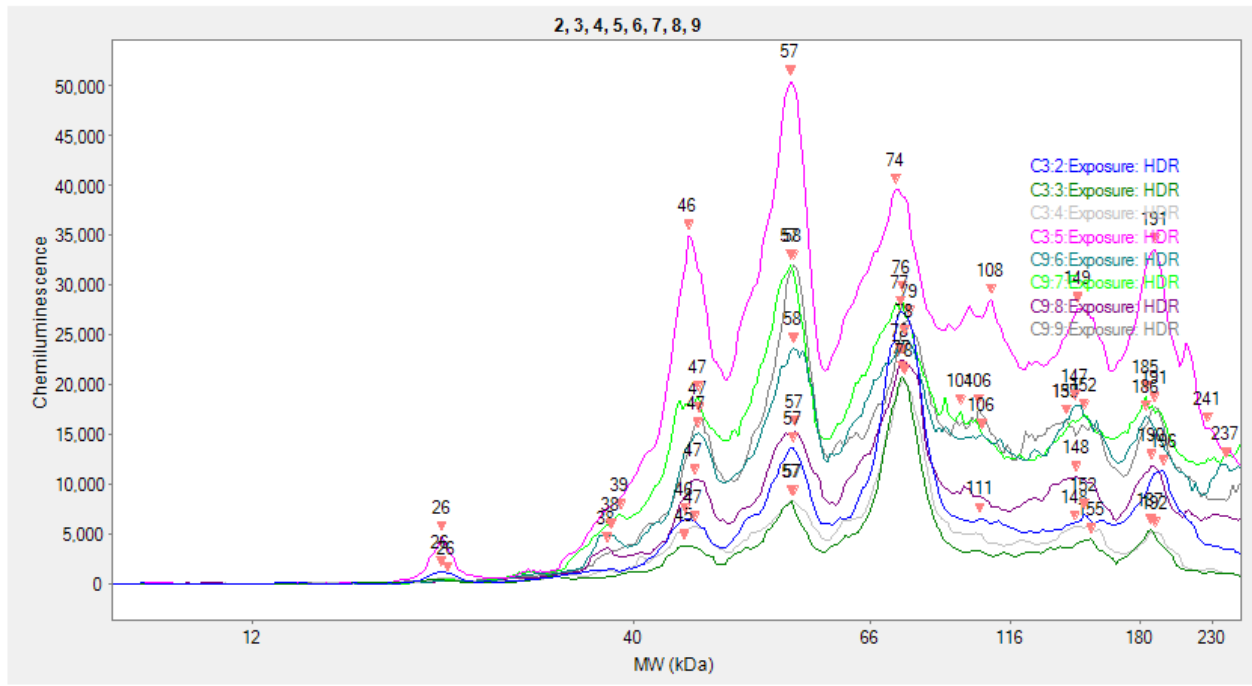
Chromatogram (0h C3 and C9 and 2h C3 and C9):
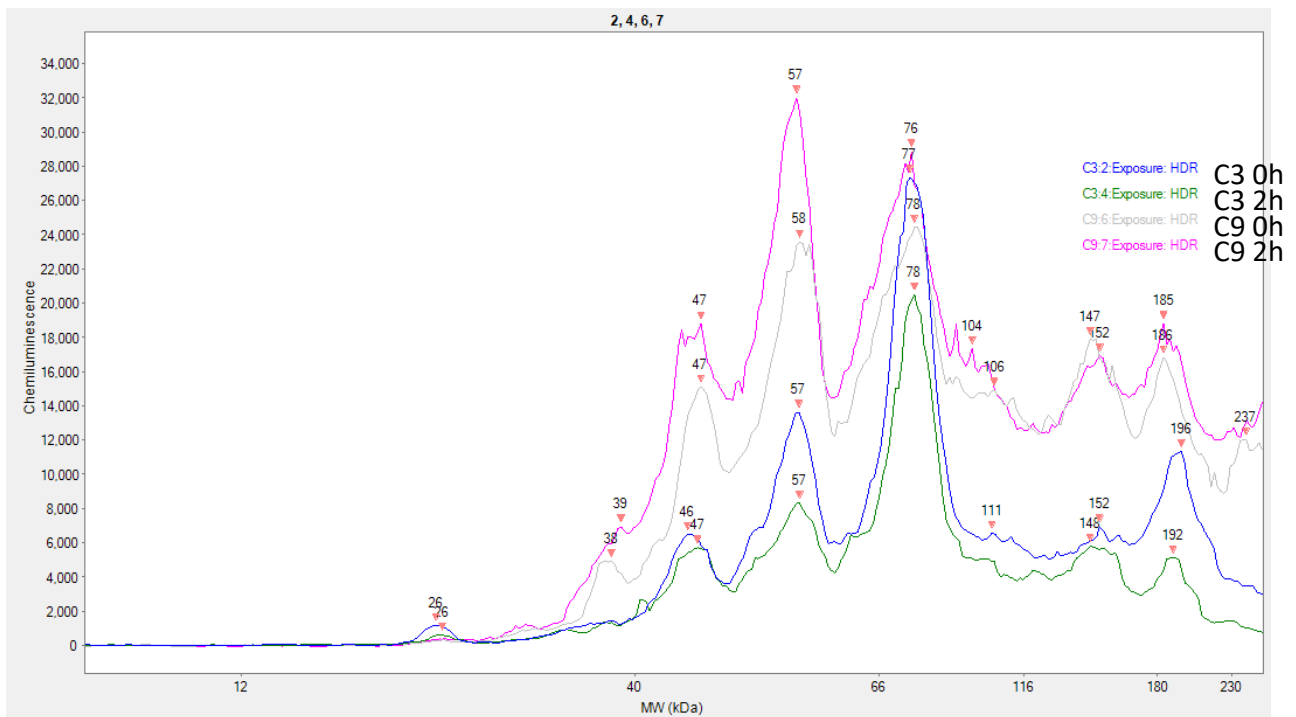
Ataxin-2-like protein (Observed in both caspase-3 and caspase-9 experiments. Found in the DegraBase)

Protein MW: 113kDa

Cleavage products expected: 87.5kDa (cleavage at LESD(246)-MS)

Observed: High nonspecific binding, hard to visualize cleavage on the western blot reconstruction, however looking at the chromatograms it is easier to tell that cleavage is observed in the caspase-3 sample, less so in the caspase-9 sample.

Chromatogram (all samples):

Chromatogram (0h C3 and C9 and 2h C3 and C9):

C3 0h
C3 2h
C9 0h
C9 2h
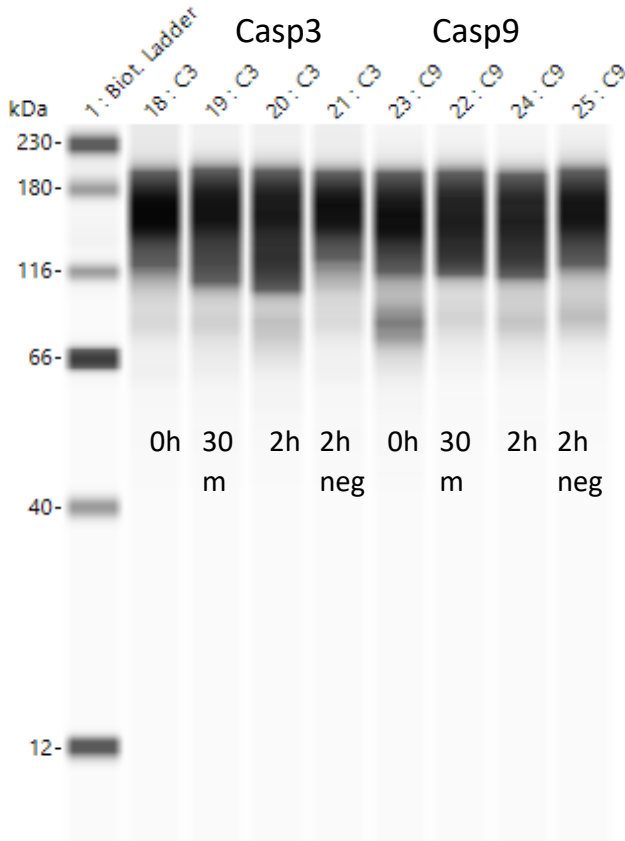
Chromatogram (0h C3 and C9 and 2h C3 and C9, separated into 2 images):

Blue = C3 0h

Green = C3 2h

Blue = C9 0h

Green = C9 2h
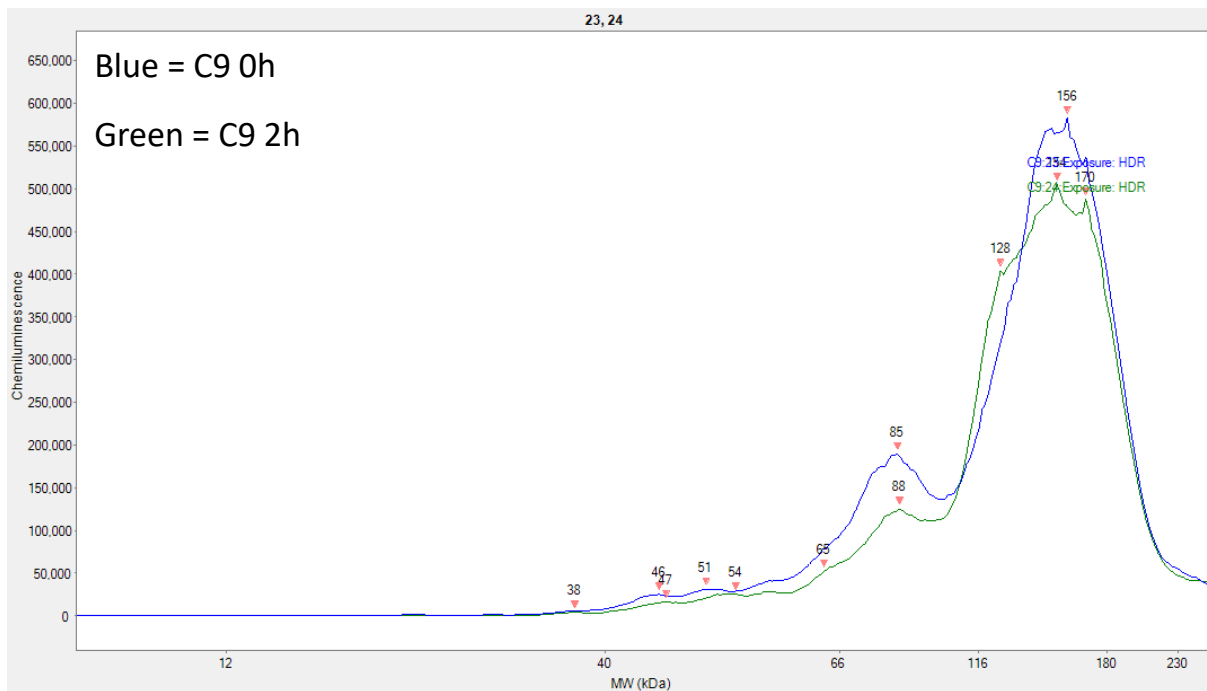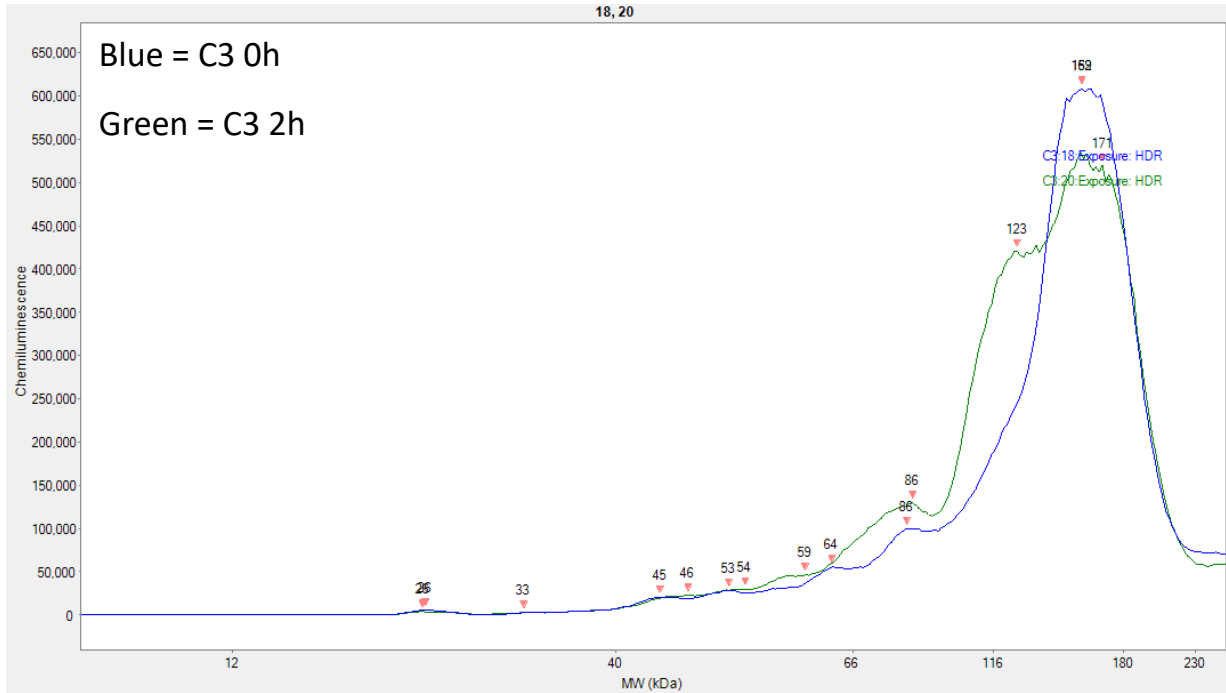
Gasdermin-D (Observed in caspase-3 experiment only. Found in the DegraBase)

Protein MW: 55kDa

Cleavage products expected: 42.8kDa (cleavage at DAMD(88)-GQ)

Observed: Cleavage in caspase-3 sample over time, no cleavage in caspase-9 sample.
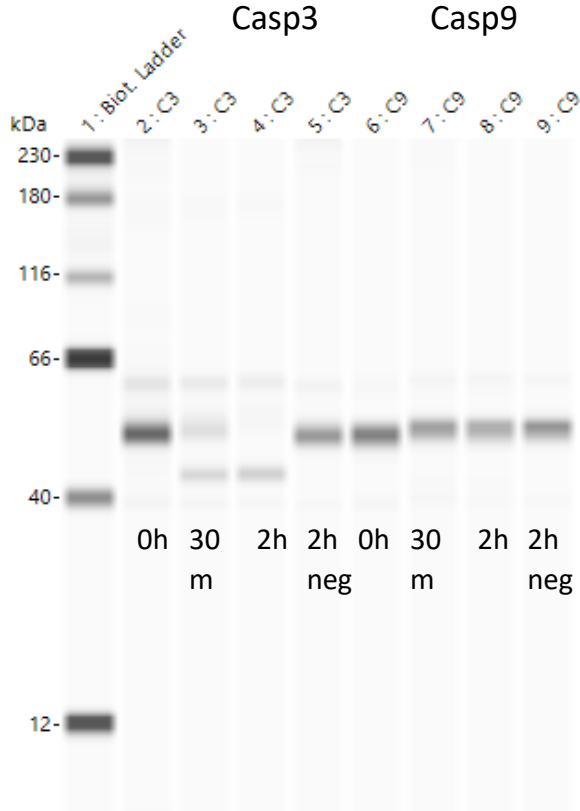
Chromatogram (all samples):

Chromatogram (0h C3 and C9 and 2h C3 and C9):
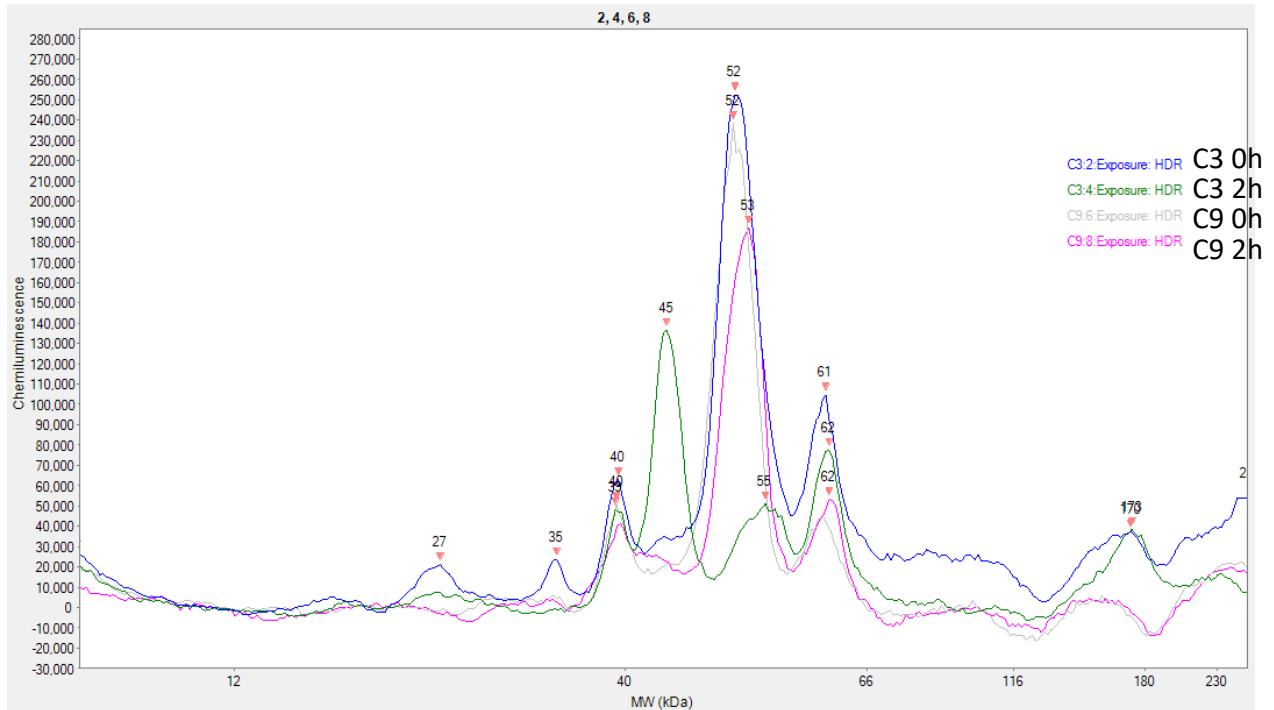
Summary

In conclusion, using capillary westerns is likely better for analysis of a single protein across multiple samples, so optimization of a single antibody can be conducted at a relatively low cost. As a result of our chosen timepoints, we were unable to view the appearance of cleaved products in most samples. As well, the results for the cleavage products above are variable in quality. To address both limitations would require significant optimization, which would be expensive given the cost of each capillary western plate. For these reasons, we opted to not continue with these experiments and use standard immunoblotting protocols for monitoring caspase-3 and -9 substrate proteolysis.

APPENDIX C

PREPARATIONS FOR A CASPASE-14 *REVERSE* N-TERMINOMICS EXPERIMENT

Preparations for a Caspase-14 Reverse N-terminomics Experiment

Caspase-14 the only human caspase presumed to play no role in cell death. In mice, it has been shown to be expressed in embryonic tissues of some organs but is undetected in all adult tissues[2]. It plays a role in keratinocyte differentiation[1] through cleavage of its one known substrate, profilaggrin[3], leading to downstream accumulation of natural moisturization factors and an increased UV resistance in the epidermis. We would like to conduct *reverse* N-terminomics, where we induce a cell lysate with active caspase-14. Through labeling of free N-termini, we will observe potential substrates of caspase-14 that can later be validated. However, purified caspase-14 has never been shown to be active in lysate. Prior to N-terminomics, we wished to observe Caspase-14 cleavage of a coumarin-based probe (Ac-WEHD-AFC)[4] both in buffer and in a Jurkat cell lysate and measure its activity. Below are the procedures undertaken for four completed assays, and their corresponding results.

This assay is complex because Caspase-14 requires a high concentration of kosmotropic salt to be active *in vitro* (typically fulfilled by using trisodium citrate)[4], which poses problems when placed in combination with cell lysates. Salts can be placed on a sliding scale (termed the Hofmeister series) that classifies them as kosmotropes or chaotropes[5]. Chaotropic salts destabilize intermolecular interactions, while kosmotropic salts stabilize intermolecular interactions. This leads to an increase in protein stability, and a decrease in protein solubility when kosmotropic salts are added to lysates. Practically, when a kosmotropic salt is added in high concentration to a cell lysis buffer, this creates a gummy, high-viscosity lysate that is difficult to work with. As a result, the assays below introduce citrate to cell lysates at the final step, when the assay is being assembled on the 96-well plate.

Reagents:

Caspase-14

- Provided from lab of Dr. Guy Salvesen (Sanford Burnham Prebys Medical Discovery Institute), purified by Scott Snipas
- 28 µM, stored in 50 µL aliquots at -80 °C (-80 OJ freezer #1, Rack 3, row 131, box 2)

Lysates

- Jurkat cell pellets – stored at -80°C (-80 OJ freezer #1, Rack 3, row 133, boxes 3-5)

Probes:

- Ac-WEHD-AFC
- Ac-DEVD-AFC
- Both stored in 10 µL, 5 mM stocks in DMSO at -20 °C (-20 OJ freezer #1, 2nd shelf, back right)

Protease inhibitors:

- phenylmethyl sulfonyl fluoride (PMSF) – Stored solid at 4 °C – prepare stocks fresh in isopropanol
- Iodoacetamide (IAM) – Stored solid at 4 °C, prepared fresh – prepare stocks fresh in dH2O
- 4-benzenesulfonyl fluoride hydrochloride (AEBSF) – Stored in 100 mM stocks in DMSO at -80 °C (-80 OJ freezer #1, Common rack)
- DEVD-fmk - Stored in 10 µL, 5mM stocks in DMSO at -20 °C (-20 OJ freezer #1, 2nd shelf, back right)
- Ethylenediaminetetraacetic acid (EDTA) – Prepared as 500 mM stock solution, stored at room temperature

Buffer reagents:

- Trisodium citrate (citrate) – Stored solid at room temperature (Chemical shelf)
- NaCl – Prepared as 5 M stock solution, stored at room temperature
- 3-[(3-Cholamidopropyl)dimethylammonio]-1-propanesulfonate (CHAPS) – Stored solid at room temperature, prepared fresh
- 2-[4-(2-hydroxyethyl)piperazin-1-yl]ethanesulfonic acid (HEPES) – prepared as 500 mM stock solution, stored at room temperature

Procedure:

Assay #1 – *In vitro* assay with purified caspase-14

Assay components:

- 1 µM purified Caspase-14
  - Pre-activated in 2X concentration (2 µM) in activity buffer
- Various Ac-WEHD-AFC concentrations
  - Final concentrations in assay plate: 100 µM, 50 µM, 25 µM, 12.5 µM, 0 µM
  - Prepared 2X concentration in activity buffer (serial dilutions)

- Starting at 200 µM, serial dilute until 25 µM
- Activity buffer
  - 0.7 M trisodium citrate
  - 100 mM HEPES pH 7.4
  - 0.1 mM EDTA
  - 0.1 % CHAPS
  - 60 mM NaCl

Final assay volume 100 µL

Final [trisodium citrate] = 0.7 M

Caspase-14 and Ac-WEHD-AFC were each separately prepared at 2X concentrations in activity buffer in 96-well plates. Probe was serially diluted. Enzyme dilutions were conducted in assay plate and placed on a shaker at room temperature for 15 minutes. Following, probe was pipetted into enzyme wells, and assay measurements were conducted (Excitation = 400 nm, Emission = 505 nm) for 2 hours. See plate layout below.

C14 + 100 µM Probe	C14 + 50 µM Probe	C14 + 25 µM Probe	C14 + 12.5 µM Probe	Buffer control

Assay #2 – Lysate assay

Final assay volume: 200 µL

Final [trisodium citrate]: 0.35 M

Components

- 1 µM or 5 µM purified Caspase-14
  - Preactivated in 4X concentration (4 µM or 20 µM) in activity buffer (50 µL/well)
- 50 µM Ac-WEHD-AFC
  - In 4X concentration in activity buffer (50 µL/well)
- For 1 sample set: 50 µM Ac-DEVD-AFC
  - To see if DEVD-fmk is inhibiting endogenous caspase-3
  - In 4X concentration in activity buffer (50 µL/well)
- 10 million/mL Jurkat cell lysate

- In 2X concentration (20 million/mL) in activity buffer lacking Trisodium citrate (100 µL/well)
- Activity buffer
  - Same composition as *in vitro* assay, with the following protease inhibitors added:
    - 1 mM phenylmethyl sulfonyl fluoride (PMSF)
    - 1 mM 4-benzenesulfonyl fluoride hydrochloride (AEBSF)
   - 5 mM Iodoacetamide (IAM)

100 million pelleted Jurkat cells (stored at -80°C) were resuspended in 500 µL activity buffer lacking trisodium citrate (with protease inhibitors). Lysis of cells was achieved by performing sonication at 20% amplitude, 2 seconds on and 5 seconds off for 2 minutes. Dithiothreitol (DTT) was then added to 20 mM to quench IAM. Lysate was then centrifuged at 8,000 g for 15 minutes to remove debris.

Caspase-14 was diluted to 4X concentration in activity buffer in a 96-well plate. Following, lysate was pipetted into enzymes wells, then probe. See plate layout below. Assay measurements were conducted for 5 hours.

Lysate + 1 µM C14	Lysate + 5 µM C14	Lysate + Buffer	Lysis Buffer + 1 µM C14	Lysis buffer + 5 µM C14

Assay #3 – Lysate assay with pre-activation period, & 10 µM DEVD-fmk

Components: same as assay #2 + 10 µM DEVD-fmk added to lysate

Lysate was prepared as in assay #2. Endogenous caspase-3 activity in lysate was inhibited with 10 µM (final) in DEVD-fmk for 15 minutes prior to assay.

Caspase-14 was diluted to 4X concentration in activity buffer in a 96-well plate, then placed on a shaker at room temperature for 15 minutes. Following, lysate was pipetted into enzymes wells, then probe. See plate layout below. Assay measurements were conducted for 5 hours.

Jurkat + DEVD-fmk + C14	Jurkat + DEVD-fmk	Jurkat + DEVD-fmk (Ac-DEVD-AFC probe)	Lysis buffer + DEVD-fmk + C14	Lysis Buffer + C14	Lysis buffer control

Assay #4 – Lysate and buffer assay at various citrate concentrations

Final assay volume: 150 µL

Final [trisodium citrate]: 0.7 M, 0.35 M, 0.175 M

Components

- Trisodium citrate buffer stocks – to be used with probe and enzyme
    - Create lysis buffer as described above, at 3 citrate concentrations (achieved by serial dilution into non-citrate lysis buffer):
        - 1.05 M, 0.525 M, 0.2625 M
        - These buffers will create final citrate concentrations of 0.7 M, 0.35 M and 0.175 M in assay plates
- 5 µM purified Caspase-14
    - Preactivated in activity buffer containing various citrate concentrations (50 µL/well)
        - See "trisodium citrate buffer stocks" above
    - Caspase-14 is prepared at 3X concentration here (15 µM), for a final concentration of 5 µM in assay plate
- 50 µM Ac-WEHD-AFC
    - In activity buffer containing various citrate concentrations (50 µL/well)
        - See "trisodium citrate buffer stocks" above
- 10 million/mL Jurkat cell lysate
    - In activity buffer lacking citrate (50 µL/well)
    - Prepared at 3X concentration (30 million/mL), for a final concentration of 10 million/mL in assay plate
- Activity buffer
    - Same composition as *in vitro* assay, with the following protease inhibitors added:
        - 1 mM phenylmethylsulfonyl fluoride (PMSF)
        - 1 mM 4-benzenesulfonyl fluoride hydrochloride (AEBSF)
        - 5 mM Iodoacetamide (IAM)
        - 10 µM DEVD-fmk

Lysate was prepared as in Assay #3, with the addition of DEVD-fmk to quench endogenous caspase-3 activity

Caspase-14 in lysis buffer (or buffer for no-enzyme controls) was added to a 96-well plate, then placed on a shaker at room temperature for 15 minutes to preactivate. Following, lysate was pipetted into enzymes wells (or an equal volume of buffer for no-lysate controls), then probe. See plate layout below. Assay measurements were conducted for 2 hours.

0.7 M Citrate +Lysate + Buffer	0.7 M Citrate +Lysate + C14	0.7 M Citrate + C14 + Buffer	0.7 M Citrate Buffer-only control	0.7 M Citrate C14 in vitro control Activity buffer, no inhibitors
0.35 M Citrate +Lysate + Buffer	0.35 M Citrate +Lysate + C14	0.35 M Citrate + C14 + Buffer	0.35 M Citrate Buffer-only control	0.7 M Citrate C14 in vitro control Activity buffer, no inhibitors
0.175 M Citrate +Lysate + Buffer	0.175 M Citrate +Lysate + C14	0.175 M Citrate + C14 + Buffer	0.175 M Citrate Buffer-only control	Empty well

Results:

Assay #1 – Caspase-14 is active in vitro (2-hour assay)
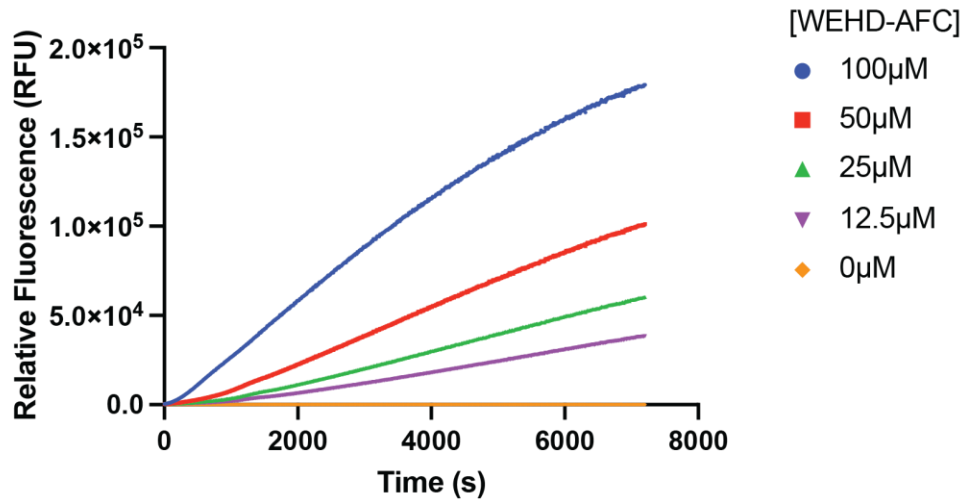
Probe cleavage is robust and increases proportionally with increasing probe concentration.

Assay #2 – Caspase-14 activity is indistinguishable from background proteolysis in lysate induced by 0.7 M citrate (5-hour assay)
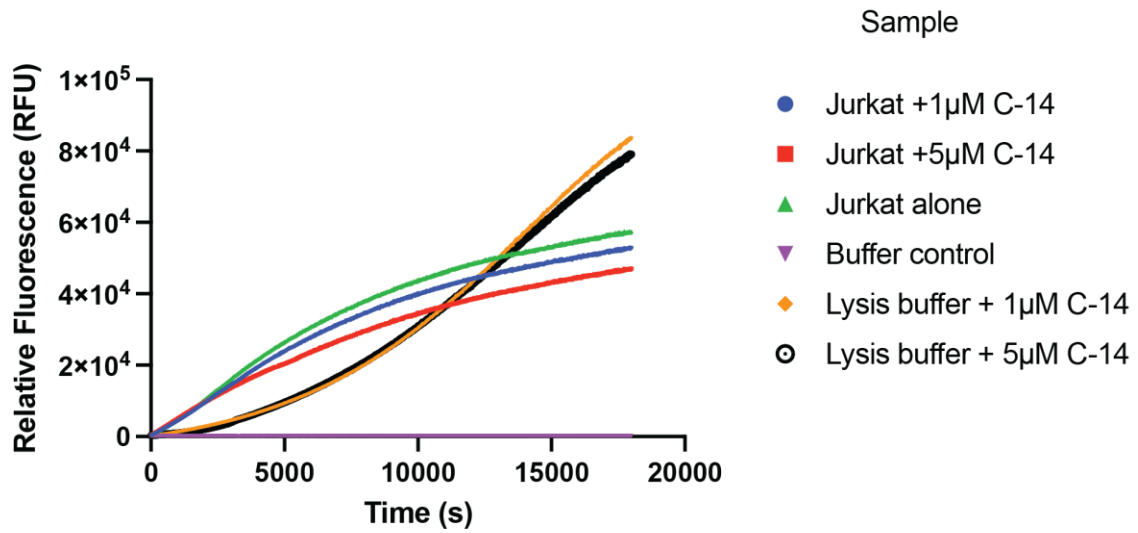
Probe cleavage is similar between Jurkat lysate treated with caspase-14 and Jurkat lysate lacking the enzyme. The added caspase-14 does not lead to an increased cleavage above background levels.

Assay #3 – Caspase-14 does not exhibit higher activity than background in lysate when preactivated, DEVD-fmk appears to not inhibit endogenous caspase-3 at 10 µM (5-hour assay)
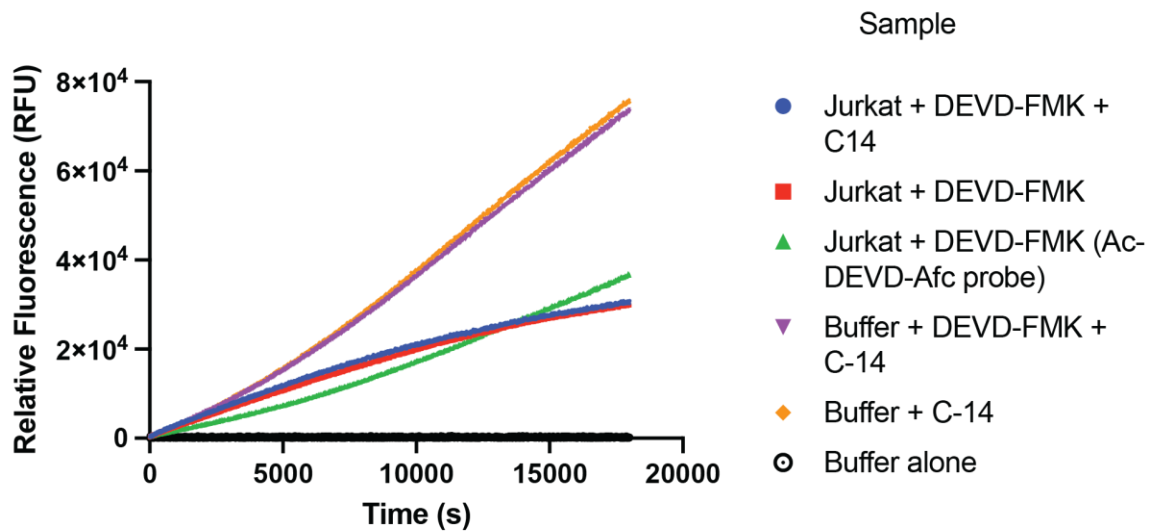
It appears some element of the lysate is inhibiting the activity of Caspase-14, and that 10 µM DEVD-fmk is insufficient to inhibit caspase-3 activity, as the Ac-DEVD-AFC probe continues to be cleaved.

Assay #4: Citrate dilution assays in lysate and in buffer – citrate concentration appears to affect Ac-WEHD-AFC probe cleavage (1.5-hour assay)

Sample-[citrate]

- ● Lysate-700
- ■ Lysate + C14-700
- ▲ Lysis buffer + C14-700
- ▼ Buffer only-700
- ▣ Lysate-350
- △ Lysate + C14-350
- ▽ Lysis buffer + C14-350
- ◇ Buffer only-350
- + Lysate-175
- ✕ Lysate + C14-175
- ☉ Lysis buffer + C14-175
- ▣ Buffer only-175

Assay #4 - Perfect
Buffer control only

- · C14 in perfect buffer
- · C14 in perfect buffer
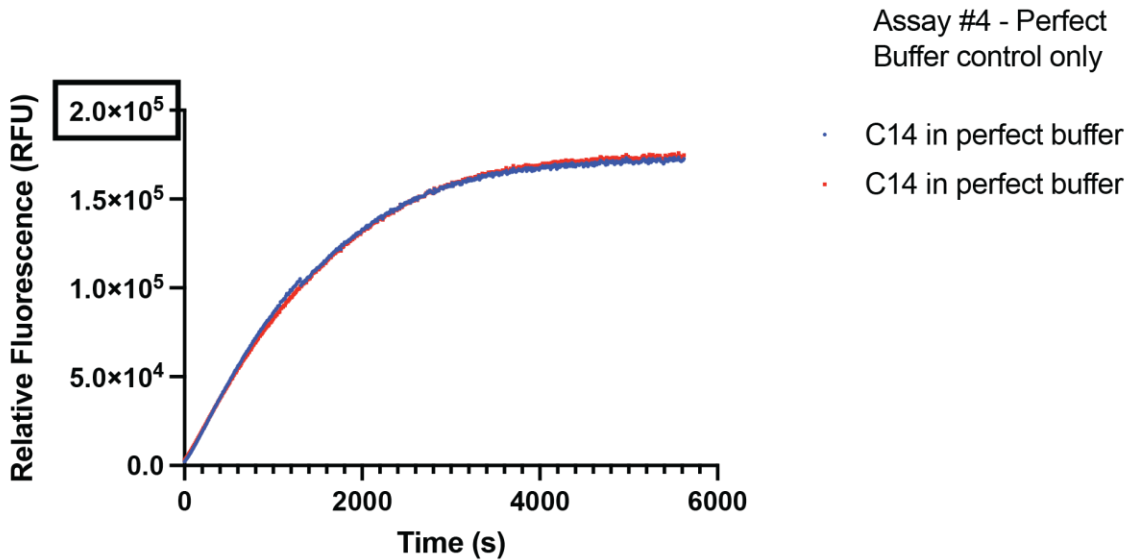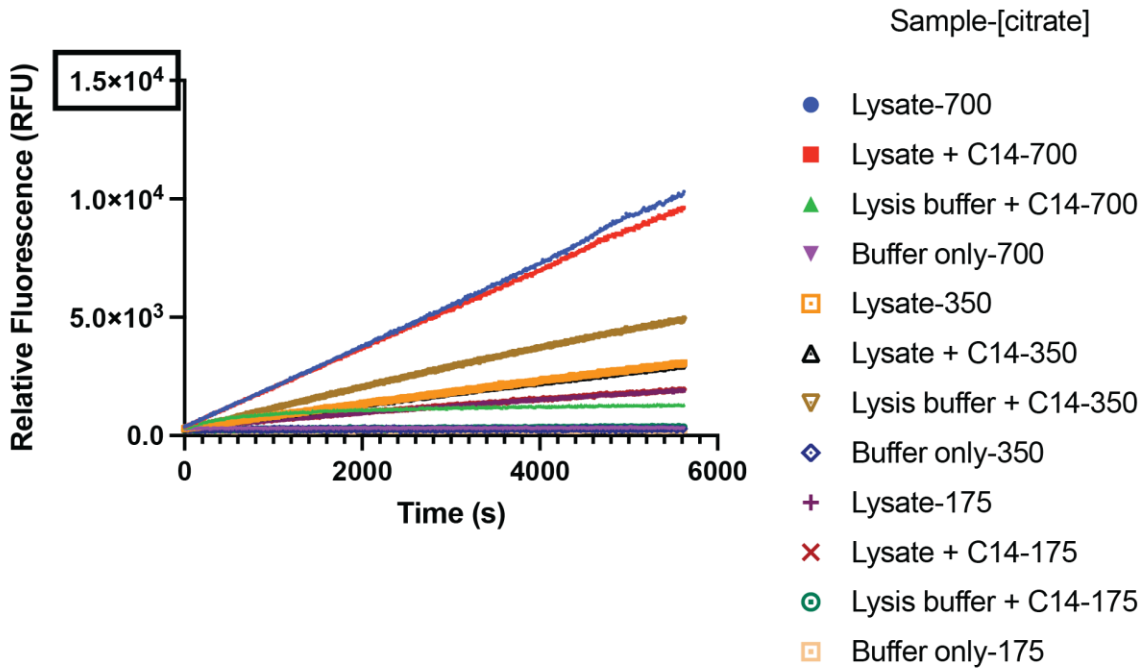
This assay demonstrated that differing concentrations of citrate directly impacted Ac-WEHD-AFC. An increase in citrate concentration correlates with an increase in probe cleavage

Upon working further with collaborator Scott Snipas in the laboratory of Dr. Guy Salvesen (Sanford Burnham Prebys Medical Discovery Institute), they were able to improve upon this assay. They were able to confirm my findings that Ac-WEHD-AFC was being cleaved in lysate in a citrate-dependent manner, using HEK-293 lysates. They also repeated the AC-WEHD-AFC lysate assay with Ac-IETD-AFC and Ac-LEHD-AFC probes and were able to demonstrate higher probe cleavage in caspase-14-induced lysates than native lysates. Using samples from these collaborators, we plan to conduct a *reverse* N-terminomics labelling experiment and identify novel proteolytic targets of Caspase-14.

Another experiment we conducted prior to N-terminomics is a labelling test, to determine whether the high citrate concentration in lysate would prevent subtiligase from labelling neo-N-termini created from proteolytic cleavage. To this end, we will prepare a lysate as done for the activity assays and incubate it with subtiligase and the TEVest6 peptide ester tag. This peptide ester tag contains biotin, which allows for lysate labelling to be monitored via immunoblotting using a fluorescent streptavidin antibody. A properly labeled lysate generates a smear along a western blot lane, as N-termini of proteins of varying lengths are labeled. If the high citrate concentration impedes labelling, then an ethanol precipitation will be conducted prior to labelling, to extract proteins and remove the citrate buffer.

Reagents:

Subtiligases:

- Wild-Type (WT) – Stored at -80°C (OJ -80 freezer #1, rack #2, row 124, box 1)
- M222A mutants – Stored at -80°C (OJ -80 freezer #1, common rack)

Lysates:

- Jurkat cell pellets – stored at -80°C (-80 OJ freezer #1, Rack 3, row 133, boxes 3-5)

Buffers:

- Pipes – Stored solid at room temperature (chemical shelf)
- KCl – Prepared as 250 mM stock solution, stored at room temperature
- EDTA – Prepared as 500 mM stock solution, stored at room temperature
- $MgCl_2$ – Prepared as 500 mM stock solution, stored at room temperature
- DTT – Prepared as 1 M stock solution, stored at -20°C (OJ -20 freezer #1, shelf 2)
- Trisodium citrate – Stored solid at room temperature (chemical shelf)

- Sucrose – Stored solid at room temperature (chemical shelf)

- NaCl – Prepared as 5 M stock solution, stored at room temperature

- CHAPS – Stored solid at room temperature (chemical shelf)

- AEBSF – stored at -80°C (-80 OJ freezer #1, Common rack)

- IAM – Stored solid at 4 °C, prepared fresh – prepare stocks fresh in dH2O

- PMSF – Stored solid at 4 °C, prepared fresh – prepare stocks fresh in isopropanol

Procedure:

Lysis buffer

- 20 mM PIPES
- 10 mM KCl
- 5 mM EDTA
- 2 mM $MgCl_2$
- 1 mM AESBSF
- 1 mM PMSF
- 5 mM IAM

Citrate buffer

- 1.4 M Trisodium citrate
- 40 mM PIPES
- 20% Sucrose
- 200 mM NaCl
- 0.2% CHAPS
- 2 mM EDTA

Casp-14 buffer condition replication

- 50 mM Tris pH 8.0
- 100 mM NaCl

Replicated lysate conditions of samples prepared by Scott Snipas (in Jurkat rather than HEK293 lysate though), with the addition of protease inhibitors. Lysed 50M Jurkat cell pellet (at -80°C) in 600 µL lysis buffer by probe tip sonication: 40% amplitude 2 s on 2 s off for 5 minutes. A 50 µL aliquot was taken for protein concentration via Bradford assay (lysate concentration was 6 mg/mL). DTT was added to 25 mM to quench IAM, following which the sample was centrifuged

at 8000 g for 10 minutes. The resulting supernatant was transferred to a new tube and centrifuged again. The final supernatant was placed in a new tube, and the sample was prepared to correlate identically with Scott Snipas's sample conditions. 200 µL of lysed cells were placed in a new tube and mixed with 500 µL of citrate buffer and 100 µL of Casp-14 buffer (did not add any caspase-14 – did not want to waste enzyme). This sample was used to proceed with the labeling protocol. The TEVest6 peptide ester tag (in 10 mM stock) was added to the samples at a 1:10 dilution, following which a 15 µL "pre-label" sample was taken and stored at 4°C. Subtiligases (WT and M222A mutant – both at 100 µM stocks) were added to 1 µM to the samples, and were left to incubate for 1 hour at room temperature. After 1 hour, a 20 µM "post-label" sample was taken, and both "pre" and "post-label" samples were analyzed via SDS-PAGE (180V for 40 minutes, Bio-Rad) and western blotting using IRDye-800 streptavidin antibody.

Results:

Streptavidin-800 labeling western blot shows successful subtiligase labeling of lysate in 0.875M citrate:

| 5 µL protein ladder | 15 µL pre-label | 20 µL post-label |
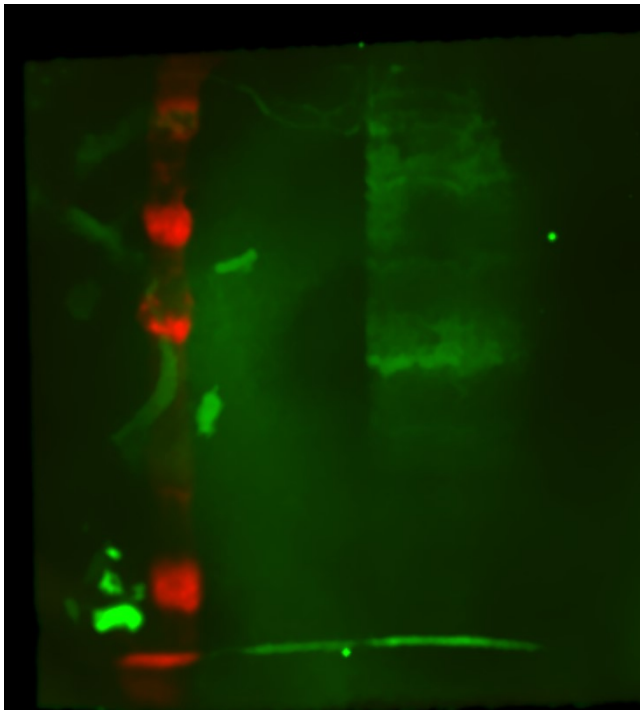
While the gel was running, it appeared like the sample lanes were expanding, explaining the larger banding pattern from the sample lanes compared to the ladder lane. The labeling western demonstrated that subtiligase could label Jurkat lysate as there was a smear of labeled proteins in the "post-label" sample compared to the "pre-label" sample. However, this labelling efficiency appears low based on the band intensity compared to previous labeling experiments with lysates of similar concentration. Based on these results, we decided to precipitate the samples in ethanol prior to subtiligase labelling.

Discussion:

Through the *reverse* N-terminomics experiment, we will identify many proteolytically cleaved substrates, though not all of them will be caspase substrates. To remove non-caspase substrates from consideration, we will filter for substrates which were cleaved with an aspartic acid at the P1 position, the hallmark of caspase cleavage. However, the validation of these target substrates cannot be done using lysates. As evidenced in Ac-WEHD-AFC probe cleavage assays in lysate, the addition of trisodium citrate to Jurkat lysates increases, as higher citrate concentration samples exhibit more probe cleavage when all other conditions remain identical. While caspase-14 cleavage is likely occurring, we cannot be confident with lysate-based validation that there is not another enzyme being activated to generate that cleavage site instead. To combat this issue, we will instead conduct validation *in vitro*, expressing or purchasing recombinant protein of the identified target and determining cleavage with recombinant caspase-14 in buffer. If the recombinant protein is cleaved, then we can assert that the protein is cleaved by caspase-14.

References:

1. S. Lippens, M.K.M. Knaapen, L. Mortier, R. Polakowska, A. Verheyen, M. Garmyn, A. Zwijsen, P. Formstecher, D. Huylebroeck, P. Vandenabeele, and W. Declercq. (2000). Epidermal differentiation does not involve the pro-apoptotic executioner caspases, but is associated with caspase-14 induction and processing. *Cell Death and Differentiation.* 7. 1218-1224

2. S. Hu, S. Snipas, C. Vincenz, G. Salvesen and V. Dixit (1998). Caspase-14 is a Novel Developmentally *Regulated Protease. Cell Biology and Metabolism*. 273(45). 29648-29653.

3. G. Denecker, P. Ovaere, P. Vandenabeele, and W. Declercq.(2008). Caspase-14 reveals its secrets. *Journal of Cell Biology*. 180(3). 451-458.

4. J. Mikolajczyk, F. Scott, S. Krajewski, D. Sutherlin and G. Salvesen (2004). Activation and Substrate Specificity of Caspase-14. *Biochemistry*. 43 (32), 10560-10569.

5. B.A. Rogers, T.S. Thompson, and Y Zhang. (2016). *Journal of Physical Chemistry.* 120. 12596-12603

APPENDIX D

THE PLUM POX VIRUS PROTEASE – A TEV PROTEASE ALTERNATIVE FOR N-TERMINOMICS

The Plum Pox Virus Protease – a TEV protease alternative for N-terminomics

Introduction:

The Plum Pox Virus (PPV) is a virus causing disease in stone fruit. It is a single-stranded RNA virus and manifests as a discoloration on fruit seeds, as well as rings on leaves. There is currently no cure to the Plum Pox Virus, making it an irritant for farmers because if there is infected fruit, the whole tree must be removed.

We intended to use the Nuclear Inclusion protein A (NIa) of the PPV as an alternative to the Tobacco Etch Virus (TEV) protease which we use in the lab for subtiligase-based N-terminomics. Our current N-terminomics protocol uses a peptide ester tag containing an ester, a biotin, a TEV protease cleavage site and an aminobutyric acid residue. The ester is required for subtiligase to ligate the tag to neo-N-termini. The biotin is required for the labeled proteins to be enriched, using neutravidin beads. The TEV protease cleavage site is required so that after on-bead trypsinization, we can use TEV protease to cleave labeled peptides from the neutravidin beads. Following TEV protease cleavage, the aminobutyric acid residue is retained on the labeled peptides to serve as an unambiguous mass tag to monitor in analysis of peptides via LC-MS/MS.

To broaden our peptide coverage, we wish to use enzymes other than trypsin to generate peptides for mass spectrometry. However, the way our tag is currently designed, this poses some issues for some enzymes we were considering, such as GluC and chymotrypsin. GluC cleaves C-terminal to glutamate residues and chymotrypsin cleaves C-terminal to large nonpolar amino acids (such as F, W and Y), both of which are present in the TEV protease cleavage site. If we used either of those enzymes to generate peptides in subtiligase-based N-terminomics, our peptides would be released from the neutravidin beads and washed away prior to TEV protease cleavage.
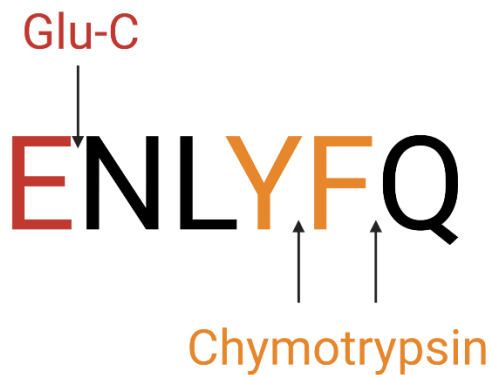
Figure 1. TEV protease cleavage site enzyme incompatibilities. The TEV protease cleavage site within our N-terminomics peptide ester tag restricts the enzyme we can use to generate peptides. We cannot use Glu-C because it would cleave c-terminal to the glutamic acid residue in the TEV site. Chymotrypsin is incompatible as well because it would lead to cleavage after the large nonpolar amino acids in the TEV site, namely tyrosine and phenylalanine. Figure made using BioRender.com.

To make our peptide ester tag compatible with multiple enzymes, we sought a different proteolytic cleavage site with the same advantages as the TEV protease, especially with respect to stringent specificity (to avoid the protease cleaving targets within our experiments). Following this we chose to begin expression of the Plum Pox Virus NIa protease.

The PPV protease is a 28kDa cysteine protease with a His46-Asp81-Cys151 catalytic triad. Its recognition site is QVVVHS/K, making it compatible with chymotrypsin and GluC (at time of writing, Erik Gomez-Cardona is developing a separate multi-enzyme probe that is GluC and chymotrypsin compatible as well).

Materials:

Primers & PPVP gblock: all in -20 Freezer #1, in an NEB box on shelf 2 labeled "Luam"; see "**Methods**" for primer sequences

Cloning restriction enzymes & materials; -20 Freezer #2

Agarose gel materials, protein expression materials – chemical shelves

Methods:

Generating gblock

The PPV NIa protease sequence was retrieved from the uniprot sequence for PPVP (accessed at https://www.uniprot.org/uniprot/P13529). The gblock was created to enter a plasmid where the protease would be expressed attached to a Maltose-Binding Protein (MBP) sequence, be purified on a Ni^{2+} affinity column, then it would self-cleave from MBP – this is similar to our current TEV protease expression and purification protocol. To do this, the gblock we created included a 6xHis tag and a PPVP cutsite, as well as a stop codon so only the protease is expressed and not the whole backbone plasmid. The sequence is below:

ac (extra bases to keep the construct in-frame once ligated), PPVP cutsite, 6xHis, PPVP Nia, stop

accaggtggtggttcaccagtccaagcatcatcatcatcatcattccaagtcactctttcgcgggttacgggactataatccg atcgcttcgtccatctgtcagctcaacaattcatctggtgctcgtcagtctgaaatgttcggcctcggtttcggggggcttaattgt gactaatcaacatcttttcaaacgtaacgatggtgaattgacaattcgctcgcaccatggcgaatttgtcgtaaaagacacc aaaacgcttaagttgctcccatgcaaagggcgcgatattgtgatcattcggttaccaaaagactttcctccattccccgaaac ggctccagttccggaccccaaccaccgaggaccgcgtctgtctcattggcagcaatttccagacgaaatcaatttcctcaa ccatgtctgaaaccagcgcaacttaccctgtagataattcccatttctggaaacattggatttcgacgaaggacggtcattgt ggtttaccaatcgtgagcacgcgcgacggctctattcttggcctgcattcgctcgcaaatagcactaacacacagaacttct acgcagctttcccagacaactttgagaccacgtatttgtcgaaccaggataatgataattggattaaacagtggcggtataa ccctgacgaggtctgctggggttctctccagcttaaacgcgacattccgcaaagtccgttcaccatctgcaaactttttaaccg acttagatggggagttcgtatatacccagtaa

The protein sequence of the NIa protease (after self-cleavage) is below: 6xHis, PPVP Nia

KHHHHHHHSKSLFRGLRDYNPIASSICQLNNSSGARQSEMFGLGFGGLIVTNQHLFKRNDGEL TIRSHHGEFVVKDTKTLKLLPCKGRDIVIIRLPKDFPPFPKRLQFRTPTTEDRVCLIGSNFQTKSIS STMSETSATYPVDNSHFWKHWISTKDGHCGLPIVSTRDGSILGLHSLANSTNTQNFYAAFPDN FETTYLSNQDNDNWIKQWRYNPDEVCWGSLQLKRDIPQSPFTICKLLTDLDGEFVYTQ

MW = 28.7kDa, E/1000 = 36.815 assuming all Cys form cystines, 36.440 assuming all Cys reduced. (From Expasy ProtParam tool)

The PPVP sequence was also cloned into the CMX3 plasmid, in a form where it would remain fused with the MBP encoded in the plasmid backbone (no self-cleavage), by removing the PPV cutsite and the 6xHis tag. The resulting protein sequence is below: 6xHis, MBP, PPVP Nia

MGSSHHHHHHGSSMKIEEGKLVIWINGDKGYNGLAEVGKKFEKDTGIKVTVEHPDKLEEKFPQ
VAATGDGPDIIFWAHDRFGGYAQSGLLAEITPDKAFQDKLYPFTWDAVRYNGKLIAYPIAVEALS
LIYNKDLLPNPPKTWEEIPALDKELKAKGKSALMFNLQEPYFTWPLIAADGGYAFKYENGKYDIK
DVGVDNAGAKAGLTFLVDLIKNKHMNADTDYSIAEAAFNKGETAMTINGPWAWSNIDTSKVNY
GVTVLPTFKGQPSKPFVGVLSAGINAASPNKELAKEFLENYLLTDEGLEAVNKDKPLGAVALKS
YEEELAKDPRIAATMENAQKGEIMPNIPQMSAFWYAVRTAVINAASGRQTVDEALKDAQTNSS
SNNNNNNNNNNLGIEENLYFQGQSKSLFRGLRDYNPIASSICQLNNSSGARQSEMFGLGFGGL
IVTNQHLFKRNDGELTIRSHHGEFVVKDTKTLKLLPCKGRDIVIIRLPKDFPPFPKRLQFRTPTTE
DRVCLIGSNFQTKSISSTMSETSATYPVDNSHFWKHWISTKDGHCGLPIVSTRDGSILGLHSLA
NSTNTQNFYAAFPDNFETTYLSNQDNDNWIKQWRYNPDEVCWGSLQLKRDIPQSPFTICKLLT
DLDGEFVYTQ

MW = 72.3kDa, E/1000 = 104.655 assuming all Cys form cystines, 104.280 assuming all Cys reduced. (From Expasy ProtParam tool)

Primer sequences

For amplifying the gblock (gblock orders only come with 100µg of DNA usually):

- Forward: LA_003 primer at -20C
  accaggtggtggttcaccagtc → %GC=59.1% tm=61.4C
- Reverse: LA_004 primer at -20C
  ttactgagtatagacaaattcgccgtccaagtc → %GC=42.4%, tm=59.6C

For ligating the gblock into pRK793:

- Forward: LA_001 primer at -20C
  25bp until SacI cut end + 23bp into gblock
  aaagacgcgcagactaattcgagctaccaggtggtggttcaccagtccaa → 54.2%GC, Tm=70.5C
  insert overlap tm = 60.3C

- Reverse: LA_006 primer at -20C

  gcctgcaggtcgactctagaggatcttactgggtatatacgaactccccatc → 51.9%GC, Tm 68.4C

  insert overlap tm: 57.2

For removing the PPVP cutsite:

- Forward: LA_008

  tccaagtcactctttcgcgg → %GC=55% Tm= 57.4C

- Reverse: LA_004

  ttactgggtatatacgaactccccatctaagtc (same primer as for amplifying the gblock) → GC% = 42.4% Tm =59.6C

For ligating the modified gblock into CMX3:

- Forward: LA_009

  Gaggaaaacctgtattttcagggccagtccaagtcactctttcgcggg → %GC= 52.1% Tm=69.4C

  Insert overlap Tm: 59.5C

- Reverse: LA_010

  gtggtggtggtgctcgattactgggtatatacgaactccccatc → %GC= 52.3% Tm= 67.7%

  Insert overlap Tm: 57.9C

Gibson assembly:

The PPV protease was cloned into the pRK793 plasmid backbone through restriction enzyme digests and Gibson assembly using the protocol below (See Gibson Cloning Protocol in Julien Lab google drive for full protocol). I used the restriction digest-based protocol, where only the insert is amplified via PCR, and ligated into a digested vector.

With the insert, Gibson PCR was conducted with the LA_001 and LA_006 primers. The PCR mix was: 1 µL of 0.5 ng/µL template, 5µL of 10x Q5 Buffer (Thermo Fisher Scientific), 2.5µL 10µM forward primer primer, 2.5µL 10µM reverse primer, 1µL 10mM dNTP's (Thermo Fisher Scientific), 37.5 µL ddH$_2$O, 0.5 µL Q5 polymerase (Thermo Fisher Scientific). The PCR cycle was: 98C x 2min, **98C x 15sec, 56C x 30sec, 72C x 3 minutes (30s/kBase, the vector is 6400bp)**, repeating the bold 30x, 72C x 10min, 12C forever (in case left overnight). Following the Gibson reactions, a 5µL aliquot of each product (along with DNA loading dye) was run on 0.8% agarose gel electrophoresis at 100V for 45 minutes to confirm PCR success. Once confirmed, a PCR cleanup kit (Truin Science) was used to purify the products. The concentration of the products was verified using a NanoDrop. To perform the Gibson Assembly, 25ng of double-digested vector

(SacI/BamHI for pRK793, XhoI/NdeI for CMX3) was mixed with a 4-fold molar excess of insert in a total volume of 5 µL. A separate vector-only control was also prepared in 5 µL. These DNA mixtures were each added to 15 µL of HiFi Assembly MasterMix (New England BioLabs), then incubated at 50°C for 30 minutes in a thermocycler. After the cycle is complete, 2 µL of the assembly mixture is transformed into XL10 cells (see **Transformations** protocol below).
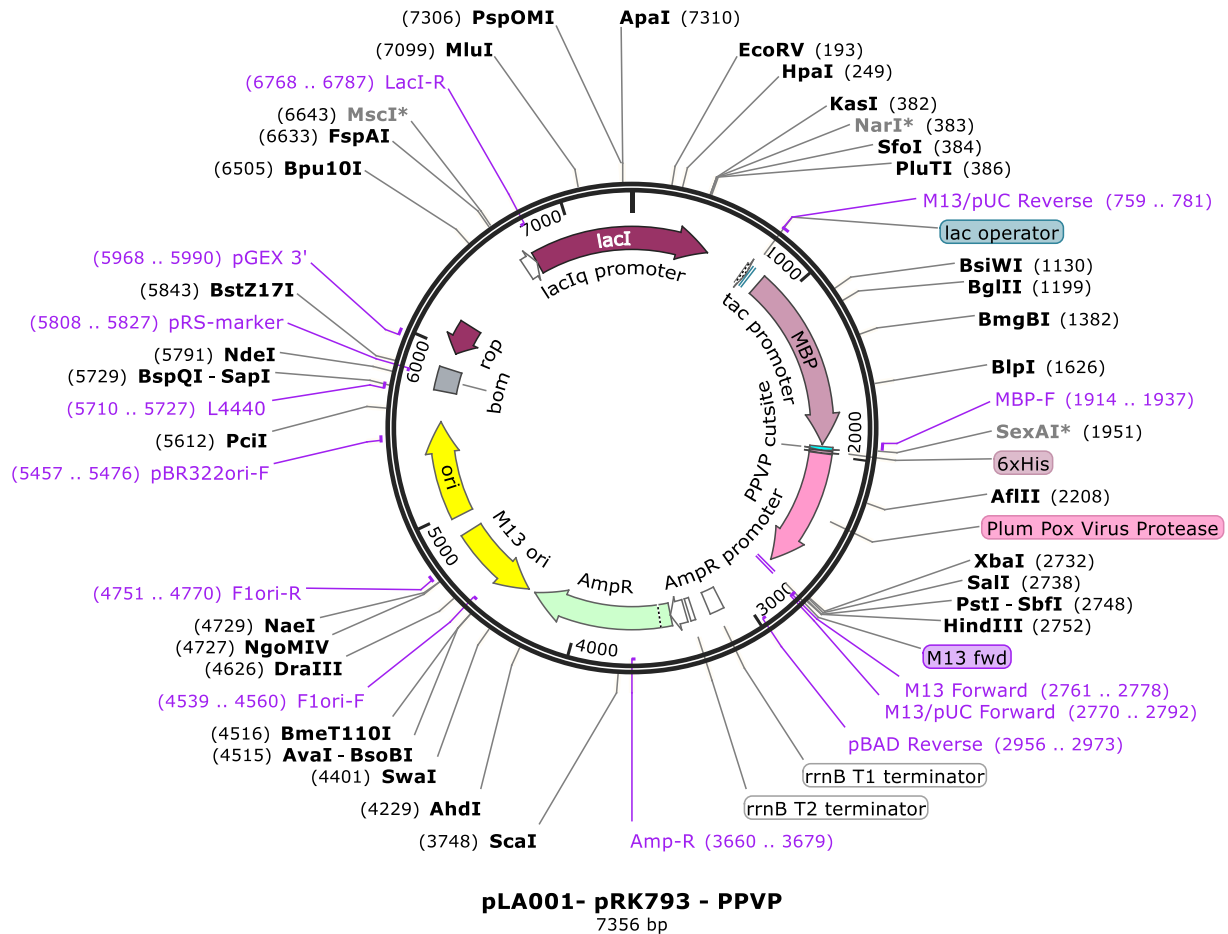

pLA001- pRK793 - PPVP
7356 bp

Figure 2. pRK793-PPVP sequence diagram. Sequence diagram of the PPVP gblock sequence cloned into pRK793, the TEV protease plasmid. To make this plasmid, the TEV protease sequence was removed from the plasmid via restriction enzyme digestion, following which Gibson assembly was conducted to ligate the PPVP sequence in its place. Sequence diagram made with SnapGene.

The PPV protease was also cloned into the CMX3 plasmid backbone through restriction enzyme digests and Gibson assembly. Prior to this however, a new PPV protease sequence was created

via primer amplification, to cut out the PPV cutsite and 6xHis tag, to leave just the protease sequence. The protocol used was the same as above, using the primers LA_009 and LA_010 instead.
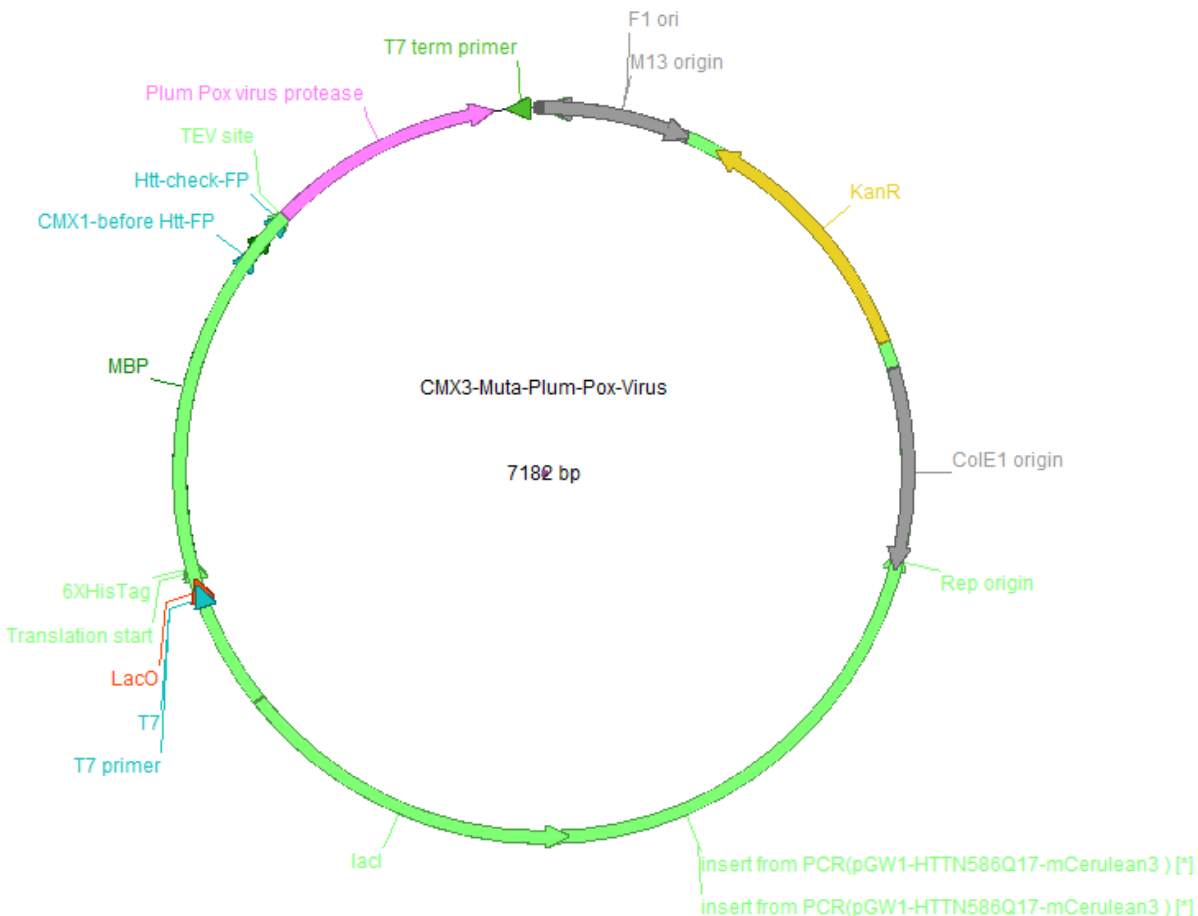
Figure 3. CMX3-PPVP sequence diagram. Sequence diagram of the PPVP gblock sequence cloned into CMX3. To make this plasmid, restriction enzyme digestion was conducted to create an opening for the plasmid, following which Gibson assembly was conducted to ligate the PPVP sequence in its place. See Figure 4 for details on the plasmid backbone. Sequence diagram made with ApE.

Transformations

Transformations of Gibson assembly: DNA stocks ranged from 50-200 ng/µL. 2 µL of Gibson assembly DNA was added to 50 µL competent XL10 *E. Coli* and incubated for 15 minutes on ice. Then transformation was heat shocked by incubation in a 42°C water bath, followed by an

incubation on ice for 2 minutes. 450 µL of LB was added to the cells, following which they were incubated at 37°C in a shaking incubator at 200 rpm for 1 hour. The cells were centrifuged at 1000 rpm for 5 minutes and most of the media removed, leaving 100 µL. Cells were resuspended in that 100 µL, 50 µL of which was plated on LB agar plates with 100 µg/mL ampicillin. Plates were incubated overnight at 37°C. Plates were stored at 4°C. Individual candidate colonies were selected, miniprepped (using QIAgen kits), and submitted for Sanger sequencing. Candidates whose sequencing results returned successful were transformed for expression (see below).

Transformations for expression: DNA stocks ranged from 50-200 ng/µL. 2 µL of stock DNA was added to 50 µL competent BL21(DE3)pLysS *E. Coli* and incubated for 15 minutes on ice. Then transformation was heat shocked by incubation in a 42°C water bath, followed by an incubation on ice for 2 minutes. 450 µL of LB was added to the cells, following which they were incubated at 37°C in a shaking incubator at 200 rpm for 1 hour. The cells were centrifuged at 1000 rpm for 5 minutes and most of the media removed, leaving 100 µL. Cells were resuspended in that 100 µL, which was plated in its entirety on LB agar plates with 100 µg/mL ampicillin and 12.5 µg/mL chloramphenicol. Plates were incubated overnight at 37°C. Plates were stored at 4°C.

Protease expression and purification

The PPV protease was purified using the same protocol as the TEV protease, see below:

Recombinant His-tagged PPV Protease was expressed in BL2DE31pLysS. 1 colony was added to 8 mL 2xYT media supplemented with ampicillin and chloramphenicol. The following morning, 4 mL of the starter culture was used to inoculate 3 L of 2xYT (Fisher Scientific) supplemented with 100 µg/mL ampicillin and 12.5 µg/mL chloramphenicol at 37°C until the O.D. of 0.6 was reached. We then induced expression for 5 h at 30°C using 0.3 mM IPTG (Fisher Scientific). Cells pellets were collected by centrifugation of the culture at 4,000 g for 20 minutes at 4°C. The pellet was resuspended in 45 mL of Lysis buffer (1X PBS+10 mM imidazole+500 mM NaCl+ 2 mM BME). Cells were lysed through high-pressure homogenization (Avestin Emusiflex C3, in the Overduin Lab [we now have one in the lab as well]), then centrifuged at 40,000 g for 45 minutes at 4°C. The clarified protein supernatant was passed through a 1-mL Ni^{2+} affinity HisTrapFF column (GE Heathsciences), following which protein was collected off the column using a linear elution gradient (Elution buffer: 1X PBS, 500 mM imidazole, 100 mM NaCl, 2 mM BME, 10% glycerol). The eluted protein purity was confirmed via SDS-PAGE, then pooled. The protein was buffer exchanged using an Econopac DG10 column (Bio-Rad), eluting in storage buffer (25 mM Tris pH 7.5, 100 mM NaCl, 1 mM EDTA, 10% glycerol, 2 mM DTT). Protein concentration was

determined using a Bradford protein assay (Bio-Rad) and A280 (Expasy Protparam for pRK793-PPVP: MW 28.7 kDa, E/1000= 36.815 assuming all Cys form cystines, 36.440 assuming all Cys reduced. CMX3-PPVP: MW 72.3kDa, E/1000=104.655 assuming all Cys form cystines, 104.280 assuming all Cys reduced). Protein was supplemented with 10% glycerol, divided into aliquots and flash-frozen in liquid nitrogen, followed by storage at -80°C.

SDS-PAGE and native PAGE analysis

10% SDS-PAGE gels were prepared as per standard protocols in the lab. 10% native PAGE gels were prepared with the same protocol, omitting SDS.

SDS-PAGE samples were mixed with 4X loading dye (250mM Tris pH 6.8, 8% SDS, 0.2% bromophenol blue, 20% glycerol, 20% β-mercaptoethanol [BME]), while the native PAGE samples were mixed with a 2X sample buffer lacking SDS and BME (20% glycerol, 0.02% bromophenol blue, 0.16M Tris)

SDS-PAGE gels were run in SDS running buffer (0.192 M glycine, 0.025 M Tris, 3.5 mM SDS) at 180V for 40 minutes. Native-PAGE gels were run in native running buffer (0.192 M glycine, 0.025 M Tris, no SDS). Afterwards, both gels were placed in Coomassie blue dye (0.1% Coomassie Brilliant Blue R250, 50% methanol, 10% glacial acetic acid) for 20 minutes on an orbital shaker at room temperature. Following this, the dye was discarded and the gels were briefly rinsed with water, then placed in destaining solution (40% methanol, 10% glacial acetic acid). The gels were either destained overnight at room temperature on an orbital shaker, or in the microwave in 10-second intervals for 1 minute.

Anti-6xHis tag western blots

Using a prepared 10% acrylamide SDS-PAGE gel, electrophoresis of 5 µL of PPVP purification products was performed at 180V for 40 minutes. The resulting gel was transferred onto a PVDF (Polyvinylidene fluoride) membrane (GE Healthsciences) using a Mini Trans Blot ® wet transfer apparatus (Bio-Rad), transferring for 75 minutes at 35 V, using Towbin's transfer buffer (25 mM Tris base, 192 mM glycine, pH 8.3). The transferred membrane was then blocked for 45 minutes at room temperature on an orbital shaker with a 10% fish skin gelatin buffer. Following this, a mouse anti-his tag antibody (Thermo Fisher Scientific) was added at a 1:1000 dilution in the same 10% fish skin gelatin buffer and incubated at room temperature for 1 hour at room temperature. The membrane was then washed 3 times in 1X TBST (Tris-buffered saline, 0.1% Tween-20),

following which it was treated with a goat anti-mouse IR680 fluorescent secondary antibody (Li-Cor Biosciences) and incubated at room temperature for 1 hour. The membranes were subsequently washed with the same method as for the primary antibody, then visualized at a 2-minute exposure time at 680 nm.

Cleavage tests

In vitro cleavage tests were performed by Erik Gomez-Cardona, in which a standard *E. Coli* lysate was labeled with a peptide ester tag containing a PPVP cleavage sequence (the tag was termed PlumBEst1). Samples were also enriched on neutravidin beads following the subtiligase-based N-terminomics protocol. These labeled proteins in solution were then treated with the purified PPVP. Samples were taken after every step in the protocol (Pre-labeling, post-labeling, pre-cleaving, post-cleaving), and monitored via western blot using a fluorescent streptavidin tag.

Results:

PPV protease constructs

pRK793-PPVP cloning

The PPV protease gblock was amplified using the Gibson primers LA_001 and LA_006 to create the ends for ligation into pRK793 (see agarose gel below). As seen in the gel, the PCR product migrates slightly higher, meaning the construct was lengthened as per the primers.
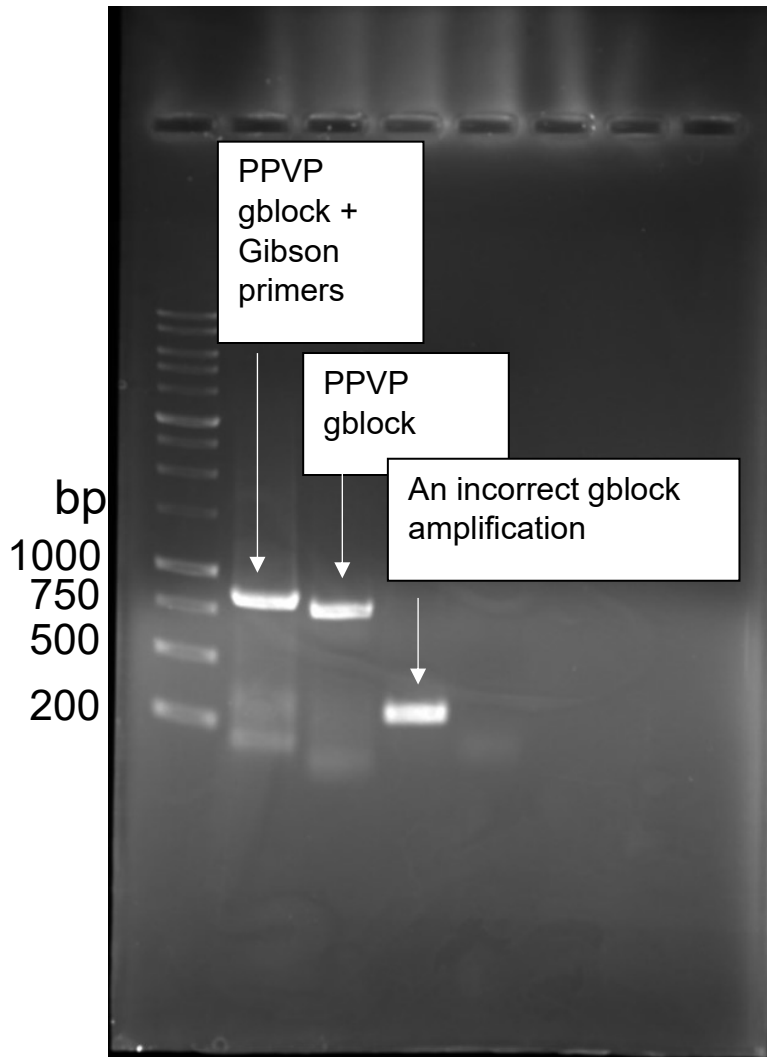
Figure 5. PCR product of PPV gblock amplified with primers for pRK793 assembly. The PCR product migrates at a slightly higher base-pair length than the original gblock, meaning that the Gibson primers have lengthened the construct and prepared it for ligation into the pRK793 plasmid.

Following amplification, the Gibson assembly took place, leading to successful colony growth on XL10 and a correct plasmid product determined via Sanger sequencing.

CMX3-PPVP cloning

Prior to ligating into the CMX3 plasmid, I performed a PCR to remove the PPV protease cutsite and the His-tag from the gblock, using the primers LA_004 and LA_008. As well, like with the previous construct, the PPV protease gblock was amplified using Gibson primers, this time LA_009 and LA_010, to create the ends for ligation into CMX3 (see agarose gel below for

products of both PCR reactions). The same slightly higher migration of the PCR product is observed, indicating that the primer lengthened the construct.
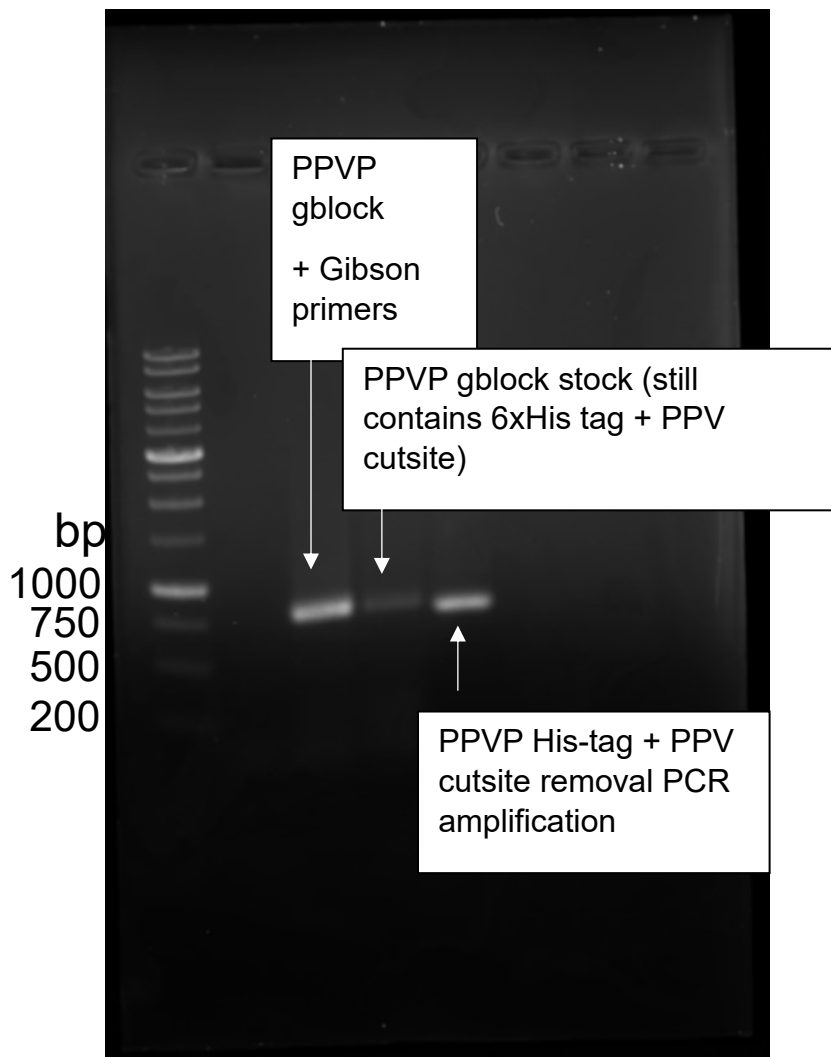
Figure 6. PCR product of PPV gblock to remove PPVP cutsite, and PCR to amplify with primers for CMX3 assembly. The PCR product of the PPVP cutsite and His-tag removal migrates lower than the gblock stock, indicating that these elements were removed successfully. The Gibson PCR product, like that of Figure 5, migrates at a slightly higher base-pair length than its non-PCR counterpart, indicating that the primers have prepared it for ligation into CMX3.

As with the pRK793 construct, the Gibson assembly led to successful transformations in XL10, with Sanger sequencing confirming that the assembly worked properly.

pRK793-PPVP purification leads to two protein products

When we purified the pRK793-PPVP construct, the protein product eluted in a single peak observed on the chromatogram of the HisTrapFF column. When analyzing the purification fractions on SDS-PAGE, we observed 2 bands on SDS-PAGE: one one at ~28kDa, consistent with full-length PPVP, and one at ~24kDa. We presumed that the band at 24kDa was a truncated product, after running a second purification batch and observing the same result. We then decided to pool the purified protein product to conduct cleavage tests.
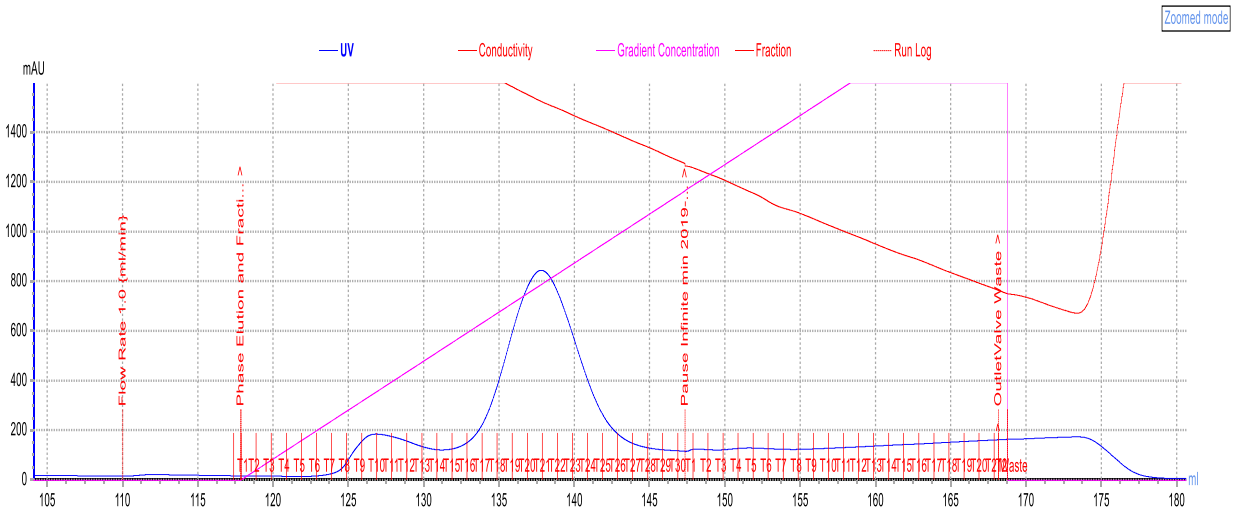
Figure 7. Chromatograph from pRK793-PPVP purification. A shallow peak is seen from fractions 9-12, and a taller peak is observed from fractions 17-26, whose height exceeds 800 mAU.

| Pellet | Sup | F/T | Wash | F15 | F19 | F22 | F30 |
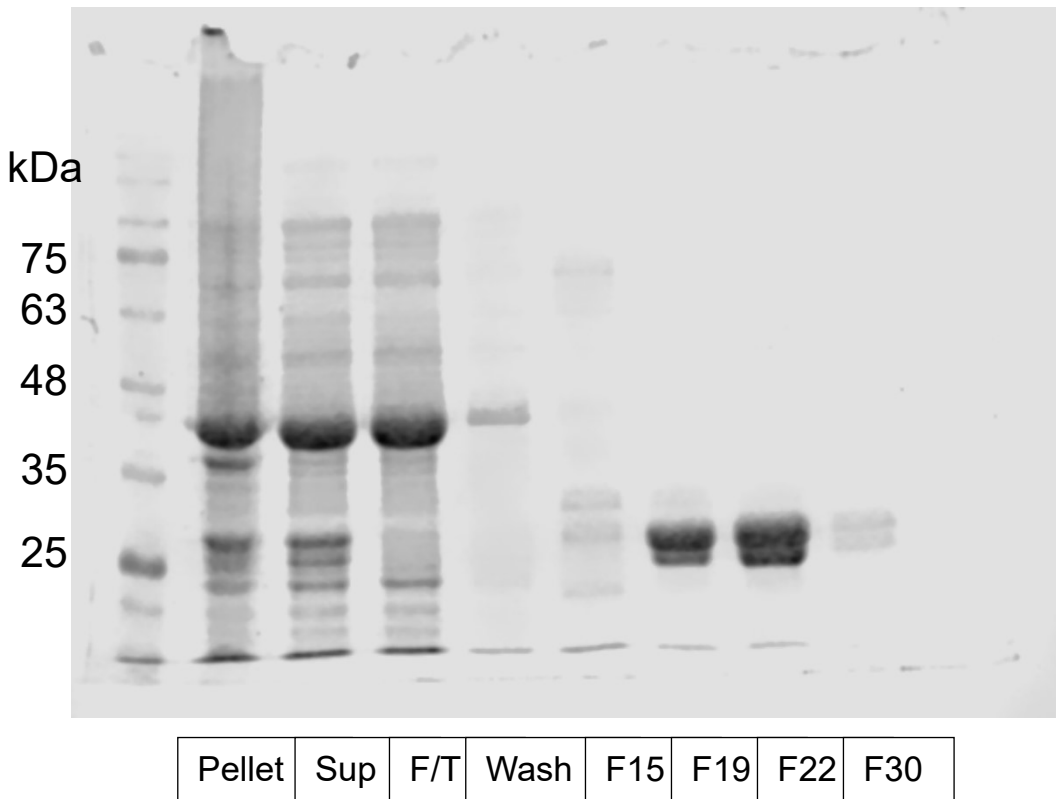
Figure 8. pRK793-PPVP His-tag purification gel. SDS-PAGE gel of PPVP purification using the pRK793-PPVP construct on a HisTrapFF column with a gradient imidazole elution. The purification product is visible in fractions 19-30, with its highest concentration around fraction 22. In these fraction, two bands are visible – one at ~28kDa, consistent with full-length PPVP, and one at ~24kDa, presumably a truncated product.

Purified protein does not cleave PlumBEst1 off of labeled lysates

Following purification, Erik Gomez-Cardona performed a cleavage test to see if the protein product could cleave the PlumBEst1 tag off labeled *E. coli* lysates. This was conducted in tandem to a control experiment using the TEVest6 tag and the TEV protease, which we knew would succeed. A western blot was conducted using a fluorescent streptavidin tag to label biotinylated (tagged) proteins. The appearance of signal between the pre-label and post-label sample would demonstrate that the TEVest6 and PlumBEst1 tags are successfully added to neo-N-termini. Following this, the disappearance of signal between the pre-cleavage and post-cleavage sample would demonstrate that the TEV protease and the PPV protease are able to cleave their respective tags. The blot we conducted (see below) demonstrates that both the TEVest6 and the PlumBEst1 tags are successfully labeled onto lysates, however only the TEV protease can cleave its tag off the labeled proteins. The pre-cleavage and post-cleavage samples for the PlumBEst1-labeled samples have the same intensity, indicating that the purified PPV protease is inactive.
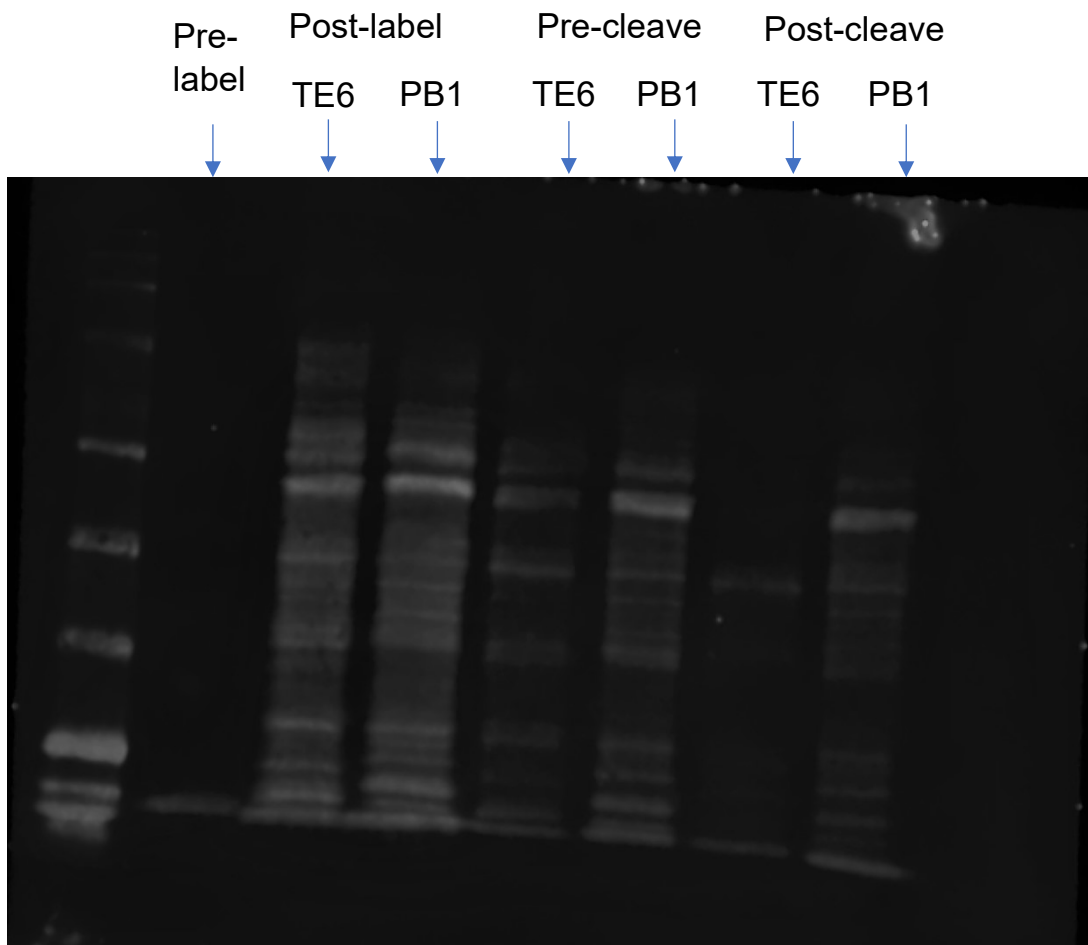
Figure 9. PlumBEst1 cleavage test streptavidin fluorescent tag blot. Pre-label, post-label, pre-cleavage and post-cleavage samples of *E. coli* lysates labeled with TEVest6 and PlumBEst1 and subsequently cleaved with their respective enzymes (TEV protease and PPV protease, respectively). Both tags successfully label lysates, but only the TEV protease can cleave its tag, meaning the purified PPV protease is inactive.

Anti-His western blot of PPV protease purification revealed that truncated product was his-tagged

To further investigate the truncation product observed, we conducted an anti-his tag western blot to see if the truncation was an N- or C-terminal truncation (see below). The anti-his tag antibody bound to both products, so we concluded that a portion of the C-terminal end of the purified product was being truncated. From here we moved onto native PAGE to assess aggregation.
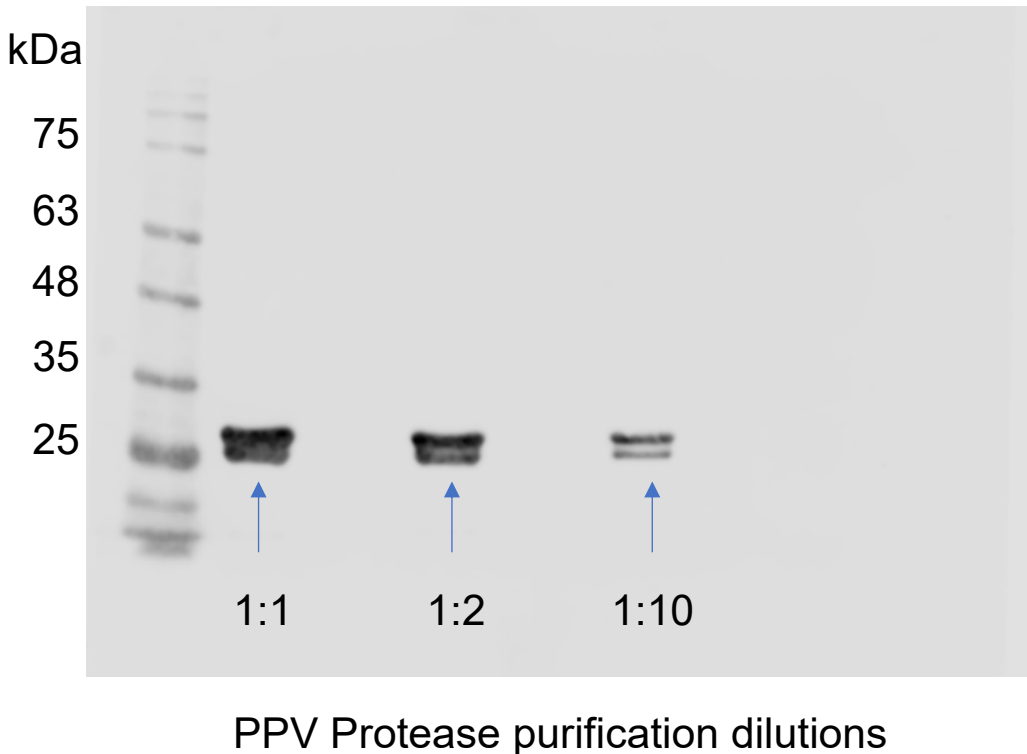

PPV Protease purification dilutions

Figure 10. Anti-6xHis tag western blot of PPV protease purification, at various dilutions. Several dilutions were performed in case a high signal was achieved, to be able to distinguish between the full-length and truncated protein product. As seen in the 1:10 fraction, the anti-his tag antibody binds to both products, meaning that this truncated product is a C-terminal truncation.

Native PAGE

Finally, native PAGE was conducted on the pooled and stored PPV protease, to determine if the protein was aggregated. A sample of the TEV protease was added to the native PAGE as a reference for what should be seen (see below). The PPV protease sample do not appear to even enter the gel, while the TEV protease enters the gel and is clearly visible. After this, we decided to move on and create a new construct.
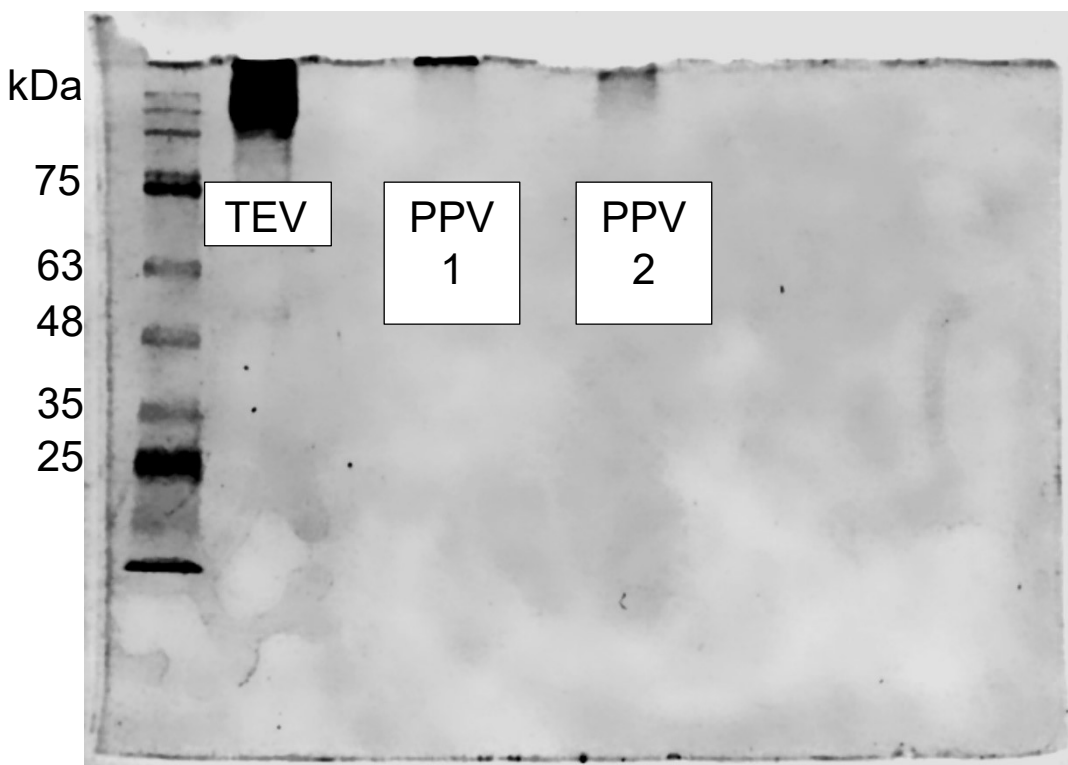

Figure 11. Native PAGE of frozen protease aliquots. The purified TEV protease succeeds in slowly migrating into the gel, while both PPV protease preps do not, suggesting that the PPV protease is aggregated in some way.

Modified TEV protease construct cloning

After the PPV protease purification was unsuccessful, we decided to create a new PPV protease construct, this time with a construct which would retain the MBP upon expression and purification, in an attempt to keep the protein stable and to avoid creating another truncation product. To attempt to express this construct, we inserted the PPV protease sequence into a new backbone plasmid, CMX3. This plasmid already contained a his-tag, so we cloned a truncated version of the PPV protease gblock, removing the 6 histidine residue codons from the sequence. We then ligated this construct in using Gibson assembly, then transformed and sequenced several candidates. Three candidates transformed successfully and were sent for Sanger sequencing, all

of which returned correct. Each of these plasmids was used in an expression attempt. Sadly, none of these constructs were able to successfully express any protein.

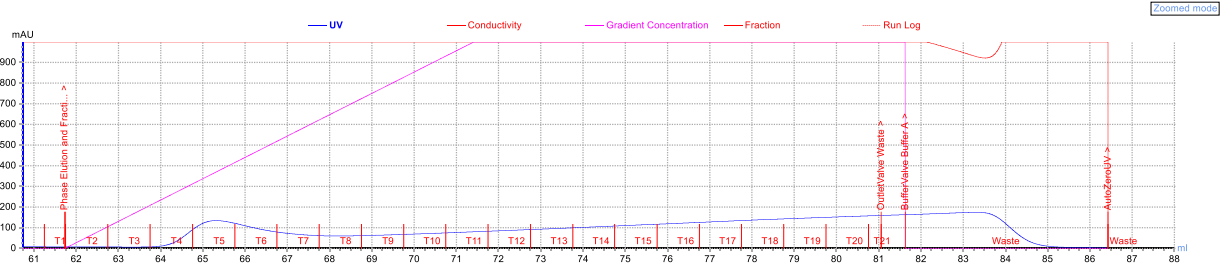**Modified TEV protease construct expression unsuccessful**

Figure 12. CMX3-PPVP chromatogram, showing no protein expression. The chromatogram does now seem to have a peak, indicating that no protein was expressed. The slight increase in mAU over time is due to the increasing concentration of imidazole over time (it is a gradient dilution).
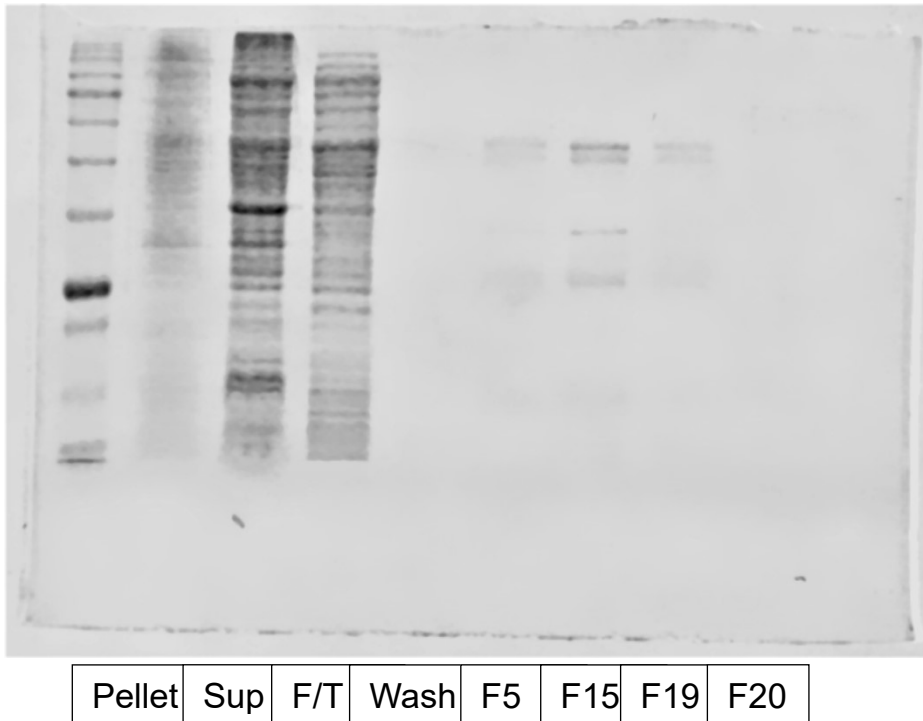

| Pellet | Sup | F/T | Wash | F5 | F15 | F19 | F20 |

Figure 13. CMX3-PPVP His-tag purification gel. SDS-PAGE gel of PPVP purification using the CMX3-PPVP construct on a HisTrapFF column with a gradient imidazole elution. There are no purification products visible.

From this point we elected to pause the project for the time being, to address our other protein expression problems before revisiting, as we noticed that the CMX3 plasmid was under a T7-inducible promoter while our other plasmid was not, and other members of the lab purifying protein under T7-inducible promoters were also having issues, leading us to believe that there might be issues with our competent cells as well.

Conclusions:

As of now, there are many avenues where our various PPV purifications could have gone wrong. Our initial construct using the TEV protease plasmid backbone is likely a bad candidate as it was successfully expressed yet did not cleave a synthetic PPV site peptide. The second construct using the CMX3 plasmid backbone could potentially work, as later in the year we determined that the BL21(DE3)pLysS cells used in the expression no longer carries DE3 (and so could not express protein). It is worth re-doing the expression with proper BL21(DE3)pLysS cells first, to fully determine whether the CMX3-PPV construct expresses an active protease. If this is not successful, the next course of action which should be taken is to re-clone the PPV protease sequence into a new expression plasmid, also containing a sequence for the Maltose Binding Protein. In this new plasmid, we should retain the MBP onto the PPV protease following expression – perhaps this will allow the protease to express more efficiently, because it was expressed as a fusion to another protein in another paper describing its purification by Zheng et al.[1]
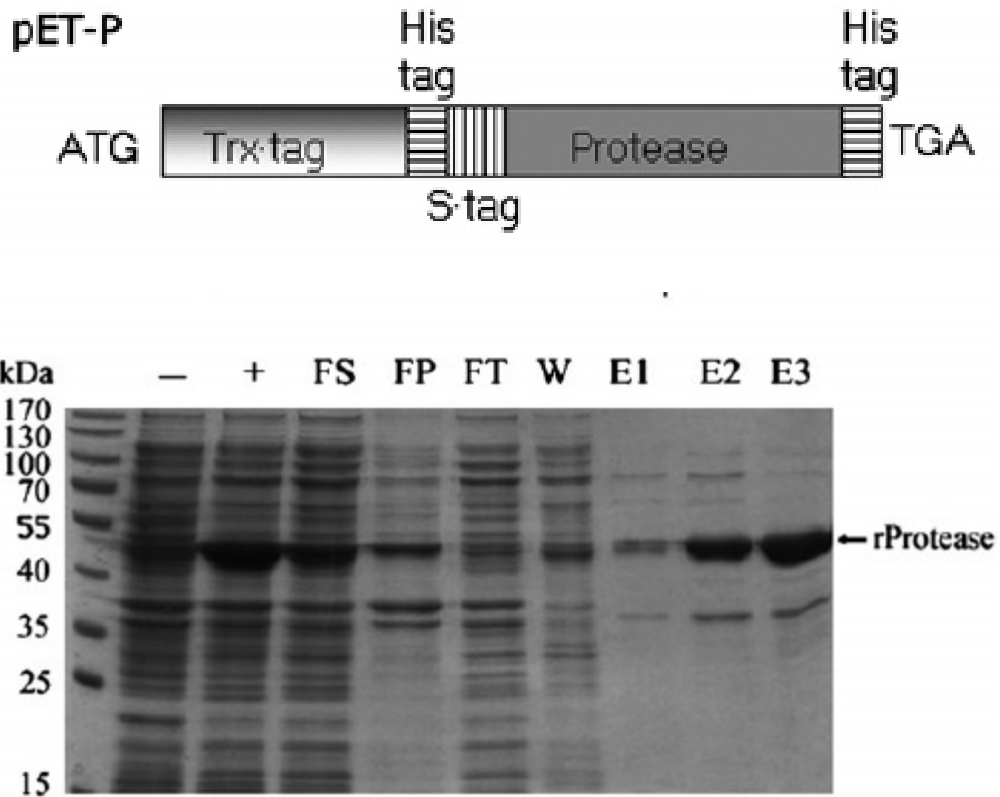
Figure 14. Recombinant PPV protease expression from Zheng et al. They employed a Trx tag to improve protein solubility and did not design their construct to cleave the tag, so the final purified protein retains it. As a result, their recombinant protein migrates at 55 kDa on SDS-PAGE.

References.

1. Zheng, N, Pérez, J.J., Zhang, Z, Dominguez, E, Garcia, J.A., and Xie, Q. (2007). Specific and efficient cleavage of fusion proteins by recombinant plum pox virus NIa protease. *Protein Expression and Purification.* 57(2). 153-162.